Expression and evaluation of a 297-amino acid fragment of the blood stage protein *Pf*C0760c from *Plasmodium falciparum*

by

Zainab Baig
BSc (*Hons*) Biochemistry

Submitted in fulfilment of the academic requirements of

Master of Science

in Biochemistry

School of Life Sciences

College of Agriculture, Engineering and Science

University of KwaZulu-Natal

Pietermaritzburg

South Africa

April 2019

Preface

The research contained in this dissertation was completed by the candidate while based in the Discipline of Biochemistry, School of Life Sciences of the College of Agriculture, Engineering and Science, University of KwaZulu-Natal, Pietermaritzburg, South Africa. The research was financially supported by The National Research Foundation.

The contents of this work have not been submitted in any form to another university and, except where the work of others is acknowledged in the text, the results reported are due to investigations by the candidate.

Declaration: Plagiarism

I, Zainab Baig, declare that:

(i) the research reported in this dissertation, except where otherwise indicated or acknowledged, is my original work;

(ii) this dissertation has not been submitted in full or in part for any degree or examination to any other university;

(iii) this dissertation does not contain other persons' data, pictures, graphs or other information, unless specifically acknowledged as being sourced from other persons;

(iv) this dissertation does not contain other persons' writing, unless specifically acknowledged as being sourced from other researchers. Where other written sources have been quoted, then:

a) their words have been re-written, but the general information attributed to them has been referenced;

b) where their exact words have been used, their writing has been placed inside quotation marks, and referenced;

(v) where I have used material for which publications followed, I have indicated in detail my role in the work;

(vi) this dissertation is primarily a collection of material, prepared by myself, published as journal articles or presented as a poster and oral presentations at conferences. In some cases, additional material has been included;

(vii) this dissertation does not contain text, graphics or tables copied and pasted from the Internet, unless specifically acknowledged, and the source being detailed in the dissertation and in the References sections.

Signed: Zainab Baig

Date: 3 September 2019

Abstract

Malaria is a mosquito-borne disease caused by parasites of the *Plasmodium* genus. There is no malaria vaccine available. The most lethal form of malaria in humans is caused by infection with *Plasmodium falciparum* parasites. The protein *Pf*C0760c from *P. falciparum* was identified as a potential malaria vaccine candidate based on the presence of alpha-helical coiled-coil motifs. This protein is conserved, and homologous proteins have been identified in *Plasmodial* species infecting humans, monkeys, mice and birds. *Pf*C0760c has not been characterised and has no known function. Conditions for the recombinant expression of a 297 amino acid fragment (N2360 – N2656) from *Pf*C0760c was optimized. The recombinant *Pf*C0760c protein (denoted further as r*Pf*C0760c$_{297}$) was expressed as an insoluble 56 kDa his$_6$-tagged fusion protein. Different conditions for the expression of soluble r*Pf*C0760c$_{297}$ were evaluated, including expression in the presence of ethanol and co-expression with *Escherichia coli* chaperones. Under different expression conditions, r*Pf*C0760c$_{297}$ remained insoluble, and was thus solubilized before nickel chelate affinity purification. 1 g cell biomass yielded ~22 mg purified r*Pf*C0760c$_{297}$ protein. Bioinformatics analyses of *Pf*C0760c revealed three conserved peptides. B-cell epitopes, and several T-cell epitopes were also predicted. *Pf*C0760c is expressed during the blood stages of the *P. falciparum* lifecycle and is found in the parasite nucleus. The absence of transmembrane domains and functional PEXEL motifs suggests that the protein is unlikely to be secreted. Chicken anti-r*Pf*C0760c$_{297}$ IgY antibodies were able to detect the homologous protein in *P. berghei*-infected mouse red blood cells. Far western blot analysis revealed protein-protein interactions between human U937 and mouse J774A.1 monocyte proteins with the r*Pf*C0760c$_{297}$. Mice immunized with r*Pf*C0760c$_{297}$ were able to raise antibodies against the protein, however succumbed to a *P. berghei* mouse malaria challenge infection. Various factors may have contributed to this outcome and further research is required in this endeavour. Further research is required for the development of a suitable malaria vaccine candidate.

Graphical Abstract

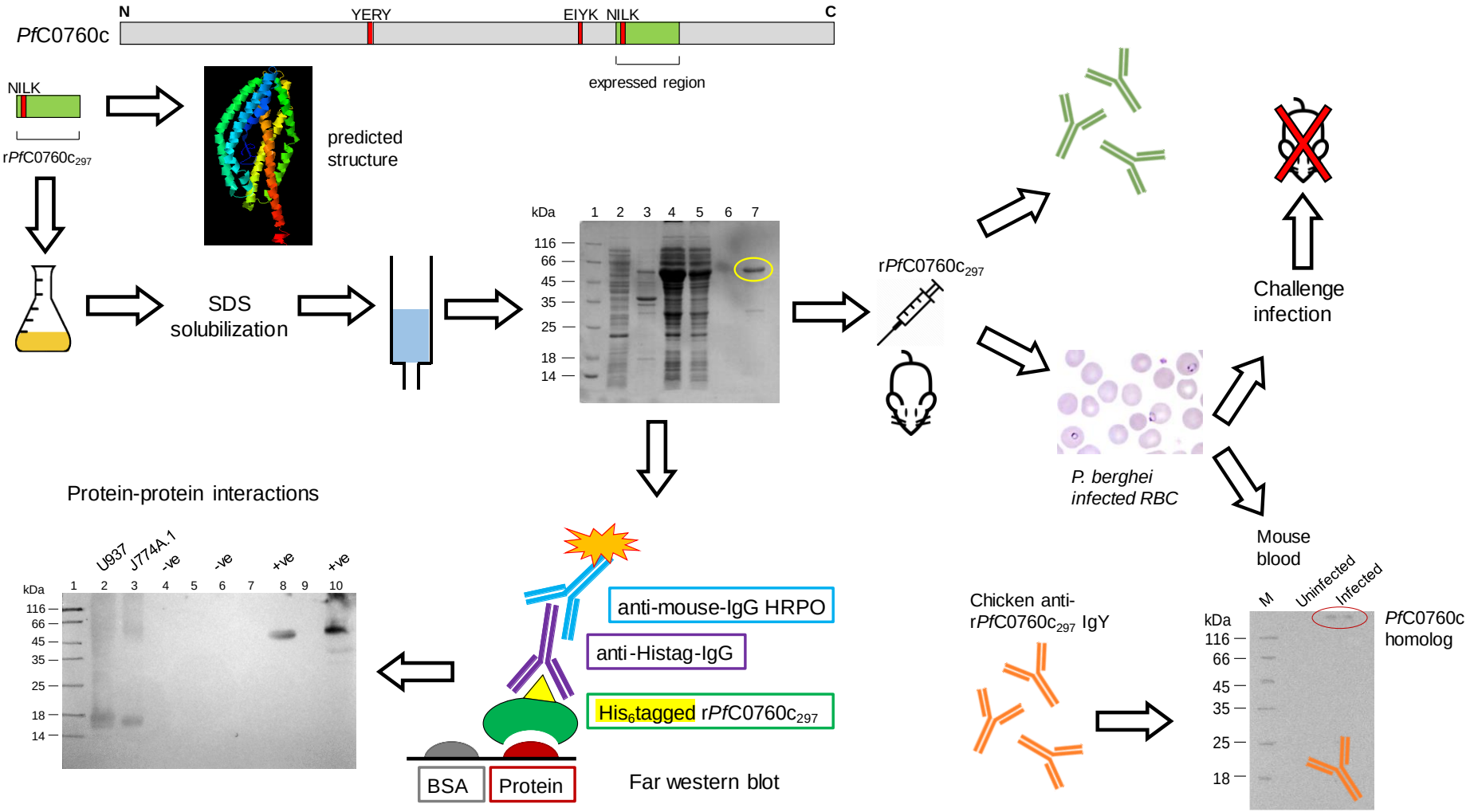

Acknowledgments

First and foremost, I would like to thank the Almighty, without whom nothing would be possible. I would like to thank the following people:

My parents, M.M. Idrees and Hajra for their continued love and support, for believing in me, for praying for me, and for every possible little thing that made a difference in my life.

Every teacher and lecturer who inspired my love for science, and helped lay my academic foundation.

My supervisor, Professor J.P. Dean Goldring for his supervision, encouragement and guidance throughout my studies as an undergraduate all the way through to postgraduate. Thank you for instilling in us good lab practice and a healthy amount of OCD.

Dr Robert G.E. Krause, Dr Kajal Fowdar and Dr Lauren Eyssen for all their helpful discussions as the project progressed. All fellow students of the Malaria Lab: Mark H, Mlondi, Abdulmalik, Eugene, Mark C, Sinothile and Sheldon, for the support and interesting, healthy debates.

Kelvin Addicott, who had previously worked with the protein, and who also did the initial cloning of the recombinant protein and raised the chicken antibodies. Thank you for always being available for a chat regarding the protein.

Professor Carola Niesler, Dr Raymond Hewer, Dr M.M. Elias Baig, Dr Farzana Baig, Quraisha Baig, Dr M.I. Adam and Rizwana Mia who always had an ear for me and provided invaluable advice.

Ebrahim Ally, who sacrificed time and mice for this project. Your continued friendship based on mutual love for tea and animals is appreciated.

Our admin ladies Charmaine, Tanya and Natalie, thank you for taking care of all the admin on our behalf. Jessica Moodley and Yegan Pillay who were always available for technical support. Ma Agnes for ensuring we always had dH_2O available.

All the cleaning staff for making our lives easier.

To my brothers Ibrahim and Muhammad, my sister-in-law Tasfiyah and my dear friends Faiaz, Alex, Tash, Tracy, Mariam, Billie, Selisha, Ryan, Jezelle, Ameer, and Tasmiyah for always being around, for a chat, love and support.

To the National Research Foundation and the University of KwaZulu-Natal, without which, this study would not have been made possible.

Table of Contents

Page

Preface ii
Declaration: Plagiarism iii
Abstract iv
Graphical Abstract v
Acknowledgments vi
Table of Contents vii
List of Tables xiv
List of Figures xv
Abbreviations xvii
Chapter 1: Literature review 1
1.1 Introduction 1
1.2 Malaria transmission and control 2
1.3 The *Plasmodium falciparum* parasite 2
1.4 The lifecycle of *Plasmodium* parasites 3
1.4.1 The sporozoite stage of the *Plasmodium* lifecycle 3
1.4.2 The merozoite stage of the *Plasmodium* lifecycle 3
1.4.3 The ring stage of the *Plasmodium* lifecycle 3
1.4.4 The trophozoite stage of the *Plasmodium* lifecycle 4
1.4.5 The schizont stage of the *Plasmodium* lifecycle 4
1.4.6 The gametocyte stage of the *Plasmodium* lifecycle 4
1.5 Severe malaria 5
1.6 Malaria diagnostic tests 6
1.6.1 Microscopy for malaria diagnosis 6
1.6.2 Rapid diagnostic tests for the detection of malaria 7
1.6.3 Polymerase chain reaction detection and diagnosis of malaria 7
1.6.4 Loop-mediated isothermal amplification for detection and diagnosis of malaria 7
1.6.5 Enzyme-linked immunosorbent assay to detect malaria 8
1.7 Antimalarial drugs 8
1.8 Survival of *Plasmodium* within a host 8
1.9 Malaria vaccines 9

1.9.1 Pre-erythrocytic stage vaccines 9
1.9.1.1 Circumsporozoite protein and the RTS,S malaria vaccine 9
1.9.1.2 Liver stage antigen-1 10
1.9.1.3 Sporozoite surface protein/thrombospondin related anonymous protein 11
1.9.1.4 Radiation attenuated sporozoites.....11
1.9.1.5 Genetically attenuated sporozoites 12
1.9.2 Malaria blood stage vaccines.....12
1.9.2.1 Apical membrane antigen 13
1.9.2.2 Merozoite surface protein 13
1.9.2.3 Erythrocyte binding antigen 14
1.9.2.4 Glutamate-rich protein 14
1.9.2.5 Hypoxanthine-guanine-xanthine phosphoribosyltransferase 15
1.9.2.6 Reticulocyte-binding protein homolog 5 15
1.9.2.7 Ring-infected erythrocyte surface antigen.....16
1.9.2.8 Trophozoite exported protein 1 16
1.9.2.9 Whole parasite blood stage vaccine 16
1.9.3 Transmission blocking vaccines.....17
1.9.3.1 The *Pf*s25 antigen.....17
1.9.3.2 The *Pf*s48/45 antigen.....17
1.9.3.3 The *Pf*s230 antigen.....18
1.9.4 Multi subunit vaccines.....18
1.9.4.1 NYVAC-*Pf*7 vaccine.....18
1.9.4.2 Multi-antigen peptide vaccines.....18
1.9.4.3 S*Pf*66 malaria vaccine 19
1.10 *Pf*C0760c as a potential malaria vaccine candidate.....19
1.11 Aims and objectives.....20
Chapter 2: Materials and methods.....21
2.1 Materials.....21
2.2 Bacterial recombinant protein expression 21
2.2.1 *E. coli* growth curves in different media.....21
2.2.2 Optimization of bacterial expression of recombinant r*Pf*C0760c$_{297}$.....22
2.2.2.1 Expression of r*Pf*C0760c$_{297}$ in LB or 2×YT media 22
2.2.2.2 Expression of r*Pf*C0760c$_{297}$ in terrific broth 22
2.2.2.3 Influence of different temperatures on the expression of r*Pf*C0760c$_{297}$ 22

2.2.2.4 Influence of shaking speed on the expression of r*Pf*C0760c$_{297}$ 22
2.2.2.5 Influence of time on the expression of r*Pf*C0760c$_{297}$ 22
2.2.2.6 Effect of IPTG concentration in LB media on the expression of r*Pf*C0760c$_{297}$ 23
2.2.3 Modification of expression conditions to yield soluble r*Pf*C0760c$_{297}$.....23
2.2.4 Solubilization of r*Pf*C0760c$_{297}$ 23
2.2.5 Purification of r*Pf*C0760c$_{297}$ 23
2.2.6 Regeneration of nickel chelate affinity matrix.....24
2.3 Co-expression of r*Pf*C0760c$_{297}$ with chaperones 24
2.3.1 Generation of competent *E. coli* BL21(DE3) cells 24
2.3.2 Transformation of competent *E. coli* BL21(DE3) cells with chaperone plasmids 25
2.3.3 Isolation of chaperone plasmid DNA from *E. coli* cells 25
2.3.4 Co-expression of r*Pf*C0760c$_{297}$ with *E. coli* chaperones.....26
2.3.5 Modification of co-expression conditions.....26
2.4 Electrophoretic techniques 26
2.4.1 Sodium dodecyl sulfate polyacrylamide gel electrophoresis.....26
2.4.2 Western blotting.....27
2.4.3 Far western blotting 28
2.5 Far dot blot 29
2.6 Cell culture techniques 30
2.6.1 Culture of human U937 and mouse J774A.1 cells 30
2.6.2 Monocyte subculture.....30
2.6.3 Trypan blue assay 30
2.7 The Bradford assay 31
2.8 Immunization of mice.....31
2.8.1 Mice used in this study 31
2.8.2 Generation of anti-r*Pf*C0760c$_{297}$ antibodies in mice 31
2.8.3 Enzyme-linked immunosorbent assay 32
2.8.4 Immunization of mice with r*Pf*C0760c$_{297}$ and challenge with *P. berghei* parasites.....32
2.8.5 Giemsa staining of *P. berghei* infected blood samples.....32
Chapter 3: Recombinant expression, solubilization and purification of r*Pf*C0760c$_{297}$ 33
3.1 Introduction.....33
3.1.1 *E. coli* as a bacterial host for recombinant protein expression.....33
3.1.2 pET expression vectors 33
3.1.3 Expression of r*Pf*C0760c$_{297}$ 34

3.2 Results 34
3.2.1 Growth profiles of transformed *E. coli* cells in different media 34
3.2.2 Evaluation of different culture conditions for r*Pf*C0760c$_{297}$ expression 35
3.2.3 Modification of expression conditions to improve solubility of r*Pf*C0760c$_{297}$ 39
3.2.4 Solubilization and purification of r*Pf*C0760c$_{297}$ 42
3.3 Discussion 43
3.3.1 Recombinant expression of r*Pf*C0760c$_{297}$ 43
3.3.2 Recombinant expression of *P. falciparum* proteins 43
3.3.3 Bacterial inclusion bodies 43
3.3.4 Growth profiles of bacterial cells 44
3.3.5 Terrific broth expresses high levels of r*Pf*C0760c$_{297}$ 44
3.3.6 The thioredoxin fusion tag 44
3.3.7 Induction of recombinant protein expression with IPTG 45
3.3.8 Expression of recombinant protein at low temperatures 45
3.3.9 Protein recombinant expression in the presence of ethanol 45
3.3.10 Solubilization of recombinant proteins 46
3.3.11 Refolding and purification of r*Pf*C0760c$_{297}$ 46
3.3.12 Alternative solubilization methods 46
3.3.13 Conclusion 47
Chapter 4: *E. coli* chaperone co-expression for the recombinant expression of soluble r*Pf*C0760c$_{297}$ 48
4.1 Introduction 48
4.1.1 Chaperones 48
4.1.2 *E. coli* chaperones 48
4.1.3 The GroEL-GroES chaperones 48
4.1.4 The *dna*K*dna*J*grp*E chaperones 49
4.2 Results 49
4.2.1 Co-expression of r*Pf*C0760c$_{297}$ with *E. coli* chaperones in LB media 49
4.2.2 Co-expression of r*Pf*C0760c$_{297}$ with *E. coli* chaperones in terrific broth 51
4.2.3 Induction of r*Pf*C0760c$_{297}$ expression with various concentrations of IPTG in LB media 52
4.2.4 Induction of chaperone co-expression with L-arabinose 53
4.4 Discussion 53
4.4.1 r*Pf*C0760c$_{297}$ is an insoluble recombinant protein 53

4.4.2 Co-expression of r*Pf*C0760c$_{297}$ with *E. coli* chaperones in terrific broth.....54
4.4.3 *P. falciparum* heat shock proteins.....54
4.4.4 Co-expression of recombinant proteins with non-*E. coli* chaperones.....55
4.4.5 Conclusion.....55
Chapter 5: Protein-protein interactions between r*Pf*C0760c$_{297}$ and monocyte proteins.....57
5.1 Introduction.....57
5.1.1 White blood cells in the immune system.....57
5.1.2 Function of monocytes.....57
5.1.3 Protein-protein interactions.....58
5.2 Results.....58
5.2.1 Selection of chicken IgY concentrations for far dot blot analysis.....58
5.2.2 Detection of monocyte peroxidase activity by dot blot analysis.....59
5.2.3 Far western blot analysis of control proteins.....59
5.2.4 Western blot analysis of monocyte proteins.....60
5.2.5 Detection of monocyte peroxidase activity by western blot.....60
5.2.6 Far western blot analysis of monocyte lysate proteins and r*Pf*C0760c$_{297}$.....61
5.3 Discussion.....61
5.3.1 U937 and J774A.1 monocytes used in this study.....61
5.3.2 Far western blot of U937 and J774A.1 monocyte proteins with r*Pf*C0760c$_{297}$.....62
5.3.3 Alternative methods to detect protein-protein interactions.....62
5.3.4 Monocyte peroxidase activity.....62
5.3.5 Interaction of monocytes with r*Pf*C0760c$_{297}$ *in vivo*.....63
5.3.6 Chicken anti-r*Pf*C0760c$_{297}$ IgY.....63
5.3.7 Conclusion.....63
Chapter 6: Bioinformatics analyses of *Pf*C0760c.....64
6.1 Introduction.....64
6.2 Methods.....64
6.2.1 Basic local alignment search tool and sequence alignment.....64
6.2.2 Presence of B-cell epitopes within *Pf*C0760c.....65
6.2.3 Prediction of T-cell epitopes within *Pf*C0760c.....65
6.2.4 Predict7 analysis of *Pf*C0760c.....65
6.2.5 *Plasmodium* export element and transmembrane domain prediction.....65
6.2.6 Functional site prediction of *Pf*C0760c using ScanPROSITE.....65
6.2.7 Prediction of protein-protein interactions of *Pf*C0760c.....66

6.2.8 Detection of conserved domains within the *Pf*C0760c protein....66
6.2.9 Prediction of the subcellular localization of *Pf*C0760c....66
6.2.10 Protein structural prediction of r*Pf*C0760c$_{297}$....67
6.3 Results....67
6.3.1 BLASTp and multiple sequence alignment....67
6.3.2 Identification of B-cell epitopes within *Pf*C0760c....73
6.3.3 Prediction of T-cell epitopes within *Pf*C0760c....74
6.3.4 Predict7 analysis of *Pf*C0760c....74
6.3.5 Identification of *Pf*C0760c PEXEL motifs....77
6.3.6 Functional site predictions of *Pf*C0760c....78
6.3.7 Prediction of protein-protein interactions of *Pf*C0760c....81
6.3.8 Prediction of conserved domains in the *Pf*C0760c protein sequence....82
6.3.9 Prediction of the subcellular localization of *Pf*C0760c....83
6.3.10 Prediction of r*Pf*C0760c$_{297}$ protein structure....84
6.4 Discussion....86
6.4.1 *Pf*C0760c is a conserved protein....86
6.4.2 Possible subcellular localization of *Pf*C0760c....86
6.4.3 Predicted function of *Pf*C0760c....87
6.4.4 Protein motifs within the *Pf*C0760c protein sequence....87
6.4.4.1 Phosphorylation motifs in *Pf*C0760c....87
6.4.4.2 Myristoylation sites within *Pf*C0760c....87
6.4.4.3 Glycosylation of *Pf*C0760c....88
6.4.4.4 Prediction of leucine zippers in *Pf*C0760c....88
6.4.4.5 Lysine acetylation of *Pf*C0760c....88
6.4.5 Predicted structure of r*Pf*C0760c$_{297}$....89
6.4.6 Conclusion....89
Chapter 7: Immunization of BALB/c mice with r*Pf*C0760c$_{297}$....90
7.1 Introduction....90
7.1.1 Mouse malaria pre-clinical trials....90
7.1.2 *P. berghei* as a model for malaria vaccines....90
7.1.3 *Pf*C0760c as a potential malaria vaccine candidate....90
7.2 Results....91
7.2.1 Detection of homologous *Pf*C0760c protein in *P. berghei*....91
7.2.2 Generation of anti-r*Pf*C0760c$_{297}$ antibodies in mice....92

7.2.3 Immunization of mice with r*Pf*C0760c$_{297}$ followed by *P. berghei* challenge 93
7.3 Discussion 94
7.3.1 Immunization with r*Pf*C0760c$_{297}$ 94
7.3.2 Solubilization of r*Pf*C0760c$_{297}$ 95
7.3.3 Conformation of r*Pf*C0760c$_{297}$ 95
7.3.4 Adjuvant used for immunization with r*Pf*C0760c$_{297}$ 96
7.3.5 Immunization of mice 96
7.3.6 Further modifications to the r*Pf*C0760c$_{297}$ immunization study 96
7.3.7 Conclusion 97
Chapter 8: General discussion and conclusions 98
8.1 Premise of this study 98
8.2 Uncharacterised *Plasmodial* proteins 98
8.3 *Pf*C0760c as a potential malaria vaccine candidate 98
8.4 r*Pf*C0760c$_{297}$ is expressed as an insoluble protein in *E. coli* 99
8.5 Expression of r*Pf*C0760c$_{297}$ in the presence of *E. coli* chaperones 99
8.6 Properties of the *Pf*C0760c protein 100
8.7 Conclusion and future work 100
References 101
Appendix A: Annotated full-length amino acid sequence of *Pf*C0760c 130
Appendix B: BLAST output from PlasmoDB and ExPASy 131

List of Tables

Table **Page**

Table 2.1: Components used in SDS-PAGE gels 27

Table 6.1: Results from NCBI BLASTp using *Pf*C0760c as the query sequence 68

Table 6.2: BLASTp analyses of the *Pf*C0760c conserved peptides YERY, EIYK and NILK ..72

Table 6.3: Detection of PEXEL motifs in the *Pf*C0760c protein sequence 78

Table 6.4: Analysis of the full-length *Pf*C0760c protein sequence using the PROSITE prediction software 80

Table 6.5: Prediction of protein-protein interactions of *Pf*C0760c with *P. falciparum* proteins using STRING 81

Table 6.6: Conserved domains of *Plasmodium* species' proteins homologous to *Pf*C0760c 82

Table 6.7: Functions of domains from *Plasmodium* species identified by CDD 83

Table 6.8: MultiLoc2 analysis of *Plasmodium* proteins of known locations.....83

Table 6.9: Analysis of *Plasmodium* proteins of known locations using the NucPred server ..84

Table B.1: PlasmoDB BLAST analysis of PfC0760c protein sequence.....131

Table B.2: Protein sequences from ExPASy were aligned with PfC0760c using Clustal Omega 132

List of Figures

Figure **Page**

Figure 1.1: Lifecycle of *Plasmodium falciparum* in *Anopheline* and human hosts. 5
Figure 2.1: Schematic representation of far dot blot or far western blot probed with r*Pf*C0760c$_{297}$. 29
Figure 3.1: Growth profiles of *E. coli* BL21(DE3) transformed with pET32a-r*Pf*C0760c$_{297}$ or pET28a-r*Pf*C0760c$_{297}$ in three types of media 35
Figure 3.2: *E. coli* BL21(DE3) cells transformed with pET32a-r*Pf*C0760c$_{297}$ or pET28a-r*Pf*C0760c$_{297}$ grown in different media.....36
Figure 3.3: Expression of r*Pf*C0760c$_{297}$ at three temperatures.....37
Figure 3.4: Expression of r*Pf*C0760c$_{297}$ in terrific broth at different shaking speeds.....37
Figure 3.5: Expression of r*Pf*C0760c$_{297}$ for different time periods 38
Figure 3.6: Comparison of IPTG concentrations for the expression of r*Pf*C0760c$_{297}$ in LB media 38
Figure 3.7: Optimized conditions for expression of r*Pf*C0760c$_{297}$.....39
Figure 3.8: Expression of r*Pf*C0760c$_{297}$ for 6 – 8 h 40
Figure 3.9: Expression of r*Pf*C0760c$_{297}$ at 20°C 40
Figure 3.10: Expression of r*Pf*C0760c$_{297}$ in the presence of 0 – 3% (v/v) ethanol.....41
Figure 3.11: Induction of r*Pf*C0760c$_{297}$ expression at stationary phase in LB media.....41
Figure 3.12: Solubilization and purification of r*Pf*C0760c$_{297}$ expressed under optimal conditions.....42
Figure 4.1: Co-expression of r*Pf*C0760c$_{297}$ with *E. coli* chaperones.....50
Figure 4.2: Co-expression of r*Pf*C0760c$_{297}$ with *E. coli* chaperones in terrific broth 51
Figure 4.3: Co-expression of r*Pf*C0760c$_{297}$ with the *dna*K*dna*J*grp*E chaperones for 8 h in terrific broth.....51
Figure 4.4: Different IPTG concentrations for the induction of r*Pf*C0760c$_{297}$ co-expression with GroEL-GroES chaperones 52
Figure 4.5: Induction of chaperone co-expression with different concentrations of L-arabinose. 53
Figure 5.1: Far dot blot analysis of chicken IgY probed with r*Pf*C0760c$_{297}$.....58
Figure 5.2: Far western blot analysis of positive and negative controls probed with increasing concentrations of r*Pf*C0760c$_{297}$.....59
Figure 5.3: Western blot of U937 and J774A.1 monocyte lysate proteins 60

Figure 5.4: Far western blot analysis of U937 and J774A.1 lysates probed with r*Pf*C0760c$_{297}$ 61
Figure 6.1: Relationship between *Pf*C0760c and homologous *Plasmodium* protein sequences.....69
Figure 6.2: Multiple sequence alignment of *Pf*C0760c and homologous *Plasmodium* proteins showing conserved peptides 71
Figure 6.3: Amino acid sequence of r*Pf*C0760c$_{297}$ 72
Figure 6.4: Multiple sequence alignment of *Pf*C0760c B-cell epitopes.....73
Figure 6.5: Predict7 analysis of the 297-amino acid sequence of r*Pf*C0760c$_{297}$ 75
Figure 6.6: Predict7 analysis of conserved *Pf*C0760c peptides 76
Figure 6.7: Predict7 analysis of B-cell epitopes from *Pf*C0760c.....77
Figure 6.8: Amino acid composition of *Pf*C0760c and r*Pf*C0760c$_{297}$. 78
Figure 6.9: Multiple sequence alignment of *Pf*C0760c with homologous proteins from *Plasmodium* species showing an acetylated lysine residue 79
Figure 6.10: Predicted models of the r*Pf*C0760c$_{297}$ generated by I-TASSER.....85
Figure 6.11: Predicted conformation of amino acids in the conserved peptide and B-cell epitope of r*Pf*C0760c$_{297}$. 85
Figure 7.1: Sequence alignment of r*Pf*C0760c$_{297}$ and homologous sequence in *P. berghei* ANKA. 91
Figure 7.2: Detection of homologous r*Pf*C0760c$_{297}$ protein in *P. berghei*-infected blood.....92
Figure 7.3: Detection of anti-r*Pf*C0760c$_{297}$ antibodies from mice immunized with r*Pf*C0760c$_{297}$ 93
Figure 7.4: Parasitaemia monitored over the course of *P. berghei* infection. 94
Figure A.1: Full-length amino acid sequence of PfC0760c with key sequences indicated...130

Abbreviations

ABTS	di-ammonium 2,2'-azino-bis(3-ethybenzothiazolinesulfonate)
ADP	adenosine diphosphate
AMA	apical membrane antigen
ATP	adenosine triphosphate
BLAST	basic local alignment search tool
BLASTp	basic local alignment search tool for protein sequences
BSA	bovine serum albumin
cAMP	cyclic adenosine monophosphate
CDD	Conserved Domain Database
cGMP	cyclic guanosine monophosphate
CSA	chondroitin sulfate A
CSP	circumsporozoite protein
C-terminal	carboxy terminal
dH_2O	distilled water
DMEM	Dulbecco's modified Eagles medium
DMSO	dimethyl sulfoxide
DNA	deoxyribonucleic acid
ECL	enhanced chemiluminescence
EBA	erythrocyte binding antigen
EDTA	ethylenediaminetetraacetic acid
ELISA	enzyme-linked immunosorbent assay
FBS	foetal bovine serum
FMP011	*falciparum* malaria protein 011
g	relative centrifugal force
GLURP	glutamate-rich protein
GTP	guanosine triphosphate
h	hours
HGPRT	hypoxanthine-guanine phosphoribosyltransferase
HGXPRT	hypoxanthine-guanine-xanthine phosphoribosyltransferase
his_6tag	hexahistidine affinity tag
HRP-2	histidine rich protein 2
HRPO	horseradish peroxidase
HSP	heat shock protein
IFN	interferon
IgG	immunoglobulin G
IgY	immunoglobulin Y from chicken egg yolk
IL	interleukin
IPTG	isopropyl β-D-1-thiogalactopyranoside
I-TASSER	Iterative Assembly Refinement
K*Pf*	chimeric *P. falciparum* HSP70
LAMP	loop-mediated isothermal amplification
LB	Luria Bertani
LDH	lactate dehydrogenase
LSA	liver stage antigen
MAP	multiple antigen peptide
min	minutes
mRNA	messenger RNA
MSP	merozoite surface protein
NCBI	National Centre for Biotechnology Information
NLS	nuclear localization signal

NTA	nitriloacetic acid
NYVAC	New York vaccine
N-terminal	amino terminal
OD	optical density
PBS	phosphate buffered saline
PCR	polymerase chain reaction
PEXEL	*Plasmodium* export element
*Pf*EMP	*P. falciparum* erythrocyte membrane protein
RAS	radiation attenuated sporozoites
RDT	rapid diagnostic test
RESA	ring-infected erythrocyte surface antigen
RH	reticulocyte-binding homologue
RON	rhoptry neck protein
RNA	ribonucleic acid
RPM	revolutions per minute
RPMI	Roswell Park Memorial Institute
rRNA	ribosomal ribonucleic acid
RT	room temperature
s	seconds
scFv	single chain antibody fragment
SDS	sodium dodecyl sulfate
SDS-PAGE	sodium dodecyl sulfate polyacrylamide gel electrophoresis
SMC	structural maintenance of chromosomes
SOB	sub-optimal broth
SOC	sub-optimal broth with catabolite
STRING	Search Tool for Recurring Instances in Neighbouring Genes
TBS	Tris buffered saline
TEMED	*N*,*N*,*N*′,*N*′-Tetramethylethane-1,2-diamine
Tex-1	trophozoite exported protein-1
TRAP	thrombospondin related anonymous protein
WHO	World Health Organization
2xYT	2 x yeast-tryptone media

Chapter 1: Literature review

1.1 Introduction

Malaria is a disease caused by the mosquito-borne parasite of the *Plasmodium* genus. Malaria affects the tropical and subtropical regions of the world. The *Plasmodium falciparum* parasite causes the most lethal form of malaria in humans (WHO, 2018). Other species of *Plasmodium* known to infect humans include *P. malariae, P. ovale* and *P. vivax* (Birkett, 2016; Muerhoff *et al*., 2010). The simian-infecting parasite *P. knowlesi* was identified as a human-infecting parasite, due to the recent increase in human *P. knowlesi* infections occurring in South East Asia (Antinori *et al*., 2012; Singh *et al*., 2004). Sub-Saharan Africa has the highest mortality caused by *P. falciparum* malaria (Targett and Greenwood, 2008; Gardner *et al*., 2002). Children younger than five years old, and pregnant women are the most vulnerable (Srinivasan *et al*., 2017; Birkett, 2016). South America, Europe, the Middle East, and Asia are also affected by malaria (Birkett, 2016). In South Africa, the KwaZulu-Natal, Mpumalanga and Limpopo provinces are affected (Maharaj *et al*., 2013).

A malaria infection is characterised by intermittent febrile episodes occurring every 48 – 72 hours following infection (Kyes *et al*., 2001) depending on which *Plasmodium* species a human host is infected with. Febrile episodes occur every day in *P. knowlesi*, every second day in *P. vivax*, every three days in *P. falciparum* infections, and every fourth day in *P. malariae* and *P. ovale* (Daneshvar *et al*., 2009; Collins and Jeffery, 2007; Garcia *et al*., 2001). These periods of fever coincide with the rupture of infected red blood cells releasing merozoites into the bloodstream which then invade new red blood cells, wherein they replicate (Absalon *et al*., 2016; Tuteja, 2007). Parasite-associated debris and metabolites released from rupturing red cells contribute to fever (Markwalter *et al*., 2016). Headaches and chills are common symptoms, as well as myalgia, abdominal pain, nausea, vomiting, malaise, and less frequently diarrhoea, cramps, loss of appetite, decreased energy, dizziness and body pains (Bartoloni and Zammarchi, 2012; Hlongwana *et al*., 2009; Trampuz *et al*., 2003).

Problems threatening malaria eradication efforts include mosquito resistance to insecticides and parasite resistance to various antimalarial drugs (Krzywinska *et al*., 2016; Pavadai *et al*., 2016; Srinivasan *et al*., 2017). The liver stage of the parasite lifecycle is asymptomatic, and this also circumvents the elimination of malaria as the infection is undetected (Dhangadamajhi *et al*., 2010; Targett and Greenwood, 2008). Clinical symptoms of malaria become evident during parasite asexual replication during the blood stages of the parasite lifecycle (Absalon *et al*., 2016; Srinivasan *et al*., 2017). Thus, an individual infected with malaria only realises that infection has begun when they experience symptoms associated with the blood stage. New

drug targets and an effective vaccine would help prevent malaria, provide new treatments to bypass parasite drug resistance, and possibly eradicate malaria in the long-term.

1.2 Malaria transmission and control

The *Plasmodium* parasites are transmitted by female *Anopheles* mosquitoes (Birkett, 2016; Gardner *et al*., 2002). Transmission of *P. knowlesi* occurs zoonotically from infected macaques to humans (Singh *et al*., 2004), although human to human transmission of *P. knowlesi* is uncommon (Beeson *et al*., 2016). Transmission of malaria can occur through blood transfusions, although this is not common (Muerhoff *et al*., 2010). Prevention of malaria transmission would require eradication of all parasites in a community (Targett and Greenwood, 2008).

Malaria persists, despite efforts to eradicate and control the spread of the disease (Gardner *et al.,* 2002). Control measures include the use of insecticide residual spraying (Sharp *et al*., 2007) and insecticide-treated bed nets, improved accessibility to diagnosis of the early stages of infection, and effective malaria drug combination therapy with artemisinin (Beeson *et al.,* 2016). Interruption of the parasite lifecycle as a malaria control measure would require control of the mosquito vector. The possibility of transgenically producing male-only offspring in *Anopheles* mosquitoes for malaria control programs is being explored (Krzywinska *et al.,* 2016).

1.3 The *Plasmodium falciparum* parasite

The genome of *P. falciparum* is rich in adenine and thymine residues, which contribute to approximately 82% of the genome (Weber, 1987). The *P. falciparum* genome comprises 23 megabases, condensed into 14 chromosomes (Gardner *et al*., 2002), and a total of 5,369 proteins are expressed (www.uniprot.org). Whilst the genome of *P. falciparum* has been completely sequenced (Gardner *et al*., 2002), there are still many proteins expressed by the parasite that has not yet been characterised (Florens *et al*., 2002). Determining the roles of these proteins will greatly expand the understanding of parasite biochemistry and the pathways enabling the parasite to develop drug resistance and evade host immune responses. Analysis of the parasite proteome may help identify prospective malaria vaccine candidates and new drug targets.

In 2017, there were 219 million reported cases of malaria, and 435 000 documented deaths related to malaria (WHO, 2018). Approximately 99% of malaria cases in Africa were caused by *P. falciparum* infections (WHO, 2018). This may be due to the capacity of *P. falciparum* to cause severe malaria, as well as limited access to diagnosis and treatment in Africa.

1.4 The lifecycle of *Plasmodium* parasites

The complex lifecycle of *P. falciparum* is characterised by an exogenous sexual stage within an *Anopheles* mosquito, and a liver and blood stage in a human host (Florens *et al*., 2002; Antinori *et al*., 2012), depicted in Figure 1.1 (Bousema *et al*., 2014). The antigens of interest that have been studied as potential vaccine candidates will be identified at the individual stages of the parasite lifecycle. These malaria vaccine candidates will be discussed further in Section 1.9.

1.4.1 The sporozoite stage of the *Plasmodium* lifecycle

During a blood meal, sporozoites pass from the salivary glands of an infected mosquito through the dermis of the human host (Krettli and Miller, 2001). Once in the host, sporozoites travel via the bloodstream to the liver, where they invade hepatocytes (Todryk and Walther, 2005) and develop into tissue schizonts (Antinori *et al*., 2012). Mature schizonts contain numerous merozoites which rupture from the hepatocytes and enter the bloodstream. Notable sporozoite antigens are the circumsporozoite protein (CSP) and the liver-stage antigen-1 (LSA-1). CSP in the form of the RTS,S vaccine is being evaluated as a malaria vaccine candidate (Khan *et al*., 2019; Hill, 2011; Targett and Greenwood, 2008).

1.4.2 The merozoite stage of the *Plasmodium* lifecycle

The merozoite stage invades red blood cells and undergoes asexual replication. Within the host red blood cells, the parasites enter a 48-hour cycle of asexual replication and division (Boyle *et al*., 2013; van Dooren *et al.,* 2005), during which they mature into ring, trophozoites and blood schizonts. Mature blood schizonts rupture, releasing merozoites that begin a new cycle of red blood cell invasion. Merozoite antigens of interest for malaria vaccine development include merozoite surface protein (MSP) -1, -2 and -3, apical membrane antigen-1 (AMA-1), reticulocyte-binding homologue 5 (RH5) and glutamate-rich protein (GLURP) (Todryk and Walther, 2005).

1.4.3 The ring stage of the *Plasmodium* lifecycle

The merozoite matures into the ring stage which has minimal biosynthetic and metabolic activity (Hawthorne *et al*., 2004). As the ring stage matures, the parasite becomes larger and comprises multiple organelles (Kozicki *et al*., 2015). Haemoglobin is catabolised by haemoglobinases (Xie *et al*., 2016) into heme, which is then transformed into brown haemozoin crystals (Bannister *et al*., 2000). Formation of haemozoin signals the conversion of the ring stage to the trophozoite stage (Kozicki *et al*., 2015). The ring-infected erythrocyte surface

antigen (RESA) is a malaria vaccine candidate expressed at this stage (Bozdech *et al*., 2003b; Newton *et al*., 2001; Brown *et al*., 1985).

1.4.4 The trophozoite stage of the *Plasmodium* lifecycle

The trophozoite stage is characterised by high concentrations of nucleic acids and increased metabolism of haemoglobin and nutrients from the erythrocyte cytoplasm (Dekel *et al*., 2017; Bozdech *et al*., 2003a; Bozdech *et al*., 2003b; Florens *et al*., 2002; Francis *et al*., 1997). Increased synthesis of ribosomes in the cytoplasm and swift development of parasite organelles is observed (Bozdech *et al.,* 2003a). This stage of the lifecycle is committed to cellular division (Bozdech *et al*., 2003a ; Florens *et al*., 2002). From the trophozoite stage of the lifecycle, the trophozoite exported protein-1 (Tex-1) is being evaluated as a potential vaccine candidate (Tiendrebeogo *et al*., 2019; Kulangara *et al*., 2012).

1.4.5 The schizont stage of the *Plasmodium* lifecycle

The schizont stage of the parasite lifecycle occurs in both the liver (tissue schizont) (Soulard *et al*., 2015) and the blood stages (blood schizont) (Bannister *et al*., 2000). The primary function of the schizont stage is for the maturation of merozoites (Bozdech *et al*., 2003a). Within the parasitophorous vacuole in infected red blood cells, newly synthesised DNA aggregates and forms nuclei (Bozdech *et al.,* 2003a; Bannister *et al.,* 2000). Exhaustion of haemoglobin and subsequent crystallization of haemozoin is associated with this stage (Bannister *et al*., 2000). Clusters of large lipid vacuoles are reserved, to be used later for membrane formation (Bannister *et al*., 2000). Organelles are subdivided into segments within the schizont, for subsequent merozoite development in a controlled series of steps (Bannister *et al*., 2000). Mature schizonts contain merozoites that rupture out of the parasitophorous vacuole membrane and the erythrocyte membrane to invade and replicate in new red blood cells (Soulard *et al*., 2015; Bozdech *et al*., 2003a).

1.4.6 The gametocyte stage of the *Plasmodium* lifecycle

After the blood stage cycle is repeated several times, a portion of the merozoites differentiates into male and female gametocytes (Miller *et al*., 2013). Gametocytes undergo five stages of maturation. The bone marrow is enriched for early gametocyte development (Joice *et al*., 2014) and only the stage V gametocytes circulate in the blood. Gametocytes are ingested by mosquitoes during feeding.

Upon entry into the mosquito midgut, the development of gametes from the ingested gametocytes begins as a response to a change in several environmental factors (Kuehn and Pradel, 2010). These include the change in host body temperature and secretion xanthurenic acid (Kuehn and Pradel, 2010). In the mosquito midgut, fertilization of gametes results in

zygotes that mature into ookinetes. The ookinete leaves the mid-gut lumen enclosed in a membrane, forming an oocyst. The oocyst ruptures as it leaves the mid-gut lumen, releasing sporozoites that invade the salivary glands (Dhangadamajhi *et al*., 2010). Transmission to the next host occurs at the mosquito's next blood meal. The gametocyte surface antigens *Pf*s230 and *Pf*s48/45 (Kapulu *et al*., 2015) are potential transmission-blocking vaccine candidates. In the mosquito midgut, *Pf*s25 is expressed in the developing parasites (Barr *et al*., 1991).

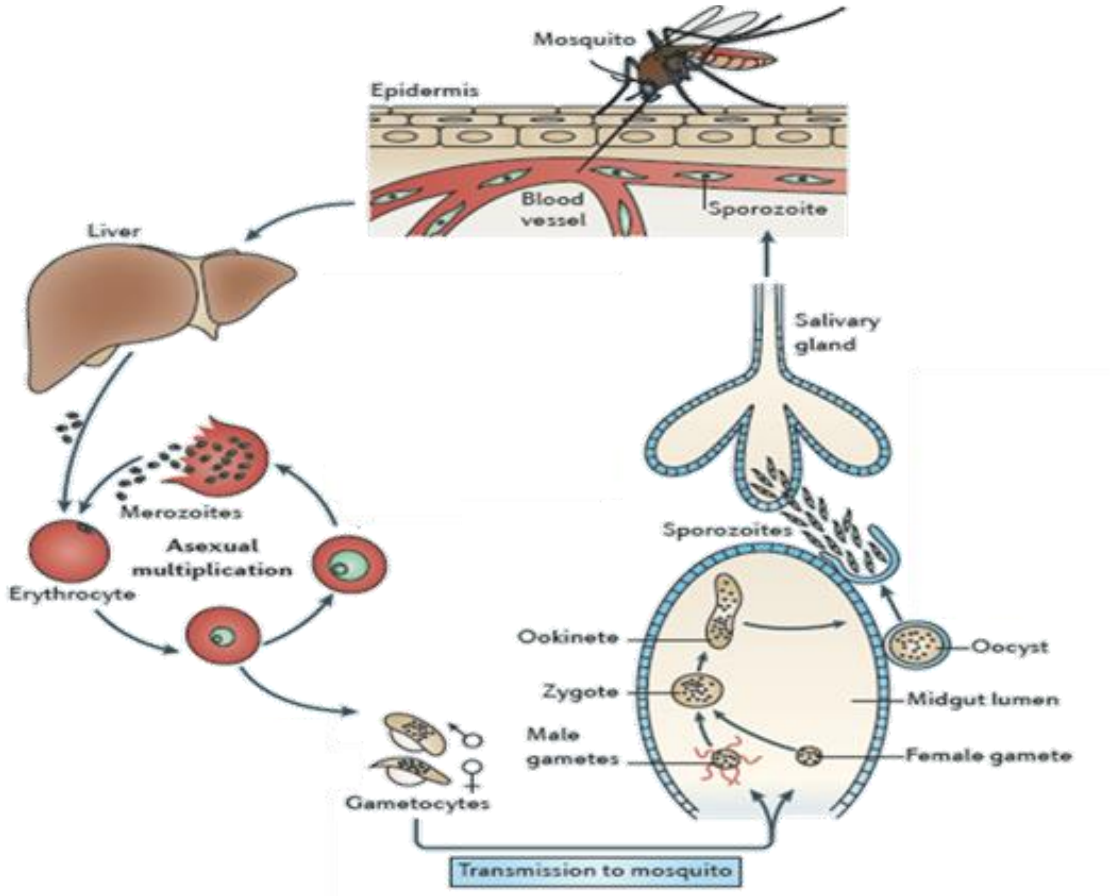

Figure 1.1: Lifecycle of *Plasmodium falciparum* in *Anopheline* and human hosts. The human host is infected with sporozoites during a blood meal by an infected female *Anopheles* mosquito. Sporozoites flow through the bloodstream and enter the liver cells, where they mature into a tissue schizont containing merozoites. Merozoites are released into the bloodstream where they begin a cycle of asexual replication. A portion of the merozoites will undergo sexual replication to produce gametocytes, which are transmitted to mosquitoes upon consumption of a blood meal. Within the midgut of the mosquito, gametocytes mature into sporozoites. These sporozoites invade the mosquito salivary glands and are then able to infect a host. Adapted from Bousema *et al*. (2014).

1.5 Severe malaria

Severe malaria is typically caused by *P. falciparum*, however, *P. knowlesi*, and rarely, *P. vivax* and *P. ovale* have also been implicated (Barber *et al*., 2013; Fatih *et al*., 2012; William *et al*., 2011;Trampuz *et al*., 2003). Complications of severe malaria include cerebral malaria, renal failure, anaemia, hypoglycaemia and acidosis (Trampuz *et al*., 2003). Some of the clinical

presentations of severe malaria include a high fever, cerebral malaria, respiratory distress, multi-organ failure, vascular obstructions, severe anaemia and metabolic acidosis (Craig *et al*., 2012). Respiratory distress or impaired consciousness were identified as indicators for high risk of malaria-associated mortality in African children (Marsh *et al*., 1995).

Cytoadherence of *P. falciparum*-infected red blood cells contribute to sequestration in major organs (Rowe *et al*., 2009; Craig *et al*., 2012). The *P. falciparum* erythrocyte membrane protein-1 (*Pf*EMP-1) family of proteins are ligands expressed on the surface of infected red blood cells. Binding of *Pf*EMP-1 proteins to CD36, chondroitin sulfate A (CSA) and intracellular adhesion molecule-1 receptors on the surface of endothelial cells, placenta and the brain respectively, has been associated with of severe malaria (Pehrson *et al*., 2016; Turner *et al*., 2013; Patel *et al*., 2004).

Cerebral malaria is characterised by a coma associated with a *Plasmodium* infection. Haemorrhage and lesions on the brain and sequestration of infected red blood cells was detected post-mortem in cerebral malaria patients (Storm and Craig, 2014). The exact mechanism for the development of cerebral malaria is unknown (Storm and Craig, 2014).

1.6 Malaria diagnostic tests

The correct diagnosis of malaria, particularly in underdeveloped subtropical rural areas, is imperative for the proper course of treatment to be followed. Malaria symptoms are often flu-like, and fevers may be misdiagnosed as dengue, typhoid or other fever-associated tropical diseases. Because *P. falciparum* malaria may become severe or progress to cerebral malaria, it is critical to correctly diagnose the infective *Plasmodial* species.

Microscopy and rapid diagnostic tests are the most widely used malaria diagnostic tools (Kho *et al*., 2016). Polymerase chain reaction analysis, loop-mediated isothermal amplification and enzyme-linked immunosorbent assays are also used for malaria diagnosis.

1.6.1 Microscopy for malaria diagnosis

Microscopic examination of Giemsa-stained blood smears for malaria diagnosis is regarded as the “gold-standard” against which other malaria diagnostic methods are compared (Wongsrichanalai *et al*., 2007). The Giemsa stain differentially stains the nucleus of cells. Red blood cells are devoid of a nucleus, thus parasite-infected red blood cells are easily distinguished from uninfected red blood cells (Dekel *et al*., 2017). Thick blood films are more sensitive for the detection of low levels of parasitaemia, and thin blood films allow for species differentiation (Moody, 2002). However, very low parasitaemia or mixed infections where the parasite species’ morphology is similar may not always be detected (; Mahende *et al*., 2016; Chew *et al*., 2012; Noedl *et al*., 2006).

1.6.2 Rapid diagnostic tests for the detection of malaria

The rapid diagnostic test (RDT) is one of the major malaria diagnostic tools used in underdeveloped areas and is designed to detect infections within approximately 15 minutes. The RDT comprises an immunochromatographic test strip impregnated with colloidal-gold coupled monoclonal antibodies against key malaria proteins (Maltha *et al*., 2013). The blood sample is applied to the test strip and flows across the strip by capillary action. A control line indicates that the blood has flowed across the test strip. In addition to the control line, a coloured line where the gold labelled antibodies complexed with a malaria antigen is captured indicates a malaria infection (Davis *et al.,* 2014; Maltha *et al*., 2013). Malaria antigens used in RDTs include the parasite-specific glycolytic enzymes aldolase and lactate dehydrogenase (LDH), and the *P. falciparum*-unique blood stage protein histidine-rich protein 2 (HRP-2) (Moody, 2002). The thioredoxin peroxidase 1 protein is a conserved blood stage *Plasmodium* protein and has recently been evaluated as a potential diagnostic target (Hakimi *et al*., 2015).

The urine malaria test is a non-invasive RDT used to detect a *P. falciparum* infection (Oyibo *et al*., 2017). Similar to RDTs that test blood, the urine malaria test detects HRP-2 in urine with recombinant monoclonal anti-HRP-2 antibodies on an immunochromatographic test strip in the form of a dipstick (Oyibo *et al*., 2017; Oguonu *et al*., 2014).

Diagnostic tests that detect HRP-2 are able to distinguish *P. falciparum* infections from other infecting species, and treatment or further testing can be managed accordingly. However, HRP-2 persists in the body fluids including blood and urine after an infection has cleared, and this could lead to false positives (Mahende *et al.,* 2016).

1.6.3 Polymerase chain reaction detection and diagnosis of malaria

Polymerase chain reaction (PCR) is a method that is more sensitive than microscopy and can detect mixed infections (Moody, 2002; Johnston *et al*., 2006). Real-time and conventional PCR assays have been developed for the identification and differentiation of *Plasmodium* species (Johnston *et al*., 2006). Genes encoding the small-subunit 18S rRNA and circumsporozoite proteins have been used to distinguish between the different *Plasmodial* species (Moody, 2002), using parasite-specific primers (Snounou *et al*., 1993). Despite its sensitivity and specificity, PCR is an expensive procedure requiring specialised equipment, trained personnel, adequate time to process samples, and stable reagents. This prevents the test from being useful in rural settings (Mahende *et al*., 2016).

1.6.4 Loop-mediated isothermal amplification for detection and diagnosis of malaria

The loop-mediated isothermal amplification (LAMP) technique is based on the amplification of nucleic acids at a constant temperature (Notomi *et al*., 2000). The LAMP diagnostic test

detects a malaria infection by amplifying *Plasmodium*-specific genes (Poon *et al*., 2006; Ocker *et al*., 2016). For the detection of a *Plasmodium* infection, the 18S rRNA gene is amplified using species-specific primers (Poon *et al*., 2006). There are several advantages of using LAMP over PCR, including the simplicity and cost of the test, the time required, and the DNA does not have to be purified first (Poon *et al*., 2006). However, the PCR remains more sensitive and specific for the detection of *Plasmodium* infections (Poon *et al*., 2006; Ocker *et al*., 2016). LAMP may detect asymptomatic malaria where an RDT may not (Cook *et al*., 2015).

1.6.5 Enzyme-linked immunosorbent assay to detect malaria

The enzyme-linked immunosorbent assay (ELISA) employs the use of enzyme-linked antibodies to detect malaria antigens. *Plasmodium* LDH (Nambati *et al*., 2018) is used for malaria diagnosis, and detection of HRP-2 is specific for *P. falciparum* (Gibson *et al*., 2017). Similar to PCR, an HRP-2 based ELISA was shown to be more sensitive than microscopy (Noedl *et al*., 2006). However, the cost of antibodies, time, expertise required, and the stability of reagents involved make ELISA a problematic method for malaria diagnosis under field conditions. The ELISA is better suited to laboratories analysing numerous samples for research purposes.

1.7 Antimalarial drugs

Many therapeutic drugs are available to treat malaria infections. Most drugs target the asexual blood stage (Bousema *et al*., 2006). Antimalarial drugs such as mefloquine are often used as prophylaxis before an individual enters a malaria endemic area (Steffen *et al*., 1993). Combination therapy with artemisinin and another antimalarial drug helps prevent recrudescence and combats antimalarial drug resistance (Bousema *et al*., 2006; Nandakumar *et al*., 2006). Malaria may also be treated symptomatically to aid patient comfort.

Antimalarial drug treatment is an effective mechanism for malaria control. However, *Plasmodium* parasites are developing resistance to frontline drugs including artemisinin, chloroquine, mefloquine, quinine, sulfadoxine-pyrimethamine and others (Fairhurst and Dondorp, 2016; Achan *et al*., 2011; Gatton *et al*., 2004; Wellems and Plowe, 2001; Nosten *et al*., 1996). Resistance to various artemisinin-combination therapies is prevalent in Southeast Asia (Fairhurst and Dondorp, 2016).

1.8 Survival of *Plasmodium* within a host

Plasmodium parasites have developed mechanisms to evade the host immune system to avoid clearance by antibodies, phagocytic cells or the spleen (Kyes *et al*., 2001). During the liver stage, the parasite envelopes itself in a parasitophorous vacuole, which protects it from host-cell proteolytic degradation (Vaughan *et al*., 2010). *P. vivax* and *P. ovale* produce dormant

hypnozoites which can revive many years later and introduce reinfection, (Beeson *et al*., 2016; Bartoloni and Zammarchi, 2012; Wipasa *et al*., 2002).

Sequestration and cytoadherence of *Plasmodium*-infected red blood cells in the organs prevent splenic clearance (Turner *et al*., 2013). The *Pf*EMP-1 family of proteins is implicated, and are capable of antigenic variation, weakening the ability of the host to clear parasitaemia (Scherf *et al*., 2008).

Plasmodium-infected mosquitoes retain higher levels of glycogen for energy storage. Infected mosquitoes increase food intake and survive better under starvation conditions compared to uninfected mosquitoes (Zhao *et al.*, 2012).

1.9 Malaria vaccines

An effective malaria vaccine should provide long-lasting protection and prevent transmission to mosquitoes (Ishizuka *et al*., 2016; Targett and Greenwood, 2008; Sinigaglia *et al*., 1988). Such a vaccine should be directed against a protein or region of a protein that is conserved within the parasite and should therefore elicit an immune response in all immunized individuals, and stimulate both B-cell and T-cell responses (Sinigaglia *et al*., 1988). There is currently no licensed malaria vaccine approved for use by the World Health Organization (WHO, 2018). The availability of an effective vaccine against malaria would help prevent infection in malaria-endemic areas, circumvent the spread of the disease, and decrease the mortality rate caused by the disease.

There is an urgent need for an effective malaria vaccine. Parasite resistance to many antimalarial drugs and artemisinin combination therapy has developed and is spreading (Pavadai *et al*., 2016). *Anopheles* mosquitoes are becoming increasingly resistant to insecticides (Beeson *et al*., 2016; Gardner *et al*., 2002).

1.9.1 Pre-erythrocytic stage vaccines

Vaccines formulated against the pre-erythrocytic liver stage are designed to prevent parasite invasion of the red blood cells (Targett and Greenwood, 2008). During the liver stage, there is a lower parasitaemia, and sufficient time for an active immune system to clear the parasitaemia (Dundas *et al*., 2018). Antigens used in the development of malaria vaccines targeting the pre-erythrocytic stage include the circumsporozoite protein and RTS,S vaccine, liver stage antigen-1, sporozoite surface protein, and attenuated sporozoites. These antigens have been shown to induce weak antibody, CD4+ and CD8+ T-cell responses (Trieu *et al*., 2011).

1.9.1.1 Circumsporozoite protein and the RTS,S malaria vaccine

The circumsporozoite protein (CSP) is a well-conserved protein and is the major coat protein of sporozoites (Coppi *et al*., 2005). The structure of CSP is comprised of a central

NANP repeat region flanked by an N- and C-terminus (Plassmeyer *et al*., 2009). Peptides derived from the NANP-repeat region of the CSP protein were chosen as a target for vaccine development, as the peptides were shown to elicit sporozoite-deactivating antibodies (Egan *et al*., 1987).

Mice immunized with full-length CSP were able to elicit strong immune responses against challenge infection and were protected (Espinosa *et al*., 2017). However, it was shown that progression to the blood stage of development circumvents the immune response against CSP (Keitany *et al*., 2016).

The RTS,S vaccine is made up of the NANP tandem-repeat tetrapeptide (R) and T-cell epitopes from the C-terminal region of CSP (T), fused to the hepatitis B surface antigen (S) and unfused S-antigen (S) (Hill, 2011; Targett and Greenwood, 2008).

Early studies of the RTS,S vaccine showed that it was able to protect against a challenge malaria infection (Stoute *et al*., 1997). The RTS,S vaccine is capable of eliciting high concentrations of antibodies against the conserved NANP repeat region, which may be able to clear sporozoites before liver cell invasion, and moderate T-cell immunogenicity (Hill, 2011). However, this vaccine candidate has not demonstrated sufficient long-term protection against a challenge malarial infection (Gosling and von Seidlein, 2016). In a phase III clinical trial, the RTS,S vaccine was more efficient when a booster dose was included for African infants (RTS,S Clinical Trial Partnership, 2015). Due to the short-term efficacy of this vaccine, it has been suggested that it may be used in future strategies to prevent transmission by vaccinating people who are at high risk of contracting malaria (Gosling and von Seidlein, 2016). Protection by this vaccine appears to be mediated by IgG_1 and IgG_3 antibodies raised against the C-terminus of CSP and NANP (Ubillos *et al*., 2018).

1.9.1.2 Liver stage antigen-1

The liver stage antigen-1 (LSA-1) is expressed during the sporozoite stage of the *P. falciparum* life cycle (Zhu and Hollingdale, 1991). LSA-1 localises to the parasitophorous vacuole, and is composed of conserved non-repeat N- and C- terminal regions, and 17-mer repeat regions (Hollingdale *et al*., 1990; Zhu and Hollingdale, 1991). LSA-1 is a conserved *P. falciparum* protein able to produce B- and T-cell responses (Fidock *et al*., 1994; Kurtis *et al*., 2001).

In a pre-clinical trial conducted in rhesus monkeys, LSA-1 induced IFNɣ- and IL-2-secreting CD4+ T-cells. This vaccine was deemed safe to administer on its own, or in conjunction with the RTS,S vaccine (Pichyangkul *et al*., 2007). In a clinical trial, volunteers immunized with low doses of LSA-1 were able to produce higher quantities of IFNɣ- and IL-2-secreting CD4+

T-cells than high doses. However, regardless of dose and adjuvant used, this vaccine did not protect individuals from a challenge infection (Cummings *et al*., 2010).

Falciparum malaria protein 011 (FMP011) is a 54 kDa protein derived from LSA-1 and encodes the N- and C-terminal peptides, and two 17-mer repeat units that vary slightly (Brando *et al*., 2007). A pre-clinical trial in mice showed that FMP011 was a promising malaria vaccine candidate due to its ability to stimulate antibody responses and IFNɣ secreted by CD4+ T-cells (Brando *et al*., 2007; Hillier *et al*., 2005). However, in a different strain of mice, minimal cellular and humoral responses were observed (Brando *et al*., 2007). Curiously, no LSA-1 homologue is found in *Plasmodium* species infecting monkeys or mice (Kurtis *et al*., 2001).

1.9.1.3 Sporozoite surface protein/thrombospondin related anonymous protein

Sporozoite surface protein-2, also known as thrombospondin related anonymous protein (TRAP) facilitates invasion of liver cells (Labaied *et al*., 2007). Host cell integrins were shown to interact directly with TRAP (Dundas *et al*., 2018).

CD8+ T-cell activity is associated with protection in mice and humans by TRAP in attenuated sporozoites and viral vector systems (Bliss *et al*., 2017; Ewer *et al*., 2013; Khusmith *et al*., 1994). Clinical trials evaluating viral-vectored TRAP with multiple epitopes elicited strong immune responses in African adults and children (Bliss *et al*., 2017; Ogwang *et al*., 2015). Immunization with TRAP in combination with the RTS,S vaccine was deemed safe and tolerable (Kester *et al*., 2014; Walsh *et al*., 2004). However, conflicting results were obtained regarding the value of the addition of TRAP to the RTS,S vaccine (Kester *et al*., 2014; Walsh *et al*., 2004).

1.9.1.4 Radiation attenuated sporozoites

Attenuation of live sporozoites may be achieved by radiation or genetic modification. Attenuation of sporozoites prevents their development, halting the lifecycle and preventing clinical manifestation of malaria (Lyke *et al*., 2017; Bijker *et al*., 2015).

Immunization with radiation attenuated sporozoites (RAS) produces mutant schizonts that cannot rupture to release invasive merozoites (Hill, 2011; Hoffman *et al*., 2002; Clyde *et al*., 1975; Nussenzweig *et al*., 1967). RAS produces antigens capable of stimulating an immune response (Hill, 2011). RAS were shown to confer sterile immunity, and protect volunteers from repeated challenge infection with nearly 100% efficacy (Lyke *et al*., 2017; Hoffman *et al*., 2002). *P. falciparum* RAS were shown to confer sterile protection mediated by IFNɣ-secreting T-cells, against homologous and heterologous controlled human malaria infections, (Lyke *et al*., 2017; Ishizuka *et al*., 2016). Antibodies, CD4+ and CD8+ T-cell responses against *Pf*CSP and *Pf*RAS antigens were correlated with protection (Seder *et al*., 2013). CD8+ T-cells are implicated in the removal of infected liver cells (Hill, 2011; Weiss *et al*., 1988).

The use of mosquitoes for RAS vaccine delivery proved to be unrealistic for conventional use (Hollingdale and Sedegah, 2016). Mosquito infection can only be confirmed after dissection of the salivary glands. It is debatable whether immunization with a needle and syringe can replace the salivary gland fluids of a mosquito to induce sufficient immunogenicity and efficiency in humans (Hill, 2011).

1.9.1.5 Genetically attenuated sporozoites

Genetic attenuation of sporozoites involves the selective knockout of genes that are associated with the development of liver stage parasites, generating mutants that are incapable of progressing to the blood stage (Bijker *et al*., 2015). Such genes include the P52, P36, sporozoite asparagine-rich protein-1, b9, and *slarp* (Mikolajczak *et al*., 2014; van Schaijk *et al*., 2014; Aly *et al*., 2008). Immunization with P52, P36, sporozoite asparagine-rich protein-1, b9 and *slarp* knockouts inhibited the parasites' ability to produce invasive merozoites (Mikolajczak *et al*., 2014; van Schaijk *et al*., 2014). Immunization with b9 and *slarp* knockout parasites resulted in complete protection from a homologous sporozoite challenge (van Schaijk *et al*., 2014). In a clinical study, P52 and P36 knockout parasites were able to confer complete sterile protection. Protection was mediated by IFNɣ and cytokine-secreting CD4+ and CD8+ T-cells (Spring *et al*., 2013).

In comparison to attenuated sporozoite approaches for a malaria vaccine, the RTS,S vaccine has failed to produce similar levels of protection against challenge malaria infections.

1.9.2 Malaria blood stage vaccines

In order to combat malaria-induced mortality and prevent the manifestation of clinical symptoms of malaria, blood stage vaccines were developed (Zhu *et al*., 2017). These vaccines are aimed at diminishing morbidity, mortality and the development of severe malaria (Lu *et al*., 2017; Thera *et al*., 2011; Ellis, *et al*., 2010; Goodman and Draper, 2010). Many of the blood stage vaccines comprise a protein antigen co-administered with an adjuvant intended to produce protective antibodies that impair parasite growth with or without other effector cells (Hill, 2011). Numerous blood-stage vaccines are based on the merozoite surface protein (MSP) and apical membrane antigen (AMA) (Hill, 2011). Other blood stage antigens include erythrocyte binding antigen (EBA), ring-infected erythrocyte surface antigen (RESA), reticulocyte-binding protein homolog (RH), glutamate-rich protein (GLURP), hypoxanthine-guanine-xanthine phosphoribosyltransferase (HGXPRT) and trophozoite exported protein (Tex). Three challenges have been encountered in the development of blood stage vaccines. Firstly, large quantities of the protein antigens may be difficult to express in the correct conformation. Secondly, only moderate antibody responses have been generated, even with

a range of adjuvants tested. Thirdly, the antigens may exhibit extensive polymorphism (Hill, 2011).

1.9.2.1 Apical membrane antigen

The apical membrane antigen-1 (AMA-1) protein is expressed in sporozoites and on the surface of merozoites and is possibly implicated in both liver and red blood cell invasion (Schussek *et al*., 2013; Silvie *et al*., 2004; Triglia *et al*., 2000). This vaccine candidate aims to induce high titres of growth inhibiting antibodies. The antibodies were shown to be strain-specific in rabbits and humans (Spiegel *et al*., 2017; Schussek *et al*., 2013; Malkin *et al*., 2005).

AMA-1 was able to provide sterile protection against challenge blood stage infections in mice (Schussek *et al*., 2013). Mice were protected from a homologous, but not heterologous blood-stage challenge infection when immunized with refolded AMA-1 (Crewther *et al*., 1996). Importantly, the data presented by Crewther *et al*. (1996) suggests that protection is conferred by the adjuvant alone; which contradicts what is stated in the document, as it is unlikely that immunization with adjuvant alone would result in protection from challenge infection.

Aotus vociferans monkeys were protected against challenge *P. falciparum* blood stage infection when immunized with the AMA-1 protein (Stowers *et al*., 2002). AMA-1 in combination with *Plasmodium* rhoptry neck protein 2 (RON-2) was protective against challenge blood stage infections in rats and *A. nancymae* monkeys (Srinivasan *et al*., 2017; Srinivasan *et al*., 2014). Superior protection was achieved with AMA-1/RON-2 compared to AMA-1 alone, although antibody titres were similar, suggesting protection is not mediated by antibodies alone (Srinivasan *et al*., 2017).

In a phase I clinical trial, AMA-1 formulated with Alhydrogel was shown to be safe and well tolerated (Malkin *et al*., 2005). Malaria naïve adults immunized with the AMA-1 ectodomain vaccine in different adjuvant systems were not protected against sporozoite challenge infection (Spring *et al*., 2009).

1.9.2.2 Merozoite surface protein

The merozoite surface protein-1 (MSP-1) protein is a conserved *Plasmodium* protein expressed on the surface of merozoites (Ling *et al*., 1994). The MSP-1 protein is approximately 200 kDa, which is cleaved into smaller fragments of 83 kDa, 28 – 30 kDa, 38 kDa and 42 kDa upon release into the blood (Holder *et al*., 1992). The 42 kDa C-terminal component ($MSP\text{-}1_{42}$) is further processed into a 33 kDa and a 19 kDa fragment ($MSP\text{-}1_{33}$ and $MSP\text{-}1_{19}$ respectively) (Holder *et al*., 1992). The $MSP\text{-}1_{19}$ fragment remains attached to the parasite membrane, and prompts an antibody response, whereas the $MSP\text{-}1_{33}$ contains T-cell epitopes (Pusic *et al*., 2011; O'Donnell *et al*., 2001; Holder *et al*., 1992). Correctly folded MSP-1 proteins are likely to be immunogenic (Ling *et al*., 1994).

Mice immunized with MSP-1_{19} were protected from a homologous challenge infection (Zhang *et al*., 2005; Ling *et al*., 1994). A heterologous immunization treatment using AMA-1 and MSP-1_{42} was able to protect *Aotus* monkeys from a challenge blood stage infection (Obaldia *et al*., 2017). MSP-1_{42} from the *P. falciparum* 3D7 and FVO strains was found to be safe and tolerable in a clinical trial. Serum antibodies raised against the recombinant refolded protein was able to recognise the native protein (Malkin *et al*., 2007). A phase IIb trial assessing MSP-1_{42} produced high titres of antibodies, which were not protective in children (Ogutu *et al*., 2009).

1.9.2.3 Erythrocyte binding antigen

Erythrocyte binding antigen (EBA) is a blood stage malaria vaccine candidate expressed in the merozoite stage of the parasite life cycle. The EBA-175 is a 175 kDa protein that has been implicated in the invasion of red blood cells by binding sialic acid on glycophorin A (Camus and Hadley, 1985).

Mice immunized with the conserved N-terminus of EBA-175 developed a robust antibody response that prevented parasite invasion of red blood cells (Pattnaik *et al*., 2007). Blood stage challenge of *A. nancymae* monkeys immunized with EBA-175 region II resulted in lower parasitaemia compared to the control group, most notably in monkeys immunized with a regimen including both plasmid DNA and protein (Jones *et al*., 2001). Higher titres of antibodies were elicited in monkeys immunized with the protein compared to immunization with plasmid DNA or a regimen of both (Jones *et al*., 2001). Non-glycosylated EBA-175 region II was evaluated in phase I clinical trials and was found to be safe and immunogenic in healthy malaria-naïve adults (El Sahly *et al*., 2010). Antibodies raised against EBA-175 region II in a phase Ia clinical trial in semi-immune individuals were able to prevent parasite growth *in vitro* (Koram *et al*., 2016).

1.9.2.4 Glutamate-rich protein

The glutamate-rich protein (GLURP) is a conserved, immunogenic protein expressed during the liver and blood stages of the *Plasmodium* life cycle (Borre *et al*., 1991). The composition of GLURP is made up of a central repeat region flanked by an N-terminal non-repeat region and an immunogenic C-terminal repeat region (Theisen *et al*., 1995).

A synthetic peptide derived from GLURP was evaluated in a phase I clinical trial, and was shown to have some adverse effects, while stimulating antibodies that are capable of inhibiting *in vitro* parasite growth (Hermsen, *et al*., 2007). The carboxy terminus was found to be the most antigenic region in Liberian individuals and was shown to be immunogenic in mice (Theisen *et al*., 1995). A correlation was observed between protection against malaria infection

and cytophilic antibodies against GLURP in Ghana, Burkina Faso and Myanmar (Meraldi *et al*., 2004; Soe *et al*., 2004; Dodoo *et al*., 2000).

1.9.2.5 Hypoxanthine-guanine-xanthine phosphoribosyltransferase

The hypoxanthine-guanine-xanthine phosphoribosyltransferase (HGXPRT) enzyme is involved in the purine salvage pathway. HGXPRT is a tetrameric enzyme that catalyses the conversion of hypoxanthine to inosine 5'-monophosphate, guanine to guanosine 5'-monophosphate and xanthine to xanthosine 5'-monophosphate (Mbewe *et al*., 2007; Belen Cassera *et al*., 2011). The enzyme appears to be vital for *Plasmodium* parasite survival, as parasites do not produce nucleotides by the *de novo* pathway (Mbewe *et al*., 2007). *Plasmodium* HGXPRT was found in both the parasite and infected red blood cell cytoplasm (Shahabuddin *et al*., 1992).

Immunization with *P. falciparum* HGXPRT was shown to stimulate a T-cell response associated with protection in mice (Makobongo *et al*., 2003). HGXPRT is immunogenic in humans, stimulating *in vitro* T-cell proliferation in individuals naturally exposed to malaria (Woodberry *et al*., 2009). Antibodies against HGXPRT were not detected (Woodberry *et al*., 2009).

However, *Plasmodium* HGXPRT is homologous to human HGPRT (Good and Doolan, 2010; Makobongo *et al*., 2003). This means that the number of people responding to the vaccine, and generating an immune response could be limited (Good and Doolan, 2010).

1.9.2.6 Reticulocyte-binding protein homolog 5

The reticulocyte-binding protein homolog 5 (RH5) antigen is a well-conserved protein expressed on the rhoptries at the parasite apex, and is involved in red blood cell invasion (Rodriguez *et al*., 2008; Baum *et al*., 2009). Antibodies directed against RH5 prevents parasite invasion of red blood cells *in vitro* (Bustamante *et al*., 2013; Baum *et al*., 2009). Mouse monoclonal antibodies raised against RH5 was able to prevent parasite invasion of red blood cells (Ord *et al*., 2014). *A. nancymae* monkeys were protected from a *P. falciparum* challenge infection after immunization with RH5, and protection was associated with a strong antibody response (Douglas *et al*., 2015). In a phase Ia clinical trial, a robust antibody response was rasied against the RH5 protein, and these antibodies were also shown to inhibit *Plasmodium* parasite growth *in vitro.* The vaccine was safe and well tolerated (Payne *et al*., 2017). For protection, it is suggested that the conformation of the protein is critical (Bustamante *et al*., 2013).

1.9.2.7 Ring-infected erythrocyte surface antigen

The ring-infected erythrocyte surface antigen (RESA) is expressed during the late schizont stage, and at the infected red blood cell membrane during the ring stage (Brown *et al*., 1985; Coppel *et al*., 1984). This protein was found to have regions of repetitive amino acid sequences (Coppel *et al*., 1984).

Immunization of Peruvian *Aotus* monkeys with the RESA repeat regions elicited high titres of antibodies associated with protection against a *P. falciparum* blood stage challenge (Collins *et al*., 1986). In young Gambian children, an association between resistance to clinical malaria and antibodies against the tetrapeptide repeat region was observed (Riley *et al*., 1991). Antibodies raised against a RESA octapeptide experimentally in rabbits and naturally in humans was able to prevent *P. falciparum* merozoite invasion of red blood cells *in vitro* (Berzins *et al*., 1986). However, the RESA protein is no longer considered a malaria vaccine candidate.

1.9.2.8 Trophozoite exported protein 1

Trophozoite exported protein 1 (Tex-1) is expressed during the blood stages of the parasite lifecycle, and its expression is significantly upregulated during the trophozoite stage (Kulangara *et al*., 2012). Tex-1 is expressed as a soluble protein in the cytoplasm, before becoming bound to the Maurer's Cleft membrane during the trophozoite stage (Kulangara *et al*., 2012). The P27 antigen is conserved and is found at the C-terminus of Tex-1, and is one of three alpha-helical coiled-coil domains (Kulangara *et al*., 2012; Villard *et al*., 2007). The second antigen identified within the Tex-1 protein is the N-terminal P27A fragment and is predicted to be intrinsically unstructured (Kulangara *et al*., 2012). Nanoparticle delivery of the P27 and P27A fragments were shown to be immunogenic in mice, both as individual proteins and as a combination (Karch *et al*., 2017). These nanoparticles were recognised by serum antibodies present in individuals from Burkina Faso (Karch *et al*., 2017). The P27A antigen has been evaluated in a phase I clinical trial (Steiner-Monard *et al*., 2018). The vaccine was safe and tolerable, and stimulated a strong antibody response that inhibited parasite invasion in red blood cells (Steiner-Monard *et al*., 2018).

1.9.2.9 Whole parasite blood stage vaccine

Immunization with whole blood stage parasites allows for the exposure of the host to multiple antigens. Such vaccinations may be with killed or live attenuated parasites (Stanisic and Good, 2015). Problems often encountered with whole parasite vaccines include their synthesis, storage and safety (Giddam *et al*., 2016).

Low doses of killed *P. chabaudi chabaudi AS* parasites were able to protect mice from a lethal blood stage challenge (Pinzon-Charry *et al*., 2010). Internalization of killed blood stage

parasites in liposomes was tested as an alternative vaccine delivery in mice. Mice immunized with these parasite-containing liposomes survived blood stage challenge and had a low parasite burden (Giddam *et al*., 2016).

Varying degrees of protection against homologous and heterologous challenge was observed in mice immunized with killed blood stage parasites (McColm and Dalton, 1983). *A. trivirgatus* monkeys immunized with mature merozoites were protected from a *P. falciparum* challenge infection (Siddiqui, 1977).

In a clinical study, immunity against *P. falciparum* was established by immunization with ultra-low doses of live *P. falciparum*-infected red blood cells (Pombo *et al*., 2002). *In vitro* analyses indicated protection was mediated by parasite-specific CD4+ T-cell responses. A CD8+ T-cell response and upregulation of IFNɣ secretion was also prevalent, with minimal parasite-specific antibody response in all volunteers (Pombo *et al*., 2002).

1.9.3 Transmission blocking vaccines

Transmission blocking vaccines are based on the sexual stages of the *Plasmodium* lifecycle. Vaccination of individuals against the sexual stages of the parasite lifecycle would not necessarily prevent clinical manifestation of malaria. Transmission blocking vaccines prevent parasite development in the mosquito midgut and hence blocks transmission (Moorthy *et al*., 2004).

1.9.3.1 The *Pf*s25 antigen

*Pf*s25 is expressed on the surface of *P. falciparum* zygotes and ookinetes in the mosquito midgut (Barr *et al*., 1991; Kaslow *et al*., 1988). *Pf*s25 is capable of inducing a strong antibody response in mice (Radtke *et al*., 2017; Goodman, *et al*., 2011). In one study, mosquitoes were fed red blood cells containing gametocytes, combined with *Pf*s25 immune sera from mice and monkeys (Barr *et al*., 1991). The antibodies from monkeys and mice inhibited the development of oocysts in the mosquitoes (Kapulu *et al*., 2015; Farrance *et al*., 2011a; Barr *et al*., 1991).

Systemic adverse events were observed in a phase Ia clinical trial evaluating *Pf*s25 and *P. vivax Pv*s25 as vaccines (Wu *et al*., 2008). Evaluation of *Pf*s25 coupled to *Pseudomonas aeruginosa* ExoProtein A in a phase I clinical trial showed that it was relatively safe. High titres of anti-*Pf*s25 antibodies were raised and were associated with transmission blocking activity (Talaat *et al*., 2016). This suggests that the *Pf*s25 vaccine may be developed further.

1.9.3.2 The *Pf*s48/45 antigen

*Pf*s48/45 is expressed on the surface of *Plasmodium* gametocytes within the blood of a human host (Kapulu *et al*., 2015). The conformation of the *Pf*s48/45 antigen was shown to be important for transmission blocking activity (Milek *et al*., 1998). It is possible to synthesise

correctly folded *Pf*s48/45 that is capable of stimulating transmission blocking antigen-specific antibodies in mice and *Papio Anubis* baboons (Chowdhury *et al*., 2009; Outchkorov *et al*., 2008). This protein has potential for evaluation in a clinical trial (Theisen *et al*., 2017).

1.9.3.3 The *Pf*s230 antigen

*Pf*s230 is expressed on the surface of *Plasmodium* gametocytes within the human host and has a 6-cysteine-rich domain in its structure (MacDonald *et al*., 2016; Kapulu *et al*., 2015). Antibodies raised in mice against a region of the *Pf*s230 protein were shown to block transmission to mosquitoes (Kapulu *et al*., 2015). Rabbits immunized with a *Pf*s230 construct were able to produce a strong antibody response capable of preventing transmission (MacDonald *et al*., 2016; Farrance *et al*., 2011b). A clinical trial of the *Pf*s230 protein is yet to be evaluated as a malaria vaccine (MacDonald *et al*., 2016).

1.9.4 Multi subunit vaccines

Multi-subunit vaccines use more than one antigen, sometimes from different stages, or include multiple antigens from the same stage. By including antigens from different stages of the parasite lifecycle in a multi-subunit vaccine the immune system is primed against these stages.

1.9.4.1 NYVAC-*Pf*7 vaccine

The NYVAC-*Pf*7 malaria vaccine is composed of the sporozoite antigens CSP and sporozoite surface protein-2, LSA-1 from the liver, AMA-1, MSP-1 and serine repeat antigen from the merozoite, and the sexual stage *Pf*s25 antigen (Tine *et al*., 1996). This vaccine was safe and well tolerated in monkeys and humans (Ockenhouse *et al*., 1998; Tine *et al*., 1996). Clinical trial evaluation of NYVAC-*Pf*7 demonstrated that this vaccine was capable of completely protecting one individual from a challenge infection (Ockenhouse *et al*., 1998). A weak antibody, but strong cellular response was observed (Ockenhouse *et al*., 1998). The antibody response was enhanced in mice primed by immunization with *Plasmodium* antigen-encoding plasmid DNA, when followed by boosting with NYVAC-*Pf*7 (Sedegah *et al*., 2004).

1.9.4.2 Multi-antigen peptide vaccines

Mouse antibodies raised against three *P. falciparum* multiple-antigen peptide (MAP) constructs were evaluated. MAP-1 consisted of epitopes from CSP. MAP-2 contained epitopes from CSP, LSA-1, MSP-1_{42} and MSP-3b and MAP-3 contained epitopes from serine repeat antigen, MSP-1_{42}, and rhoptry-associated protein (RAP) -1 and RAP-2. Antibodies raised in mice against MAP-1 was able to prevent sporozoite invasion of liver cells *in vitro*, and

anti-MAP-2 and anti-MAP-3 antibodies inhibited parasite blood stage development *in vitro* (Mahajan *et al*., 2010).

A multi-epitope malaria vaccine was designed to include B- and T-cell epitopes based on nine *P. falciparum* membrane and secretory proteins. The nine proteins are CSP, SEL-1 protein, protein kinase, protein tyrosine phosphatase, the erythrocyte membrane protein-1 ATS1 and ATS2 domains, VAR2CSA, StAR-related lipid transfer protein, and a conserved *Plasmodium* protein PFB0190. This multi-subunit vaccine has been modelled and underwent physicochemical characterisation, and is yet to be experimentally evaluated (Pandey *et al*., 2018).

1.9.4.3 S*Pf*66 malaria vaccine

The S*Pf*66 vaccine is made up of synthetic immunogenic peptides from *P. falciparum* schizont and merozoite stages (Patarroyo *et al*., 1988). Polymers of the S*Pf*66 molecule tested in mice and guinea pigs were found to be non-toxic, safe and immunogenic (López *et al*., 1994). Mice and monkeys immunized with S*Pf*66 encapsulated in poly-(d,l-lactide-co-glycolic) biodegradable microspheres developed robust and long-lasting immune responses (Rosas *et al*., 2002). Immunized monkeys developed high antibody titres, and were challenged with blood stage *P. falciparum* parasites. Of the seven monkeys, two were completely protected, one had delayed parasitaemia, and the remaining four developed patent parasitaemia (Rosas *et al*., 2002).

Initial clinical studies of S*Pf*66 vaccination followed by *P. falciparum* blood stage challenge, showed recipients developing a slight parasitaemia, which was gradually resolved (Patarroyo *et al*., 1988). In a phase III clinical trial conducted in Venezuela and a follow-up study in Colombia, the S*Pf*66 vaccine showed promise as a malaria vaccine candidate (Valero *et al*., 1996; Noya *et al*., 1994). However, further clinical studies of the S*Pf*66 vaccine in Gambia, Thailand and Tanzania failed to show protection in children (Acosta *et al*., 1999; Nosten *et al*., 1996; D'Alessandro *et al*., 1995).

1.10 *Pf*C0760c as a potential malaria vaccine candidate

*Pf*C0760c is a conserved, uncharacterised protein found in all strains of *P. falciparum*. Homologous proteins are found in species of *Plasmodium* that infect humans, monkeys, mice and birds. The gene for the 405 kDa protein is located on chromosome 3 and is 10 185 bp coding for 3394 amino acids (http://plasmodb.org).

*Pf*C0760c from the 3D7 strain was amongst the *P. falciparum* proteins identified as a potential malaria vaccine candidate due to the exhibition of alpha-helical coiled-coil protein motifs, allowing it to fold easily within the parasite (Villard *et al*., 2007). This characteristic of the protein could allow for the *in vivo* production of antibodies, which can be implicated in

protection. This protein has been recognised by antibodies in infected human sera, however, it has not yet been determined if this protein is capable of protection against malaria challenge infection in mice, humans or other animals (Villard *et al*., 2007).

1.11 Aims and objectives

This study aimed to express and purify the region spanning N2360 – N2656 of the *Pf*C0760c protein. The recombinant protein comprised of 297 amino acids including a 23mer conserved peptide. Partial characterisation of the protein was carried out by determining its interaction with human and mouse monocyte proteins. Bioinformatics analyses was used to predict the likelihood of certain characteristics of *Pf*C0760c. The r*Pf*C0760c$_{297}$ protein was evaluated for antibody production in mice. To determine whether r*Pf*C0760c$_{297}$ could protect mice against a heterologous malaria challenge infection, mice were immunized with r*Pf*C0760c$_{297}$ followed by a *P. berghei* malaria challenge infection.

Chapter 2: Materials and methods

This chapter describes the materials and methods used for expression and partial characterisation of r*Pf*C0760c$_{297}$

2.1 Materials

All reagents were purchased from Merck, Sigma or ThermoScientific with the following exceptions: methanol was purchased from RadChem (Gauteng, South Africa). Goat anti-mouse HRPO-IgG and rabbit anti-chicken HRPO-IgG were purchased from Jackson Immunochemicals (Pennsylvania, USA).

2.2 Bacterial recombinant protein expression

Expression of recombinant eukaryotic proteins is most often carried out in prokaryotic host cells. One of the most common expression systems includes the use of the Gram-negative bacterial host, *Escherichia coli* (*E. coli*) (Baneyx, 1999). The advantages of using this well-studied organism include its ability to grow and replicate rapidly, using cheap substrates. The competent BL21(DE3) strain of *E. coli* is commonly used for recombinant protein expression as it is devoid of proteases (Rosano and Ceccarelli, 2014).

2.2.1 *E. coli* growth curves in different media

All procedures were performed under aseptic conditions. Fresh 15% (v/v) glycerol stocks of *E. coli* BL21(DE3) transformed either with pET32a (pET32a-r*Pf*C0760c$_{297}$) or pET28a (pET28a-r*Pf*C0760c$_{297}$) plasmids encoding the r*Pf*C0760c$_{297}$ protein were prepared and stored at -70°C. The glycerol stocks were streaked onto LB agar (1% (w/v) tryptone, 0.5% (w/v) yeast extract, 0.085 M NaCl, 0.011 M glucose, 1.5% (w/v) bacto-agar) containing the appropriate antibiotic. Ampicillin (50 µg/ml) was used for pET32a-r*Pf*C0760c$_{297}$ cells, and kanamycin (34 µg/ml) was used for pET28a-r*Pf*C0760c$_{297}$ cells. The agar plates were inverted and incubated overnight (37°C). A single colony was inoculated into 10 ml LB media (1% (w/v) tryptone, 0.5% (w/v) yeast extract, 0.085 M NaCl, 0.011 M glucose) containing the appropriate antibiotic with a sterile tip. The cells were grown for 3 h (37°C, 220 RPM), after which absorbance at 600 nm (OD_{600}) was measured hourly for 3 h. The experiment was carried out in triplicate flasks. Growth curves were established in a similar manner for 2×YT media (1% (w/v) yeast extract, 1.6% (w/v) tryptone, 0.085 M NaCl) and terrific broth (1.2% (w/v) tryptone, 2.4% (w/v) yeast extract, 0.4% (v/v) glycerol, 0.017 M KH_2PO_4, 0.072 M K_2HPO_4).

2.2.2 Optimization of bacterial expression of recombinant r*Pf*C0760c$_{297}$

2.2.2.1 Expression of r*Pf*C0760c$_{297}$ in LB or 2×YT media

E. coli cells harbouring either the pET32a-r*Pf*C0760c$_{297}$ or the pET28a-r*Pf*C0760c$_{297}$ plasmids were used. A single colony was picked off an agar plate and inoculated into 10 ml media containing the appropriate antibiotic and grown (37°C, 220 RPM, 16 h). The overnight culture was diluted to 1% (v/v) in 10 ml fresh media, and grown (37°C, 220 RPM) until the OD_{600} was between 0.500 and 0.600. The cells were then induced with 0.3 mM isopropyl β-D-1-thiogalactopyranoside (IPTG) and grown (37°C, 220 RPM, 4 h). Cells were harvested using the Avanti J-26 XPI (Beckman Coulter, California, USA) (6000 *g*, 4°C, 5 min) with a C0850 rotor and the supernatant was discarded. Cell pellets were resuspended in 1% of the original culture volume in phosphate buffered saline (PBS) (0.014 M NaCl, 0.003 M KCl, 0.0085 M NaH_2PO_4, 0.0015 M KH_2PO_4; pH 7.2). Cells were lysed by sonication (8W, 10 s). *E. coli* harbouring the pET32a-r*Pf*C0760c$_{297}$ plasmid was chosen for further experiments. For SDS-PAGE analysis, identical volumes were taken from each sample.

2.2.2.2 Expression of r*Pf*C0760c$_{297}$ in terrific broth

A single colony from an agar plate was aseptically inoculated into 10 ml terrific broth and grown (37°C, 220 RPM, 16 h). The cells were harvested and prepared as described previously.

2.2.2.3 Influence of different temperatures on the expression of r*Pf*C0760c$_{297}$

A single colony was inoculated into 10 ml terrific broth and incubated at 25°C, 30°C or 37°C (220 RPM, 16 h). Bacterial cells were harvested and prepared as described previously. Each experiment was performed in triplicate.

2.2.2.4 Influence of shaking speed on the expression of r*Pf*C0760c$_{297}$

A single colony was inoculated into 10 ml terrific broth and incubated (37°C, 16 h), shaken at 200 RPM, 220 RPM or kept static. The experiment was performed in triplicate, and bacterial cells were harvested and prepared as described previously.

2.2.2.5 Influence of time on the expression of r*Pf*C0760c$_{297}$

A single colony was inoculated into terrific broth, and cultures were incubated (37°C, 200 RPM) for either 12, 16 or 18 h. The experiment was performed in triplicate, and bacterial cells were harvested as described previously.

2.2.2.6 Effect of IPTG concentration in LB media on the expression of r*Pf*C0760c$_{297}$

Cultures were grown in LB media as described in Section 2.2.2.1. IPTG concentrations of 0.1 mM and 0.3 mM were compared in triplicate.

2.2.3 Modification of expression conditions to yield soluble r*Pf*C0760c$_{297}$

The conditions used for expression of high yields of r*Pf*C0760c$_{297}$ were modified for expression of soluble r*Pf*C0760c$_{297}$. *E. coli* transformed with pET32a-r*Pf*C0760c$_{297}$ was grown in terrific broth. In the first experiment, cultures were grown (37°C, 200 RPM) in triplicate, and the duration of expression was terminated after 2, 4, 6 and 8 h. In the second experiment, cultures were grown (200 RPM, 16 h) in triplicate at 20°C. In the third experiment, terrific broth was supplemented with 1%, 2% and 3% (v/v) ethanol and grown (37°C, 200 RPM, 16 h). Bacterial cells were harvested and prepared as previously described.

In LB media, *E. coli* transformed with pET32a-r*Pf*C0760c$_{297}$ was grown (37°C, 200 RPM) and induced with 0.3 mM IPTG when the cells were in the stationary phase (OD_{600} above 0.700).

2.2.4 Solubilization of r*Pf*C0760c$_{297}$

A single colony was inoculated into 50 ml terrific broth and grown under optimized conditions (37°C, 200 RPM, 16 h), and cells were harvested (6000 *g*, 4°C, 20 min). Proteins were solubilized as described (Schlager *et al.*, 2012) with modifications. Briefly, the bacterial pellet was resuspended in 2 ml Triton-PBS (1% (v/v) Triton X-100 in PBS), and sonicated at 8 W for 10 s to resuspend. The suspension was frozen (-20°C, 16 h or -70°C, 1 h) then thawed at room temperature (RT), followed by centrifugation (9000 *g*, 4°C, 20 min). The supernatant was removed, and the pellet was resuspended in 5 ml lysis buffer (8 mM Na_2HPO_4, 286 mM NaCl, 1.4 mM KH_2PO_4, 2.6 mM KCl, 1% (w/v) SDS; pH 7.4) supplemented with 1 mM dithiothreitol. The solution was sonicated at 8 W twice for 2 min on ice, with a 1 min interval. The lysate was then incubated on ice for a minimum of 30 min to facilitate precipitation of SDS, after which it was centrifuged (10 528 *g* (maximum speed of C0850 rotor), 4°C, 35 min). The supernatant containing the solubilized material was ultracentrifuged (99398 *g*, 4°C, 30 min) or filtered through a 0.45 µm filter. Samples taken at various points during the solubilization were prepared for SDS-PAGE.

2.2.5 Purification of r*Pf*C0760c$_{297}$

A 1 ml bed volume of His60 Ni Superflow Resin was transferred to a plastic column. The resin was equilibrated with 10 ml wash buffer (8 mM Na_2HPO_4, 1.4 mM KH_2PO_4, 2.6 mM KCl, 0.1% (w/v) N-lauroyl sarcosine; pH 7.4). The solubilized material was applied to the resin and

equilibrated on an end-over-end rotor (1 h, RT). The unbound fraction was collected, and the resin was washed extensively with wash buffer containing 20 mM imidazole until the absorbance at 280 nm was ≤0.02. Bound protein was eluted (8 mM Na_2HPO_4, 286 mM NaCl, 1.4 mM KH_2PO_4, 2.6 mM KCl, 0.1% (w/v) N-lauroyl sarcosine, 500 mM imidazole; pH 7.4) with a linear gradient of imidazole ranging from 20 – 270 mM in 500 µl fractions. The absorbance of all the eluted samples was measured at 280 nm and an elution profile was generated. A concentration of 150 mM imidazole was chosen for further purifications. The Bradford assay (Section 2.7) was used to determine the concentration of the final pooled purified product (Bradford, 1976).

2.2.6 Regeneration of nickel chelate affinity matrix

Following purification, the resin was washed with 2 bed-volumes of MES buffer (0.02 M 2-(*N*-morpholino)ethanesulfonic acid; pH 5.0) on an end-over-end rotor for 20 min. This was followed by washing with 20 bed-volumes of distilled water (dH_2O), then the resin was stored in storage buffer (20% (v/v) ethanol, 0.01% (w/v) NaN_3) at 4°C.

Complete regeneration of the nickel affinity matrix was carried out as per manufacturer's instructions. Briefly, the nickel was stripped with 10 bed-volumes of EDTA (0.2 M EDTA; pH 7.0), then washed with 10 bed-volumes double-dH_2O. The resin was charged with 2 bed-volumes of nickel sulfate (0.1 M $NiSO_4•7H_2O$). The column was washed with 7 bed-volumes of double-dH_2O, followed by 3 bed-volumes of NaCl (0.3 M NaCl), then washed once more with 10 bed-volumes of double-dH_2O. The column was used immediately or maintained in storage buffer at 4°C until further use.

2.3 Co-expression of r*Pf*C0760c$_{297}$ with chaperones

2.3.1 Generation of competent *E. coli* BL21(DE3) cells

All procedures were performed aseptically. Generation of competent cells was performed as described (Sambrook *et al*., 1989). Briefly, untransformed *E. coli* BL21(DE3) cells from a glycerol stock were three-way streaked onto LB agar without antibiotic and incubated overnight. A single colony was inoculated into 100 ml LB media without antibiotic and incubated (37°C, 200 RPM) until the cells were in the exponential phase. The culture was aseptically transferred to falcon tubes and cooled on ice for 10 min. Cells were harvested (4000 *g*, 10 min, 4°C) and the media discarded. The bacterial cell pellets were resuspended in 20 ml ice-cold $CaCl_2$ (0.1 M $CaCl_2$, filter sterilised with 0.2 µm filter), and incubated on ice for 20 min. This was centrifuged as before, and the supernatant removed. The competent cell pellet was resuspended in 4 ml $CaCl_2$, which was used immediately. The remaining cells were stored at -70°C as 15% (v/v) glycerol stocks.

For generation of competent *E. coli* cells containing pET32a-r*Pf*C0760c$_{297}$, ampicillin was added to the LB agar and media, and the procedure was performed as described above.

2.3.2 Transformation of competent *E. coli* BL21(DE3) cells with chaperone plasmids

The chaperone plasmids used were pGro7, pKJE7 and pG-KJE8. Co-transformation was performed as described (Sambrook *et al*., 1989). Briefly, a 200 µl aliquot of competent cells was transferred to a cold 1.5 ml tube, and 50 ng (10 µl) of chaperone plasmid DNA was added and swirled gently. The preparation was incubated on ice for 30 min, then heat-shocked (42°C, 90 s). The cells were chilled on ice for 2 min, and rescued with the addition of 800 µl SOC media (0.5% (w/v) yeast extract, 2% (w/v) tryptone, 10 mM NaCl, 2.5 mM KCl, 10 mM $MgCl_2$, 20 mM $MgSO_4$, 20 mM glucose). This was incubated (37°C, 45 min), and 200 µl of the preparation was plated onto SOB agar (0.5% (w/v) yeast extract, 2% (w/v) tryptone, 10 mM NaCl, 2.5 mM KCl, 10 mM $MgCl_2$, 20 mM $MgSO_4$, 1.5% (w/v) agar) containing 20 µg/ml chloramphenicol. Plates were inverted and incubated overnight at 37°C. Single colonies on the plates indicated successful transformation. Glycerol stocks were prepared by picking single colonies and growing them as overnight cultures in LB media containing chloramphenicol. A 700 µl aliquot of the overnight culture was combined with 300 µl of 50% (v/v) glycerol and stored at -70°C.

For co-transformation of *E. coli* cells containing pET32a-r*Pf*C0760c$_{297}$ with a chaperone plasmid, the procedure was carried out as described. Ampicillin was included in the SOB agar, and glycerol stocks were prepared in media containing both chloramphenicol and ampicillin.

2.3.3 Isolation of chaperone plasmid DNA from *E. coli* cells

All procedures were performed under aseptic conditions. Glycerol stocks of *E. coli* cells harbouring the pGro7, pKJE7 or pG-KJE8 plasmids were streaked onto LB agar-chloramphenicol plates and incubated overnight (37°C). A single colony was inoculated into 2 ml LB media containing chloramphenicol, and grown overnight (37°C, 200 RPM). A 1.5 ml aliquot of the culture was transferred to a 2 ml tube and centrifuged (12 000 *g*, 30 s, 4°C). The media was removed, and the pellet resuspended in 100 µl cold glucose-Tris-EDTA buffer (50 mM glucose, 25 mM Tris-HCl, 10 mM EDTA; pH 8), then incubated on ice for 30 min. 200 µl lysis buffer (0.2 M NaOH, 1% (w/v) SDS) was added and the tube was inverted 5 times to mix. This was incubated on ice for 5 min, then 150 µl cold potassium acetate (3 M potassium, 5 M acetate) solution was added. The solution was vortexed briefly, and incubated on ice for 5 min, followed by centrifugation (12 000 *g*, 5 min, 4°C). The supernatant was transferred to a fresh sterile 2 ml tube, and 100 % ethanol was added at twice the supernatant volume. This was allowed to stand at RT for 2 min, then centrifuged (12 000 *g*, 5 min, 4°C). The supernatant was removed, and the pellet was rinsed with 1 ml cold 70% (v/v) ethanol, and centrifuged (12 000

g, 5 min, 4°C). The supernatant was aspirated, and the purified DNA pellet was resuspended in 50 µl Tris-EDTA (10 mM Tris-HCl, 1 mM EDTA), and 20 µg/ml RNAse was added.

2.3.4 Co-expression of r*Pf*C0760c$_{297}$ with *E. coli* chaperones

Glycerol stocks of the co-transformed cells were streaked onto LB agar containing chloramphenicol and ampicillin, then incubated at 37°C overnight. A single colony was inoculated into LB media containing chloramphenicol and ampicillin, and cultures were incubated overnight (37°C, 200 RPM). The overnight culture was diluted to 1% (v/v) into fresh media containing the antibiotics and supplemented with 1 mg/ml L-arabinose for induction of chaperone plasmid expression. Where the pG-KJE8 plasmid was used, 1 mg/ml tetracycline was also added. Cultures were grown (37°C, 200 RPM) until they reached the exponential phase. Induction of r*Pf*C0760c$_{297}$ expression was initiated by the addition of IPTG (0.3 mM) for 4 h. Cells were harvested and prepared for SDS-PAGE analysis as described in Section 2.4.1.

2.3.5 Modification of co-expression conditions

The temperature and shaking speed were kept constant (37°C, 200 RPM). Media supplemented with L-arabinose (1 mg/ml) was evaluated, and tetracycline (1 mg/ml) was included where the pG-KJE8 plasmid was used.

The effect of the duration of co-expression in terrific broth was evaluated with the pKJE7 plasmid, as outlined in Section 2.2.3.

Induction of r*Pf*C0760c$_{297}$ expression with different concentrations of IPTG was tested. In LB media, overnight cultures were prepared and diluted to 1% (v/v) in fresh LB media supplemented with L-arabinose. Induction with IPTG was always for 4 h. The following concentrations of IPTG were tested: 0, 0.05 mM, 0.1 mM, 0.2 mM and 0.3 mM.

In a separate experiment, the following concentrations of L-arabinose were tested: 0 mM, 0.25 mM, 0.5 mM, 0.75 mM and 1 mg/ml in LB media. Cultures were induced with IPTG (0.3 mM).

2.4 Electrophoretic techniques

2.4.1 Sodium dodecyl sulfate polyacrylamide gel electrophoresis

Sodium dodecyl sulfate polyacrylamide gel electrophoresis (SDS-PAGE) is a biochemical technique developed by Laemmli (1970), that is used to separate proteins by size and assess protein purity.

The reagents used were as follows: monomer solution (30% (w/v) acrylamide, 0.8% (w/v) bisacrylamide), running gel buffer (1.5 M Tris-HCl; pH 8.8), SDS stock solution (10% (w/v) SDS), initiator stock (10% (w/v) ammonium persulfate), stacking gel buffer (0.5 M Tris-HCl;

pH 6.8), and tank buffer (0.25 M Tris-HCl, 0.192 M glycine, 0.1% (w/v) SDS; pH 8.3). The monomer solution, running and stacking gel buffers were filtered through Whatman No.1 filter paper. All reagents except the SDS stock solution were stored at 4°C. The monomer solution and initiator were stored in amber bottles. The tank buffer was always freshly prepared.

For SDS-PAGE analysis, samples were combined 1:1 with treatment buffer (0.125 M Tris-HCl, 4% (w/v) SDS, 20% (w/v) glycerol, 10% (v/v) β-mercaptoethanol, bromophenol blue tracker dye; pH 6.8). From the *E. coli* culture experiments described in Sections 2.2.2 and 2.2.3, identical volumes from each culture were analysed. The treatment buffer was stored without β-mercaptoethanol, (which was also omitted for non-reducing SDS-PAGE gels). Samples were boiled (95°C, 5 min) prior to analysis. A reduced, unstained molecular weight marker (Catalog number 26610, ThermoScientific, Gauteng, South Africa) containing proteins of known molecular weight was run alongside samples.

The running gel was prepared according to Table 2.1, and the gels were cast in a BioRad™ Mini-PROTEAN® Tetra vertical electrophoresis gel casting system. Gels were overlaid with dH_2O and allowed to polymerise. The dH_2O was removed, and the stacking gel was pipetted on top of the polymerised running gel, and a comb was inserted to form the wells. The gels were assembled onto the gasket and immersed in the SDS-PAGE tank containing tank buffer. 5 – 10 µl of prepared SDS-PAGE samples were loaded onto SDS-PAGE gels.

A current of 20 mA per gel was applied until the tracker dye migrated to the bottom of the gel. The gels were stained overnight with Coomassie Brilliant Blue R250 staining solution (1.25% (w/v) Coomassie Brilliant Blue R250, 50% (v/v) methanol, 10% (v/v) acetic acid). Gels were rinsed with dh_2O, then destained (50% (v/v) methanol, 10% (v/v) acetic acid) until protein bands were clearly visible. The gels were placed into dH_2O until they reverted to their original size, then photographed.

Table 2.1: Components used in SDS-PAGE gels.

Reagent	12.5% running gel	4% stacking gel
Monomer solution	6.25 ml	940 µl
Running gel buffer	3.75 ml	-
Stacking gel buffer	-	1.75 ml
dH_2O	4.75 ml	4.3 ml
SDS stock solution	150 µl	70 µl
TEMED	7.5 µl	15 µl
Initiator	150 µl	70 µl

2.4.2 Western blotting

An effective, sensitive and accurate method to determine the presence of a protein in a gel, is to transfer the proteins from the gel onto a nitrocellulose membrane and probe the blot with antigen-specific antibodies (Towbin *et al*., 1979).

Following SDS-PAGE, gels, nitrocellulose membranes (6 × 8 cm) and blotting paper (8 × 10 cm) were equilibrated in western blotting buffer (0.05 M Tris, 0.192 M glycine, 20% (v/v) methanol, 0.01% (v/v) SDS) for 5 min. Following equilibration, the components were assembled into the western blot apparatus. The tank was filled with western blotting buffer, and a current of 40 mA was applied for 16 h. After protein transfer, nitrocellulose was stained with Ponceau S (0.1% (w/v) Ponceau S in methanol), and the molecular weight markers were marked in pencil. The western blot was destained by rinsing with dH_2O and a few drops of concentrated NaOH. The blot was blocked with 5% (w/v) milk powder in Tris-buffered saline (TBS) (0.02 M Tris, 0.2 M NaCl; pH 7.4) (2 h, RT or overnight, 4°C). Blots were washed with TBS (3 × 5 min), and incubated with primary antibody (2 h, RT or overnight, 4°C). Blots were washed as before, then incubated with secondary antibody (1 h, RT), then washed as before. The substrate was prepared by combining 2 ml of a 4-chloro-1-naphthol stock solution (0.017 M 4-chloro-1-naphthol in methanol, stored at -20°C) with 8 ml TBS and 4 µl H_2O_2 to yield the substrate (0.0034 M 4-chloro-1-naphthol, 3.92 mM H_2O_2). The substrate was prepared fresh each time before use. The blot was incubated with the substrate in the dark until a coloured precipitate developed.

Antibodies were prepared in 0.5% (w/v) BSA in TBS. The chicken anti-r*Pf*C0760c$_{297}$ IgY (affinity purified in-house; Addicott, 2014) was used at a concentration of 1 µg/ml. Mouse anti-hexahistidine tagged (his$_6$tag) IgG and goat anti-mouse HRPO-IgG were prepared 1:6000. The rabbit anti-chicken HRPO-IgG was prepared at 1:15 000.

To test for endogenous peroxidase activity, proteins were electrophoretically transferred or dotted onto nitrocellulose. The blots were blocked with 5% (w/v) milk powder-TBS (2 h, RT). The enhanced chemiluminescence (ECL) substrate (Section 2.4.3) was applied to the western blot, and the 4-chloro-1-naphthol substrate was applied to the dot blot.

2.4.3 Far western blotting

The far western blot is performed identically to a western blot, apart from an additional incubation step, and some amendments (Wu *et al*., 2007). Monocyte proteins were analysed by non-reducing SDS-PAGE and western blot.

A total of 5 µg of control proteins was loaded. Following SDS-PAGE and transfer to nitrocellulose, blots were blocked (8% (w/v) milk powder TBS, 0.1% Tween-20) (2 h, RT or overnight, 4°C). Blots were probed with 100 µg r*Pf*C0760c$_{297}$ (2 h, RT or overnight, 4°C). Protein-protein interactions were detected with mouse anti-his$_6$tag IgG (2 h, RT or overnight, 4°C) and goat anti-mouse HRPO-IgG (1 h, RT). Blots were washed between incubations (3 × 8 min) with TBS-T (TBS, 0.1% (v/v) Tween). Both antibodies and r*Pf*C0760c$_{297}$ were prepared in 0.5% (w/v) BSA-TBS-T. The ECL substrate was used for increased sensitivity. Stocks of p-

iodophenol (0.1 M *p*-iodophenol in DMSO) and luminol (40 mg/ml luminol in DMSO) were prepared and stored at -20°C. The ECL reagent (0.5 mM *p*-iodophenol, 1.13 mM luminol, 24.5 mM H_2O_2) was prepared in Tris-HCl (0.1 M Tris-HCl; pH 8.5). A 500 µl aliquot of the substrate was pipetted onto the blot directly before image capture. The far dot or western blot schematic is depicted in Figure 2.1. Following incubation of the prey proteins on the blot with r*Pf*C0760c$_{297}$, anti-his$_6$tag antibodies detect the his$_6$tagged-r*Pf*C0760c$_{297}$ protein bound to proteins on the blot. Positive and negative controls are included to ensure that the results are not non-specific in nature.

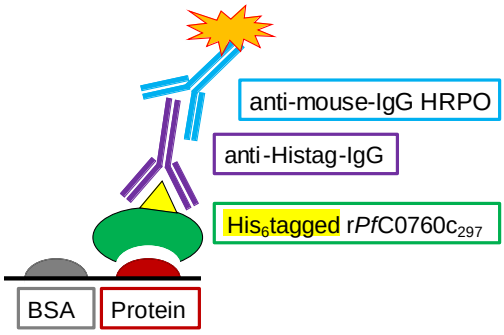

Figure 2.1: Schematic representation of far dot blot or far western blot probed with r*Pf*C0760c$_{297}$. Prey protein is dotted or transferred onto nitrocellulose. After blocking with milk-TBS, blots are probed with the bait protein, his$_6$tagged-r*Pf*C0760c$_{297}$. Mouse anti-his$_6$tag IgG and goat anti-mouse HRPO-IgG are used for detection. The blots are then developed with the substrate.

2.5 Far dot blot

Dot blots allow for the detection of an antigen within a sample using antigen-specific antibodies. The far dot blot is performed similarly to that of a far western blot, however, proteins are not transferred electrophoretically, but rather, are dotted directly onto a nitrocellulose membrane.

Amounts of 1 µg, 10 µg and 50 µg chicken anti-rabbit albumin IgY and chicken anti-r*Pf*C0760c$_{297}$ IgY were dotted onto nitrocellulose and airdried. A volume of 0.5 µl was used. Blots were probed with 5 µg r*Pf*C0760c$_{297}$ (1 h, RT), followed by incubation with mouse anti-his$_6$tag IgG (1:6000) (2 h, RT) and goat anti-mouse HRPO-IgG (1:6000) (1 h, RT). The r*Pf*C0760c$_{297}$ protein and antibodies were prepared in 0.5% (w/v) BSA-TBS. The 4-chloro-1-naphthol substrate was applied.

For the detection of peroxidase activity, a maximum volume of 0.5 µl monocyte lysates and 1 µg control proteins were dotted onto a nitrocellulose membrane and airdried. Blots were blocked (5% (w/v) milk powder in TBS) (2 h, RT), then the 4-chloro-1-naphthol substrate was applied.

2.6 Cell culture techniques

Tissue culture of mammalian cells is a useful research tool allowing for the cultivation of cells derived from humans or animals. These cells can be used for various *in vitro* studies aimed at determining cell-interactions with other materials, such as drugs, proteins, cytokines or chemokines.

2.6.1 Culture of human U937 and mouse J774A.1 cells

Cell culture of malaria-naïve monocytes was performed as recommended by the European Collection of Authenticated Cell Cultures under aseptic conditions. Briefly, human U937 monocytes were cultured in RPMI 1640 media (90% (v/v) RPMI, 10% (v/v) FBS, 1% (v/v) PenStrep) and mouse J774A.1 monocytes were cultured in DMEM (90% (v/v) DMEM, 10% (v/v) FBS, 1% (v/v) PenStrep), stored at 4°C. PenStrep (Catalog number P4333, Sigma-Aldrich, Gauteng, South Africa) constituted 10 000 U penicillin and 10 mg/ml streptomycin before dilution. 4 ml pre-warmed media (37°C) was transferred to a 25 cm^3 culture flask and equilibrated (37°C, 5 % CO_2). Stock cultures preserved in liquid nitrogen containing 1 ml monocytes was thawed (37°C). Thawed monocytes were gently pipetted into the respective pre-warmed media. The flasks were incubated (37°C, 5 % CO_2) until they reached confluency.

2.6.2 Monocyte subculture

Confluent cells were harvested (1000 *g*, 5 min) and the spent media was removed. The cells were resuspended in 3 ml of the appropriate media. In three 25 cm^3 flasks, 1 ml of the cell suspension was added to each flask containing 4 ml of fresh, equilibrated media and incubated (37°C, 5% CO_2). Once the cells reached confluency, one of the three flasks were sub-cultured as outlined. The cells from the remaining two flasks were harvested (1000 *g*, 5 min). These cells were washed twice with 5 ml cold PBS (1000 *g*, 5 min). The cell pellets were resuspended in 100 µl cold PBS and kept on ice. The Halt™ Protease Inhibitor Cocktail (100×) (ThermoFisher, Gauteng, South Africa) was added to each cell suspension, and cells were lysed by sonication (3 W, 10 s). Cells were stored at -20°C until further use.

2.6.3 Trypan blue assay

The trypan blue assay was used to assess cell viability (Strober, 2001). A volume of 50 µl of cells was combined with 50 µl of the trypan blue dye (0.4% (w/v) trypan blue in PBS), and equilibrated for 1 min. Cell viability was assessed microscopically using a haemocytometer. Viable cells remain unstained, and non-viable cells were stained dark blue.

2.7 The Bradford assay

The Bradford assay was used to determine the concentration of protein samples (Bradford, 1976). A protein standard curve was prepared using BSA at concentrations ranging from 0 – 100 µg in triplicate. These were made up to 100 µl, followed by addition of 900 µl of the Bradford reagent. Solutions equilibrated for 2 min, and the absorbance was measured at 595 nm.

To measure the concentration of a protein sample, 900 µl of the Bradford reagent was combined with 95 µl dH_2O and 5 µl of the protein sample. Samples were equilibrated and measured as above. The protein concentration was estimated using the standard curve.

2.8 Immunization of mice

Mouse models provide an important tool to allow for the study of human diseases (Perlman, 2016), that may provide valuable insight into the pathology and progression of human diseases. *P. berghei*, *P. chabaudi* and *P. yoelii* are species that specifically infect mice, and are used to mimic different aspects of human *Plasmodial* infections (Huang *et al*., 2015; Wykes and Good, 2009).

2.8.1 Mice used in this study

Female BALB/c mice (8 – 10 weeks) were housed at the UKZN Animal House Unit under recommended conditions. Food, water and enrichment were provided *ad libitum*. Once a week, mice were given sunflower seeds and apple slices. Immunized and control mice were housed in separate labelled cages, and mouse tails were labelled with permanent marker. Ethical approval was obtained from the University of KwaZulu-Natal Animal Ethics Committee (004/15/animal).

2.8.2 Generation of anti-r*Pf*C0760c$_{297}$ antibodies in mice

An experimental group of 5 mice were immunized with 100 µg r*Pf*C0760c$_{297}$, and the control group consisting of 2 mice received the elution buffer (Section 2.2.5). Antigen was emulsified in Freund's Complete Adjuvant for primary immunization, and Freund's Incomplete Adjuvant for subsequent immunizations, and triturated. Mice were immunized intraperitoneally with a 26G needle with a final volume of 100 µl on days 0, 14 and 28. On day 42, mice were anaesthetized with isoflurane and sacrificed by cervical dislocation. Blood was harvested by cardiac puncture and collected in EDTA-coated or heparinised vacutainers. The blood was transferred to a sterile 2 ml tube and allowed to separate overnight at 4ºC. Serum was collected in a sterile 2 ml tube for further analysis.

2.8.3 Enzyme-linked immunosorbent assay

ELISA is sensitive immunochemical technique that is used for the detection and quantification of an antigen using antigen-specific antibodies.

A Nunc Maxisorp ELISA plate was coated overnight at 4°C with 1 µg/ml r*Pf*C0760c$_{297}$ (100 µl). Plates were washed 3 times with PBS-T (0.1% (v/v) Tween-20 in PBS), then inverted and tapped to remove excess buffer. Plates were blocked with 200 µl 5% (w/v) powdered milk-PBS-T (2 h, 37°C), then washed as before. The antibodies were diluted in 0.5% (w/v) BSA-PBS-T. Mouse serum was diluted 10^{-3} – 10^{-7} (100 µl) and incubated (2 h, 37°C). The serum from a non-immune mouse was included. Plates were washed as before. The goat anti-mouse HRPO-IgG antibody was prepared (1:6000 in 0.5% (w/v) BSA-PBS-T) and 100 µl was incubated (1 h, 37°C). The ABTS substrate (0.97 mM ABTS, 4.9 mM H_2O_2) was prepared in citrate-phosphate buffer (0.15 M citrate-phosphate; pH 5.0). The substrate was added (150 µl) and plates were incubated in the dark (1 h, RT) before the absorbance was measured at 405 nm.

2.8.4 Immunization of mice with r*Pf*C0760c$_{297}$ and challenge with *P. berghei* parasites

In the challenge model, female BALB/c mice (6 – 8 weeks old) were immunized on the same schedule as outlined (Section 2.8.1), and challenged with 10^5 *P. berghei* ANKA infected red blood cells on day 40. Parasitaemia was monitored every second day by collecting blood via tail-prick and smeared onto a glass slide. After challenge, mice were anaesthetized and sacrificed as before when the parasitaemia was higher than 15%. All r*Pf*C0760c$_{297}$-immunized mice were sacrificed on the same day.

2.8.5 Giemsa staining of *P. berghei* infected blood samples

Glass slides with blood smears were fixed with 100% methanol for 30 s and allowed to airdry, then stained with Giemsa (10% (v/v) Giemsa stain in PBS). Slides were viewed with a Zeiss microscope under oil immersion at 1000× magnification. A total of 500 blood cells were counted, and the percentage parasitaemia calculated.

Chapter 3: Recombinant expression, solubilization and purification of r*Pf*C0760c$_{297}$

3.1 Introduction

3.1.1 *E. coli* as a bacterial host for recombinant protein expression

Bacteria are advantageous hosts used for recombinant protein expression. The benefits of using *Escherichia coli* for bacterial recombinant expression include rapid growth in inexpensive media, and high yield of recombinant protein (Larentis *et al*., 2014; Baneyx, 1999). Optimizing conditions that improve cell mass generally leads to a greater yield of target protein (Kilikian *et al*., 2000). The BL21 (DE3) strain of *E. coli* is a commonly used host, as it lacks functional *Lon* and *OmpT* proteases. These proteases are responsible for cleaving foreign proteins including recombinant proteins (Ahmad *et al*., 2018; Rosano and Ceccarelli, 2014).

Media used for cultivation of bacteria, such as *E. coli* used in expression systems primarily comprise tryptone, yeast extract and NaCl. Yeast extract is a source of vitamins and minerals, and tryptone provides nitrogen (Lessard, 2013). Luria Bertani (LB) media includes glucose, whereas 2× yeast-tryptone (2×YT) media and terrific broth do not. Terrific broth contains glycerol. Metabolism of glycerol produces acidic products which help to delay an increase in pH, and the potassium phosphate salts buffer the media (Kram and Finkel, 2015). Depletion of carbohydrates during bacterial cultivation causes the cells to metabolise amino acids, which releases ammonia into the culture medium, leading to an increase in pH (McFall and Newman, 1996).

Terrific broth is an autoinduction media, which does not require the addition of IPTG to initiate recombinant protein expression. Cells grown in autoinduction media preferentially metabolise glucose during proliferation. Glucose depletion results in the cells switching to glycerol and lactose metabolism. Metabolism of lactose initiates recombinant protein expression of *lac*-controlled proteins (Rosano and Ceccarelli, 2014).

3.1.2 pET expression vectors

The pET expression vectors use the inducible bacteriophage T7 promoter, which when induced, activates host T7 RNA polymerase (Studier, 2005; Rosenberg *et al*., 1987). Endonucleases are used to insert the complementary DNA of the target gene, which is cloned into the multiple cloning site region downstream of the T7 promoter. An antibiotic resistance marker is incorporated into the vector to select for transformed cells (Lodish *et al*., 2000; Baneyx, 1999). Recombinant protein expression is induced by binding of lactose or its analogue, isopropyl β-D-1-thiogalactopyranoside (IPTG) to the *lac* promoter (Ahmad *et al*.,

2018). Often with the use of expression vectors, recombinant proteins are expressed with fusion tags.

His_6tagged fusion proteins can easily be affinity purified from *E. coli* lysates by passing soluble material over an immobilised metal ion affinity chromatography matrix (Baneyx, 1999). The column is comprised of nickel or cobalt attached to nitrilotriacetic acid (NTA) or carboxylmethylaspartate respectively, which is coupled to a support resin (Rosano and Ceccarelli, 2014; Bornhorst and Falke, 2000). The imidazole-ring on the histidine molecule forms coordination bonds with the metal ions (Bornhorst and Falke, 2000). The contaminating *E. coli* proteins remain unbound. Bound protein is eluted using imidazole, or changes in the ionic strength or pH of the elution buffer.

3.1.3 Expression of r*Pf*C0760c$_{297}$

A region spanning the amino acids N2360 – N2656 from the N-terminus of the *Pf*C0760c protein (denoted further as r*Pf*C0760c$_{297}$) was previously cloned into pET32a and pET28a expression vectors and transformed into *E. coli* BL21 (DE3) host cells. The predicted size of untagged r*Pf*C0760c$_{297}$ is 36 kDa (Gasteiger *et al*., 2005). The expected size of r*Pf*C0760c$_{297}$ from pET32a is 56 kDa, and pET28a is 42 kDa. The larger sizes are attributed to the presence of a his_6tag, S-tag and thioredoxin on pET32a, and a his_6tag and T7 tag on pET28a. The T7 tag is used to enhance recombinant protein expression, and the his_6tag and S-tags are used for detection of the fusion protein (Bornhorst and Falke, 2000; Raines *et al*., 2000; Olins, *et al*., 1988). The thioredoxin tag contributes to protein solubility (LaVallie *et al*., 1993).

In this chapter, growth profiles for transformed *E. coli* were established in different media. The conditions for high levels of r*Pf*C0760c$_{297}$ expression were optimized. Adjustment of expression conditions was evaluated for the expression of soluble r*Pf*C0760c$_{297}$.

3.2 Results

3.2.1 Growth profiles of transformed *E. coli* cells in different media

E. coli BL21(DE3) cells containing either pET32a-r*Pf*C0760c$_{297}$ or pET28a-r*Pf*C0760c$_{297}$ were grown in LB or 2×YT and were not induced, or grown in terrific broth. The absence of turbidity after the first 2 h post-inoculation indicated minimal growth and likely constituted the lag phase. After 3 h post-inoculation, the OD_{600} was measured hourly. The results shown are the mean absorbance of triplicate cultures, and the standard deviation for each triplicate set is indicated.

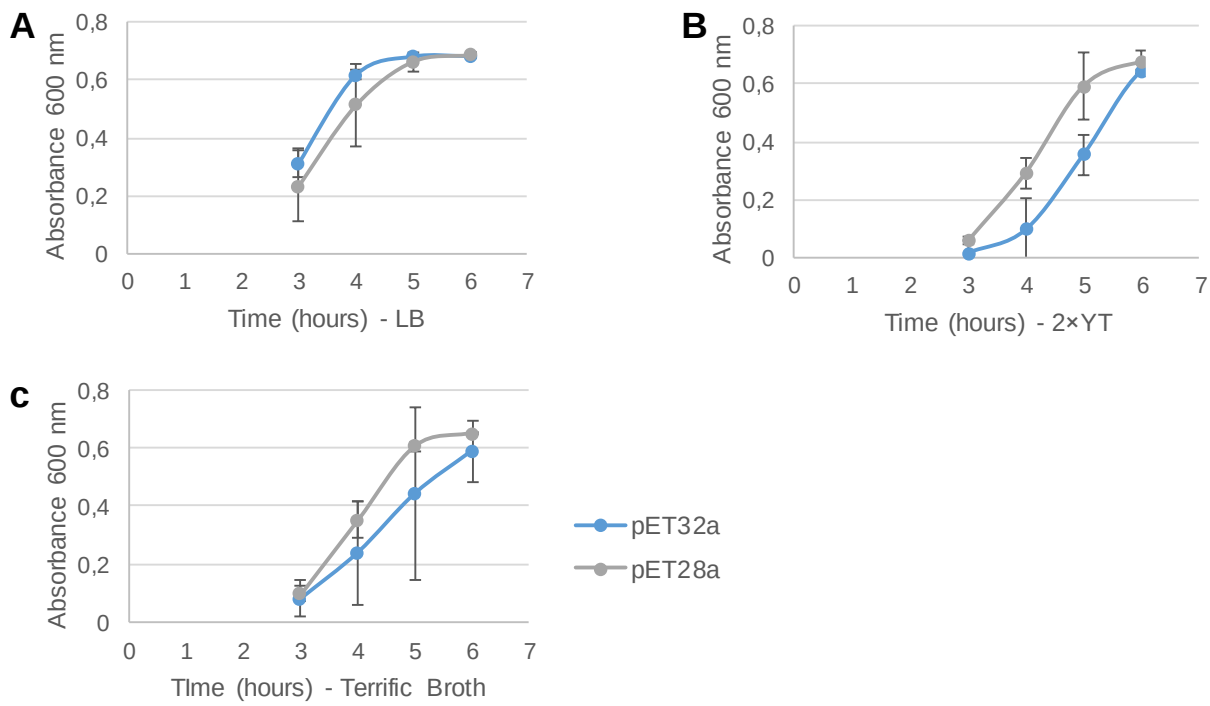

Figure 3.1: Growth profiles of *E. coli* BL21(DE3) transformed with pET32a-r*Pf*C0760c$_{297}$ or pET28a-r*Pf*C0760c$_{297}$ in three types of media. The absorbance of triplicate cultures was measured at 600 nm hourly from 3 – 6 h. The mean absorbance and standard deviations are indicated for cultures grown in **(A)** LB media, **(B)** 2×YT media and **(C)** terrific broth.

Measurable growth begins after approximately 3 h, which increases as the exponential phase begins. The stationary phase is reached when the cell growth slows down. There appears to be more bacteria present at 3 h in the LB cultures (Figure 3.1A) than in cultures grown in 2×YT and terrific broth (Figure 3.1B and C). This is likely due to the number of cells used to inoculate the media. Individual colonies were picked to inoculate cultures, which contributed to the observed variations in the standard deviations.

3.2.2 Evaluation of different culture conditions for r*Pf*C0760c$_{297}$ expression

The conditions for the expression of high quantities of r*Pf*C0760c$_{297}$ were explored. The temperature and shaking speed were kept constant for all three types of media tested. Where LB and 2×YT media were used, the concentration of IPTG and the duration of induction was kept constant.

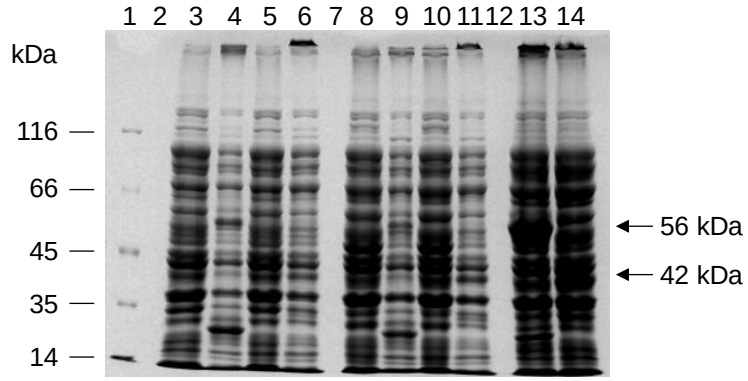

Figure 3.2: *E. coli* BL21(DE3) cells transformed with pET32a-r*Pf*C0760c$_{297}$ or pET28a-r*Pf*C0760c$_{297}$ grown in different media. Bacterial lysates were resolved on 12.5% reducing SDS-PAGE and proteins were stained with Coomassie Blue. Lane 1: molecular weight marker. Uninduced and induced lysates were from cultures grown in LB (lanes 3 – 6) and 2×YT (lanes 8 – 11) media. Lanes 3 and 4, 8 and 9: pET32a-r*Pf*C0760c$_{297}$. Lanes 5 and 6, 10 and 11: pET28a-r*Pf*C0760c$_{297}$. Lanes 13 and 14: pET32a-r*Pf*C0760c$_{297}$ and pET28a-r*Pf*C0760c$_{297}$ respectively in terrific broth.

The size of r*Pf*C0760c$_{297}$ expressed from pET32a and pET28a was approximately 56 kDa and 42 kDa respectively. The protein expression profiles of uninduced and induced *E. coli* is illustrated (Figure 3.2). The r*Pf*C0760c$_{297}$ is absent in uninduced *E. coli* grown in LB media (lanes 3 and 5) and 2×YT media (lanes 8 and 10). A 56 kDa band is present in IPTG-induced *E. coli* cells containing pET32a-r*Pf*C0760c$_{297}$ grown in LB and 2×YT media (lanes 4 and 9). There is a large amount of the 56 kDa r*Pf*C0760c$_{297}$ protein produced in terrific broth with the pET32a plasmid (lane 13). A thin band of 42 kDa is present in induced *E. coli* cells containing pET28a-r*Pf*C0760c$_{297}$, irrespective of the media used (lanes 6, 11 and 14). The 42 kDa r*Pf*C0760c$_{297}$ expressed with pET28a is not clearly visible (lane 14). A prominent band at approximately 30 kDa is present in all induced *E. coli* containing pET32a (lanes 4, 9 and 13) which is absent in uninduced cultures. A lower protein band intensity is noted in IPTG-induced *E. coli* in proteins ranging in size from 14 kDa to >116 kDa in cultures (lanes 4, 6, 9 and 11) compared to uninduced cultures (lanes 3, 5, 8 and 10). *E. coli* cells transformed with pET32a-r*Pf*C0760c$_{297}$ grown in terrific broth were chosen for further evaluation.

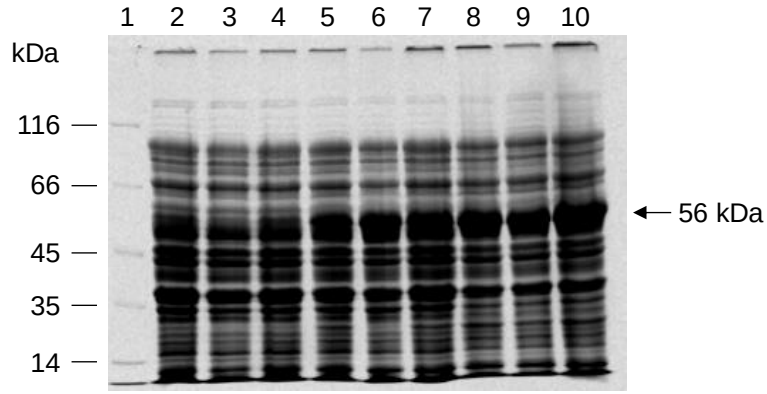

Figure 3.3: Expression of r*Pf*C0760c$_{297}$ in terrific broth at three temperatures. Bacterial lysates were resolved on 12.5% reducing SDS-PAGE, and proteins were stained with Coomassie Blue. Lane 1: molecular weight marker. Cultures were grown in triplicate at the following temperatures: Lanes 2 – 4: 25°C. Lanes 5 – 7: 30°C. Lanes 8 – 10: 37°C.

Three different temperatures, 25°C, 30°C and 37°C were tested for host cell growth and protein expression. The 56 kDa r*Pf*C0760c$_{297}$ band is prominent in cultures grown at all three temperatures (Figure 3.3, lanes 2 – 10). At 25°C, there is less r*Pf*C0760c$_{297}$ that is expressed (lanes 2 – 4) compared to cultures incubated at 30°C (lanes 5 – 7) and 37°C (lanes 8 – 10). The amount of r*Pf*C0760c$_{297}$ expressed at 30°C and 37°C are similar.

As 37°C had previously been used to express the protein (Addicott, 2014), this temperature was used in subsequent experiments.

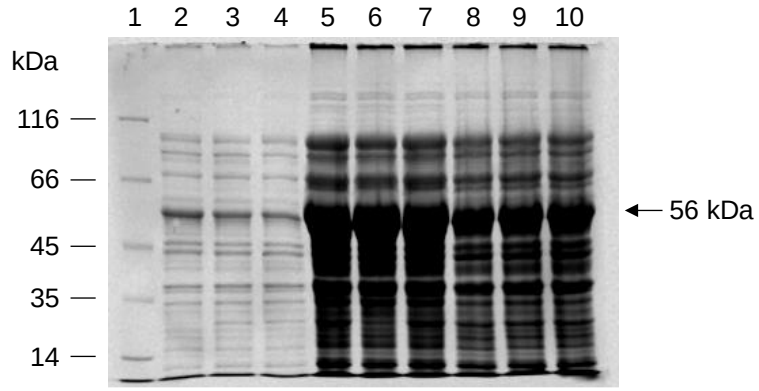

Figure 3.4: Expression of r*Pf*C0760c$_{297}$ in terrific broth at different shaking speeds. Bacterial lysates were resolved on 12.5% reducing SDS-PAGE, and proteins were stained with Coomassie Blue. Lane 1: molecular weight marker. Lanes 2 – 4: static cultures. Lanes 5 – 7: 200 RPM. Lanes 8 – 10: 220 RPM.

The shaking speeds at 200 and 220 RPM were compared to static cultures. The r*Pf*C0760c$_{297}$ protein is expressed at all the shaking speeds tested (Figure 3.4, lanes 2 – 10). Poor cell growth and hence poor expression of r*Pf*C0760c$_{297}$ is observed in static cultures (lanes 2 – 4). Higher concentrations of r*Pf*C0760c$_{297}$ and *E. coli* proteins are observed in cultures shaken at 200 RPM (lanes 5 – 7) compared to cultures shaken at 220 RPM (lanes 8 – 10). Thus, 200 RPM was used in further experiments.

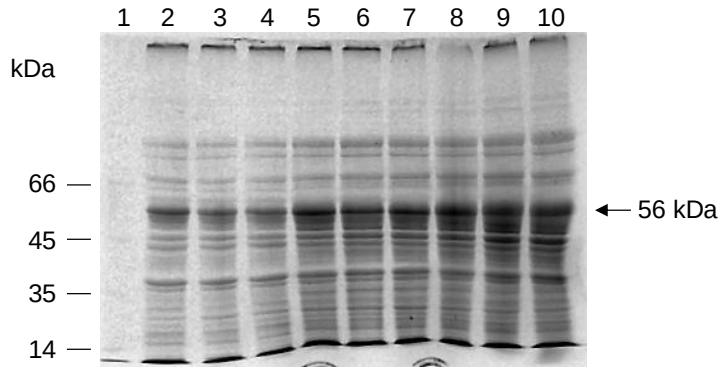

Figure 3.5: Expression of r*Pf*C0760c$_{297}$ for different time periods. Bacterial lysates were resolved on 12.5% reducing SDS-PAGE, and proteins were stained with Coomassie Blue. Lane 1: molecular weight marker. Lysates were analysed from triplicate cultures incubated for: lanes 2 – 4: 12 h; lanes 5 – 7: 16 h; and lanes 8 – 10: 18 h.

Durations of 12, 16 and 18 h incubation in terrific broth was tested. The r*Pf*C0760c$_{297}$ protein is expressed along with *E. coli* host proteins in all cultures (Figure 3.5). There is noticeably less protein present in the cultures incubated for 12 h (lanes 2 – 4) compared to cultures that were incubated longer (lanes 5 – 10). The amount of host and recombinant proteins expressed is comparable in cultures incubated for 16 h and 18 h. A duration of 16 h was chosen for further experiments.

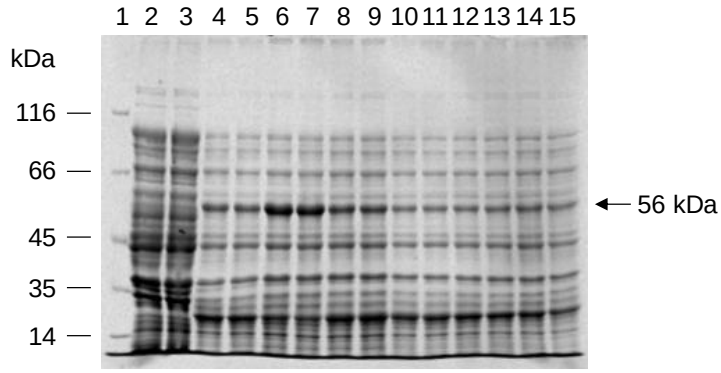

Figure 3.6: Comparison of IPTG concentrations for the expression of r*Pf*C0760c$_{297}$ in LB media. Bacterial lysates were resolved on 12.5% reducing SDS-PAGE and proteins were stained with Coomassie Blue. Lane 1: molecular weight marker. Lanes 2, 3: duplicate uninduced samples. Duplicate samples of three cultures induced with 0.1 mM IPTG (lanes 4 and 5, 6 and 7, 8 and 9), and 0.3 mM IPTG (lanes 10 and 11, 12 and 13, 14 and 15).

Concentrations of 0.1 mM and 0.3 mM IPTG were compared for induction of r*Pf*C0760c$_{297}$ expression in LB media. There is a distinct difference between the uninduced culture (lanes 2 and 3) and the induced cultures (lanes 4 – 15), regardless of the IPTG concentration used for induction (Figure 3.6). Similar to Figure 3.2, there appears to be less protein present in the induced cultures compared to the uninduced cultures. The 56 kDa r*Pf*C0760c$_{297}$ protein band is present in all the induced cultures, as well as a band at approximately 30 kDa (lanes 4 – 15). Better expression of r*Pf*C0760c$_{297}$ was achieved by induction with 0.1 mM IPTG (lanes 4 – 9)

compared to 0.3 mM IPTG (lanes 10 – 15). A higher concentration of the r*Pf*C0760c$_{297}$ protein is present in one of the cultures induced with 0.1 mM (lanes 6 and 7) compared to replicates induced with the same concentration, and cultures induced with 0.3 mM IPTG. There is slightly better production of *E. coli* host proteins in the presence of 0.1 mM IPTG (lanes 4 – 9) compared to 0.3 mM (lanes 10 – 15).

Overall, better expression of r*Pf*C0760c$_{297}$ was achieved using terrific broth. Terrific broth was therefore used for the subsequent expression and purification of r*Pf*C0760c$_{297}$. Cultures were grown at 37°C for 16 h and shaken at 200 RPM.

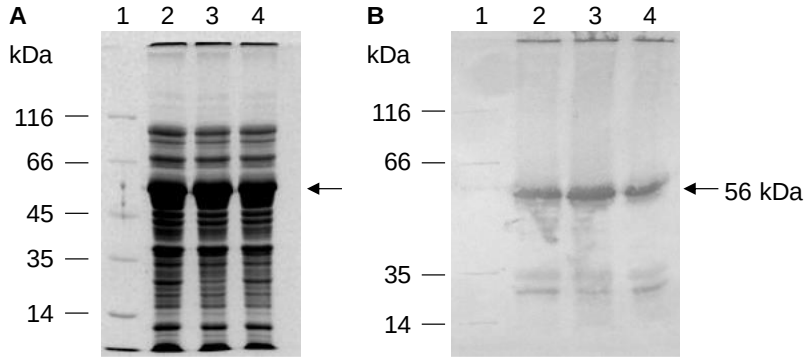

Figure 3.7: Optimized conditions for expression of r*Pf*C0760c$_{297}$. (A) Bacterial cell lysates were resolved on 12.5% reducing SDS-PAGE. Proteins were stained with Coomassie Blue. Lane 1: molecular weight marker. Lanes 2 – 4: samples from triplicate cultures. **(B)** Western blot of an identical gel was probed with mouse anti-his$_6$tag IgG and detected with goat anti-mouse HRPO-IgG.

Expression under the chosen conditions resulted in overexpression of r*Pf*C0760c$_{297}$ (Figure 3.7A). The 56 kDa r*Pf*C0760c$_{297}$ protein was detected with monoclonal mouse anti-his$_6$tag IgG (Figure 3.7B). Two additional bands at approximately 34 kDa and 30 kDa were also detected.

The conditions used to express high quantities of r*Pf*C0760c$_{297}$ resulted in the formation of insoluble protein aggregates called inclusion bodies (data not shown). Soluble r*Pf*C0760c$_{297}$ is required to study the protein.

3.2.3 Modification of expression conditions to improve solubility of r*Pf*C0760c$_{297}$

Modifications of the expression conditions were evaluated to determine whether soluble r*Pf*C0760c$_{297}$ could be expressed. The changes in expression conditions included the duration of expression under optimal conditions, a lower temperature of expression (Flick *et al*., 2004; Baneyx, 1999), expression in the presence of ethanol (Chhetri *et al*., 2015; Steczko *et al*., 1991), and induction of r*Pf*C0760c$_{297}$ expression in LB media during the stationary phase (Flick *et al*., 2004).

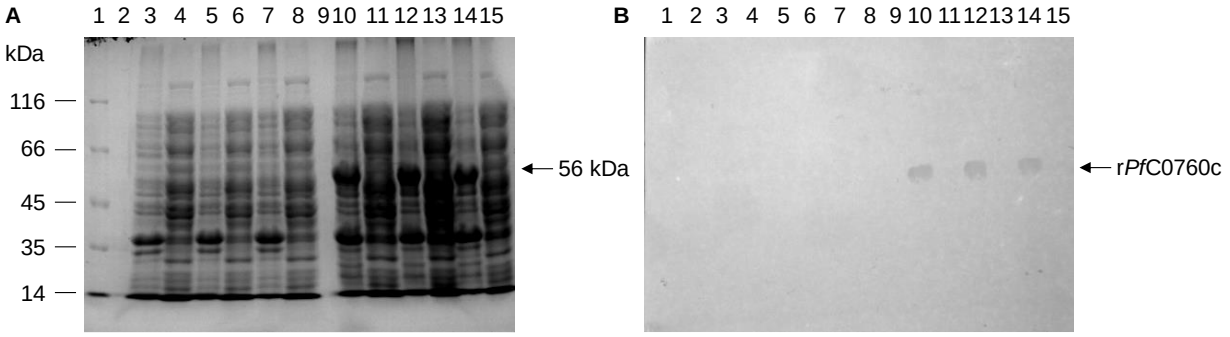

Figure 3.8: Expression of r*Pf*C0760c$_{297}$ for 6 – 8 h. Cultures were grown for 6 and 8 h in terrific broth. Bacterial lysates were resolved on 12.5% reducing SDS-PAGE, and proteins were stained with Coomassie Blue. **(A)** Lane 1: molecular weight marker. Insoluble and soluble fractions were analysed respectively. Lanes 3 and 4, 5 and 6, 7 and 8: triplicate after 6 h expression; and lanes 10 and 11, 12 and 13, 14 and 15: triplicate cultures after 8 h expression. **(B)** Western blot of an identical gel probed with mouse anti-his$_6$tag IgG and detected with goat anti-mouse HRPO-IgG.

The duration of expression was shortened. After 4 h of incubation, minimal growth was observed. Samples were therefore taken after 6 and 8 h. The 56 kDa r*Pf*C0760c$_{297}$ protein is undetected in both the insoluble and soluble fractions after 6 h of expression (Figure 3.8A and B, lanes 3 – 8). An increase in *E. coli* host protein expression is observed after 8 h, and the 56 kDa r*Pf*C0760c$_{297}$ protein is visible in the insoluble fraction (Figure 3.8A and B, lanes 10 – 15). Soluble r*Pf*C0760c$_{297}$ is undetected (Figure 3.8A and B, lanes 11, 13 and 15). Interestingly, the 34 kDa and 30 kDa protein bands that were present after 16 h of expression (Figure 3.7B) are absent after half the incubation time (Figure 3.8B, lanes 10 – 15). Reducing the duration of expression under optimal conditions does not produce soluble r*Pf*C0760c$_{297}$.

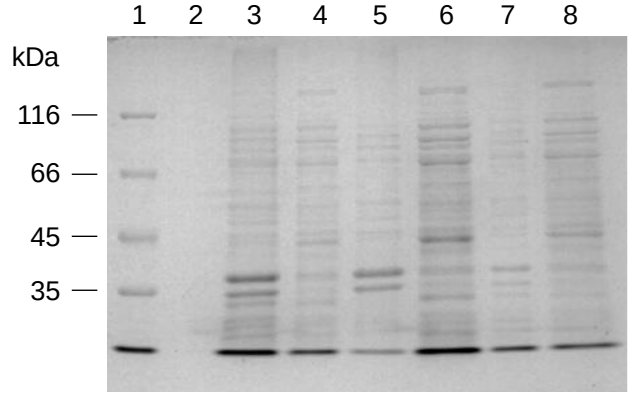

Figure 3.9: Expression of r*Pf*C0760c$_{297}$ at 20°C. Bacterial lysates were resolved on 12.5% reducing SDS-PAGE, and proteins were stained with Coomassie Blue. Lane 1: molecular weight marker. Lanes 3, 5, 7 contain insoluble fractions, and lanes 4, 6 and 8 contain soluble fractions from triplicate cultures.

Expression at a lower temperature was evaluated to determine if soluble recombinant protein could be produced (Sørensen and Mortensen, 2005). Figure 3.3 showed substantial growth at a temperature as low as 25°C. Growth at a lower temperature of 20°C was evaluated in terrific broth for 16 h. Expression at 20°C resulted in very little overall protein expression

(Figure 3.9). A 56 kDa r*Pf*C0760c$_{297}$ protein band is indistinguishable in the soluble and insoluble fractions (lanes 3 – 8).

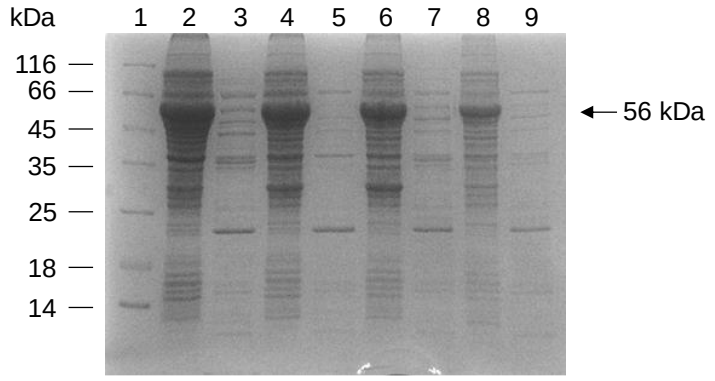

Figure 3.10: Expression of r*Pf*C0760c$_{297}$ in the presence of 0 – 3% (v/v) ethanol. Bacterial lysates were resolved on 12.5% reducing SDS-PAGE, and proteins were stained with Coomassie Blue. Lane 1: molecular weight marker. Insoluble and soluble fractions were analysed for each culture supplemented with the following concentrations of ethanol: lanes 2 and 3: 0%; lanes 4 and 5: 1% (v/v); lanes 6 and 7: 2% (v/v); lanes 8 and 9: 3% (v/v).

Expression of r*Pf*C0760c$_{297}$ was evaluated in the presence of ethanol. Terrific broth was prepared with increasing concentrations of ethanol and cultures were grown under the conditions outlined previously. The presence of ethanol in the culture media shows a marked decrease in the expression of r*Pf*C0760c$_{297}$ as the concentration of ethanol increases (Figure 3.10, lanes 4 – 9). The absence of ethanol shows the highest expression of r*Pf*C0760c$_{297}$, with the majority remaining in the insoluble fraction (lanes 2 and 3). There is no detectable r*Pf*C0760c$_{297}$ in the soluble fractions (lanes 5, 7 and 9).

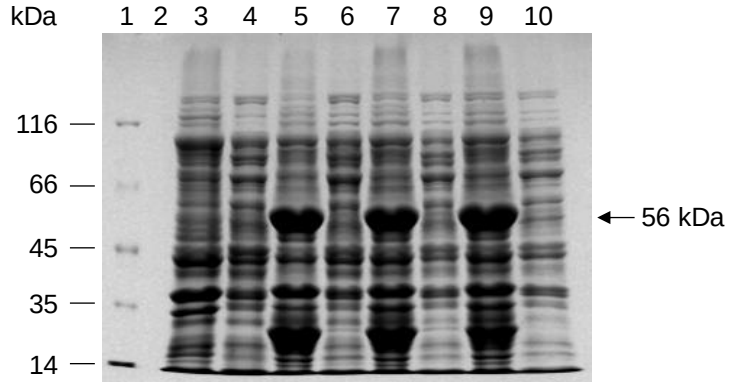

Figure 3.11: Induction of r*Pf*C0760c$_{297}$ expression at the stationary phase in LB media. Bacterial lysates were resolved on 12.5% reducing SDS-PAGE, and proteins were stained with Coomassie Blue. Lane 1: molecular weight marker. Lanes 3 and 4: cell lysates from uninduced *E. coli*. Lanes 5 and 6, 7 and 8, 9 and 10 contain insoluble and soluble fractions from triplicate induced cultures.

Cultures grown in LB media were induced with 0.3 mM IPTG in the stationary phase when the OD$_{600}$ was between 0.7 and 0.8 (Figure 3.11). The 56 kDa r*Pf*C0760c$_{297}$ band was absent in uninduced cultures (lanes 3 and 4). Induction at the stationary phase of cell growth resulted in improved expression levels of r*Pf*C0760c$_{297}$, which was insoluble (lanes 5 – 10). Presence

of soluble r*Pf*C0760c$_{297}$ protein is not evident in induced cultures (lanes 6, 8 and 10). The 30 kDa band is prominent in the insoluble fractions (lanes 5, 7 and 9). There is considerably more recombinant protein expressed when cultures were induced during the stationary phase in LB media compared to induction in the exponential phase (Figure 3.2, lanes 3 – 6).

Since none of the adjustments that were tested allowed for the expression of soluble r*Pf*C0760c$_{297}$, the r*Pf*C0760c$_{297}$ protein was solubilized before purification for downstream experiments.

3.2.4 Solubilization and purification of r*Pf*C0760c$_{297}$

After expression of r*Pf*C0760c$_{297}$, the insoluble fraction of the *E. coli* lysate was solubilized in a buffer containing the chaotropic detergent SDS under reducing conditions (Schlager *et al*., 2012).

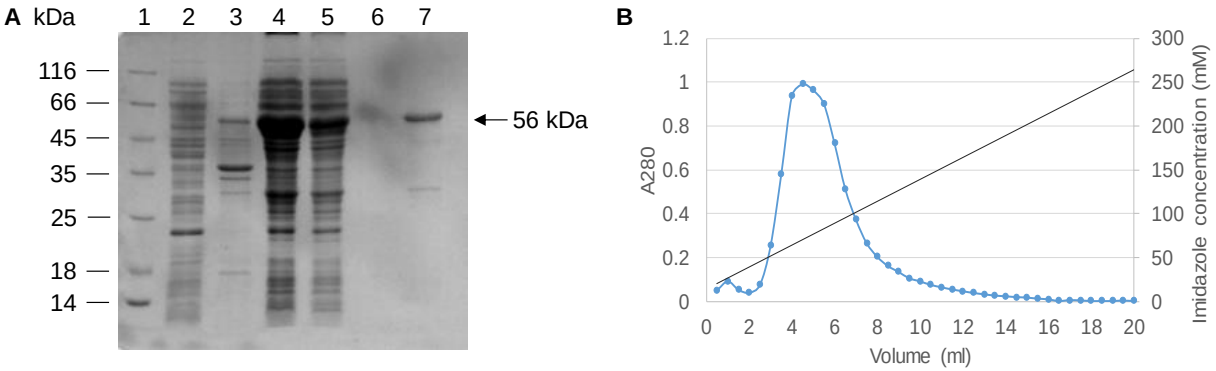

Figure 3.12: Solubilization and purification of r*Pf*C0760c$_{297}$ expressed under optimal conditions. The r*Pf*C0760c$_{297}$ protein was solubilized with SDS before affinity purification using nickel chelate affinity chromatography. Proteins were resolved on 12.5% reducing SDS-PAGE and stained with Coomassie Blue. **(A)** Lane 1: molecular weight marker. Lane 2: supernatant after Triton X-100 wash. Lane 3: pellet after SDS solubilization. Lane 4: solubilized material applied to the nickel column. Lane 5: unbound fraction. Lane 6: final wash with 20 mM imidazole. Lane 7: pooled purified r*Pf*C0760c$_{297}$. **(B)** Elution of r*Pf*C0760c$_{297}$ from a nickel column using an imidazole gradient from 20 – 270 mM.

The solubilization and purification of r*Pf*C0760c$_{297}$ from an *E. coli* lysate is illustrated (Figure 3.12A). Proteins are released after the bacterial cell pellet is washed with Triton X-100, and a faint band corresponding to r*Pf*C0760c$_{297}$ is noted (lane 2). Fewer insoluble proteins remain after treatment with SDS (lane 3), and the majority of r*Pf*C0760c$_{297}$ and many *E. coli* host proteins are solubilized (lane 4). The solubilized material was loaded onto a nickel NTA resin for purification, and the unbound fraction contained some r*Pf*C0760c$_{297}$ (lane 5). No protein was detected in the final wash (lane 6). The purified protein fractions were pooled (lane 7). The concentration of purified r*Pf*C0760c$_{297}$ was determined by the Bradford assay, and 22 mg of r*Pf*C0760c$_{297}$ was purified from 1 g of cell biomass from a 50 ml culture. From the imidazole gradient, a concentration of 150 mM imidazole was chosen for further purifications (Figure 3.12B).

3.3 Discussion

3.3.1 Recombinant expression of r*Pf*C0760c$_{297}$

To study and determine the biological functions of a protein, it must first be made available in a native, purified form. Proteins may be isolated from tissues however, a sufficient protein yield may be costly to acquire (Villaverde and Carrió, 2003). Isolation of sufficient native *Pf*C0760c would require large volumes of *P. falciparum*-infected red blood cells. Recombinant expression of proteins is an important technique, which can overcome these drawbacks (Tsumoto *et al*., 2003).

3.3.2 Recombinant expression of *P. falciparum* proteins

P. falciparum proteins are difficult to recombinantly express, as they tend to aggregate, or are not expressed (Mehlin *et al*., 2006). Expression of 1000 *P. falciparum* open reading frames in *E. coli* revealed only 63 soluble proteins (Mehlin *et al*., 2006). Proteins rich in asparagine-repeat regions such as *Pf*C0760c are more likely to form insoluble aggregates (Muralidharan and Goldberg, 2013). The genome of *P. falciparum* is rich in adenine and thymine residues, which is thought to contribute to recombinant proteins forming insoluble inclusion bodies (Flick *et al*., 2004; Gardner *et al*., 2002). As a result, *P. falciparum* proteins require codons that are rarely used by *E. coli* (Birkholtz *et al*., 2008). The genomic sequence of *Pf*C0760c is 49% adenine and 30% thymine residues. Unexpectedly, it was found that the adenine-thymine richness did not influence the solubility of *P. falciparum* proteins (Vedadi *et al*., 2007; Mehlin *et al*., 2006).

3.3.3 Bacterial inclusion bodies

Expression of large amounts of foreign protein in a bacterial host expression system is likely to form insoluble inclusion bodies (Schlager *et al*., 2012; Singh and Panda, 2005). Typically, inclusion bodies comprise inactive, misfolded protein aggregates that require solubilization and refolding before purification (Singh and Panda, 2005; Villaverde and Carrió, 2003; Baneyx, 1999).

Reducing conditions in bacterial cytosol prevent the formation of disulfide bonds, contributing to protein aggregation (Singh and Panda, 2005; Prinz *et al*., 1997). The full-length *Pf*C0760c protein contains 34 cysteine residues, 5 of which are present in r*Pf*C0760c$_{297}$. These cysteines may participate in disulfide bonding, which stabilises the protein structure (Wedemeyer *et al*., 2000). The 5 cysteine residues are possibly unable to form disulfide bonds or are not paired correctly. This has not been evaluated.

Other factors that contribute to inclusion body formation include the expression conditions, the size and amino acid sequence of the protein, thermal stress, a basic pI, and higher degree of disorder. (Mehlin *et al*., 2006; Villaverde and Carrió, 2003; Schein, 1989).

3.3.4 Growth profiles of bacterial cells

As expected, the growth profiles of transformed *E. coli* cells exhibited variations in growth rate. Different colonies were used for replicates as opposed to using a single seed culture.

In the transformed *E. coli* cells, minimal metabolic activity and cell density was observed in the lag phase (Madar *et al*., 2013), accounting for the first 2 h post-inoculation (Figure 3.1). During the lag phase, cells adapt to the growth conditions. Cells are not necessarily increasing in number, but the expression of genes that utilize the carbon source for the production of energy and building blocks is upregulated (Madar *et al*., 2013).

A sharp increase in cell growth indicates the exponential phase (Figure 3.1) (Maier, 2000). Cultures are usually induced to express recombinant protein in this phase, ensuring a large population of healthy cells, which should result in the high expression of recombinant protein.

The stationary phase constitutes equal amounts of multiplying and dying cells (Maier, 2000). Cell death is likely attributed to an accumulation of toxic metabolites, decreasing nutrients, or cell death signals, and is indicated by a plateau in the growth curve (Kram and Finkel, 2015).

3.3.5 Terrific broth expresses high levels of r*Pf*C0760c$_{297}$

E. coli bacteria transformed with pET32a and grown in terrific broth expressed large quantities of r*Pf*C0760c$_{297}$ (Figure 3.2). pET32a was chosen as it allowed the expression of a thioredoxin fusion protein (LaVallie *et al*., 1993). Terrific broth is a nutrient-rich auto-induction media (Lessard, 2013), that enhanced the expression of r*Pf*C0760c$_{297}$ and *E. coli* host proteins (Figure 3.2). The adenine-thymine richness of the *P. falciparum* genome can cause premature termination of the mRNA translation, which leads to truncated protein production (Flick *et al*., 2004). This could account for the 34 kDa and 30 kDa bands detected on the western blot by the mouse anti-his$_6$tag IgG antibodies (Figure 3.7B).

3.3.6 The thioredoxin fusion tag

The solubility of previously insoluble proteins was improved when expressed as thioredoxin fusion proteins. These included mammalian cytokines, WT1 tumour suppressor and its zinc finger domain expressed at a low temperature, and sea cucumber lysozyme (Cong *et al*., 2014; Fagerlund *et al*., 2012; LaVallie *et al*., 1993). Although r*Pf*C0760c$_{297}$ was expressed as a thioredoxin fusion protein, it remained insoluble. The *Canis* IFNα and IL-2 tyrosine kinase remained insoluble as thioredoxin fusion proteins (Yang *et al*., 2015; Joseph and Andreotti, 2008). Soluble *Canis* IFNα was obtained by fusion to the Nus tag, or by expression at a low

temperature when fused to thioredoxin (Yang *et al*., 2015). Thioredoxin fusion proteins may not be expressed as soluble proteins at higher temperatures, hence lower temperatures of expression should be evaluated.

3.3.7 Induction of recombinant protein expression with IPTG

IPTG is not metabolised by the cells and may have a toxic effect on bacterial host cells (Ahmad *et al*., 2018; Larentis *et al*., 2014; Kosinski *et al*., 1992). This is demonstrated by decreased protein synthesis, and upregulation of stress proteins similar to the response caused by heat shock (Kosinski *et al*., 1992). Presence of high concentrations of IPTG impaired the expression of *E. coli* host proteins (Figure 3.2 and 3.6).

The solubility and yield of the *Pf*EMP-1 domains were improved when expression was induced during the late stationary phase (Flick *et al*., 2004). A lower rate of protein expression during the stationary phase may facilitate correct protein folding (Flick *et al*., 2004). The yield of r*Pf*C0760c$_{297}$ was improved when cells were induced at the stationary phase, yet it remained insoluble. This could possibly be attributed to the high concentration of the accumulated protein.

3.3.8 Expression of recombinant protein at low temperatures

Expression at lower temperatures is known to improve the solubility of proteins (Sørensen and Mortensen, 2005; Schein, 1989). Slower growth of cells may allow for efficient protein folding, but sacrifices the yield of recombinant protein (Flick *et al*., 2004; Schein, 1989). Therefore, a lower temperature was expected to result in lower r*Pf*C0760c$_{297}$ and host protein expression (Figure 3.3). No soluble r*Pf*C0760c$_{297}$ was detected.

The falcipain-2 protease enzyme from *P. falciparum* was expressed as an inclusion body in *E. coli*, and failed to express in *Pichia pastoris* (Goh *et al*., 2003). Expression of falcipain-2 protease in *E. coli* TB1 as a maltose binding protein-fusion protein at a low temperature produced soluble protein (Goh *et al*., 2003). Thus, a lower temperature of recombinant protein expression in *E. coli* host cells may be a feasible avenue to explore to produce soluble recombinant protein.

3.3.9 Protein recombinant expression in the presence of ethanol

The presence of ethanol could possibly enhance protein solubility by inducing a stress response, forcing the cell to upregulate the expression of heat shock proteins (HSPs) (Ziemienowicz *et al*., 1993; Steczko *et al*., 1991; Lindquist and Craig, 1988). HSPs, also known as chaperones, help prevent protein aggregation by correctly folding misfolded proteins. On the contrary, increasing concentrations of ethanol suppressed the expression of r*Pf*C0760c$_{297}$ and host proteins, and did not improve r*Pf*C0760c$_{297}$ solubility (Figure 3.10).

3.3.10 Solubilization of recombinant proteins

Solubilization of inclusion bodies requires protein unfolding using high concentrations of a denaturant (Tsumoto *et al*., 2003). Solubilization is usually performed under reducing conditions to prevent oxidation of cysteine residues, and remove existing disulfide bonds within the inclusion bodies (Wingfield, 2001; Fischer *et al*., 1993). Solubilization of proteins with detergents is likely to form an ordered structure, folded into alpha-helices (Schlager *et al*., 2012; Tsumoto *et al*., 2003).

Protein solubilization with SDS is advantageous as it is cheap, the procedure is rapid and simple, and excess detergent is easily removed by cooling and centrifugation (Schlager *et al*., 2012). N-lauroyl sarcosine is a milder detergent compared to SDS, and is used for solubilization and refolding (Schlager *et al*., 2012; Burgess, 1996). The majority of the r*Pf*C0760c$_{297}$ protein was solubilized with SDS (Figure 3.12A) and was maintained in the soluble form with a low concentration of N-lauroyl sarcosine. SDS was successfully used to solubilize 17 different his$_6$tagged proteins and muscle proteins from different types of fish (Schlager *et al*., 2012; Rehbein and Karl, 1985). N-lauroyl sarcosine was used to solubilize RNA polymerase σ factors (Burgess, 1996).

3.3.11 Refolding and purification of r*Pf*C0760c$_{297}$

Gradual removal of the denaturant allows the protein to refold at an intermediate concentration of the denaturant (Tsumoto *et al*., 2003; Burgess, 1996). In this case, replacing SDS with a lower concentration of N-lauroyl sarcosine facilitates protein refolding (Schlager *et al*., 2012; Rogl *et al*., 1998). Aggregation during refolding and purification is prevented by the N-lauroyl sarcosine likely coating the exposed hydrophobic surfaces of the protein (Burgess, 1996).

For further analysis, the his$_6$tagged r*Pf*C0760c$_{297}$ protein was purified by nickel chelate affinity chromatography. A concentration of 20 mM imidazole was used in the wash buffer to help prevent non-specific binding of contaminant proteins to the resin. N-lauroyl sarcosine was included in the wash and elution buffers to maintain soluble r*Pf*C0760c$_{297}$.

3.3.12 Alternative solubilization methods

Other methods of protein solubilization from inclusion bodies include the use of urea or guanidine-HCl, which both denature protein (Singh and Panda, 2005; Wingfield, 2001). Using urea or guanidine-HCl for protein solubilization results in a flexible, disordered protein structure (Tsumoto *et al*., 2003). Solubilization with urea would require the urea solubilization solution to be freshly prepared before each experiment, as urea solutions have a propensity to decompose into ammonium cyanate, which would need to be removed (Wingfield, 2001).

Before further analysis, an additional dialysis step is necessary to remove the urea. Low concentrations of urea coupled with an alkaline pH shock was able to solubilize purified inclusion bodies containing human growth hormone (Singh and Panda, 2005).

There are several advantages of using SDS for solubilization rather than urea or guanidine-HCl. These include the low cost of SDS, ease of use, and the speed of protein solubilization (Schlager *et al*., 2012). In the SDS and N-lauroyl sarcosine protocol (Schlager *et al*., 2012), 34 mM of SDS was used, compared to 6 – 8 M urea or guanidine-HCl.

Various strategies may still be investigated to determine whether the solubility of r*Pf*C0760c$_{297}$ may be improved while maintaining a satisfactory yield. These include expression at low temperatures for longer periods of time, co-expression with *E. coli* chaperones, co-expression of *Plasmodium* chaperones, or expression with other vectors, fusion tags, or hosts. All these strategies would have to be evaluated and compared to the current strategy for yield and solubility.

3.3.13 Conclusion

Although high levels of the r*Pf*C0760c$_{297}$ protein was produced, r*Pf*C0760c$_{297}$ was prone to aggregation in inclusion bodies. The r*Pf*C0760c$_{297}$ protein was therefore solubilized and purified before subsequent studies.

Chapter 4: *E. coli* chaperone co-expression for the recombinant expression of soluble r*Pf*C0760c$_{297}$

4.1 Introduction

4.1.1 Chaperones

Proteins that prevent anomalous interactions between macromolecules are known as molecular chaperones (Bell *et al*., 2011). Heat shock proteins (HSPs) are a group of molecular chaperones that help to correctly fold misfolded or aggregated proteins to allow for correct protein conformation (Ryabova *et al*., 2013; Nishihara *et al*., 1998). As the name suggests, HSPs are expressed as a stress response to increased temperatures and other stresses in the cell (Bell *et al*., 2011; Lindquist and Craig, 1988). In bacterial recombinant protein expression, co-expression with chaperones may aid in the expression of soluble recombinant protein (Sørensen and Mortensen, 2005; Hartl and Hayer-Hartl, 2002).

4.1.2 *E. coli* chaperones

After bacterial ribosomal protein synthesis, some proteins may require chaperones to fold correctly (de Marco, 2007). These proteins may be *E. coli* host proteins, or plasmid-encoded recombinant proteins. Two plasmid-encoded *E. coli* chaperone systems were investigated for the expression of soluble r*Pf*C0760c$_{297}$. The pGro7 plasmid carries the GroEL-GroES chaperone system, the pKJE7 plasmid carries the *dna*K*dna*J*grp*E chaperone system, and the pG-KJE8 plasmid carries both the GroEL-GroES and *dna*K*dna*J*grp*E chaperone systems (Nishihara *et al*., 1998). These plasmids all encode a chloramphenicol resistance marker, and an *ara*B promoter triggered by L-arabinose for expression of the chaperones (Nishihara *et al*., 1998). The pG-KJE8 plasmid encodes a *Pzt*-1 promoter, which requires the addition of tetracycline for induction (Nishihara *et al*., 1998).

4.1.3 The GroEL-GroES chaperones

Correct folding of misfolded proteins by the GroEL-GroES chaperone system occurs in a controlled series of steps. The GroEL protein (60 kDa) forms a double-ringed cylinder, where each ring is composed of seven identical subunits (Ryabova *et al*., 2013; Mayhew *et al*., 1996). After protein synthesis, misfolded protein binds to the inner surface of GroEL. GroES (10 kDa) binds to the top of the GroEL cylinder and folding of the misfolded protein occurs within the GroEL chamber (Ryabova *et al*., 2013; Martin, 1998). The correctly folded protein is released from the chamber upon hydrolysis of ATP, along with dissociation of GroES from GroEL (Mayhew *et al*., 1996).

4.1.4 The *dna*K*dna*J*grp*E chaperones

The *dna*K*dna*J*grp*E chaperone system consists of a chaperone and two co-chaperones. The *dna*K chaperone (70 kDa) belongs to the HSP70 protein family (Bell *et al*., 2011; Glover and Lindquist, 1998; Schönfeld *et al*., 1995; Schröder *et al*., 1993). The *dna*J co-chaperone (40 kDa) is a HSP40 protein (Schönfeld *et al*., 1995; Glover and Lindquist, 1998), and the co-factor *grp*E (22 kDa) acts as a nucleotide exchange factor (Gamer *et al*., 1996; Schönfeld *et al*., 1995). The mechanism of protein folding with the *dna*K*dna*J*grp*E chaperones occurs as follows: firstly, the *dna*J co-chaperone binds to the misfolded protein, and this complex interacts with the *dna*K chaperone. The ATP attached to the *dna*K chaperone is hydrolysed to ADP (Szabo *et al*., 1994). The *dna*J co-chaperone speeds up hydrolysis of ATP to ADP (Bell *et al*., 2011). The release of ADP is facilitated by *grp*E (Szabo *et al*., 1994), allowing fresh ATP to bind, which triggers the release of the correctly folded protein (Szabo *et al*., 1994).

In this chapter, co-expression of r*Pf*C0760c$_{297}$ with the GroEL-GroES and *dna*K*dna*J*grp*E chaperone systems was explored under different expression conditions, aiming to express soluble r*Pf*C0760c$_{297}$.

4.2 Results

4.2.1 Co-expression of r*Pf*C0760c$_{297}$ with *E. coli* chaperones in LB media

Competent *E. coli* BL21(DE3) cells containing pET32a-r*Pf*C0760c$_{297}$ were co-transformed with plasmids encoding *E. coli* chaperones.

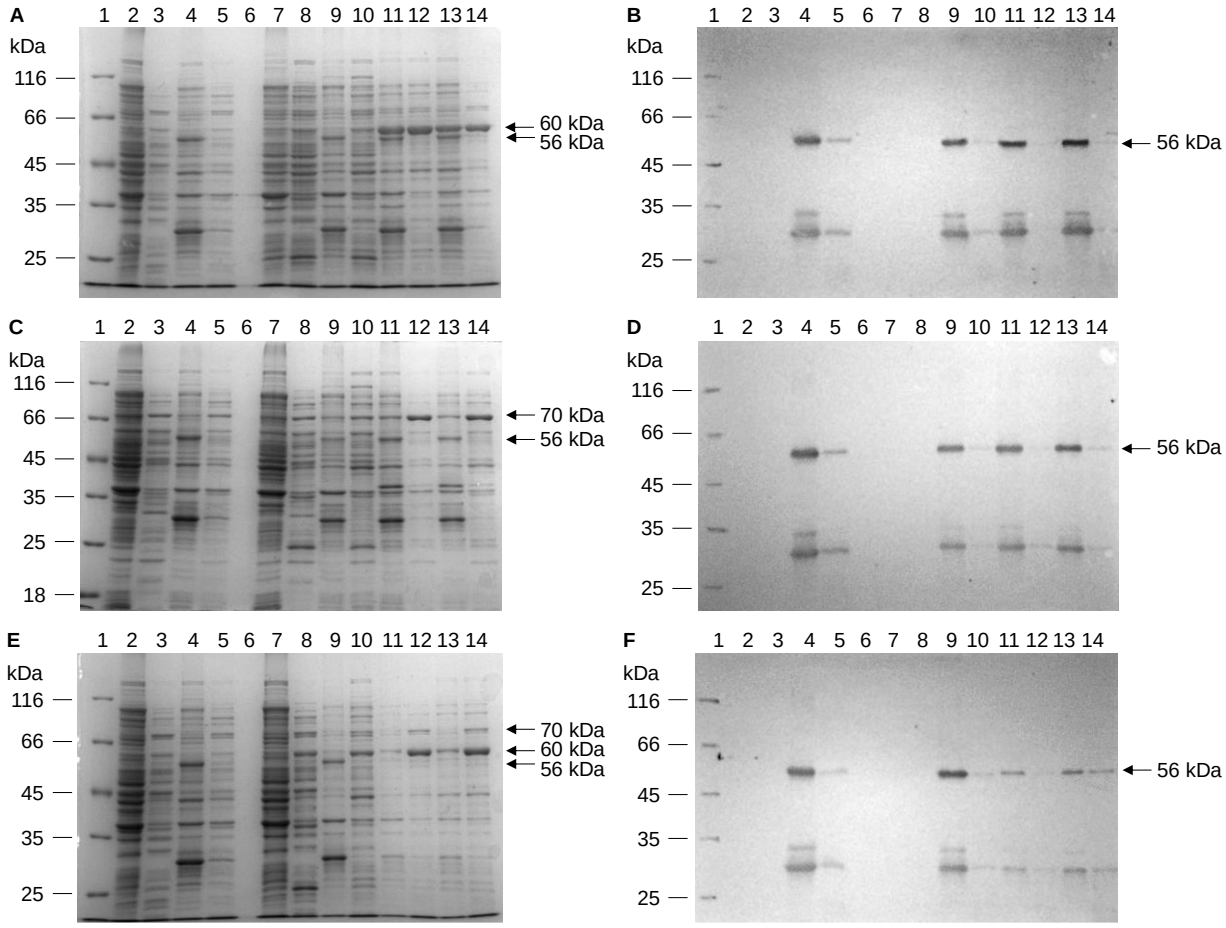

Figure 4.1: Co-expression of r*Pf*C0760c$_{297}$ with *E. coli* chaperones. *E. coli* BL21(DE3) cells expressing r*Pf*C0760c$_{297}$ were grown with the chaperones: **A, B:** GroEL-GroES; **C, D:** *dna*K*dna*J*grp*E; **E, F:** GroEL-GroES and *dna*K*dna*J*grp*E. **A, C, E:** Proteins were resolved on 12.5% reducing SDS-PAGE and stained with Coomassie Blue. Lane 1: molecular weight marker. Insoluble and soluble fractions were loaded for each sample in consecutive lanes. Lanes 2 – 5 contain pET32a-r*Pf*C0760c$_{297}$ cell lysates. Lanes 2 and 3: uninduced, lanes 4 and 5: induced. Lanes 7 – 14 contain lysates from co-transformed cells. Lanes 7 and 8: uninduced cells, lanes 9 and 10: co-transformed cells expressing r*Pf*C0760c$_{297}$, lanes 11 and 12, 13 and 14: duplicate cultures co-expressing r*Pf*C0760c$_{297}$ and chaperones. **B, D, F:** Western blots of gels in A, C, E were probed with chicken anti-r*Pf*C0760c$_{297}$ IgY and rabbit anti-chicken HRPO-IgG.

Expression of r*Pf*C0760c$_{297}$ was not detected in uninduced cultures (Figure 4.1A – F, lanes 2, 3, 7 and 8). Induced cultures express r*Pf*C0760c$_{297}$ (56 kDa), along with a 34 kDa and a 30 kDa band detected by the chicken anti-r*Pf*C0760c$_{297}$ IgY in the western blot. Most of these proteins were in the insoluble fraction (Figure 4.1A – F, lanes 4, 5, and 9 – 14). Where expression of the chaperones was not induced, the expression of r*Pf*C0760c$_{297}$ was unaffected (Figure 4.1A – F, lanes 7 and 8). Co-expression of any of these chaperones does not improve the solubility of r*Pf*C0760c$_{297}$ (Figure 4.1A – F, lanes 11 – 14). The GroEL and *dna*K chaperones are shown at 60 kDa (Figure 4.1A and C, lanes 11 – 14) and 70 kDa respectively (Figure 4.1C and E, lanes 11 – 14). These chaperones are present in low concentrations in cells that have not been co-transformed (Figure 4.1A, C and E, lanes 2 – 5) and in uninduced

cells (Figure 4.1A, C and E, lanes 7 – 10). Overall, the chaperones did not improve the solubility of r*Pf*C0760c$_{297}$ under the conditions evaluated.

4.2.2 Co-expression of r*Pf*C0760c$_{297}$ with *E. coli* chaperones in terrific broth

Conditions for high yields of r*Pf*C0760c$_{297}$ were established in Chapter 3 (Figure 3.2). These conditions were used to evaluate the co-expression of the *E. coli* chaperones with r*Pf*C0760c$_{297}$.

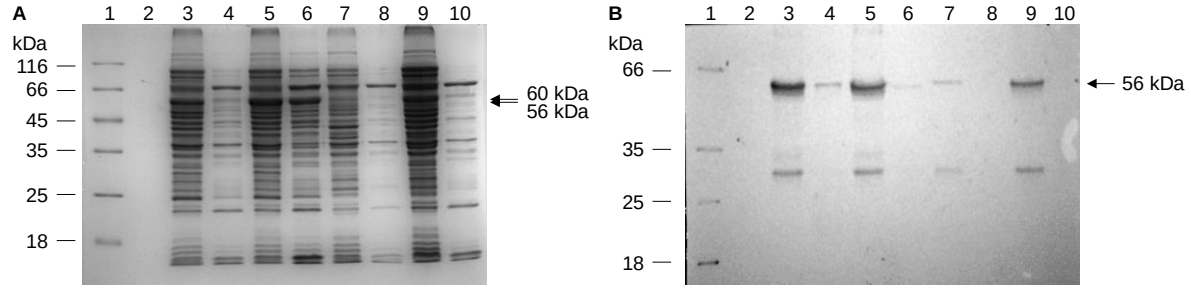

Figure 4.2: Co-expression of r*Pf*C0760c$_{297}$ with *E. coli* chaperones in terrific broth. (A) Proteins were resolved on 12.5% reducing SDS-PAGE and stained with Coomassie Blue. Lane 1: molecular weight marker. Insoluble and soluble fractions were analysed for each sample in consecutive lanes. Lanes 3 and 4: uninduced GroEL-GroES. Lanes 5 – 10: induced co-expression of r*Pf*C0760c$_{297}$ and *E. coli* chaperones. Lanes 5 and 6: GroEL-GroES. Lanes 7 and 8: *dna*K*dna*J*grp*E. Lanes 9 and 10: GroEL-GroES and *dna*K*dna*J*grp*E. **(B)** Western blot of an identical gel probed with chicken anti-r*Pf*C0760c$_{297}$ IgY and rabbit anti-chicken HRPO-IgG.

Similar quantities of r*Pf*C0760c$_{297}$ were produced in terrific broth in the presence and absence of GroEL-GroES chaperones, with the majority of r*Pf*C0760c$_{297}$ found in the insoluble fraction (Figure 4.2A and B, lanes 3 – 6). Soluble r*Pf*C0760c$_{297}$ was not detected upon co-expression with *dna*K*dna*J*grp*E, or both chaperones (Figure 4.2A and B, lanes 7 - 10). Low concentrations of the insoluble 34 kDa protein detected in the presence and absence of GroEL-GroES (lanes 3 and 5). The 30 kDa band is detected in all the insoluble fractions (lanes 3, 5, 7, and 9).

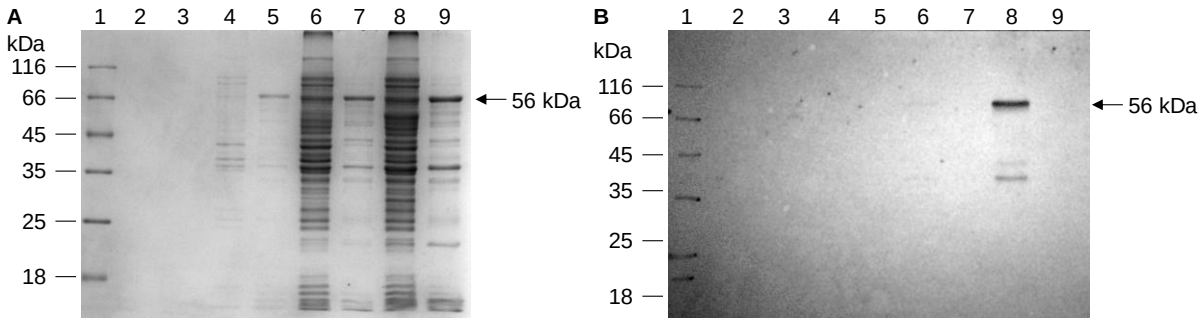

Figure 4.3: Co-expression of r*Pf*C0760c$_{297}$ with the *dna*K*dna*J*grp*E chaperones for 8 h in terrific broth. r*Pf*C0760c$_{297}$ was co-expressed with *dna*K*dna*J*grp*E and samples were removed every 2 h. **(A)** Proteins were resolved on 12.5% reducing SDS-PAGE and stained with Coomassie Blue. Lane 1: molecular weight marker. Insoluble and soluble fractions were analysed in consecutive lanes: lanes 2 and 3: 2 h, lanes 4 and 5: 4 h, lanes 6 and 7: 6 h, lanes 8 and 9: 8 h. **(B)** Western blot of an identical gel was probed with chicken anti-r*Pf*C0760c$_{297}$ IgY and rabbit anti-chicken HRPO-IgG.

Previously, r*Pf*C0760c$_{297}$ was expressed as an insoluble protein in terrific broth between 6 and 8 hours (Figure 3.8). r*Pf*C0760c$_{297}$ was co-expressed with the *dna*K*dna*J*grp*E chaperones in terrific broth and samples were taken every 2 hours. No protein is detected after the first 2 h of co-expression, as there is little cell growth (Figure 4.3A, lanes 2 and 3). After 4 h, a few proteins are seen, and r*Pf*C0760c$_{297}$ is not detected by western blot (Figure 4.3A and B, lanes 4 and 5). Similar to the result presented in Figure 3.9, a small amount of insoluble r*Pf*C0760c$_{297}$ was detected after 6 h, which increased after 8 h expression and remained insoluble (Figure 4.3B, lanes 6 – 9). The presence of the *dna*K*dna*J*grp*E chaperones had no effect on the solubility of r*Pf*C0760c$_{297}$ when grown in terrific broth.

4.2.3 Induction of r*Pf*C0760c$_{297}$ expression with various concentrations of IPTG in LB media

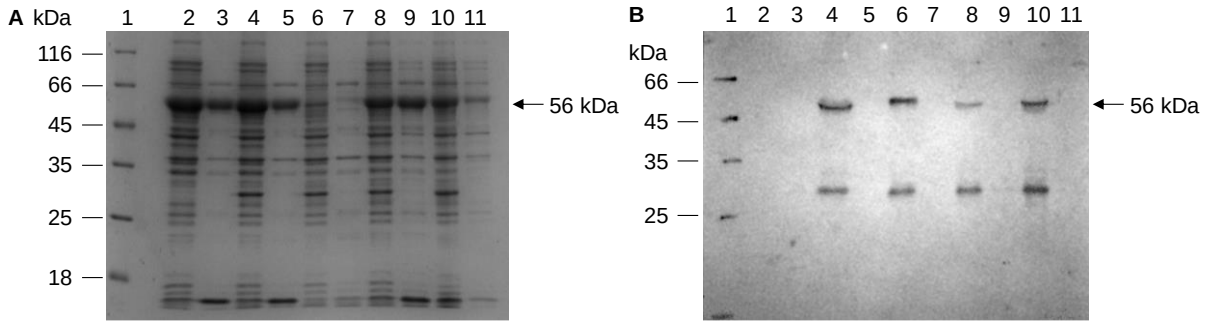

Figure 4.4: Different IPTG concentrations for the induction of r*Pf*C0760c$_{297}$ co-expression with GroEL-GroES chaperones. (A) Proteins were resolved on 12.5% reducing SDS-PAGE and stained with Coomassie Blue. Lane 1: molecular weight marker. Insoluble and soluble fractions were analysed for each sample in consecutive lanes. Cells were induced with the following concentrations of IPTG: lanes 2 and 3: 0 mM, lanes 4 and 5: 0.05 mM, lanes 6 and 7: 0.1 mM, lanes 8 and 9: 0.2 mM, and lanes 10 and 11: 0.3 mM. **(B)** Western blot of an identical gel was probed with chicken anti-r*Pf*C0760c$_{297}$ IgY and rabbit anti-chicken HRPO-IgG.

The concentration of IPTG for soluble r*Pf*C0760c$_{297}$ expression was evaluated in Chapter 3 (Figure 3.6). Co-expression of r*Pf*C0760c$_{297}$ in the presence of 0 – 0.3 mM IPTG with the GroEL-GroES chaperones were evaluated (Figure 4.4, lanes 2 – 11). A concentration of 0.2 mM IPTG reduces the expression of GroEL (Figure 4.4A, lanes 6 and 7). Soluble r*Pf*C0760c$_{297}$ was not detected when the concentrations of IPTG was varied in the presence of GroEL (Figure 4.4B, lanes 5, 7, 9, 11). The amount of r*Pf*C0760c$_{297}$ expressed with the different concentrations of IPTG is similar in the presence of induced GroEL-GroES (Figure 4.5B, lanes 4, 6, 8 and 10).

4.2.4 Induction of chaperone co-expression with L-arabinose

To determine whether soluble r*Pf*C0760c$_{297}$ could be expressed with lower amounts of the *E. coli* chaperones present, the concentration of L-arabinose was varied. Tetracycline and IPTG were kept at a fixed concentration.

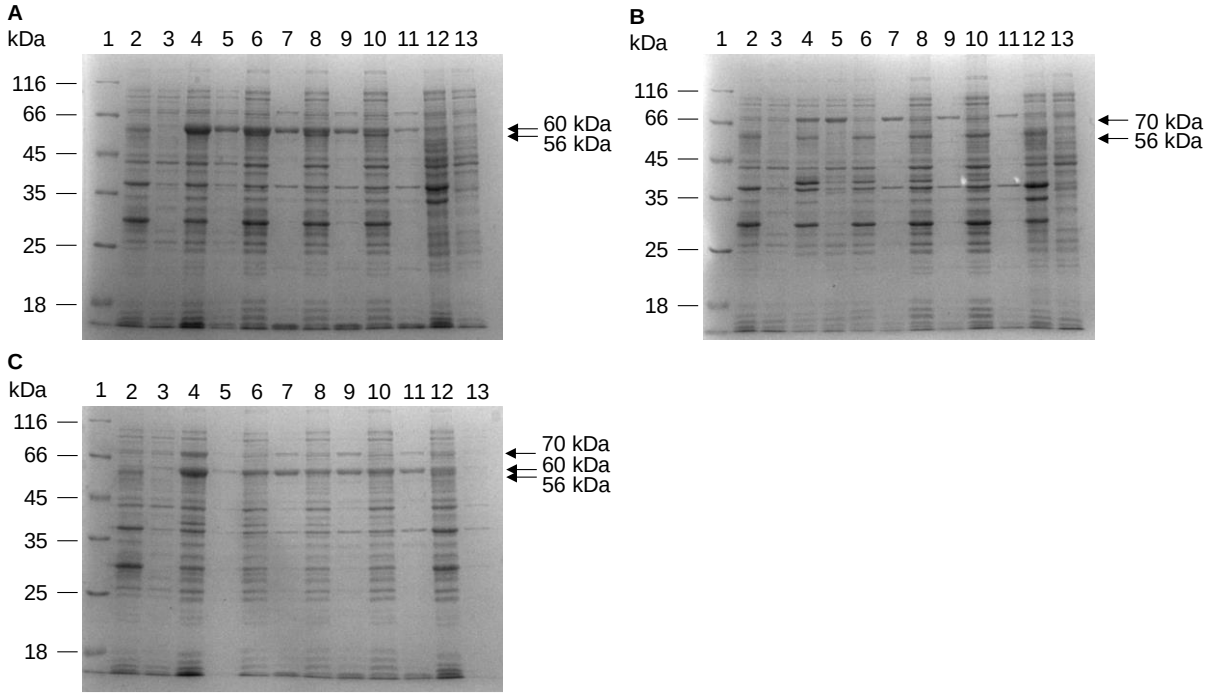

Figure 4.5: Induction of chaperone co-expression with different concentrations of L-arabinose. L-arabinose from 1 – 0 mg/ml was used to induce chaperone co-expression with r*Pf*C0760c$_{297}$. Proteins were resolved on 12.5% reducing SDS-PAGE stained with Coomassie Blue. r*Pf*C0760c$_{297}$ was co-expressed with **(A)** GroEL-GroES, **(B)** *dna*K*dna*J*grp*E, **(C)** GroEL-GroES and *dna*K*dna*J*grp*E. Lane 1: molecular weight marker. Insoluble and soluble fractions were analysed for each sample in consecutive lanes. Lanes 2 and 3: cells expressing r*Pf*C0760c$_{297}$. The following concentrations of L-arabinose were used: lanes 4 and 5: 1 mg/ml, lanes 6 and 7: 0.75 mg/ml, lanes 8 and 9: 0.5 mg/ml, lanes 10 and 11: 0.25 mg/ml and lanes 12 and 13: 0 mg/ ml.

r*Pf*C0760c$_{297}$ is present at similar concentrations, regardless of the chaperone used or the concentration of L-arabinose (Figure 4.5A – C). As expected, a decrease in the L-arabinose concentration decreases the amount of the GroEL and *dna*K*dna*J*grp*E chaperones expressed (Figure 4.5A – C, lanes 4 – 13). A change in the amount of the *E. coli* chaperones expressed did not influence the expression of soluble r*Pf*C0760c$_{297}$.

4.4 Discussion

4.4.1 r*Pf*C0760c$_{297}$ is an insoluble recombinant protein

The r*Pf*C0760c$_{297}$ protein was expressed in insoluble inclusion bodies under different growth conditions (Chapter 3). The data obtained after chaperone co-expression under the

different conditions indicate that co-expression of the *E. coli* chaperones did not have a detectable influence on the expression of soluble r*Pf*C0760c$_{297}$.

Chaperones have been shown to improve the solubility of proteins that are prone to aggregation. Co-expression with GroEL-GroES or *dna*K*dna*J*grp*E improved the solubility of aggregation-prone proteins from mutant *E. coli* cells deficient in HSPs, Japanese cedar pollen protein Cryj2 and recombinant humanised anti-epidermal growth factor receptor scFv antibody (Veisi *et al*., 2015; Nishihara *et al*., 1998; Gragerov *et al*., 1992).

The GroEL-GroES and *dna*K*dna*J*grp*E chaperones act synergistically to prevent protein aggregation (Gragerov *et al*., 1992). Five insoluble proteins co-expressed with different combinations of ClpB, GroEL-GroES, and *dna*K*dna*J*grp*E chaperones resulted in soluble expression (de Marco *et al*., 2007). Induction of both GroEL-GroES and *dna*K*dna*J*grpE* chaperones did not improve r*Pf*C0760c$_{297}$ solubility (Figure 4.1F).

Like r*Pf*C0760c$_{297}$, some proteins remain insoluble when co-expressed with chaperones (de Marco *et al*., 2007). IL-2 tyrosine kinase and four *P. falciparum* glideosome proteins co-expressed with GroEL-GroES and both GroEL-GroES and *dna*K*dna*J*grp*E remained insoluble when expressed at low temperatures (Joseph and Andreotti, 2008). The solubility of recombinant myosin A, gliding-associated protein-45 and gliding-associated protein-50 from *P. falciparum* was not improved when co-expressed with GroEL-GroES and *dna*K*dna*J*grp*E (Guerra *et al*., 2016).

4.4.2 Co-expression of r*Pf*C0760c$_{297}$ with *E. coli* chaperones in terrific broth

Terrific broth produced large amounts of r*Pf*C0760c$_{297}$, but doesn't induce expression of plasmid-encoded chaperones. However, co-expression with any chaperone produced lower amounts of r*Pf*C0760c$_{297}$ in terrific broth. The majority of the r*Pf*C0760c$_{297}$ remained insoluble (Figure 4.3).

r*Pf*C0760c$_{297}$ is expressed between 4 and 6 hours and is insoluble. It is possible that the chaperones are absent at this time, which can be confirmed by western blot with chaperone-specific antibodies. Presence of the chaperone at the time of r*Pf*C0760c$_{297}$ expression could determine whether they are capable of folding r*Pf*C0760c$_{297}$. In the presence of large amounts of GroEL, the r*Pf*C0760c$_{297}$ remains insoluble (Figure 4.1 and Figure 4.5A). Soluble r*Pf*C0760c$_{297}$ may not be detected due to insufficient lysis observed in Figures 4.4 and 4.5.

Interestingly, the truncated forms of r*Pf*C0760c$_{297}$ are absent after 6 – 8 hours (Figure 3.8B), but present with *dna*K*dna*J*grp*E co-expression (Figure 4.3B).

4.4.3 *P. falciparum* heat shock proteins

The genome of *P. falciparum* encodes 6 HSP70 proteins and 43 HSP40 proteins, suggesting that chaperones play a key role in parasite survival (Botha *et al*., 2007).

Plasmodium chaperones function under a range of conditions, including the temperature of the mosquito host, natural body temperature of a human, and human body temperature during a febrile incident (Przyborski *et al*., 2015; Bell *et al*., 2011). It is therefore likely, that *Plasmodium* proteins require chaperone-assisted folding and protection under stressful conditions.

4.4.4 Co-expression of recombinant proteins with non-*E. coli* chaperones

Production of soluble IL-2 tyrosine kinase was achieved by co-expression with the Cpn60/10 chaperone in *Oleispira antarctica* at low temperatures (Joseph and Andreotti, 2008). Co-expression of proteins in *E. coli* with chaperones from the same species have been reported to improve the yield of soluble recombinant protein. The solubility of human cytochrome P450 1A2 and the long tail fibre protein gp37 from bacteriophage T4 were improved upon co-expression with same-species chaperones (Bartual *et al*., 2010; Ahn *et al*., 2004).

P. falciparum PFI1155w is an asparagine-repeat rich protein that formed inclusion bodies in a mammalian expression system. The solubility of *P. falciparum* PFI1155w was improved upon co-expression with the *P. falciparum* HSP110 chaperone (Muralidharan *et al*., 2012). *P. falciparum* HSP70 has been successfully expressed in *E. coli*, and improved the yield of soluble *P. falciparum* GTP cyclohydrolase I (Stephens *et al*., 2011; Matambo *et al*., 2004). A chimeric HSP70 (K*Pf*) was engineered to co-operate with *E. coli* chaperones, and bind to *Plasmodium* proteins to enable folding (Makhoba *et al*., 2016; Shonhai *et al*., 2005). Co-expression of K*Pf* improved the quality of *P. falciparum* S-adenosylmethionine decarboxylase (Makhoba *et al*., 2016). *P. falciparum* HSP70 (Accession: P11144.2) and *E. coli dna*K (Accession: P0A6Y8.2) share ~44% amino acid sequence identity. The *P. falciparum* HSP70 and K*Pf* are attractive candidates for co-expression with r*Pf*C0760c$_{297}$.

Other chaperone co-expression avenues that may be explored include co-expression at lower temperatures and removal of the IPTG inducer after induction of recombinant protein expression. Other chaperones may also be evaluated for co-expression with r*Pf*C0760c$_{297}$ in *E. coli*, such as *Pf*HSP70, K*Pf* and *Pf*HSP110 from *P. falciparum*, or *E. coli* ClpB or trigger factor. Chemical additives and different host cells may also be evaluated (Prasad *et al*., 2011).

4.4.5 Conclusion

None of the co-expression conditions that were evaluated in this study improved the solubility of r*Pf*C0760c$_{297}$. The optimized expression conditions allowed for higher expression of insoluble r*Pf*C0760c$_{297}$ compared to all the chaperone co-expression conditions. Based on the results presented in this chapter, and the ethanol experiment in Chapter 3, it is concluded that these *E. coli* chaperones are unable to correctly fold the r*Pf*C0760c$_{297}$ protein to allow for

its solubility. There is no evidence to suggest that the chaperones did or did not bind to r*Pf*C0760c$_{297}$.

Chapter 5: Protein-protein interactions between r*Pf*C0760c$_{297}$ and monocyte proteins

5.1 Introduction

5.1.1 White blood cells in the immune system

White blood cells form an integral part of the innate immune system and are synthesized in the bone marrow (Serbina *et al*., 2008). These cells develop from a hematopoietic stem cell and differentiate into different cell types in the bone marrow. Unlike red blood cells, white blood cells are nucleated. Basophils, eosinophils, neutrophils, lymphocytes and monocytes are types of white blood cells, which are phenotypically different and perform specific immune functions (Tajuddin *et al*., 2016). White blood cell counts can be used as markers for infection, and are significantly low in acute *P. falciparum* and *P. vivax* malaria infections (Tangpukdee *et al*., 2008).

5.1.2 Function of monocytes

Monocytes are a group of mononuclear white blood cells derived from hematopoietic stem cells, with a bean-shaped nucleus (Chua *et al*., 2013; Geissmann *et al*., 2003). They are the largest of the white blood cells that circulate in the bloodstream. Monocytes can further be divided into subsets based on the expression of different cell surface markers or receptors. Phagocytic monocytes express CD14, and monocytes involved in the activation of T-cells express CD16 (Serbina *et al*., 2008). On the cell surface, human monocytes express CD11b, CD11c and CD14, and mouse monocytes express CD11b and F4/80 (Geissmann *et al*., 2003). During an infection, CD11b-mediated activation of inflammatory cells is vital for parasite clearance (Serbina *et al*., 2008).

Upon entry into tissues, monocytes differentiate into tissue-specific macrophages. Monocytes in the blood may also differentiate into dendritic cells, which can enter lymph nodes (Kantari *et al*., 2008). The functions of monocytes, dendritic cells and macrophages include phagocytosis of pathogens, apoptotic cells and infected red blood cells, antigen presentation to T-cells, and the release of proinflammatory cytokines and chemokines (Zhou *et al*., 2015; Kantari *et al*., 2008; Ziegler-Heitbrock, 2007). These functions are usually receptor-mediated. During a *Plasmodium* infection, monocyte-mediated phagocytosis is initiated by binding of complement and IgG to infected red blood cells (Turrini *et al*., 1992).

Pattern recognition receptors expressed on the surface of monocytes detect an infection by recognition of pathogen-associated molecular patterns expressed by parasites or other pathogens (Sampaio *et al*., 2018; Kawai and Akira, 2009). Toll-like receptors are pattern

recognition receptors that are involved in *Plasmodium* parasite recognition (Kawai and Akira, 2009).

5.1.3 Protein-protein interactions

Protein-protein interactions are defined as the intentional, specific physical contact and molecular docking between intracellular proteins or in an *in vivo* system (De Las Rivas and Fontanillo, 2010). Identification of protein-protein interactions is important for the determination of *in vivo* protein function and drug efficiency (Rao *et al*., 2014). Proteins seldom work alone when performing biological functions (De Las Rivas and Fontanillo, 2010). Interaction of a protein of unknown function with a protein of known function could help delineate the function of the unknown protein (Rao *et al*., 2014). Interaction of host immune proteins and cell surface receptors with parasite proteins may help understand disease pathogenesis. Understanding these interactions may also help clarify mechanisms underlying host immune detection of pathogens (Kawai and Akira, 2009). Disease management and novel drug design may be improved by interpretation of host immune interactions with *Plasmodium* parasites (Chua *et al*., 2013).

In this study, proteins from U937 and J774A.1 cell lysates were analysed for protein-protein interactions with r*Pf*C0760c$_{297}$. Since *Pf*C0760c is an uncharacterized protein with no known function or defined interactions, this study was conducted to determine if there are any mammalian proteins that interact with *Pf*C0760c. The *Pf*C0760c protein is predicted to localize in the parasite nucleus. Therefore, interactions of *Pf*C0760c with monocytes and macrophages may occur after immunological processing of parasite-infected host cells.

5.2 Results

5.2.1 Selection of chicken IgY concentrations for far dot blot analysis

Figure 5.1: Far dot blot analysis of chicken IgY probed with r*Pf*C0760c$_{297}$. Concentrations of 1, 10 and 50 µg of **(A)** chicken anti-r*Pf*C0760c$_{297}$ IgY and **(B)** chicken anti-rabbit albumin IgY were dotted onto nitrocellulose. Blots were incubated with 5 µg r*Pf*C0760c$_{297}$, and interactions were detected with mouse anti-his$_6$tag IgG and goat anti-mouse HRPO-IgG.

Protein-protein interactions between his$_6$tagged r*Pf*C0760c$_{297}$ and anti-r*Pf*C0760c$_{297}$ and anti-rabbit albumin chicken IgY antibodies were assessed by far dot blot. r*Pf*C0760c$_{297}$ complexed to chicken IgY were detected with mouse anti-his$_6$tag IgG and goat anti-mouse HRPO-IgG (Figure 5.1). No interaction is evident with 1 µg, a faint signal is observed with 10 µg, and a stronger signal is observed with 50 µg chicken anti-r*Pf*C0760c$_{297}$ IgY (Figure 5.1A).

No interaction is observed with chicken anti-rabbit albumin IgY (Figure 5.1B). These antibodies were used as positive and negative controls respectively in further protein-protein interaction studies with r*Pf*C0760c$_{297}$.

5.2.2 Detection of monocyte peroxidase activity by dot blot analysis

Monocytes exhibit peroxidase activity (Bodel *et al*., 1977). To determine whether monocyte-intrinsic peroxidase activity was evident in a dot blot, monocyte lysates were dotted onto nitrocellulose along with control proteins, and the substrate was applied. No peroxidase activity was evident in either the U937 or J774A.1 monocytes under these conditions (data not shown). The control proteins BSA, chicken anti-rabbit albumin IgY, chicken anti-r*Pf*C0760c$_{297}$ IgY and the r*Pf*C0760c$_{297}$ did not show peroxidase activity (data not shown). Therefore, reactions with r*Pf*C0760c$_{297}$ are due to the binding of the bait protein r*Pf*C0760c$_{297}$ to prey proteins on the blot, and not due to intrinsic monocyte peroxidase activity as a result of the addition of the peroxidase substrate.

5.2.3 Far western blot analysis of control proteins

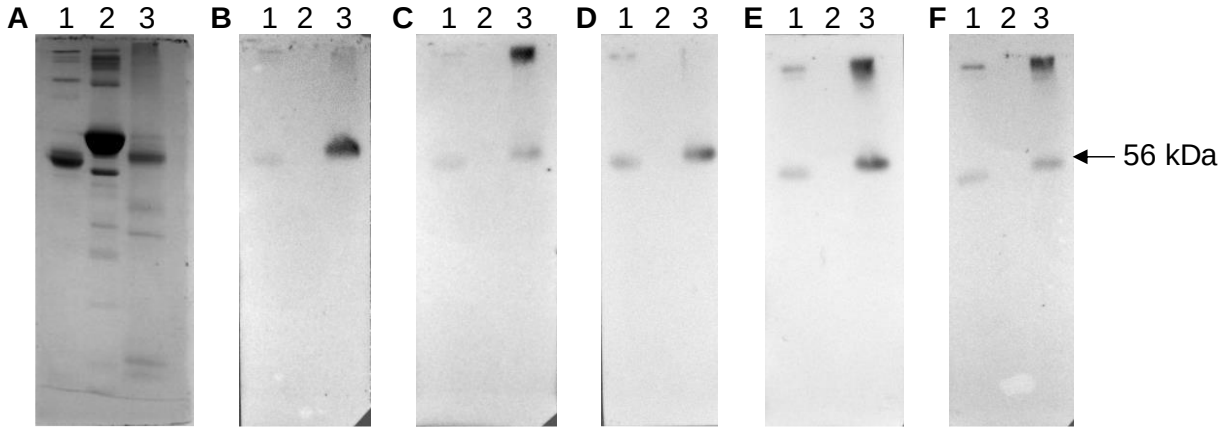

Figure 5.2: Far western blot analysis of positive and negative controls probed with increasing concentrations of r*Pf*C0760c$_{297}$. (A) Proteins were resolved on 12.5% non-reducing SDS-PAGE and stained with Coomassie Blue. Lane 1: chicken anti-r*Pf*C0760c$_{297}$ IgY, lane 2: BSA, lane 3: r*Pf*C0760c$_{297}$. Far western blots of identical gels were probed with increasing concentrations of r*Pf*C0760c$_{297}$: **(B)** 5 µg, **(C)** 10 µg, **(D)** 25 µg, **(E)** 50 µg and **(F)** 100 µg. Interactions were detected with mouse anti-his$_6$tag IgG and goat anti-mouse HRPO-IgG, and developed by ECL.

The bait protein used in all far western blot analyses was the r*Pf*C0760c$_{297}$ protein. To determine a suitable concentration of r*Pf*C0760c$_{297}$ for incubation, chicken anti-r*Pf*C0760c$_{297}$ IgY, BSA and r*Pf*C0760c$_{297}$ were analysed by far western blot. In the chicken anti-r*Pf*C0760c$_{297}$ IgY sample, several protein bands are present (Figure 5.2A, lane 1). The highest concentration of chicken anti-r*Pf*C0760c$_{297}$ IgY is present at a size which is smaller (lane 1) than the 56 kDa r*Pf*C0760c$_{297}$ (lane 3). Two protein bands in the chicken anti-r*Pf*C0760c$_{297}$ IgY sample interacted with a range of concentrations of r*Pf*C0760c$_{297}$ (Figure 5.2B – F, lane 1). This does not appear to be a concentration-dependent interaction. No

interaction was observed between BSA and r*Pf*C0760c$_{297}$ (Figure 5.2B – F, lane 2). r*Pf*C0760c$_{297}$ is detected by mouse anti-his$_6$tag IgG (Figure 5.2B – F, lane 3).

5.2.4 Western blot analysis of monocyte proteins

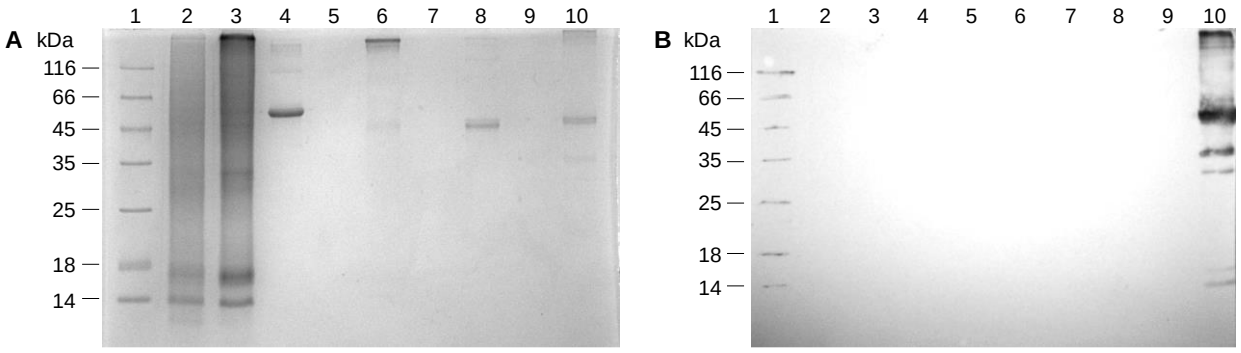

Figure 5.3: Western blot of U937 and J774A.1 monocyte lysate proteins. (A) Proteins were resolved on 12.5% non-reducing SDS-PAGE and stained with Coomassie Blue. Lane 1: molecular weight marker. Lane 2: U937 lysate. Lane 3: J774A.1 lysate. Lane 4: BSA. Lane 6: chicken anti-rabbit albumin IgY. Lane 8: chicken anti-r*Pf*C0760c$_{297}$ IgY. Lane 10: r*Pf*C0760c$_{297}$. **(B)** Western blot of an identical gel probed with mouse anti-his$_6$tag IgG and goat anti-mouse HRPO-IgG, and developed by ECL.

To ensure that the primary and secondary antibodies in the detection system do not bind non-specifically to monocyte lysate proteins, a western blot was performed. The U937 and J774A.1 monocyte lysate proteins and control proteins were probed with mouse anti-his$_6$tag IgG (Figure 5.3). The sizes of the proteins from the U937 and J774A.1 lysates ranged from smaller than 14 kDa to larger than 116 kDa (Figure 5.3A, lanes 2, 3). The mouse anti-his$_6$tag IgG antibody and the goat anti-mouse HRPO-IgG did not detect any human or mouse monocyte lysate proteins or control proteins (Figure 5.3B, lanes 2 – 8). Purified r*Pf*C0760c$_{297}$ was detected with the mouse anti-his$_6$tag IgG antibody (Figure 5.3B, lane 10). The primary antibody binds specifically to his$_6$tag-r*Pf*C0760c$_{297}$. BSA (Figure 5.3A, lane 4) appears smaller in size compared to the 66 kDa band in the molecular weight marker, as non-reducing conditions were used.

5.2.5 Detection of monocyte peroxidase activity by western blot

To determine if intrinsic monocyte peroxidase activity could be detected, monocyte lysate proteins and controls were assessed. Following electrophoretic protein transfer, the U937 and J774A.1 monocyte lysate proteins and the control proteins displayed no peroxidase activity (data not shown). This corroborates the results obtained by dot blot (Section 5.2.2).

5.2.6 Far western blot analysis of monocyte lysate proteins and r*Pf*C0760c$_{297}$

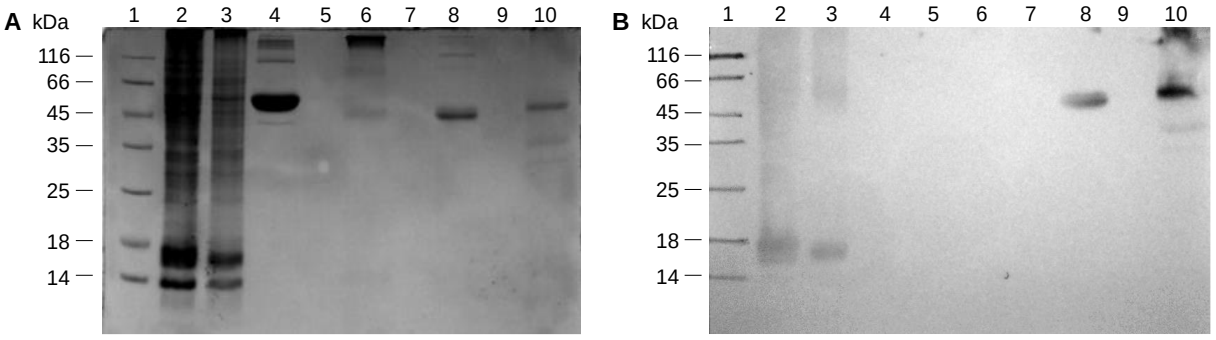

Figure 5.4: Far western blot analysis of U937 and J774A.1 lysates probed with r*Pf*C0760c$_{297}$. Monocytes were analysed for protein-protein interactions with the r*Pf*C0760c$_{297}$ protein. **(A)** Proteins were resolved on 12.5% non-reducing SDS-PAGE and stained with Coomassie Blue. Lane 1: molecular weight marker. Lane 2: U937 lysate. Lane 3: J774A.1 lysate. Lane 4: BSA. Lane 6: chicken anti-rabbit albumin IgY. Lane 8: chicken anti-r*Pf*C0760c$_{297}$ IgY. Lane 10: r*Pf*C0760c$_{297}$. **(B)** Far western blot of an identical gel probed with r*Pf*C0760c$_{297}$. r*Pf*C0760c$_{297}$-complexes were detected with mouse anti-his$_6$tag IgG and goat anti-mouse HRPO-IgG. Results were determined by ECL.

It was determined that the substrate, primary and secondary antibodies do not produce false positive results. These conditions were used to perform a far western blot to determine the binding of r*Pf*C0760c$_{297}$ to monocyte lysate proteins. An interaction is evident between several monocyte proteins and r*Pf*C0760c$_{297}$ (Figure 5.4B lanes 2 and 3). No interaction was detected with BSA and chicken anti-rabbit albumin IgY (Figure 5.4B lanes 4 and 6). In the chicken anti-rabbit albumin IgY sample, a prominent band of high molecular weight along with additional bands at 75 kDa and 45 kDa are present (Figures 5.4A, lane 6). The chicken anti-r*Pf*C0760c$_{297}$ IgY positive control showed a positive reaction, indicating that r*Pf*C0760c$_{297}$ is able to bind proteins on the blot, and these interactions can be detected (Figure 5.4B, lane 8). The r*Pf*C0760c$_{297}$ protein was detected with the mouse anti-his$_6$tag IgG antibody (Figure 5.4B, lane 10). The experiment was repeated, and identical results were obtained (data not shown). Thus, an interaction between the monocyte lysate proteins and r*Pf*C0760c$_{297}$ is evident.

5.3 Discussion

5.3.1 U937 and J774A.1 monocytes used in this study

The human U937 cell line was propagated from a patient with generalised histiocytic lymphoma (Sundström and Nilsson, 1976). The mouse J774A.1 cell line was derived from a mouse reticulum cell sarcoma (Ralph and Nakoinz, 1975). These cell lines were chosen as they were available, well characterised, simple to culture, and are immune cells likely to interact with parasite-infected red blood cells in the bloodstream.

Partial characterisation of r*Pf*C0760c$_{297}$ was performed by determining its protein-protein interactions with these mammalian cells by means of far western blot analysis. The *Pf*C0760c protein is predicted to be localized to the *Plasmodium* parasite nucleus. It is speculated that this protein may have other functions that are not associated with the nucleus.

5.3.2 Far western blot of U937 and J774A.1 monocyte proteins with r*Pf*C0760c$_{297}$

Protein-protein interactions between monocyte lysates and the r*Pf*C0760c$_{297}$ protein were assessed using the far western blot technique (Wu *et al*., 2007). This technique is able to detect specific proteins from a combination of proteins interacting with a bait protein, which may be useful in determining host-parasite interactions (Li *et al*., 2015). The bait protein may be biotinylated and detected with streptavidin, or radiolabelled and detected by autoradiography, or detected by an antibody (Hall, 2004). Far western blot analysis has successfully been used to determine protein-protein interactions between laminin and fibronectin with bacterial cell wall and extracellular matrix proteins (Li *et al*., 2015), DNA replication proteins with DNA repair proteins (Walsh *et al*., 2012), and erythropoietin with the erythropoietin receptor (Fecková *et al*., 2016).

The far western blot showed interactions between a range of monocyte proteins from a human and mouse cell line, with r*Pf*C0760c$_{297}$. The far western blot was performed under non-reducing conditions, as it seemed unlikely that a reduced form of the monocyte proteins would offer the correct structure for protein-protein interactions (Hall, 2004). The far western blot results indicate that an interaction between r*Pf*C0760c$_{297}$ with both cell lines is present, and not a result of non-specific binding of the antibodies or intrinsic monocyte peroxidase activity.

5.3.3 Alternative methods to detect protein-protein interactions

Coupling of r*Pf*C0760c$_{297}$ to an AminoLink™ resin, and passing the monocyte lysate over the resin may reveal protein-protein interactions between monocyte proteins and r*Pf*C0760c$_{297}$. Identification of these proteins may help elucidate the function of *Pf*C0760c. Other *in vitro* methods for detection of protein-protein interactions include tandem affinity purification, co-immunoprecipitation, protein arrays, protein fragment complementation, phage display, X-ray crystallography and nuclear magnetic resonance spectroscopy (Rao *et al*., 2014).

5.3.4 Monocyte peroxidase activity

Monocytes display peroxidase activity, which is localised to granules (Kantari *et al*., 2008). Monocytes prepared in PBS and in non-reducing SDS-PAGE treatment buffer did not display peroxidase-like activity. It is possible that these monocytes do not possess peroxidase activity, or cell lysis and storage conditions may have contributed to loss of peroxidase activity.

5.3.5 Interaction of monocytes with r*Pf*C0760c$_{297}$ *in vivo*

Bioinformatics analyses (Chapter 6) indicates that r*Pf*C0760c$_{297}$ is likely associated with the parasite nucleus. No feasible *Plasmodium* export element (PEXEL) and transmembrane motifs were identified. This suggests that *Pf*C0760c is unlikely to migrate to the infected red blood cell surface to facilitate cell-cell interactions. Therefore, it could be argued that an interaction may exist between monocyte lysate proteins and r*Pf*C0760c$_{297}$ as a result of phagocytosis, or processing of the infected red blood cells for antigen presentation. Thus, it could be shown by experimentation whether an interaction exists between the surface of intact monocytes and r*Pf*C0760c$_{297}$.

5.3.6 Chicken anti-r*Pf*C0760c$_{297}$ IgY

A prominent band at 45 kDa was present in the chicken anti-r*Pf*C0760c$_{297}$ IgY antibody samples on non-reducing SDS-PAGE (Figure 5.2A, lane 1, 5.3A and 5.4A, lane 8). A band of high molecular weight was also observed. The size of IgY antibodies under non-reducing conditions is ~170 kDa (Sun *et al*., 2001). The F_{ab} region of IgY is 45 kDa (Sun *et al*., 2001). It is not understood why a higher concentration of protein is observed at 45 kDa. A dominant band of high molecular weight and a faint band at 45 kDa is observed for the anti-rabbit albumin IgY antibody sample (Figures 5.6A, 5.7A and 5.8A, lane 6).

5.3.7 Conclusion

Based on the far western blot, it can be concluded that r*Pf*C0760c$_{297}$ interacts with monocyte proteins. These interactions may be explored further by means of an AminoLink™ resin coupled to r*Pf*C0760c$_{297}$ with the monocyte lysate passed through to identify specific monocyte proteins, or *in vivo* studies. These studies may also be evaluated with native, full-length *Pf*C0760c. Different types of cells may also be tested for protein-protein interactions with r*Pf*C0760c$_{297}$. Specific *Plasmodium* proteins or mammalian proteins may be used as prey proteins to determine protein-protein interactions with *Pf*C0760c.

Chapter 6: Bioinformatics analyses of *Pf*C0760c

6.1 Introduction

Bioinformatics is an invaluable tool that uses computational resources to organise and analyse biological data (Luscombe *et al*., 2001; Kearse *et al*., 2012). Data organization involves the use of databases, web services and search tools; and data analysis makes use of algorithms and statistical modelling (Kearse *et al*., 2012). Bioinformatics may be used to assess DNA, RNA, and amino acid sequences. Analyses by bioinformatics tools and databases may predict some features of a protein, such as its subcellular localization, structure, and characteristics, which may then be confirmed experimentally. Examples of databases that are routinely used include the National Centre for Biotechnology Information (NCBI) (https://www.ncbi.nlm.nih.gov/), and the ExPASy Bioinformatics Resource Portal (http://ww.expasy.org/).

In this chapter, various bioinformatics tools were used to predict properties of the *Pf*C0760c protein. Conserved peptides, epitope prediction, subcellular localization and possible protein structure were among the characteristics that were predicted.

6.2 Methods

6.2.1 Basic local alignment search tool and sequence alignment

The Basic Local Alignment Search Tool (BLAST) is a bioinformatics tool used to compare sequence data (Altschul *et al*., 1990). The full-length amino acid sequence of *Pf*C0760c in the FASTA format was uploaded to the Protein BLAST (BLASTp) server (https://blast.ncbi.nlm.nih.gov/Blast.cgi), and the default BLASTp parameters were used. Sequences from human-, simian-, murine- and avian-infecting *Plasmodium* species were chosen. The BLASTp analysis was also performed using PlasmoDB (https://plasmodb.org/) and ExPASy (https://web.expasy.org/blast/). Multiple sequence alignment of the sequences obtained from the NCBI BLASTp server was performed using Clustal Omega (http://www.ebi.ac.uk/Tools/msa/clustalo/). Multiple sequence alignment aims to compare homologous sequences (Sievers *et al*., 2011). This program was designed to give fast and accurate sequence alignments (Sievers *et al*., 2011). The *Plasmodium* sequences (in the FASTA format) was uploaded to the server and the alignment was generated. The sequences were manually searched for conserved peptides.

6.2.2 Presence of B-cell epitopes within *Pf*C0760c

The B-cell epitopes were experimentally determined using immune sera (Villard *et al*., 2007). The Immune Epitope Database and Analysis Resource (https://www.iedb.org/) was also scanned for additional B-cell epitopes.

6.2.3 Prediction of T-cell epitopes within *Pf*C0760c

SYFPEITHI (http://www.syfpeithi.de/) (Rammensee *et al*., 1999) is a database compiled of ligands and peptide motifs that are known to bind to MHC I and MHC II molecules (Rammensee *et al*., 1999). The *Pf*C0760c sequence was scanned for octamers, nonamers, decamers, and endecamers, as well as MHC II 15-mers.

6.2.4 Predict7 analysis of *Pf*C0760c

Predict7 predicts protein structural features using algorithms for protein properties including hydrophilicity, surface probability, antigenicity and flexibility (Cármenes *et al*., 1989). Hydrophilicity values are calculated according to a Hopp and Woods (1981) scale, surface probability by Emini *et al*. (1985) and Janin *et al*. (1978), antigenicity by Welling *et al*. (1985) and flexibility by Karplus and Schulz (1985). The *Pf*C0760c amino acid sequence is too long for analyses and hence was split into two segments.

6.2.5 *Plasmodium* export element and transmembrane domain prediction

The *Pf*C0760c full-length amino acid sequence was scanned manually for the presence of a PEXEL motif with the sequence (K/R)xLx(E/Q) (Marti *et al*., 2005). The PSEApred server (Verma *et al*., 2008) is a server that is used to predict the secretion of malaria proteins (http://www.imtech.res.in/raghava/pseapred/). Prediction of transmembrane domains was performed using the TMHMM prediction server (Krogh *et al*., 2001), which uses a hidden Markov model (http://www.cbs.dtu.dk/services/TMHMM-2.0/).

6.2.6 Functional site prediction of *Pf*C0760c using ScanPROSITE

Prediction of functional sites within an uncharacterised protein may help define certain characteristics. The full-length *Pf*C0760c amino acid sequence was first manually analysed to determine the amino acid composition. The ScanPROSITE tool (de Castro *et al*., 2006) was used to predict possible phosphorylation, glycosylation and myristoylation sites (http://prosite.expasy.org/scanprosite/).

To check the validity of the leucine zipper prediction, the full-length amino acid sequence was uploaded to the 2ZIP server (http://2zip.molgen.mpg.de/). As the server searches for the

leucine zipper motif, it simultaneously employs a coiled-coil prediction algorithm to rule out false positives (Bornberg-Bauer *et al*., 1998).

6.2.7 Prediction of protein-protein interactions of *Pf*C0760c

Due to the uncharacterised nature of *Pf*C0760c, determining the protein-protein interactions with other *P. falciparum* proteins would be of interest. The full-length *Pf*C0760c amino acid sequence was uploaded to the Search Tool for Recurring Instances of Neighbouring Genes (STRING) network (https://string-db.org/). The STRING network aims to predict physical and functional interactions between proteins (Szklarczyk *et al*., 2015). Proteins are retrieved based on their genes occurring in the neighbourhood of the query sequence within the genome (Snel *et al*., 2000). The expressed proteins are likely to interact with one another (Snel *et al*., 2000).

6.2.8 Detection of conserved domains within the *Pf*C0760c protein

Protein domains may be evolutionarily conserved. The presence of conserved domains may help determine possible functions and subcellular localization of uncharacterised proteins. For the identification of conserved domains within the protein, the full-length amino acid sequence of *Pf*C0760c and homologous *Plasmodium* proteins were uploaded to NCBI's Conserved Domain Database (CDD) (https://www.ncbi.nlm.nih.gov/Structure/cdd/wrpsb.cgi). This database compares a query sequence to its compilation of a manually curated collection of protein domains and protein family models (Marchler-Bauer *et al*., 2017). These models and domains were gathered from various sources including Pfam, Simple Modular Architecture Research Tool, Clusters of Orthologous Groups, TIGRFAMS, the NCBI Protein Clusters collection, and NCBI's internal data collection effort (Marchler-Bauer *et al*., 2017).

6.2.9 Prediction of the subcellular localization of *Pf*C0760c

Determination of protein subcellular localization may give an indication of the function the protein may perform (Blum *et al*., 2009). The MultiLoc2 program uses a support vector machine to predict the subcellular localization of proteins based on amino acid composition, presence of known protein sorting signals, gene ontology terms and phylogenetic profile of a protein (Blum *et al*., 2009) (http://abi.inf.uni-tuebingen.de/Services/MultiLoc2).

NucPred is a program that is able to distinguish proteins that spend time in the nucleus from non-nuclear associated proteins (Brameier *et al*., 2007). To confirm the data obtained from MultiLoc2, the NucPred server (https://nucpred.bioinfo.se/cgi-bin/single.cgi) was used. Nuclear-associated proteins are identified by the presence of nuclear localization signals (NLS) (Brameier *et al*., 2007). Proteins destined for transport to the nucleus after exo-nuclear synthesis contain these NLSs. These signals help mediate transport of these proteins to the nucleus (Brameier *et al*., 2007). NucPred works by assigning a "per-residue" score to each

amino acid based on its location in a sequence, and therefore its influence on a nuclear classification (Brameier *et al*., 2007). The *Pf*C0760c protein sequence was uploaded to the NucPred server to predict its presence in the nucleus.

6.2.10 Protein structural prediction of r*Pf*C0760c$_{297}$

The *Pf*C0760c protein was predicted to exhibit alpha-helical coiled-coil motifs (Villard *et al*., 2007). The 3-D structure of *Pf*C0760c has not yet been determined, thus, the Iterative Assembly Refinement (I-TASSER) program (Zhang, 2008) was used to predict the possible 3-D structure (http://zhanglab.ccmb.med.umich.edu/I-TASSER/). The I-TASSER first threads the query sequence against a representative Protein Data Bank library using various alignment algorithms. A full-length model is then generated using continuous fragments cut from the threading aligned regions. The structure trajectories are clustered. The models are refined, and those with the least energy are chosen from each cluster (Zhang, 2008).

The full-length of the amino acid sequence was too long for the I-TASSER server to process, hence the r*Pf*C0760c$_{297}$ sequence was uploaded. A confidence score (C-score) is assigned to each model, where a high confidence is indicated by a high C-score.

6.3 Results

6.3.1 BLASTp and multiple sequence alignment

The *Pf*C0760c amino acid sequence (Accession: O77384.1) was used as a query sequence for BLASTp analysis. The expect value, or E-value, defines the statistical significance of the match (Boratyn *et al*., 2013). From the BLASTp output, different *Plasmodium* sequences were chosen for further analysis. The details of each *Plasmodial* sequence is shown in Table 6.1.

Table 6.1: Results from NCBI BLASTp using *Pf*C0760c as the query sequence.

***Plasmodium* species**	**Protein**	**Accession no.**	**Length**	**E-value**
P. falciparum	conserved, unknown function	O77384.1	3394	-
P. vivax	conserved, unknown function	SCO72376.1	2954	2×10^{-146}
P. malariae	conserved, unknown function	SBT01363.1	3628	0
P. knowlesi	conserved, unknown function	XP_002258886.1	2941	6×10^{-141}
P. reichenowi	conserved, unknown function	SOV75936.1	3436	0
P. cynomolgi	hypothetical protein PCYB_083240	XP_004222110.1	3058	1×10^{-97}
P. coatneyi	uncharacterised protein PCOAH_00021130	XP_019914485.1	2831	2×10^{-149}
P. gonderi	conserved, unknown function	GAW80650.1	3313	1×10^{-166}
P. inui	hypothetical protein C922_02043	XP_008815864.1	2930	4×10^{-92}
P. gaboni	conserved, unknown function	SOV10972.1	3438	0
P. berghei	conserved, unknown function	SCO59523.1	2841	5×10^{-80}
P. berghei ANKA	conserved, unknown function	XP_672614.2	2840	5×10^{-80}
P. yoelii	conserved, unknown function	XP_726266.2	2891	1×10^{-11}
P. yoelii 17X	hypothetical protein YYC_02699	ETB60413.1	2879	1×10^{-78}
P. chabaudi chabaudi	conserved, unknown function	SCM20838.1	2870	6×10^{-163}
P. chabaudi adami	conserved, unknown function	SCM20066.1	2860	6×10^{-162}
P. vinckei vinckei	hypothetical protein YYE_01881	XP_008623771.1	2818	2×10^{-161}
P. vinckei petteri	hypothetical protein YYG_01058	EUD73968.1	2854	3×10^{-161}
P. gallinaceum	conserved, unknown function	CRG94286.1	2890	2×10^{-79}

Plasmodial human malaria species included *P. malariae, P. vivax* and *P. knowlesi*; simian malaria species included *P. knowlesi*, *P. reichenowi*, *P. cynomolgi*, *P. coatneyi*, *P. gonderi*, *P. inui*, *and P. gaboni*; mouse malaria species included *P. berghei, P. berghei* ANKA, *P. yoelii, P. yoelii* 17X, *P. chabaudi chabaudi, P. chabaudi adami*, *P. vinckei vinckei*, and *P vinckei petteri*. An avian malaria species, *P. gallinaceum*, was also identified. BLASTp analysis indicated that these *Plasmodium* proteins were all conserved with unknown functions. No homologous human proteins were identified using NCBI BLASTp or ExPASy (Appendix B, Table B.2). The sequences shown in Table 6.1 were aligned using Clustal Omega.

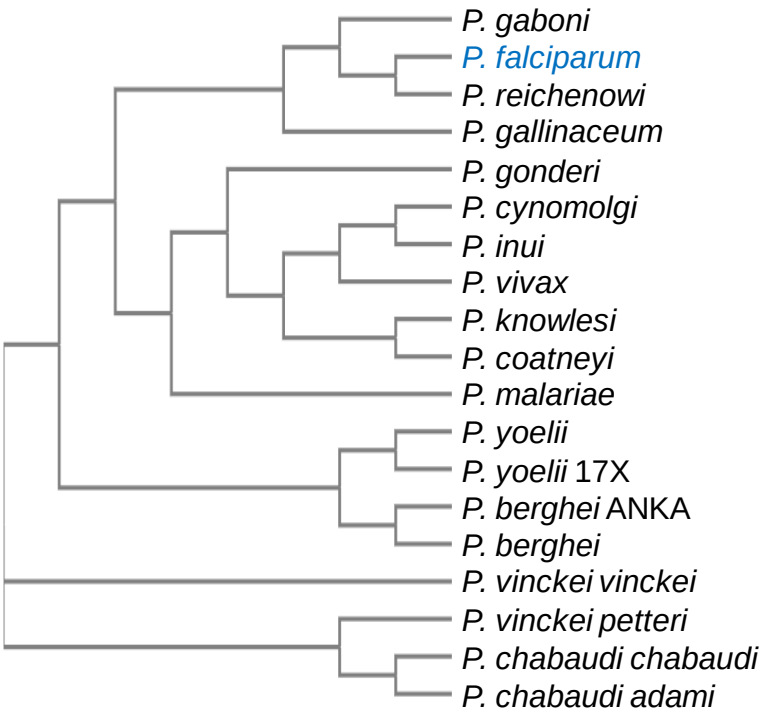

Figure 6.1: Relationship between *Pf*C0760c and homologous *Plasmodium* protein sequences. The cladogram was generated after sequence alignment using Clustal Omega.

The output from Clustal Omega generated a cladogram showing the relationship between the *Pf*C0760c and homologous *Plasmodium* protein sequences. Curiously, the closest-related proteins to *Pf*C0760c were *P. reichenowi* and *P. gaboni* infecting simians, and surprisingly, the avian-infecting parasite *P. gallinaceum* (Figure 6.1). Homologous *Pf*C0760c proteins from *Plasmodium* species infecting humans are related to simian-infecting species. As expected, the sequences from mouse malaria were all closely related to each other.

A

```
P. gaboni                HLHNI-EDKYKNIYERYFNLFNFNFSNVELSFDLFLRRFDKILR    1119
P. falciparum            HIHNI-EDKYKKVYERYFNLFNFNFSNVELSFDLLIRRFDKILR    1205
P. reichenowi            HIHNI-EDKYKKVYERYFNLFNFNFSNVELSFDLLIRRFDKILR    1161
P. gonderi               NLYSM-DEKEKNVYERYYNLFNLNFSNVEISFDLLLNRFEKIVK     944
P. cynomolgi             NLFDM-EAKYKVVYERYFNLFNLNFSNVEISFDLLLNRFERIIR     869
P. inui                  NLHDM-EEKYKLVYERYFNLFNLNFSNVEISFDLLLNRFERIIR     874
P. vivax                 NLVDVMEAKNKLVYERYFNLFNLNFSNVEISFELLLNRFERIIR     903
P. knowlesi              NLFDM-EEKYKVVYERYFNLFNLNFSNVEISFDLLMNRFERIIR     863
P. coatneyi              NLFDM-EEKYKVVYERYFNLFNLNFSNVEISFDLLLNRFERIIR     858
P. yoelii                NLFNV-ETKHKNVYERYFNLFNLNFSNVEISFDLLLKRFYKILR     943
P. yoelii 17X            NLFNV-ETKHKNVYERYFNLFNLNFSNVEISFDLLLKRFYKILR     940
P. berghei ANKA          NLFNV-ETKHKNVYERYFNLFNLNFSNVEISFDLLLKRFYKILR     939
P. berghei               NLFNV-ETKHKNVYERYFNLFNLNFSNVEISFDLLLKRFYKILR     939
P. vinckei vinckei       NLFNS-ETKHKNVYERYFNLFNLNFSNVEISFDLLLKRFYQILR     941
P. vinckei petteri       NLFNN-ETKHKNVYERYFNLFNLNFSNVEISFDLLLKRFYKILR     941
P. chabaudi chabaudi     NLFNV-ETKHKNVYERYFNLFNLNFSNVEISFDLLLKRFYKILR     941
P. chabaudi adami        NLFNV-ETKHKNVYERYFNLFNLNFSNVEISFDLLLKRFYKILR     941
P. malariae              NLYSIMDDKYKNVYERYFNLFNLNFSNVEISFDLLLRRFHQIVR    1047
P. gallinaceum           NLYNI-ENEYKTIYERYFNLFNLNFSNVELSFDLLLRRFNKILR     826
                         :: .  : : * :****:****:******:**:*::.** :*::
```

B

```
P. gaboni                NKEKNSSEEIYKYINENIDLTSELEKKNDIIDNYKNELKEKNEE    2091
P. falciparum            NKERNLSQEIYKYINENIDLTSELEKKNDMLENYKNELKEKNEE    2209
P. reichenowi            NKERNLSQEIYKYINENIDLTSELEKKNDMLENYKNELKEKNEE    2185
P. gonderi               NEKTTVSVEIYKYINENIDLTAELENKNEFIDKLKEEVKEKEDQ    1778
P. cynomolgi             TANTDVSLEIHKYISENIDLTAELENRNEVIEQCREEAKQKDKE    1672
P. inui                  ASTTDMPLEIHKYISENIDLTAELENRNEVIEQCREEARQKEME    1706
P. vivax                 GGTSKGPLEIYKYIGENIDLTAELENRNEVIEQCREEAREKDQQ    1693
P. knowlesi              GNTSNVSLEIHKYISENIDLTAELENRNEVIEQCKEETRQKDKE    1675
P. coatneyi              ANPSNVSLEIHKYISENIDLTAELENRNEVIEQCREEAKQKDKE    1672
P. yoelii                SQNNQLSLEIYKYINENIDLTAELENKNDVIEQMKEDIKNKNKE    1773
P. yoelii 17X            SQNNQLSLEIYKYINENIDLTAELENKNDVIEQMKEDIKNKNKE    1770
P. berghei ANKA          SQNNQVSLEIYKYINENIDLTAELENKNDIIEQMKEDVKNKNKE    1721
P. berghei               SQNNQVSLEIYKYINENIDLTAELENKNDIIEQMKEDVKNKNKE    1721
P. vinckei vinckei       TQDNQVSLEIYKYINENIDLTAELENKNDIIEQMKEELNNKNME    1774
P. vinckei petteri       SQDNQVSLEIYKYINENIDLTAELENKNDMIEQMKEELNNKNME    1773
P. chabaudi chabaudi     SQDNQVSLEIYKYINENIDLTAELENKNDIIEQMKEELNNKNME    1773
P. chabaudi adami        SQDNQVSLEIYKYINENIDLTAELENKNDIIEQMKEELNNKNME    1773
P. malariae              NEQQNVSLEIYKYINENIDLTAELENKYDVIEKCKDEIKVKNDE    1905
P. gallinaceum           RNNEHISLEIYKYINENIDLTAELENKNELLDKFKEEIKQKNDE    1611
                                 **:***.******:***:: :.::: ::: . *: :
```

C

```
P. gaboni              DNIIIIKFNILKLFKLGSCYLYIINRNLKEIQILKNQIISLEES    2315
P. falciparum          DNIIIIKFNILKLFKLGSCYLYIINRNLKEIQMLKNQILSLEES    2416
P. reichenowi          DNIIIIKFNILKLFKLGSCYLYIINRNLKEIQMLKNQILSLEES    2440
P. gonderi             EQIVIIKQNILKLFKLGSCYLYIINRNMKEIQVLKNQVNSLEQS    1952
P. cynomolgi           EHIVIIKQNILKLFKLGSCYLYIINRNMKEIQILKNQVSSLKQN    1837
P. inui                EHIVIIKQNILKLFKLGSCYLYIINRNLKEIQILKNQVSSLKES    1863
P. vivax               EHIVIIKQNILKLFKLGSCYLYIINRNMKEIQILKNQVSSLKQS    1850
P. knowlesi            EHIVIIKQNILKLFKLGSCYLYIINRNLKEIQVLKNEVSSLKQS    1832
P. coatneyi            EHIVVIKQNILKLFKLGSCYLYIINRNLKEIQILKNQVSSLKQS    1826
P. yoelii              DHITLIKQNILKMFKLGSCYLYIINRNLKEIKILKDKIHSFEEN    1964
P. yoelii 17X          DHITLIKQNILKMFKLGSCYLYIINRNLKEIKILKDKIHSFEEN    1961
P. berghei ANKA        DHITLIKQNILKMFKLGSCYLYIINRNLKEIKILKDKINYLEEN    1987
P. berghei             DHITLIKQNILKMFKLGSCYLYIINRNLKEIKILKDKINYLEEN    1985
P. vinckei vinckei     DHITLIKQNILKMFKLGSCYLYIINRNLKEIKILKDKINSLEEN    1961
P. vinckei petteri     DHITLIKQNILKMFKLGSCYLYIINRNLKEIKILKDKINSLEEN    1959
P. chabaudi chabaudi   DHITLIKQNILKMFKLGSCYLYIINRNLKEIKILKDKINSLEDN    1959
P. chabaudi adami      DHITLIKQNILKMFKLGSCYLYIINRNLKEIKILKDKINSLEEN    1959
P. malariae            ENIIVIKQNILKLFKLGSCYLYIINRNLKEIQILKKQVSSLEEN    2146
P. gallinaceum         DNIIIIKQNILKLFKLSSCYLYIINRNLKEIQNLKNQVSCLEQS    1770
                       ::* :** ****:***.**********:***: **.::  ::::.
```

D

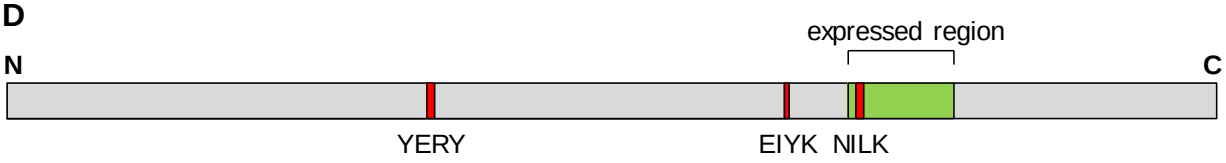

Figure 6.2: Multiple sequence alignment of *Pf*C0760c and homologous *Plasmodium* proteins showing conserved peptides. Sequences were obtained by NCBI BLASTp and aligned with Clustal Omega. Conserved peptides are indicated in red. *Pf*C0760c is shown from **(A)** N1163 – N1205, **(B)** N2166 – N2209, **(C)** N2373 – N2416. The . indicates a similar residue, the : indicates similar physicochemical properties, and * indicates an exact match. **(D)** Schematic of full-length *Pf*C0760c indicating the positions of the three conserved peptides in red, and the expressed region in green.

The homologous *Pf*C0760c *Plasmodial* sequences shown in Table 6.1 were aligned using Clustal Omega, and three conserved peptides were identified (Figure 6.2). A conserved 26-mer (N1175 – N1200) (denoted further as YERY), 17-mer (N2174 – N2190) (denoted further as EIYK) and 23-mer (N2381 – N2403) (denoted further as NILK) were identified. The YERY peptide, which was also found using sequences from ExPASy, corresponds to YERY(F/Y)NLFN(F/L)NFSNVE(L/I)SF(D/E)L(L/F)(I/L/M)(R/N/K)RF (Figure 6.2A). Alignment of homologous *Plasmodium Pf*C0760c protein sequences from PlasmoDB revealed an identical conserved sequence, where the first substitution of phenylalanine to tyrosine is not seen. This substitution is only observed in the *P. gonderi* sequence, which was absent from the PlasmoDB BLASTp result. The EIYK and NILK peptides were EI(Y/H)KYI(N/G/S)ENIDLT(A/S)ELE and NILK(L/M)FKL(G/S)SCYLYIINRN(L/M)KEI respectively (Figure 6.2B and 6.2C), and identical results were obtained with the sequences from ExPASy and PlasmoDB. The NILK peptide is found within the r*Pf*C0760c$_{297}$ sequence. Apart from the substitution of arginine and leucine in *Pf*C0760c with lysine and methionine

respectively in *Plasmodium* species infecting mice (Figure 6.2A and 6.2C), there is no noticeable pattern in the differences observed within the conserved sequences. Accession numbers for the *Plasmodium* sequences obtained from PlasmoDB and ExPASy are included in Appendix B (Tables B.1 and B.2). The schematic of the *Pf*C0760c protein sequence indicates the positions of the conserved peptides and the expressed region (Figure 6.2D) within the *Pf*C0760c amino acid sequence.

The conserved peptides were subject to NCBI BLASTp analysis. A threshold was included, where matches with an E-value above 0 were not considered. Species already present in Table 6.1 were also excluded.

Table 6.2: BLASTp analyses of the *Pf*C0760c conserved peptides YERY, EIYK and NILK.

***Plasmodium* species**	**Protein**	**Accession no.**	**E-value**		
			YERY	**EIYK**	**NILK**
P. fragile	hypothetical protein AK88_00579	XP_012333650.1	1×10^{-15}	2×10^{-5}	1×10^{-15}
P. relictum	conserved, unknown	CRG99782.1	2×10^{-13}	2×10^{-8}	1×10^{-15}
P. ovale wallikeri	conserved, unknown	SBT34370.1	NA	NA	2×10^{-8}
P. ovale curtisi	conserved, unknown	SBS82982.1	2×10^{-6}	NA	4×10^{-7}

NA: not applicable, E-values above threshold

Four additional *Plasmodium* species were identified (Table 6.2). These included *P. fragile* which infects simians, *P. relictum* which infects birds, and *P. ovale wallikeri* and *P. ovale curtisi* which infects humans. A match between the conserved peptides YERY and EIYK with *P. ovale wallikeri*, and the EIYK peptide with *P. ovale curtisi* is unlikely.

NYLVNNLQLNKDNDNIIIIKFNILKLFKLGSCYLYIINRNLKEIQMLKNQILSLEESIKSLNEFINNLKNENEKN

ELIKINNFEEILKLKNNLQDNESCIQNLNNYLKKNEELNKINVKNIFKYKGYIIHLIQQSNVFCKIFKHFNENKI

IDQSIINKLLYLKKSFDFYMYDSVIQEIRENKNIIINQDFLTDEYFKHIQTFTKTCNVLIQRGYLSILKDTNNDF

FIQNKQSNQQGNQNGNHINMCNIYPDDEINVTADQQIFDGTENVQQSLQNEEDYVNNEEMYTDKMDLDNNMN

Figure 6.3: Amino acid sequence of r*Pf*C0760c$_{297}$. The conserved peptide sequence and B-cell epitope are indicated in red and blue boxes respectively.

The 297-amino acid sequence of r*Pf*C0760c$_{297}$ is illustrated, and the conserved NILK peptide and a B-cell epitope is indicated (Figure 6.3). The alignments of the conserved NILK peptide and B-cell epitope are shown in Figures 6.2C and Figure 6.4B.

6.3.2 Identification of B-cell epitopes within *Pf*C0760c

Two B-cell epitopes were identified by Villard *et al.* (2007). The multiple sequence alignment is illustrated. No additional B-cell epitopes were identified by the Immune Epitope Database and Analysis Resource.

A

```
P. gaboni                IIDNYKNELKEKNEEIYKLNDHINMLSNNCKKLKESIIMMENYK    2120
P. falciparum            MLENYKNELKEKNEEIYKLNNDIDMLSNNCKKLKESIMMMEKYK    2238
P. reichenowi            MLENYKNELKEKNEEIYKLNNDIDMLSNNCKKLKESIMMMEKYK    2214
P. gonderi               FIDKLKEEVKEKEDQIRKLNDNMSNMSHSMDKLKESVIIMEKYK    1807
P. cynomolgi             VIEQCREEAKQKDKEINKLHDEIAALSRSMTKLKESLLVMEQYK    1701
P. inui                  VIEQCREEARQKEMEIQKLHDDIASLSRSMTKLKESLIVMEQYK    1735
P. vivax                 VIEQCREEAREKDQQIKKLHEDVDALTRSMAKLKDSLSVMEQYK    1722
P. knowlesi              VIEQCKEETRQKDKEIKKLHDDIAALSCSITKLKESLMLMEQYK    1704
P. coatneyi              VIEQCREEAKQKDKEIKKLHEEITTLSSNIAKMKESLTLMEQYK    1701
P. yoelii                VIEQMKEDIKNKNKEIAKLNKDVINLSTNYDKLKESIYMMEKHK    1802
P. yoelii 17X            VIEQMKEDIKNKNKEIAKLNKDVINLSTNYDKLKESIYMMEKHK    1799
P. berghei ANKA          IIEQMKEDVKNKNKEIAKLNKDVINLSANYDKLKESIYMMEKHK    1800
P. berghei               IIEQMKEDVKNKNKEIAKLNKDVINLSANYDKLKESIYMMEKHK    1800
P. vinckei vinckei       IIEQMKEELNNKNMELAKLNKDVINLSANYDKLKESIYMMEKHK    1803
P. vinckei petteri       MIEQMKEELNNKNMELAKLNKDIINLSTNYDKLKESIYMMEKHK    1802
P. chabaudi chabaudi     IIEQMKEELNNKNMELAKLNKDVINLSTNYDKLKESIYMMEKHK    1802
P. chabaudi adami        IIEQMKEELNNKNMELAKLNKDVINLSTNYDKLKESIYMMEKHK    1802
P. malariae              VIEKCKDEIKVKNDEIDKLNKDISILSKRCNQFEESLIIMEKHK    1934
P. gallinaceum           LLDKFKEEIKQKNDEINKLNDEILKLSRSCNKLNESIMIMEKHK    1640
                         .::: ::: . *: :: **:..:  ::    ::::*: :**::*
```

B

```
P. gaboni                NRNLKEIQILKNQIISLEESIKSLNEFINNLKNENEKNELIKIN    2339
P. falciparum            NRNLKEIQMLKNQILSLEESIKSLNEFINNLKNENEKNELIKIN    2440
P. reichenowi            NRNLKEIQMLKNQILSLEESIKSLNEFINNLKNENEKNELIKIN    2464
P. gonderi               NRNMKEIQVLKNQVNSLEQSIESLNEFIKNLKNENKQNEIIRVN    1976
P. cynomolgi             NRNMKEIQILKNQVSSLKQNIQTQNEFIHNLKAKNKNNEVIQVN    1861
P. inui                  NRNLKEIQILKNQVSSLKESIQTQNEFIQSLKTKNKNNEVIQVN    1887
P. vivax                 NRNMKEIQILKNQVSSLKQSIQTQNAFIQSLKKENKKNEVIQVN    1874
P. knowlesi              NRNLKEIQVLKNEVSSLKQSIQTQNEFIQSLKTKNEKDRVIQVS    1856
P. coatneyi              NRNLKEIQILKNQVSSLKQSIQTQNEFIQSLKTKNEKNEVIQVN    1850
P. yoelii                NRNLKEIKILKDKIHSFEENIQSLNLFINNLKDQHKNNEMIKIN    1988
P. yoelii 17X            NRNLKEIKILKDKIHSFEENIQSLNLFINNLKDQHKNNEMIKIN    1985
P. berghei ANKA          NRNLKEIKILKDKINYLEENIQSLNLFINNLKDQNKNNEVIKIN    2011
P. berghei               NRNLKEIKILKDKINYLEENIQSLNLFINNLKDQNKNNEVIKIN    2009
P. vinckei vinckei       NRNLKEIKILKDKINSLEENIQSLNVFINNLKDQNKNNEVIKIN    1985
P. vinckei petteri       NRNLKEIKILKDKINSLEENIQSLNLFINNLKDQNKNNEVIKIN    1983
P. chabaudi chabaudi     NRNLKEIKILKDKINSLEDNIQSLNLFINNLKDQNKNNEVIKIN    1983
P. chabaudi adami        NRNLKEIKILKDKINSLEENIQSLNLFINNLKDQNKNNEVIKIN    1983
P. malariae              NRNLKEIQILKKQVSSLEENIESLNQFINNLKDENNKNELINVS    2170
P. gallinaceum           NRNLKEIQNLKNQVSCLEQSIESLNKFIDNLKDENNKNELIKVN    1794
                         ***:***: **.::  :::.*:: * **..** ::::::.:*.:.
```

Figure 6.4: Multiple sequence alignment of *Pf*C0760c B-cell epitopes. Epitopes were identified (Villard *et al*., 2007), and sequences were aligned with Clustal Omega. Conserved amino acids are indicated in blue. The *P. falciparum* regions from **(A)** N2194 – N2238 and **(B)** N2396 - N 2440 are shown. The . indicates a similar residue, the : indicates similar physicochemical properties, and * indicates an exact match.

The B-cell epitopes appear to be conserved between *Pf*C0760c, *P. reichenowi* and *P. gaboni* (Figure 6.4A and 6.4B). The first *Pf*C0760c B-cell epitope (N2208 – N2235) is a 29-mer with the sequence EEIYKLNNDIDMLSNNCKKLKESIMMMEK and is found downstream from the conserved EIYK peptide. The second B-cell epitope (N2401 – 2429) is a 28-mer with the sequence KEIQMLKNQILSLEESIKSLNEFINNLKN found within the recombinant sequence, overlapping the conserved NILK peptide. Identification of these B-cell epitopes suggests that *Pf*C0760c has immunogenic regions.

6.3.3 Prediction of T-cell epitopes within *Pf*C0760c

Using the SYFPEITHI epitope prediction server, numerous (more than 100) T-cell epitopes were obtained using the cloned region *Pf*C0760c sequence (data not shown). The program predicted numerous octamers, nonamers, decamers, and endecamers; and these epitopes overlap each other. Numerous MHC II epitopes were found for H2-Ad, H2-Ak, H2-Ed, H2-Ek, HLA-DRB1*0101, HLA-DRB1*0301, HLA-DRB1*0401 (DR4Dw4), HLA-DRB1*0701, HLA-DRB1*1101, and HLA-DRB1*1501 (DR2b). Epitopes were also found in the conserved sequence. Prediction of multiple T-cell epitopes suggests that the *Pf*C0760c protein is immunogenic.

6.3.4 Predict7 analysis of *Pf*C0760c

Predict7 uses statistical modelling to determine protein characteristics and was used to predict the hydrophilicity, surface probability, flexibility and antigenicity of r*Pf*C0760c$_{297}$ (Figure 6.5). These characteristics were also analysed for the individual conserved peptide sequences (Figure 6.6) and B-cell epitopes (Figure 6.7).

The r*Pf*C0760c$_{297}$ protein is largely hydrophobic, with 10 hydrophilic peaks across the 297-amino acid region (Figure 6.5). Three peaks are observed for flexibility of the protein, and one peak for antigenicity. Large portions of the r*Pf*C0760c$_{297}$ protein have a high surface prediction, however, these regions are predicted to have a low hydrophilicity.

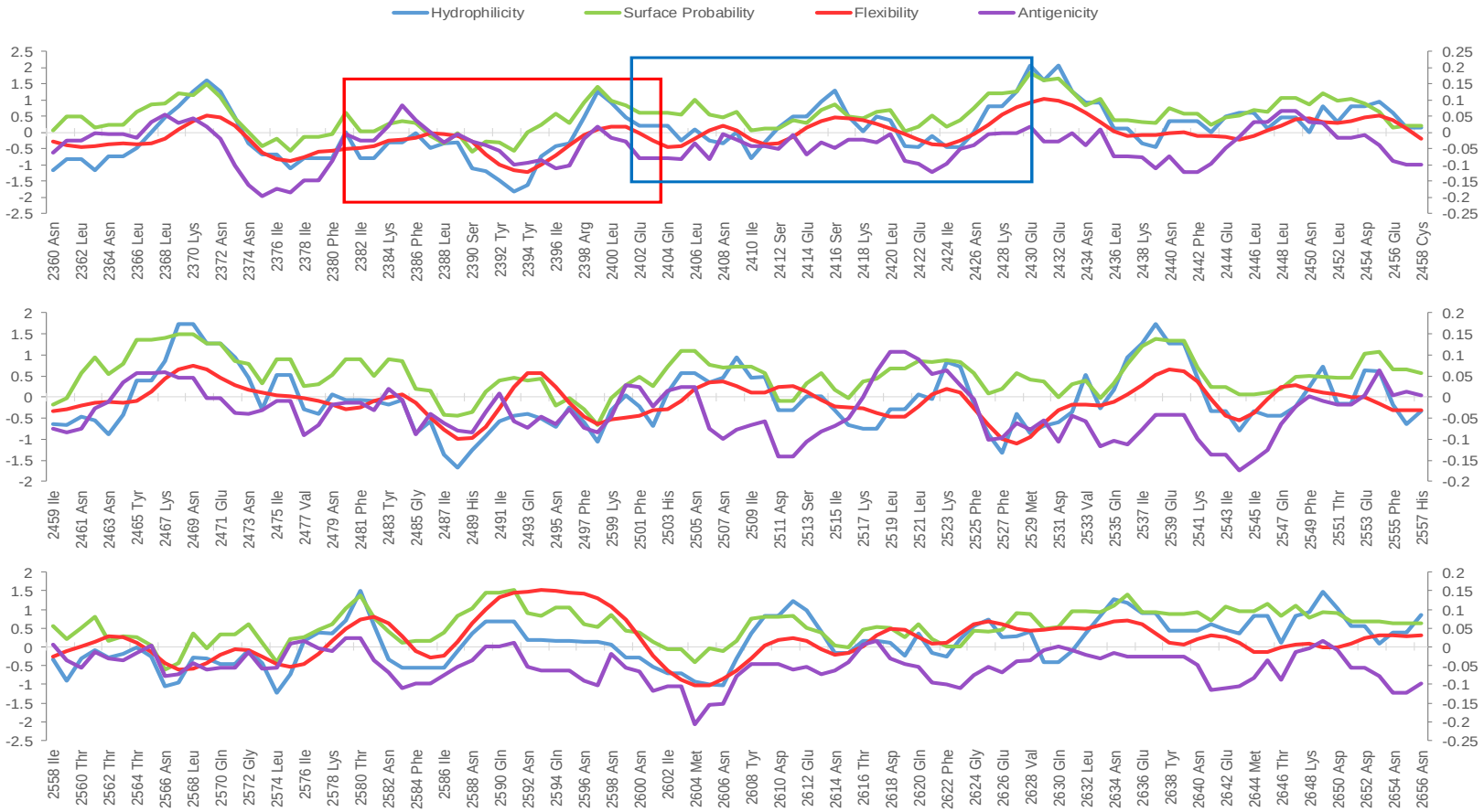

Figure 6.5: Predict7 analysis of the 297-amino acid sequence of r*Pf*C0760c$_{297}$. The region from N2360 – N2656 was cloned. The conserved NILK peptide and 28-mer B-cell epitope are indicated in the red and blue boxes respectively. Hydrophilicity and surface probability are indicated on the primary axis, flexibility and antigenicity are indicated on the secondary axis.

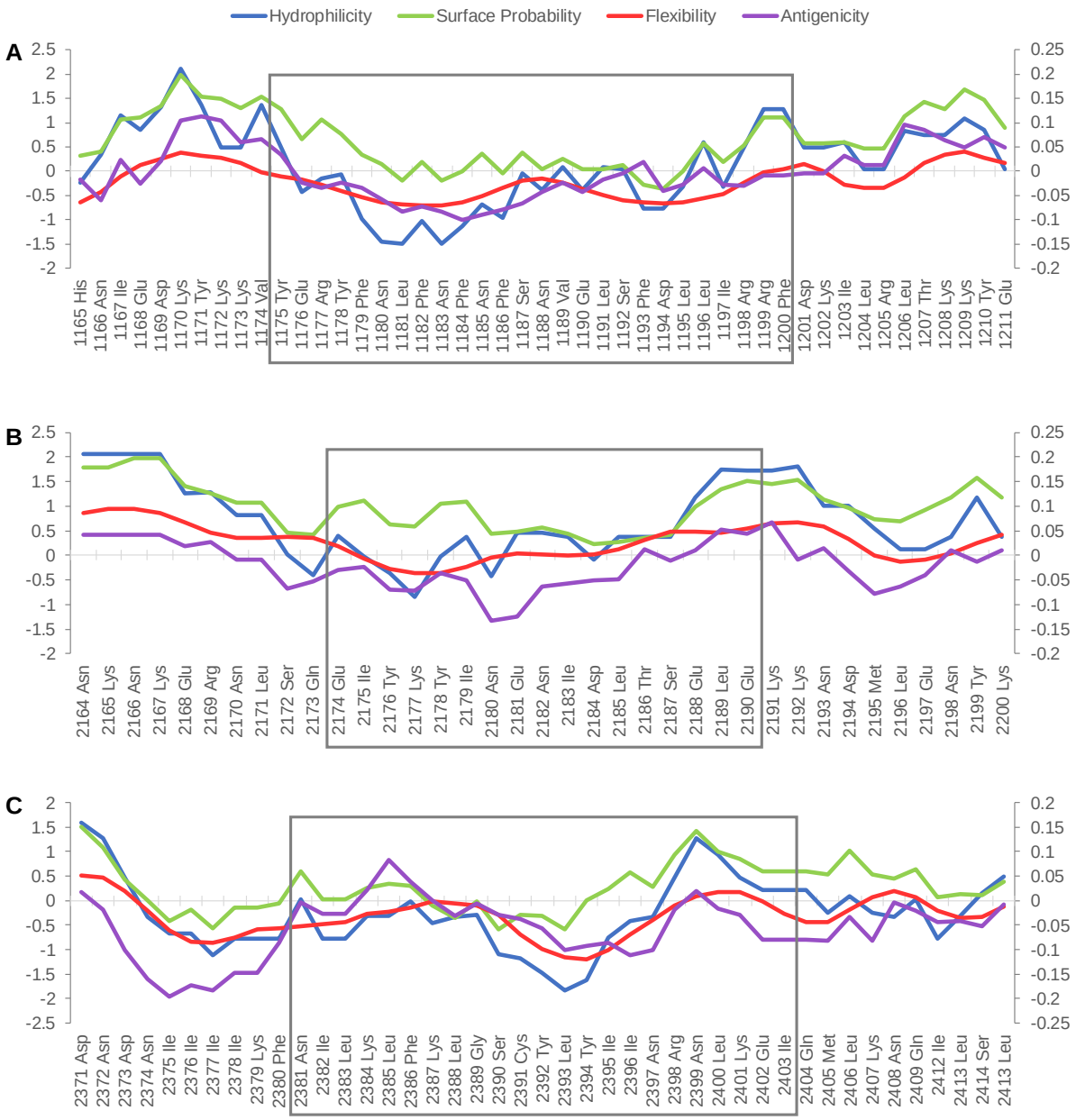

Figure 6.6: Predict7 analysis of conserved *Pf*C0760c peptides. Conserved peptides were identified after multiple sequence alignment. Hydrophilicity and surface probability are indicated on the primary axis, antigenicity and flexibility are indicated on the secondary axis. The following peptides were analysed: **(A)** N1165 – N1211, and the conserved peptide YERY is from N1175 - N1200, **(B)** N2163 – N2179, and the conserved EIYK peptide is from N2174 – N2190 and **(C)** N2371 – N2413 and the conserved peptide NILK is from N2381 – N2403.

The conserved YERY peptide is predicted to have a largely inflexible structure, with low hydrophilicity, surface probability and antigenicity (Figure 6.6A). The N-terminal of the EIYK peptide is predicted to have surface exposure, however with low hydrophilicity, antigenicity and flexibility, with the C-terminal having a higher hydrophilicity and flexibility (Figure 6.6B). The NILK peptide found in the recombinant protein sequence has a low probability of hydrophilicity, surface exposure, flexibility and antigenicity. These probabilities are increased at the C-terminal of the peptide (Figure 6.6C).

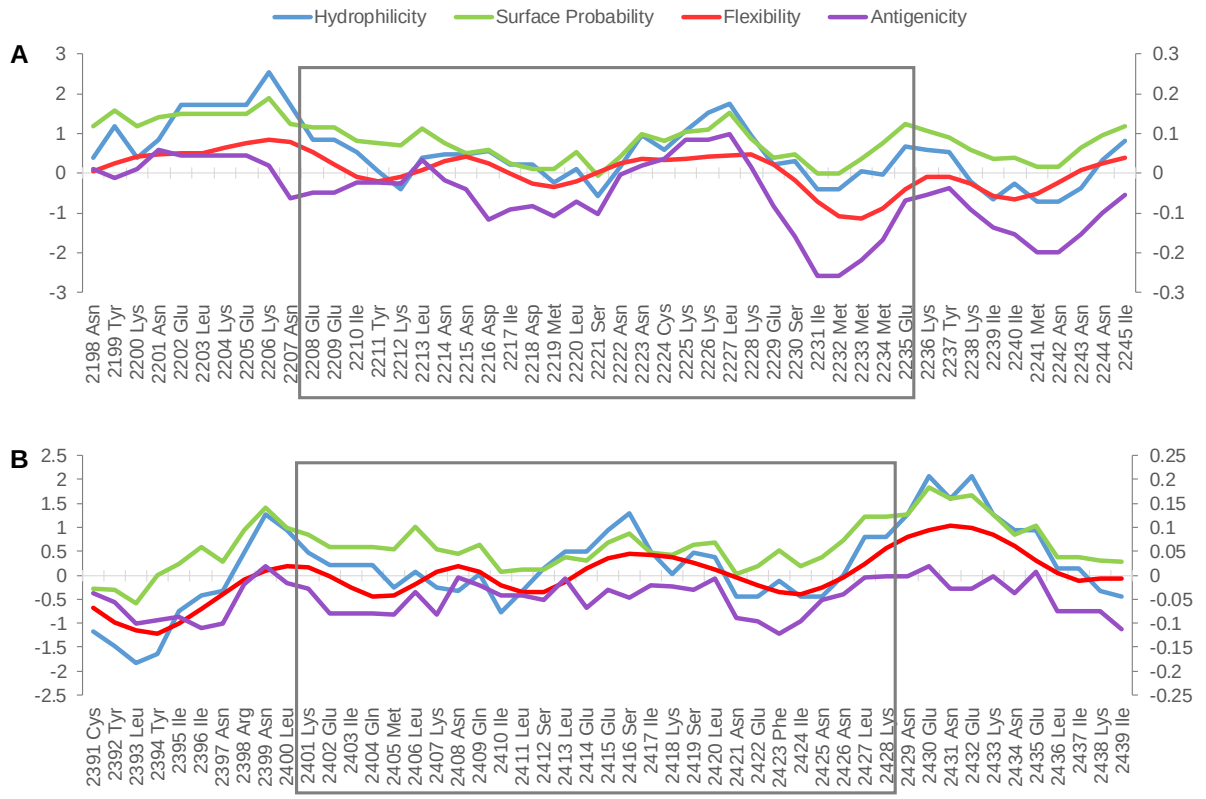

Figure 6.7: Predict7 analysis of B-cell epitopes from *Pf*C0760c. B-cell epitopes were identified (Villard *et al*., 2007). Hydrophilicity and surface probability are indicated on the primary axis, antigenicity and flexibility are indicated on the secondary axis. Peptides shown are from **(A)** N2198 – N2245 with the N2208 – 2235 29-mer B-cell epitope and **(B)** N2391 – 2439 with the N2401 – 2428 28-mer B-cell epitope. (Villard *et al*., 2007).

A single region was observed within the 29-mer B-cell epitope corresponding to hydrophilicity, surface exposure, flexibility and antigenicity (Figure 6.7A), and a single region was observed for the 28-mer B-cell epitope, although at this peak, there is low antigenicity (Figure 6.7B)

6.3.5 Identification of *Pf*C0760c PEXEL motifs

To predict whether *Pf*C0760c is a secreted protein, the amino acid sequence was manually scanned for *Plasmodium* export element motifs with the consensus sequence (K/R)xLx(Q/E) (Marti *et al*., 2005).

Table 6.3: Detection of PEXEL motifs in the *Pf*C0760c protein sequence.

Sequence	Position	Sequence	Position
KYLRQ	298 – 304	KHLEQ	1845 – 1849
KLLNE	704 – 708	RNLSQ	2169 – 2173
KKLDE	718 – 722	RNLKE*	2398 – 2402
KQLQE	1299 – 1303	KKLKE*	2225 – 2229
KSLQE	1596 – 1600	KSLNE*	2418 – 2422

* indicates sequences found within the cloned region.

Ten PEXEL motifs were found within the *Pf*C0760c protein, three of which are present in the recombinant protein (Table 6.3). For secretion, a *Plasmodium* PEXEL motif should lie at the N-terminus of the amino acid sequence (Marti *et al*., 2005). The PEXEL motif closest to the N-terminus corresponds to the sequence KYLRQ from position 298 – 304. Thus, the *Pf*C0760c is unlikely to be secreted as none of the PEXEL motifs lie close to the N-terminus. PSEApred is a database comprising *P. falciparum* secreted and non-secreted proteins, which confirmed that *Pf*C0760c is not a secreted protein (data not shown) (Verma *et al*., 2008). No transmembrane helices were predicted by TMHMM for *Pf*C0760c (data not shown) (Krogh *et al*., 2001).

6.3.6 Functional site predictions of *Pf*C0760c

To help characterise the *Pf*C0760c protein, the prevalence of each amino acid was manually determined. The amino acid prevalence is expressed as a percentage of the length of the sequences (Figure 6.8A and 6.8B).

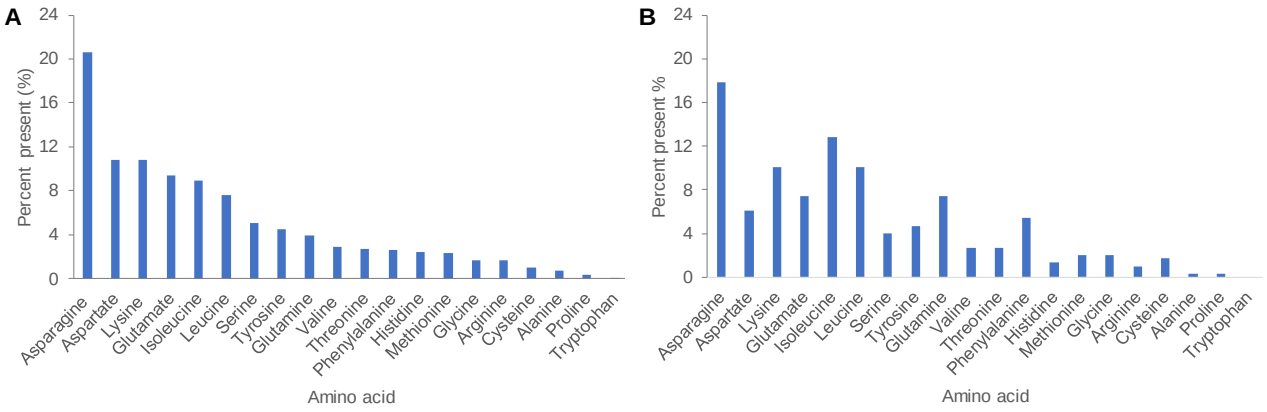

Figure 6.8: Amino acid composition of *Pf*C0760c and r*Pf*C0760c$_{297}$. Amino acids were expressed as a percentage of the sequences. **(A)** Full-length (3394 amino acids) *Pf*C0760c and **(B)** r*Pf*C0760c$_{297}$ (297 amino acids) sequences were analysed.

The polar amino acid asparagine is the most prevalent amino acid, accounting for 21% and 18% in the full-length and recombinant sequences respectively. Alanine, proline and tryptophan are the least prevalent amino acids in both sequences, and these are non-polar

residues. Only three tryptophan residues are present in the full-length protein, and none in the recombinant protein.

Within the full-length sequence, 34 cysteine residues are present, which are likely to participate in disulfide bond formation (Sevier and Kaiser, 2002). 4 of these cysteine residues are conserved at positions N123, N176, N2391 and N3128. The cysteine at position N2391 is found in the r*Pf*C0760c$_{297}$ sequence. However, data obtained from PredictProtein, using the DISULFIND tool did not predict any disulfide bonds (data not shown) (Ceroni *et al*., 2006).

Aspartate and lysine each account for ~11% of the protein, and 69 lysine residues are conserved throughout the species. The lysine residue at position N1269 of *Pf*C0760c was found to be acetylated in the trophozoite nucleus (Miao *et al*., 2013). The multiple sequence alignment showing the *Pf*C0760c lysine at position N1269 is shown (Figure 6.9).

```
P. gaboni                    INEKYLLLEKEYEEYQNKNLFINEQLE   1206
P. falciparum PfC0760c       INEKYLILEKEYEEYQNKNIFINAQIE   1292
P. reichenowi                INEKYFILEKEYKEYQNKNLFINEQIE   1248
P. gonderi                   MNTKHTMLENECKEHICKNNLLNGKYE   1031
P. cynomolgi                 VVNNHAVLQNECKEHKCKNDLLIDKYE   956
P. inui                      VINSHAVLQNECKEHKCKHDLLIEKYE   961
P. vivax                     VANNHAILQNECKEHKCKNDLLSDKYE   990
P. knowlesi                  MVNSQVILQNECKEHKCKHDLLVDKYE   950
P. coatneyi                  VLNNQVVLQNECKEHKCKHDHLLDMYE   945
P. yoelii                    ISEKYFQLEKEYNEYKNNNSLILEQYE   1030
P. yoelii 17X                ISEKYFQLEKEYNEYKNNNSLILEQYE   1027
P. berghei ANKA              INEKYFQLEKEYNEYKNNNCIIMEQYE   1026
P. berghei                   INEKYFQLEKEYNEYKNNNCIIMEQYE   1026
P. vinckei vinckei           INEKYFQLEKEYNEYKNNNSLILEQYE   1028
P. vinckei petteri           INEKYFQLEKEYNEYKNNNSLILEQYE   1028
P. chabaudi chabaudi         INEKYFQLEKEYNEYKNNNSLILEQYE   1028
P. chabaudi adami            INEKYFQLEKEYNEYKNNNSLVLEQYE   1028
P. malariae                  FNEKYLLLQNEYEECKNKNIFINELCE   1134
P. gallinaceum               FNEKYILLQNEFHQYKNKYIFIIEEFE   913
                             .  .   *::* .:   :   :    *
```

Figure 6.9: Multiple sequence alignment of *Pf*C0760c with homologous proteins from *Plasmodium* species showing an acetylated lysine residue. The *Pf*C0760c sequence shown is from N1266 – N1292. The acetylated lysine residue is N1269 in *Pf*C0760c, indicated in orange. The . indicates a similar residue, the : indicates similar physicochemical properties, and * indicates an exact match.

The acetylated lysine residue at position N1269 on *Pf*C0760c is not conserved between the species (Figure 6.9). The aligned lysine residue in the *P. cynomolgi*, *P. inui*, *P. vivax*, *P. knowlesi*, *P. coatneyi* and *P. inui* sequences were substituted with asparagine and serine residues.

To predict potential sites for enzymatic targeting and functional sites, the full-length amino acid sequence of *Pf*C0760c was uploaded to the ScanPROSITE tool. The program scans the protein sequence against a database comprising different motifs.

Table 6.4: Analysis of the full-length *Pf*C0760c protein sequence using the PROSITE prediction software.

Motif	Location
Tyrosine Phosphorylation (K/RxxxD/ExxxY)	15 - 21; 100 - 107; 222 - 230; 395 - 401; 581 - 589; 704 - 712; 729 - 735; 1026 - 1032; 1084 - 1090; 1119 - 1127; 1222 - 1230; 1659 - 1667; 1736 - 1742; 1845 - 1852; 2204 - 2211; 2353 - 2361; 2522 - 2530; and 2800 - 2807.
Casein Kinase II Phosphorylation (S/T*xxD/E)	129 - 132 S; 172 - 175 T; 177 - 180 S; 534 - 537 T; 579 - 582 S; 619 - 622 S; 750 - 753 S; 755 - 758 T; 781 - 784 S; 847 - 850 S; 865 - 868 T; 923 - 926 S; 950 - 953 S; 988 - 991 S; 1049 - 1052 S; 1067 - 1070 S; 1085 - 1088 S; 1122 - 1125 T; 1133 - 1136 S; 1187 - 1190 S; 1436 - 1439 S; 1587 - 1590 S; 1597 - 1600 S; 1621 - 1624 T; 1633 - 1636 S; 1660 - 1663 S; 1934 - 1937 S; 1960 - 1963 T; 1996 - 1999 T; 2055 - 2058 T; 2082 - 2085 S; 2111 - 2114 T; 2159 - 2162 T; 2187 - 2190 S; 2271 - 2274 S; 2279 - 2282 S; 2290 - 2293 S; 2310 - 2313 T; 2412 - 2415 S; 2419 - 2422 S; 2580 - 2583 T; 2806 - 2809 T; 2820 - 2823 S; 2844 - 2847 T; 2962 - 2965 S; 2978 - 2981 S; 3040 - 3043 S; 3064 - 3067 T; 3132 - 3135 S; 3133 - 3136 S; 3271 - 3274 S; 3280 - 3283 T; 3315 - 3318 S; 3329 - 3332 S; and 3386 – 3389 T.
Protein Kinase C Phosphorylation site (S/T*xK/R)	177 - 179 S; 199 - 201 S; 368 - 370 S; 542 - 544 S; 546 - 548 S; 555 - 557 S; 560 - 562 S; 579 - 581 S; 597 - 599 S; 781 - 783 S; 865 - 867 T; 890 - 892 S; 896 - 898 T; 1104 - 1106 S; 1207 - 1209 T; 1436 - 1438 S; 1442 - 1444 S; 1484 - 1486 S; 1555 - 1557 S; 1625 - 1627 S; 1926 - 1928 T; 2031 - 2033 S; 2159 - 2161 T; 2304 - 2306 S; 2416 - 2418 S; 2646 - 2648 T; 2994 - 2996 S; and 3315 - 3317 S.
N-Myristoylation site (G[N/I]xx[N/G/S][N/S/M/D])	28 - 33; 519 - 524; 2595 - 2600; 2599 - 2604; 2706 - 2711; and 2935 - 2940.
N-Glycosylation site (Nxxx)	258 - 261; 287 - 290; 346 - 349; 366 - 369; 374 - 377; 408 - 411; 539 - 542; 553 - 556; 594 - 597; 611 - 614; 617 - 620; 767 - 770; 1047 - 1050; 1065 - 1068; 1083 - 1086; 1120 - 1123; 1185 - 1188; 1431 - 1434; 1440 - 1443; 1456 - 1469; 1471 - 1474; 1499 - 1502; 1532 - 1535; 1658 - 1661; 1890 - 1893; 1917 - 1920; 2157 - 2160; 2170 - 2173; 2269 - 2272; 2300 - 2303; 2455 - 2458; 2614 - 2617; 2715 - 2718; 2773 - 2776; 2813 - 2816; 2816 - 2819; 2937 - 2940; 2941 - 2944; 2945 - 2948; 3050 - 3053; 3125 - 3128; 3141 - 3144; 3295 - 3298; and 3305 - 3308.
cAMP- and cGMP- dependent protein kinase phosphorylation site ([K/R][K/R]xx)	430 - 433; 878 - 881; 879 - 882; 893 - 896; 1384 - 1387; and 2998 – 3001
Leucine zipper (LxxxxxxLxxxxxxLxxxxxxL)	2406 – 2427

*Serine or threonine residue required for phosphorylation. Presence of serine (S) or threonine (T) residue is indicated with the sequence.
Underlined sequences indicate that the sequence falls within the cloned region. Sequences shown in red indicate that the sequence is found within the conserved peptides YERY or EIYK.

The positions of the amino acid sequences within *Pf*C0760c that are predicted to participate in tyrosine phosphorylation, casein kinase II phosphorylation, protein kinase C phosphorylation, N-myristoylation, glycosylation, and cAMP- and cGMP-dependent protein kinase phosphorylation sites, as well as a leucine zipper are shown (Table 6.4). There are

many sites within the full-length *Pf*C0760c protein for phosphorylation, most of which are for casein kinase II. Three casein kinase II phosphorylation sites, two protein kinase C phosphorylation, N-myristoylation and glycosylation sites, and one leucine zipper are predicted in the recombinant protein. The leucine zipper falls within the B-cell epitope. A casein kinase II phosphorylation site is found in the conserved YERY peptide sequence (1187 – 1190), and the serine is conserved in all the *Plasmodial* species. It is therefore likely for phosphorylation to occur at this site. A casein kinase II phosphorylation site is found within the conserved EIYK sequence (2187 – 2190); however, the serine residue is only conserved between *P. falciparum*, *P. gaboni* and *P. reichenowi.* A site for N-linked glycosylation is found in the YERY peptide (1185 – 1188) with the sequence NFSN and is conserved in all the *Plasmodial* species.

To validate that the structure represented by the leucine zipper motif, the *Pf*C0760c protein was analysed using the 2ZIP server (Bornberg-Bauer *et al*., 1998). The predicted leucine zipper motif was rejected as a valid leucine zipper due to the presence of adjacent coiled-coil structures (data not shown). The r*Pf*C0760c$_{297}$ amino acid sequence was also scanned using ScanPROSITE, and the same sequences corresponding to those indicated in blue (Table 6.4) were obtained (data not shown).

6.3.7 Prediction of protein-protein interactions of *Pf*C0760c

Due to the uncharacterised nature of *Pf*C0760c, it would be of interest to determine if any proteins in the *P. falciparum* proteome interact with *Pf*C0760c, which may possibly give an indication to its function. The STRING database was scanned using the full-length *Pf*C0760c protein as the query sequence (Szklarczyk *et al*., 2015; Snel *et al*., 2000).

Table 6.5: Prediction of protein-protein interactions of *Pf*C0760c with *P. falciparum* proteins using STRING.

Protein Accession	Protein
PF07_0024	Inositol phosphatase
PFF1185w	Smarca-related protein; SNF2 helicase
PF10_0079	Conserved unknown
PFF0445w	Conserved unknown
PF10_0232*	Chromodomain-helicase DNA binding protein homolog

Protein indicated by * has been experimentally proven to interact with *Pf*C0760c

*Pf*C0760c was predicted to interact with 5 *P. falciparum* proteins, including inositol phosphatase and Smarca-related protein (Table 6.5). Two proteins with unknown functions were identified. The interaction between *Pf*C0760c and chromodomain-helicase DNA binding protein homolog (PF10_0232) was experimentally determined by means of a high throughput yeast two-hybrid screening assay (LaCount *et al*., 2005). This suggests that *Pf*C0760c has some functions associated with the parasite nucleus.

6.3.8 Prediction of conserved domains in the *Pf*C0760c protein sequence

The presence of conserved domains within a protein sequence may help determine its function. The NCBI CDD was used to search the *Pf*C0760c sequence and homologous *Plasmodium* protein sequences for conserved domains.

Table 6.6: Conserved domains of *Plasmodium* species' proteins homologous to *Pf*C0760c.

***Plasmodium* species**	**Conserved domain**	**Position**
P. falciparum	SMC N-terminus	139 - 404, 1190 - 1420, 1688 - 2023
P. gaboni	SMC N-terminus	144 - 412, 1113 - 1865, 1812 - 1945
P. reichenowi	SMC N-terminus	139 - 404, 1125 - 1916, 1856 - 2244
P. gonderi	SMC N-terminus	157 - 471, 914 - 1479, 1239 - 1843
	*dna*J with C-terminal Zn finger	2411 – 2574
P. cynomolgi	SMC N-terminus	232 - 1081, 854 - 1585, 1291 - 1891
	Rad50 zinc hook motif	213 – 399
	Na^+/Ca^{2+} exchanger	2065 – 2292
P. inui	SMC N-terminus	122 - 407, 1283 - 1638, 1681 - 1918
	Na^+/Ca^{2+} exchanger	2311 - 2427, 2542 - 2802, 2737 - 2929
P. vivax	SMC N-terminus	122 - 418, 885 - 1193, 1085 - 1742
	Na^+/Ca^{2+} exchanger	2112 – 2317
	Tat-binding protein	1835 – 1920
P. knowlesi	SMC N-terminus	135 - 436, 854 - 1589, 1270 - 1918
	Glutenin subunit	2477 – 2638
	Na^+/Ca^{2+} exchanger	2063 - 2300, 2292 - 2536
P. coatneyi	SMC N-terminus	102 - 385, 854 - 1447, 1191 - 1724
	Na^+/Ca^{2+} exchanger	2440 - 2699, 2624 - 2831
P. yoelii	SMC N-terminus	181 - 410, 925 - 1164, 1236 - 1825
P. yoelii 17X	SMC N-terminus	181 - 410, 922 - 1161, 1233 - 1822
P. berghei ANKA	SMC N-terminus	126 - 407, 926 - 1353, 1279 - 1819
P. berghei	SMC N-terminus	126 - 407, 926 - 1353, 1279 - 1819
P. vinckei vinckei	SMC N-terminus	141 - 433, 923 - 1148, 1237 - 1877
	Midasin	2542 – 2818
	Rho	2660 – 2784
P. vinckei petteri	SMC N-terminus	126 - 409, 923 - 1148, 1281 - 1821
	Na^+/Ca^{2+} exchanger	2164 – 2369
	Midasin	2587 – 2814
P. chabaudi chabaudi	SMC N-terminus	183 - 456, 947 - 1494, 1237 - 1823
	Midasin	2618 - 2830
	CDC45-like protein	2755 – 2822
P. chabaudi adami	SMC N-terminus	183 - 456, 947 - 1494, 1237 - 1823
	CDC45-like protein	2752 - 2821.
P. malariae	SMC N-terminus	225 - 471, 1050 - 1919
	DUF1777	2646 – 2789
	Rho	2594 – 2711
P. gallinaceum	SMC N-terminus	107 - 384, 873 - 1672, 1509 - 1844

Within the *Pf*C0760c sequence, three domains consistent with the N-terminal domains of the structural maintenance of chromosomes (SMC) protein superfamily were predicted. All the homologous *Pf*C0760c proteins contain two or three SMC domains. The second most commonly observed domain amongst the species is the sodium/calcium (Na^+/Ca^{2+}) exchanger protein.

Table 6.7: Functions of domains from *Plasmodium* species identified by CDD.

Domain	Function
SMC	Chromosome segregation ATPase's
Rho	Transcription termination factor Rho
*dna*J with Zn finger	Molecular chaperone with Zn finger domain
DUF1777	Unknown
Na^+/Ca^{2+} exchanger	Sodium/Calcium exchanger: regulates intracellular Ca2+
Tat binding protein	Role in degradation of ubiquitinated proteins
Rad50 Zn hook	Chromosome maintenance
Midasin	ATPase; involved in ribosome maturation
CDC45	Required for initiation of DNA replication initiation

The CDD identified 9 different domains that are prevalent in *Pf*C0760c and homologous *Plasmodium* proteins. The functions of these domains are illustrated in Table 6.7. The SMC, Rho, Tat binding protein, Rad50 Zn hook, midasin and CDC45 domains are all associated with nuclear functions. DUF1777 is uncharacterised.

6.3.9 Prediction of the subcellular localization of *Pf*C0760c

To predict the subcellular location of *Pf*C0760c, the amino acid sequence was uploaded to the MultiLoc2 prediction program. The *Pf*C0760c protein was predicted to be localised to the nucleus with a confidence of 63%. To validate this result, the *Pf*C0760c amino acid sequence was uploaded to the NucPred server. The results indicated that the *Pf*C0760c is located in the nucleus with a 97% confidence.

To validate the findings from both MultiLoc2 and NucPred, protein sequences with known locations were uploaded to each server. The cytoplasmic protein *P. falciparum* aldolase (Knapp *et al*., 1990) and the nuclear protein *P. falciparum* DNA-guided RNA polymerase III (Oehring *et al*., 2012) were chosen. High confidence scores indicate the predicted location of the proteins.

Table 6.8: MultiLoc2 analysis of *Plasmodium* proteins of known locations.

Accession no.	*P. falciparum protein*	% Confidence			
		Cytoplasm	Nucleus	Mitochondria	Secreted
AAA29716.1	Aldolase	73	7	19	1
P27625	DNA-guided RNA polymerase III	4	90	1	5

The MultiLoc2 server was able to correctly predict the subcellular location of both aldolase and DNA-guided RNA polymerase III (Table 6.8).

Table 6.9: Analysis of *Plasmodium* proteins of known locations using the NucPred server.

Accession no.	Protein	NucPred Score (%)
AAA29716.1	Aldolase	9
P27625	DNA-guided RNA polymerase III	93

NucPred correctly predicted the nuclear localization of the DNA-guided RNA polymerase III enzyme with a score of 93 % (Table 6.9). Aldolase had a low NucPred score of 9, indicating that it is unlikely to be found in the nucleus. The results presented in Tables 6.8 and 6.9 indicate that the data obtained from both the MultiLoc2 and NucPred servers are reliable.

6.3.10 Prediction of r*Pf*C0760c$_{297}$ protein structure

It had previously been determined that *Pf*C0760c possessed multiple coiled-coil motifs (Villard *et al*., 2007). To date, there is no published data available showing the structure of *Pf*C0760c. Thus, the I-TASSER 3-D protein structural prediction server was used. Longer amino acid sequences provide a significant limitation with such programs. The amino acid sequence for the r*Pf*C0760$_{297}$ protein was used for structural analysis. Five possible models were generated. All five predicted models for *Pf*C0760c show helices separated by uncoiled segments (Figure 6.10). A clustered conformation of helices is observed with different arrangements (Figure 6.10A – C). Helices separated by strands and arranged in a linear pattern were also observed (Figure 6.10D and 6.10E). The highest C-score indicates the most likely structure, illustrated in Figure 6.10A, which shows a non-linear arrangement of stretches of helices separated by strands.

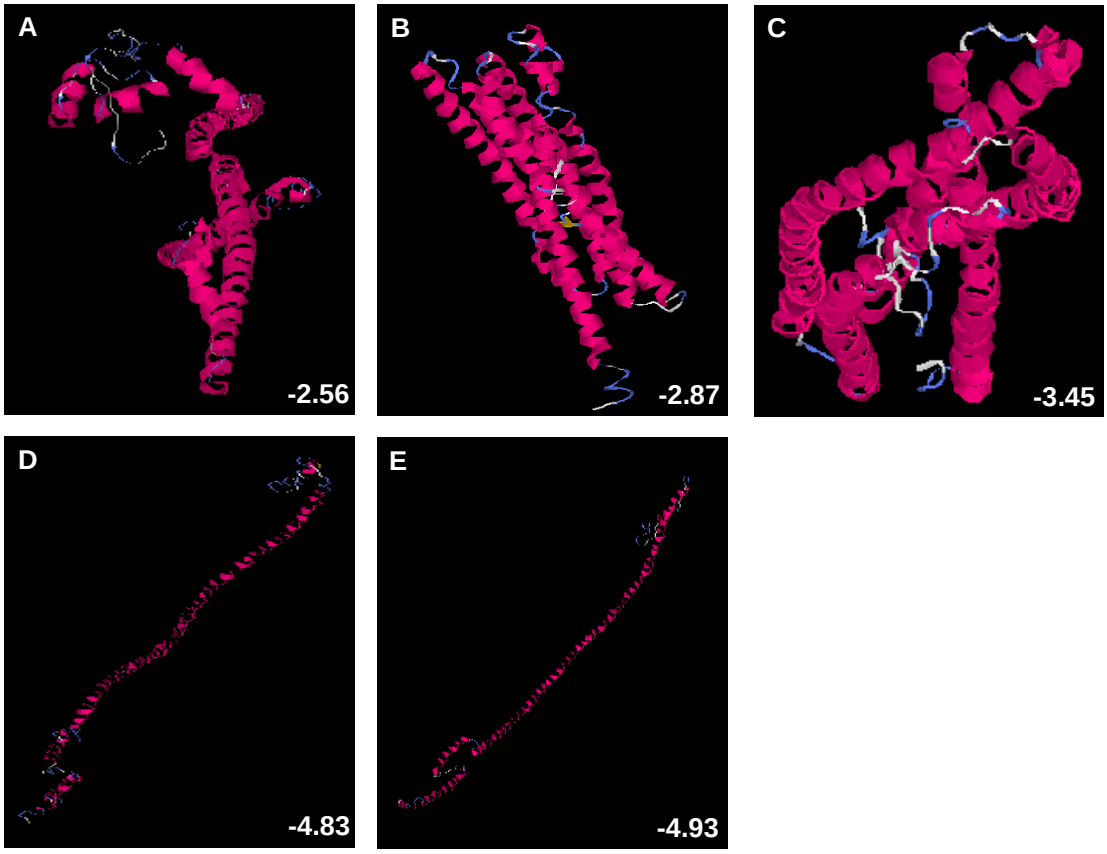

Figure 6.10: Predicted models of the r*Pf*C0760c$_{297}$ generated by I-TASSER. The recombinant amino acid sequence spanning N2360 – N2656 was uploaded to the I-TASSER server, producing 5 possible different models **(A – E)**. The C-score for each model is indicated at the bottom right (Zhang, 2008).

The I-TASSER server also predicted the possible conformation of each amino acid in the r*Pf*C0760c$_{297}$ sequence, along with a confidence score. A higher confidence score indicates the prediction is likely to be true. The conserved peptide and flanking B-cell epitope within r*Pf*C0760c$_{297}$ were analysed.

```
Sequence    NYLVNNLQLNKDNDNIIIIKFNILKLFKLGSCYLYIINRNLKEIQMLKNQILSLEESIKSLNEFINNLKNENEKNELIKINNFEEILKLKNNLQD
Prediction CCCCCCSSCCCCCCCSSSSSSCHHHHHHCCCSSSSSSCCCHHHHHHHHHHHHHHHHHHHHHHHHHHHHHHCCCCCCSSSSCCHHHHHHHHHHCC
Conf.Score 943112022678774699981478884336569987537629999999998889999999999999875414467447747899999986031144
           H:Helix; S:Strand; C:Coil
```

Figure 6.11: Predicted conformation of amino acids in the conserved peptide and B-cell epitope of r*Pf*C0760c$_{297}$. The black box indicates the conserved peptide and overlapping B-cell epitope. The conserved peptide is underlined in red, and the B-cell epitope is underlined in blue. A confidence score is indicated.

The conserved peptide is predicted to have a helix and strand flanked and separated by coils, and the B-cell epitope containing the leucine zipper sequence motif is predicted to be in a helical conformation (Figure 6.11). For the conserved peptide, the helix and strands are predicted with a high confidence, whereas the coiled sections have varying degrees of

confidence for each amino acid. The B-cell epitopes' helical prediction is met with high confidence scores, with only the last two amino acids having slightly lower confidence scores.

6.4 Discussion

6.4.1 *Pf*C0760c is a conserved protein

The *Pf*C0760c protein is conserved amongst different strains and isolates of *P. falciparum*. Homologous proteins to *Pf*C0760c were found in 18 other *Plasmodial* species infecting humans, simians, mice and birds, suggesting that *Pf*C0760c is likely an important protein for parasite metabolism.

Multiple sequence alignment of the homologous protein sequences revealed three conserved peptides. This is two more conserved sequences than the previously detected NILK peptide conserved in the *Plasmodium* species (Addicott, 2014). Identification of the additional conserved peptides is due to updated databases and sequences since the previous study. Conserved peptides may participate in protein-protein interactions, provide structural motifs or may be highly immunogenic. Conserved sites for casein kinase II phosphorylation were predicted in the YERY and EIYK peptides, and a conserved site for N-linked glycosylation was predicted in the YERY peptide. BLASTp analysis of the three conserved peptides revealed three additional protein homologs from *P. fragile*, *P. relictum*, and *P. ovale*. However, the *P. ovale* homologues did not align with all the conserved peptides (Table 6.2), and this possibly accounts for the absence of *P. ovale* species from the original BLASTp output (Table 6.1).

Within the conserved peptides, a few amino acid substitutions were observed. This could possibly be attributed to substitutions of single nucleotides in the codons used, or mistakes during sequencing.

6.4.2 Possible subcellular localization of *Pf*C0760c

Protein function is often associated with the subcellular localization, therefore the subcellular localization of *Pf*C0760c was bioinformatically evaluated (Blum *et al*., 2009). Using the MultiLoc2 and NucPred servers, the *Pf*C0760c protein was predicted to be found in the parasite nucleus with high confidence (Blum *et al*., 2009; Brameier *et al*., 2007). This result coincides with two studies placing *Pf*C0760c in the nucleus of *P. falciparum* (Miao *et al*., 2013; Oehring *et al*., 2012). Subcellular localization can be experimentally confirmed by immunostaining *P. falciparum* parasites with fluorescent- or nanoparticle-labelled *Pf*C0760c-specific antibodies.

There is no evidence to suggest whether *Pf*C0760c is transported across the parasite membrane. Ten PEXEL motif sequences were found in the *Pf*C760c protein. A true PEXEL motif lies approximately 80 amino acids downstream from the N-terminus (Marti *et al*., 2005).

None of the PEXEL motifs are within this range, therefore *Pf*C0760c is unlikely to be transported.

Protein-protein interactions were predicted for inositol phosphatase (PF07_0024), Smarca-related protein (PFF1185w) and chromodomain helicase DNA binding protein (PF10_0232). All three proteins are associated with the nucleus (Shah *et al*., 2013; Oehring *et al*., 2012; Wu *et al*., 2009), further supporting the nuclear localization of *Pf*C0760c.

6.4.3 Predicted function of *Pf*C0760c

Structural maintenance of chromosome (SMC) proteins are vital to parasite survival as they play an important role in stabilizing the chromosome (Harvey *et al*., 2002). The characteristic SMC protein structure features a central hinge region between two long coiled-coils flanked by globular domains at the N- and C-terminals (Harvey *et al*., 2002; Melby *et al*., 1998). Eukaryotic SMC proteins dimerise with heterologous SMC proteins, and complex with other proteins to form cohesin, condensin and the SMC5/6 complex (Wu and Yu, 2012). Cohesin facilitates separation of sister chromatids, condensin is involved in chromosome condensation, and SMC5/6 is involved in DNA repair mechanisms (Brooker and Berkowitz, 2014; Wu and Yu, 2012). SMC domains were predicted in the middle of the *Pf*C0760c sequence and its homologous proteins, corresponding to the N-terminal globular domain. SMC globular C-terminus, coiled-coils and hinge domains were not predicted. It is debatable whether *Pf*C0760c is likely to participate in the structural maintenance of chromosomes purely based on these results. A possible reason for this may be due to the absence of these domains in the *Pf*C0760c sequence or the CDD.

6.4.4 Protein motifs within the *Pf*C0760c protein sequence

6.4.4.1 Phosphorylation motifs in *Pf*C0760c

Multiple motifs were predicted for phosphorylation by several kinases, two of which were conserved. Protein phosphorylation is involved in the activation and deactivation of proteins and enzymes, and is often implicated in signal transduction pathways (Ardito *et al*., 2017). Phosphorylation is the driving force for trafficking of nuclear-associated proteins (Jans, 1995).

6.4.4.2 Myristoylation sites within *Pf*C0760c

Myristate is a saturated fatty acid that is attached to an N-terminal glycine residue, catalysed by N-myristoyltransferase (Thinon *et al*., 2014; Farazi *et al*., 2001). This process occurs either during or post-translation (Thinon *et al*., 2014; Farazi *et al*., 2001). It is an essential, irreversible process required for signal transduction pathways, weak interactions between proteins and membrane proteins, and protein targeting (Farazi *et al*., 2001). The N-myristoyltransferase

enzyme has been validated as an antimalarial drug target (Wright *et al*., 2014). The *Pf*C0760c protein is predicted to have several N-myristoylation motifs, indicating that *Pf*C0760c may participate in signal transduction pathways or protein-protein interactions.

6.4.4.3 Glycosylation of *Pf*C0760c

N-linked glycosylation involves the transfer of a lipid-associated carbohydrate to the nitrogen atom of an asparagine side chain (Burda and Aebi, 1999). N- and O-linked glycosylation are important for stability and folding of proteins, protein targeting and recognition (Nalivaeva and Turner, 2001). O-linked glycosylated proteins are typically found in the membrane or are transported proteins (Nalivaeva and Turner, 2001). The hydrophilicity of carbohydrates contributes to protein solubility by ensuring correct protein folding (Nalivaeva and Turner, 2001). N-linked glycosylation is essential for parasite development (Kimura *et al*., 1996).

Several sites for N-linked glycosylation were predicted for the *Pf*C0760c protein, one of which lies within the conserved YERY peptide. These sites have not been confirmed experimentally.

6.4.4.4 Prediction of leucine zippers in *Pf*C0760c

Leucine zippers are associated with the basic leucine zipper family of diverse transcription factors (Nijhawan *et al*., 2008). The characteristic motif for a leucine zipper, which is a common feature of some DNA-binding proteins, has a leucine in every 7th position over a stretch of approximately 30 amino acids (Landschulz *et al*., 1988). A basic domain flanks the leucine zipper, and the latter is found nine amino acids from the C-terminus (Nijhawan *et al*., 2008). A leucine zipper motif was found in the *Pf*C0760c sequence, which together with the SMC domain prediction, suggests a role in the nucleus. However, conflicting results were obtained regarding the leucine zipper motif found in the *Pf*C0760c sequence. The leucine zipper motif was not found at the C-terminus of *Pf*C0760c, nor is it conserved.

6.4.4.5 Lysine acetylation of *Pf*C0760c

Acetylation of lysine residues is a reversible, highly regulated post-translational modification associated with cellular signalling (Miao *et al*., 2013; Choudhary *et al*., 2014). Acetyl groups are transferred from the acetyl coenzyme A cofactor by lysine acetyltransferases, and deacetylation in the nucleus is mediated by sirtuin deacetylases (Choudhary *et al*., 2014). A single lysine residue was predicted to be acetylated in *Pf*C0760c (Miao *et al*., 2013). It is possible that *Pf*C0760c has a signalling role in the parasite nucleus.

6.4.5 Predicted structure of r*Pf*C0760c$_{297}$

Typically, alpha-helical coiled-coils comprise heptad repeats, with non-polar amino acids occupying the first and fourth positions of the heptad (Burkhard *et al*., 2001). The *Pf*C0760c was reported to possess an alpha-helical coiled-coil structure, and on this basis, a potential malaria vaccine candidate (Villard *et al*., 2007). Using the I-TASSER server, alpha helices were illustrated in all the predicted structures (Figure 6.10). Crystallization of the full-length protein may be used to confirm the structure of *Pf*C0760c (McPherson and Gavira, 2014).

6.4.6 Conclusion

*Pf*C0760c is an uncharacterised, conserved *P. falciparum* protein predicted to function in the nucleus, and interact with nuclear-associated proteins. The subcellular localization can be experimentally confirmed by staining the parasite nucleus, and counter-staining with labelled anti-*Pf*C0760c antibodies. Further characterisation of protein-protein interactions of r*Pf*C0760c$_{297}$ with *P. falciparum* proteins may be experimentally evaluated by far-western blot. A DNA-binding assay may be used to assess the interaction between DNA and *Pf*C0760c.

Chapter 7: Immunization of BALB/c mice with r*Pf*C0760c$_{297}$

7.1 Introduction

7.1.1 Mouse malaria pre-clinical trials

Mouse models have often been used to test vaccines, and the immune response and longevity of a vaccine can be assessed (Teixeira and Gomes, 2013). It is difficult to copy the internal environment of a host in an *in vitro* study. An alternative is to use animal models such as mice (Wykes and Good, 2009). Inbred, gene knockout or transgenic mice may be used to understand the immune response to a vaccine (Teixeira and Gomes, 2013). For the study of the effects of a vaccine or the immunopathology of disease, advantages of using animal models such as mice include the availability of inbred or congenic mice, obtainability of ethical approval, practicality (Minkah *et al*., 2018; Wykes and Good, 2009), and mice are easily housed and monitored. Pre-clinical trials are conducted in animals to ensure safety and immunogenicity before trials are conducted in humans.

The drawbacks of using mouse models include the fact that the outcome in humans cannot always be predicted (Teixeira and Gomes, 2013). Additionally, *Plasmodial* parasites infecting humans are unable to develop *in vivo* in rodents (Minkah *et al*., 2018).

7.1.2 *P. berghei* as a model for malaria vaccines

P. berghei, *P. chabaudi* and *P. yoelii* are often used to model different aspects of human *Plasmodial* infections (Huang *et al*., 2015; Wykes and Good, 2009). *P. berghei* can cause a lethal malaria infection in mice, and cerebral malaria (Wykes and Good, 2009). However, some laboratory strains of mice such as BALB/c are not susceptible to cerebral malaria (Wykes and Good, 2009). Hence, the selection of both the infective *Plasmodial* species and mouse strain should be carefully considered.

7.1.3 *Pf*C0760c as a potential malaria vaccine candidate

Since the *Pf*C0760c protein is conserved, homologous proteins are present in *Plasmodial* species infecting humans, monkeys, birds and mice, including *P. berghei* (Chapter 6). In this study, the r*Pf*C0760c$_{297}$ protein was evaluated for its potential to elicit an antibody response in BALB/c mice. It was then further evaluated in a *P. berghei* mouse malaria challenge model.

7.2 Results

7.2.1 Detection of homologous *Pf*C0760c protein in *P. berghei*

Proteins homologous to *Pf*C0760c were identified by BLASTp analysis, including proteins from *Plasmodial* species infecting mice (Chapter 6). The *Pf*C0760c amino acid sequence was aligned with the homologous sequence from *P. berghei*. The alignment between the *P. falciparum* recombinant protein sequence and the corresponding sequence in *P. berghei* is shown in Figure 7.1.

```
P. falciparum       N-YLVNNLQLNKDNDNIIIIKFNILKLFKLGSCYLYIINRNLKEIQ    2404
P. berghei ANKA     NLSSSESREFSVSSDHITLIKCNILKMFKLGSCYLYIINRNLKEIK    1975
                    *    :. ::. ..*:* :** ****:****************:.

P. falciparum       MLKNQILSLEESIKSLNEFINNLKNENEKNELIKINNFEEILKLKN    2450
P. berghei ANKA     ILKDKINYLEENIQSLNLFINNLKDQNKNNEVIKINNEEQIIQLKN    2021
                    :**::*  ***.*:*** ******:*::**:***** *:*::***

P. falciparum       NLQDNESCIQNLNNYLKKNEELNKINVKNIFKYKGYIIHLIQQSNV    2496
P. berghei ANKA     SLQNNENCISNLNDNLKQKDEMNNSNIKNLIKYKSFIINLVHQSNI    2067
                    .**:**.**.***: **:::*:*: *:**::***.:**:*::***:

P. falciparum       FCKIFKHFNENKIIDQSIINKLLYLKKSFDFYMYDSVIQEIRENKN    2542
P. berghei ANKA     FFHIFKIMNTQKVIQNSIYNQLTQLRKELDFYLNDYIMISELENKE    2113
                    * :*** :* :*:*::** *:*  *:*.:***: * :: .  ***:

P. falciparum       I----------IINQDFLTDEYFKHIQTFTKTCNVLIQRGYLSILK    2578
P. berghei ANKA     KLNLSNIENNLLNIVSTFSYENYEHIQIFTNKFNFIIERGKVSIFS    2159
                               :   . :: * ::*** **:. *.:*:** :**:.

P. falciparum       DTNN---------DFFIQNKQSNQQGNQNGNHINMCNIYPDDEINV    2615
P. berghei ANKA     DGKIHPSQNDQTNNFFSNINSYFQNQNQYNNALNFKDLN-ENTIET    2204
                    * :          :** : :.  *: ** .* :*: ::  :: *:.

P. falciparum       TADQQIFDGTENVQQSLQNEEDYVNNEEMYTDKMDLDNN-------    2654
P. berghei ANKA     PKDTQV--QTVQIYQETQNEEENIKNENIATQVNNQNDQIDALKNE    2248
                      * *:   * :: *. ****: ::**:: *:  : :::

P. falciparum       ------MN    2656
P. berghei ANKA     EYNDDQMY    2256
                           *
```

Figure 7.1: Sequence alignment of r*Pf*C0760c$_{297}$ and homologous sequence in *P. berghei* ANKA. The recombinant sequence of *Pf*C0760c (077384.1) from N2360 – N2656 was aligned with the *P. berghei* ANKA sequence (XP_672614.2) from N1929 – N2256. The conserved peptide is indicated by a red box, and a B-cell epitope is indicated by a blue box (Villard *et al*., 2007). The . indicates a similar residue, the : indicates similar physicochemical properties, and * indicates an exact match.

Of the 297 amino acids in the r*Pf*C0760c$_{297}$ sequence, 134 amino acids were conserved (Figure 7.1), accounting for 45% amino acid conservation between the r*Pf*C0760c$_{297}$ sequence and corresponding *P. berghei* sequence. Within the conserved peptide, a single amino acid substitution of leucine to methionine is observed (red box). 19 amino acids are conserved within the 29-mer B-cell epitope.

Polyclonal chicken IgY antibodies had previously been raised in-house against the r*Pf*C0760c$_{297}$ protein (Addicott, 2014). These antibodies were used to determine the presence of the homologous protein in a *P. berghei*-infected mouse blood sample.

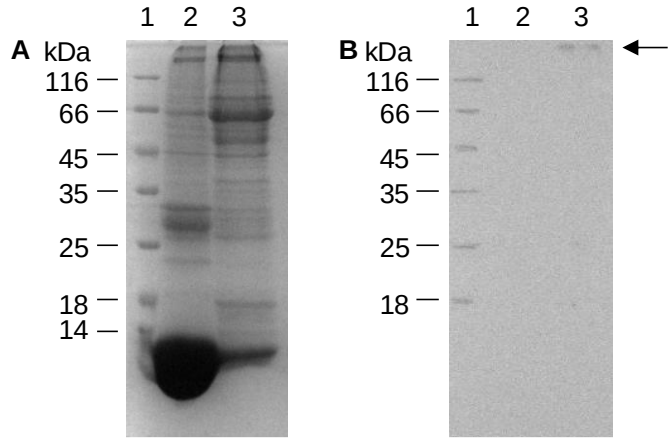

Figure 7.2: Detection of homologous r*Pf*C0760c$_{297}$ protein in *P. berghei*-infected blood. Uninfected and *P. berghei*-infected mouse blood was analysed. **(A)** Blood lysates were resolved on 12.5% reducing SDS-PAGE, and proteins were stained with Coomassie Blue. Lane 1: molecular weight marker. Lane 2: uninfected mouse blood lysate. Lane 3: *P. berghei*-infected mouse blood lysate. **(B)** Western blot of an identical gel probed with chicken anti-r*Pf*C0760c$_{297}$ IgY and detected with rabbit anti-chicken HRPO-IgG.

The protein profile under reducing conditions for a sample of uninfected and *P. berghei*-infected mouse blood shows proteins ranging in size from below 14 kDa to above 116 kDa (Figure 7.2A). The western blot shows a single band of high molecular weight detected in the *P. berghei* infected blood sample (Figure 7.2B, lane 3). No protein was detected by western blot in the uninfected blood sample (lane 2).

7.2.2 Generation of anti-r*Pf*C0760c$_{297}$ antibodies in mice

Mice were immunized with r*Pf*C0760c$_{297}$ on days 0, 14 and 28. On day 42, mice were sacrificed, and blood was collected. The serum was separated from the red blood cells and a checkerboard ELISA was performed. The serum from two mice immunized with buffer alone, and one non-immune mouse was also included for comparison.

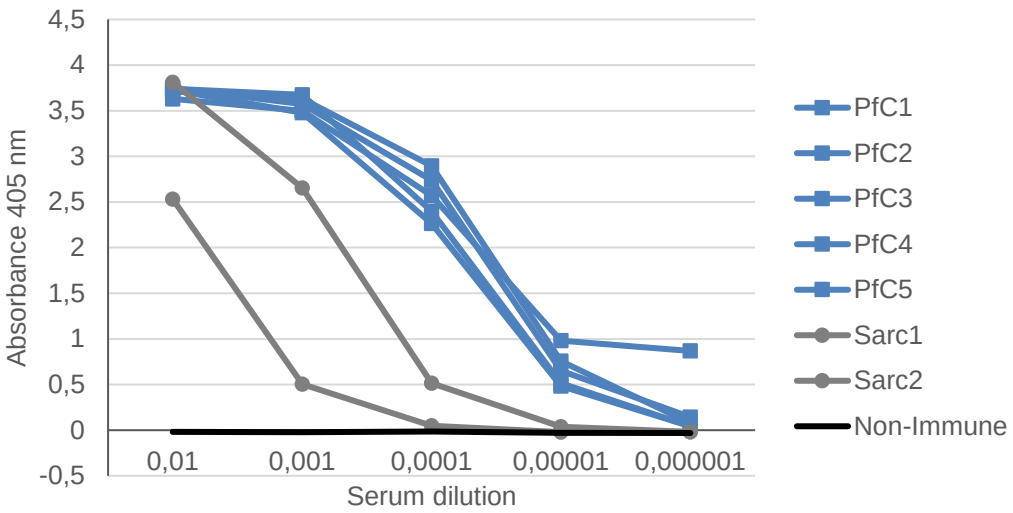

Figure 7.3: Detection of anti-r*Pf*C0760c$_{297}$ antibodies from mice immunized with r*Pf*C0760c$_{297}$. Mice were immunized with r*Pf*C0760c$_{297}$ (PfC; square marker) or buffer (Sarc; round marker) on days 0, 14 and 28. A non-immune mouse was included. Serum was collected and analysed in a checkerboard direct ELISA for antibodies against r*Pf*C0760c$_{297}$. Plate was coated with decreasing concentrations of r*Pf*C0760c$_{297}$. Serial dilutions of mouse serum were prepared. Anti-r*Pf*C0760c$_{297}$ antibodies were detected with goat anti-mouse HRPO-IgG. ABTS-H_2O_2 was used as the substrate.

Mice immunized with r*Pf*C0760c$_{297}$ was able to elicit an antibody response. It was also noted that at higher serum concentrations, there are antibodies present in the control samples Sarc1 and Sarc2. The non-immune mouse serum showed no antibody response to the r*Pf*C0760c$_{297}$ antigen.

7.2.3 Immunization of mice with r*Pf*C0760c$_{297}$ followed by *P. berghei* challenge

The capacity of r*Pf*C0760c$_{297}$ to protect mice from a malaria infection was assessed in a mouse malaria challenge model. BALB/c mice were immunized with solubilized r*Pf*C0760c$_{297}$ on days 0, 14 and 28, and challenged with 10^5 *P. berghei* parasitized red blood cells on day 40. Parasitaemia was monitored every second day by Giemsa-stained blood smears. Control mice were immunized with buffer.

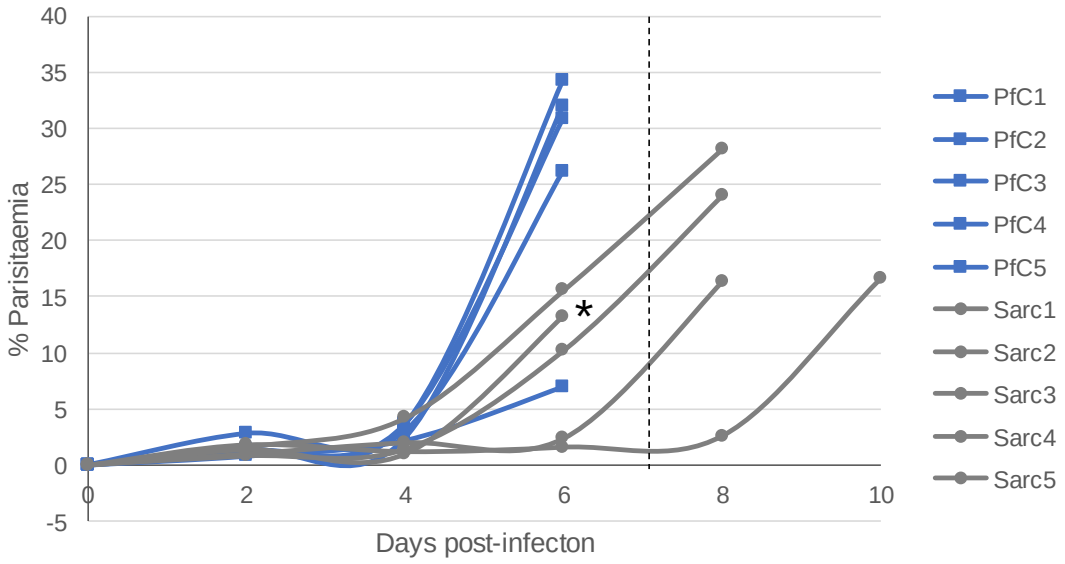

Figure 7.4: Parasitaemia monitored over the course of *P. berghei* infection. Two groups of five mice were immunized with r*Pf*C0760c$_{297}$ (PfC; square marker) or the elution buffer (Sarc; round marker). r*Pf*C0760c$_{297}$-immunized mice were sacrificed on day 7 after challenge (dashed line). Control mice Sarc1 and Sarc2 were sacrificed on day 8, Sarc5 was sacrificed on day 9 and Sarc3 was sacrificed on day 10. The * indicates mouse death.

Parasitaemia in all mice remained below 5% from days 0 – 4 after challenge. A sharp increase in parasitaemia was observed on day 6 in four of the five r*Pf*C0760c$_{297}$-immunized mice with parasitaemia above 25%. The remaining r*Pf*C0760c$_{297}$-immunized mouse had a parasitaemia of ~7% by day 6. All the r*Pf*C0760c$_{297}$-immunized mice were euthanized on day 7. Parasitaemia was monitored for the control mice, and as the parasitaemia approached 20%, mice were euthanized. One mouse, Sarc4 was deceased on day 7, and the last recorded parasitaemia was below 15% on day 6. Sarc1 and Sarc2 control mice were euthanized on day 8, and the parasitaemia was ~24% and 28% respectively. In the Sarc3 mouse, the parasitaemia remained below 5% until day 8 and increased to ~16% on day 9, and was sacrificed on day 10 at a parasitaemia of 19%. The parasitaemia in Sarc5 increased from 2% to ~16% between days 6 and 8 and the mouse was euthanized on day 9 at a parasitaemia of 20%.

7.3 Discussion

7.3.1 Immunization with r*Pf*C0760c$_{297}$

Mice immunized with the r*Pf*C0760c$_{297}$ protein generated an antibody response. However, mice immunized with r*Pf*C0760c$_{297}$ followed by challenge with *P. berghei* blood stage parasites were not protected. One of the five r*Pf*C0760c$_{297}$-immunized mice had a lower parasitaemia on day 6 post-infection compared to the rest of the r*Pf*C0760c$_{297}$-immunized mice (Figure 7.4). This suggests that immunization with the r*Pf*C0760c$_{297}$ protein may have an influence on the

parasitaemia. However, this is not significant, and the experiment needs to be repeated. Three of the 5 control mice were able to survive for at least 8 days post-infection before sacrifice, with one mouse surviving for 10 days post-infection before sacrifice. The cause of death of the remaining mouse was not determined. Various factors could have contributed to the failure of r*Pf*C0760c$_{297}$ to protect the mice, including the choice of adjuvant, the antigen dose, the route of immunization, and the immunization schedule (Jones *et al*., 2001; Hu *et al*., 1989; Playfair and de Souza, 1986). *Pf*C0760c$_{297}$ is predicted to be a *Plasmodium* nuclear protein. Thus, based on the predicted subcellular localization and lack of protection observed in mice, it is possible that *Pf*C0760c$_{297}$ may not be a good malaria vaccine candidate.

7.3.2 Solubilization of r*Pf*C0760c$_{297}$

The r*Pf*C0760c$_{297}$ protein was solubilized using the SDS detergent, as outlined by Schlager *et al*. (2012). Residual SDS from the solubilization procedure could be present in the immunized mice. According to the SDS Material Safety Data Sheet, the LD_{50} in rats was established at 1288 µg/g. The concentration of SDS in the solubilization buffer is 1% (w/v), thus in the final immunization preparation, less than 0.05 µg of SDS was present, which is well below the LD_{50}. Hence, it is unlikely that the presence of residual SDS could have affected the outcome of the immunization. To evaluate the toxicity of SDS in mice, mice can be immunized with SDS alone and the outcome can be assessed.

7.3.3 Conformation of r*Pf*C0760c$_{297}$

The structure of *Pf*C0760c has not been determined at present, but several structures of r*Pf*C0760c$_{297}$ have been predicted (Figure 6.10). Although disulfide bonds were not predicted by the DISULFIND tool (Ceroni *et al*., 2006), r*Pf*C0760c$_{297}$ appears to be smaller in size when electrophoresed under non-reducing conditions (Figure 5.3 and 5.4, lane 10) compared to reducing conditions (Figure 3.12, lane 7). This suggests that disulfide bonds are present in the recombinant protein, as the protein is more compact and mobile (Scheele and Jacoby, 1982). Five cysteine residues are present in the r*Pf*C0760c$_{297}$ sequence, indicating that there may be two possible disulfide bonds. There are 34 cysteine residues present in the entire *Pf*C0760c sequence and are likely to participate in disulfide bond formation, allowing the protein to fold into the correct structure, possibly forming 17 disulfide bonds. Since the structure of *Pf*C0760c is unknown, the pairs of cysteine residues participating in disulfide bond formation are unknown. Several methods are described for the identification of disulfide bonds within a protein, including a combination of protein mass spectrometry and unique sequence tags (Shen *et al*., 2010), and immobilized trypsin and MALDI-TOF analysis (Tang and Speicher, 2004). Site-directed mutagenesis may help identify cysteine residues participating in disulfide bond formation, by mutating specific cysteine residues to serine residues (Hattori *et al*., 2015).

The importance of immunization with correctly folded protein is indicated by a study by Ling *et al.* (1994). The MSP-1 protein was reduced and alkylated, thus changing the protein conformation. Mice immunized with this modified protein were unable to resolve a challenge infection, whereas mice immunized with the correctly folded MSP-1 protein were able to resolve the infection (Ling *et al*., 1994). This is an indication that the correct conformation of the antigen is imperative for providing protective immunity. Rabbits immunized with correctly folded RH5 from *P. falciparum* were able to generate antibodies that were able to prevent *in vitro* invasion and growth of *P. falciparum* parasites (Bustamante *et al*., 2013).

7.3.4 Adjuvant used for immunization with r*Pf*C0760c$_{297}$

Freund's Adjuvants are water-in-mineral oil based, and the Freund's Complete adjuvant contains deactivated *Mycobacterium tuberculosis* (Opie and Freund, 1937). The presence of *M. tuberculosis* encourages antibody production by stimulating the immune system (Trott *et al*., 2008). Comparing the use of Freund's Complete and Incomplete adjuvants for immunization in mice showed that the antibody titres are influenced by the choice of adjuvant for primary and booster immunizations (Hu *et al*., 1989). The combination of Freund's Complete adjuvant for primary immunization and boosting with Freund's Incomplete adjuvant provoked the highest antibody response compared to other combinations of these adjuvants (Hu *et al*., 1989). This combination was used in the r*Pf*C0760c$_{297}$-immunization study. Freund's Adjuvants are prohibited for use in humans due to their negative side effects (Gaspar *et al*., 2018; Apostólico *et al*., 2016). It is unlikely that the toxicity of Freund's adjuvant would have affected the outcome of the immunization in mice, as the mice would not have survived. No other adjuvants were tested. Evaluation of different adjuvants may alter the outcome of the experiment. Some adjuvants that may be tested include MagicMouse^{TM}, aluminium hydroxide, Montanide ISA50 or TiterMax^{TM} (Greenfield, 2019; Leenaars *et al*., 1998; Bennet *et al*., 1992).

7.3.5 Immunization of mice

It was evident that the mice were able to mount an antibody response against the r*Pf*C0760c$_{297}$ protein (Figure 7.3). The antibody response was not evaluated in the mice that were challenged with *P. berghei* parasites. It is assumed that the mice which were immunized and challenged with *P. berghei*-infected red blood cells were able to mount similar antibody responses to the vaccine. It is therefore unclear at this stage the reason for the lack of protection in the r*Pf*C0760c$_{297}$-immunized mice.

7.3.6 Further modifications to the r*Pf*C0760c$_{297}$ immunization study

Several modifications of this study can be evaluated. For immunization of mice, the concentration of the r*Pf*C0760c$_{297}$ antigen can be varied and the antibody response can be

evaluated prior to challenge infection. The number of *P. berghei* parasites that are used for the challenge infection can be decreased. The corresponding region to r*Pf*C0760c$_{297}$ in the *P. berghei* sequence (Figure 7.1) can be tested in an immunization study to determine if it is capable of protecting against a homologous challenge infection. In this study, the T-cell response of the immunized and control mice was not evaluated. The T-cell responses in mice can be evaluated indirectly by the ELISPOT assay or proliferation assays (Brinke *et al*., 2017; Leehan and Koelsch 2015).

7.3.7 Conclusion

Chicken anti-r*Pf*C0760c$_{297}$ IgY antibodies were able to recognise the homologous protein in *P. berghei* infected mouse blood. Mice immunized with solubilized r*Pf*C0760c$_{297}$ were able to raise antibodies against the protein. However, immunization of mice with r*Pf*C0760c$_{297}$ did not protect them from a *P. berghei* challenge infection.

Chapter 8: General discussion and conclusions

8.1 Premise of this study

The lack of a malaria vaccine is a major obstacle preventing the control and eradication of malaria (Bygbjerg *et al*., 2018; Crompton *et al*., 2010). Many malaria proteins have been researched for vaccine development, and none have shown long-term protection (Wykes, 2013). The most developed malaria vaccine is the RTS,S vaccine, which has been evaluated in clinical trials, but has not yet demonstrated satisfactory protection against malaria (Gosling and von Seidlein, 2016). To date, vaccination with attenuated sporozoites delivered by the bite of an infected mosquito has been shown to be the most effective vaccine at preventing clinical malaria (Lyke *et al*., 2017; Ishizuka *et al*., 2016; Spring *et al*., 2013; Hoffman *et al*., 2002). However, this mode of vaccination is not viable in humans (Hollingdale and Sedegah, 2016). Thus, there is a need to identify and evaluate new *Plasmodial* proteins for malaria vaccines.

8.2 Uncharacterised *Plasmodial* proteins

The *Pf*C0760c protein is uncharacterised. Uncharacterised proteins may provide an invaluable tool for understanding, and possibly combatting diseases that are not well understood or deemed incurable. Characterisation of proteins with yet unknown functions may help delineate the pathogenesis of disease, enzymatic functions of the protein, substrates required by the protein, and pathways used by the parasite for disease progression. Detection of conserved functional domains within these proteins may lead to classification according to function or functional groups and substrate domains. Uncharacterised proteins may also provide new drug targets or potential vaccine candidates.

8.3 *Pf*C0760c as a potential malaria vaccine candidate

The *Pf*C0760c protein is a conserved malaria protein displaying alpha-helical coiled-coil domains. Several other *Plasmodial* proteins were identified as potential malaria vaccine candidates based on the presence of alpha-helical coiled-coil domains (Villard *et al*., 2007). Alpha-helical coiled-coil motifs are capable of folding correctly into stable structures, are likely to be recognised by “conformational dependent” antibodies, and are easily produced (Villard *et al*., 2007). An antibody response against a B-cell epitope (Figure 6.4B) of *Pf*C0760c was found in adult human sera from individuals in Burkina Faso, Tanzania and Colombia (Villard *et al*., 2007). Many T-cell epitopes were predicted within the *Pf*C0760c sequence (Rammensee *et al*., 1999). This suggests that *Pf*C0760c is immunogenic in humans.

8.4 r*Pf*C0760c$_{297}$ is expressed as an insoluble protein in *E. coli*

High levels of r*Pf*C0760c$_{297}$ expression was achieved in *E. coli* host cells using terrific broth, which resulted in aggregation of the protein in insoluble inclusion bodies. Modifications of the expression conditions did not produce soluble r*Pf*C0760c$_{297}$. Incorrect folding of the r*Pf*C0760c$_{297}$ protein in the *E. coli* cells could contribute to the expression of insoluble protein.

However, several studies have shown that biologically active protein can be produced within bacterial inclusion bodies (Nahálka, 2008; Nahálka *et al*., 2006; García-Fruitós *et al*., 2005). Expression of recombinant Aβ42 fused to green fluorescent protein at 18°C – 42°C formed inclusion bodies. However, at lower temperatures of expression, higher fluorescence was noted within the inclusion bodies, suggesting that a higher ratio of correctly folded Aβ42 protein was present (de Groot and Ventura, 2006). At a lower temperature of expression, soluble r*Pf*C0760c$_{297}$ was undetected, and the quality of the inclusion bodies was not assessed.

8.5 Expression of r*Pf*C0760c$_{297}$ in the presence of *E. coli* chaperones

The addition of ethanol to the growth media of an *E. coli* culture encourages the expression of *E. coli* chaperones (Ziemienowicz *et al*., 1993; Steczko *et al*., 1991; Lindquist and Craig, 1988) However, there is no evidence in this study to suggest that the expression of the *E. coli* chaperones was affected by the addition of ethanol, or that the *E. coli* chaperones are able to bind to the r*Pf*C0760c$_{297}$ protein. Western blot using chaperone-specific antibodies may illustrate the effects of ethanol on the expression of *E. coli* chaperones. The addition of ethanol to the culture media resulted in reduced expression of r*Pf*C0760c$_{297}$, which remained insoluble (Figure 3.10).

In a separate experiment, *E. coli* cells were co-transformed with plasmids encoding the *E. coli* chaperones GroEL-GroES and *dna*K*dna*J*grp*E, which were co-expressed with r*Pf*C0760c$_{297}$. The *E. coli* chaperones GroEL-GroES and *dna*K*dna*J*grp*E had no impact on the expression of soluble r*Pf*C0760c$_{297}$ under several different conditions tested.

Upregulation of the expression of *E. coli* chaperones was observed in Figure 4.5A, where higher concentrations of the inducer L-arabinose resulted in better expression of the 60 kDa GroEL chaperone. Upregulation of the expression of *E. coli* chaperones can be confirmed by western blot of *E. coli* lysates using antibodies raised against each chaperone. The GroEL and *dna*K chaperones bind to unfolded proteins (Ryabova *et al*., 2013; Martin, 1998). Binding of the *E. coli* chaperones GroEL or *dna*K to the r*Pf*C0760c$_{297}$ protein may be evaluated *in vitro* using an AminoLink™ column coupled to the chaperones, and passing a lysate of *E. coli* cells expressing r*Pf*C0760c$_{297}$. Bound proteins can be eluted and analysed for the presence of r*Pf*C0760c$_{297}$. Far western blot analysis using insoluble r*Pf*C0760c$_{297}$ as the prey protein and

purified GroEL or *dna*K chaperones as the bait proteins. Antibodies raised against the chaperones can be used to confirm binding of the chaperones to r*Pf*C0760c$_{297}$.

8.6 Properties of the *Pf*C0760c protein

Sequence alignment of *Pf*C0760c with the homologous proteins from *Plasmodium* species infecting humans, monkeys, mice and birds revealed three conserved peptides. Bioinformatics analyses predicted various protein characteristics, including the structure, which has yet to be experimentally confirmed.

*Pf*C0760c is expressed during the sporozoite, merozoite and gametocyte stages of the *P. falciparum* life cycle (Florens *et al*., 2002). Nuclear proteomic studies and bioinformatics analysis have suggested that this protein localises to the parasite nucleus (Oehring *et al*., 2012; Blum *et al*., 2009; Brameier *et al*., 2007). This can be confirmed microscopically using nanoparticle- or fluorescent-labelled antibodies.

8.7 Conclusion and future work

The solubilized r*Pf*C0760c$_{297}$ was unable to protect mice from a heterologous *P. berghei* challenge infection. Using the current expression conditions for high yields of r*Pf*C0760c$_{297}$, an alternative means to purify soluble, correctly folded protein may be investigated. r*Pf*C0760c$_{297}$ can be purified under reducing conditions followed by dialysis to remove the reducing agent. Additionally, the r*Pf*C0760c$_{297}$ protein can be fused to the green-fluorescent reporter protein to assess the presence of correctly folded r*Pf*C0760c$_{297}$ (de Groot and Ventura, 2006). Alternatively, the r*Pf*C0760c$_{297}$ inclusion bodies may be purified (Carrió *et al*., 2000), which can then be used to immunize mice. A different region of the *Pf*C0760c protein including the conserved EIYK or YERY peptides may be considered for immunization. Mice may be immunized with the homologous *Pf*C0760c protein from *P. berghei* and challenged with a homologous *P. berghei* infection. Additionally, changes in the immunization regime may be evaluated, where mice are immunized, then infected with *Plasmodium* parasites, followed by drug-cure (Makobongo *et al*., 2003). These mice can then be challenged with a *Plasmodium* infection. A different strain of mice may also be immunized and challenged, and the outcome compared to the current study (Brando *et al*., 2007). To determine whether the *Pf*C0760c protein is vital for parasite survival, a *Pf*C0760c gene knockout study may be conducted in *Plasmodium* parasites, and these parasites can be cultured and assessed for viability.

References

Absalon, S., Robbins, J.A., and Dvorin, J.D. (2016) An essential malaria protein defines the architecture of blood-stage and transmission-stage parasites. *Nature Communications.* **7:** doi: 10.1038/ncomms11449.

Achan, J., Talisuna, A.O., Erhart, A., Yeka, A., Tibenderana, J.K., Baliraine, F.N., Rosenthal, P.J., and D'Alesandro, U. (2011) Quinine, an old anti-malarial drug in a modern world: role in the treatment of malaria. *Malaria Journal.* **10:** doi: 10.1186/1475-2875-10-144.

Acosta, C.J., Galindo, C.M., Schellenberg, D., Aponte, J.J., Kahigwa, E., Urassa, H., Armstrong Schellenberg, J.R.M., Masanja, H., Hayes, R., Kitua, A.Y., Lwilla, F., Mshinda, H., Menendez, C., Tanner, M., and Alonso, P.L. (1999) Evaluation of the S*Pf*66 vaccine for malaria control when delivered through the EPI scheme in Tanzania. *Tropical Medicine and International Health.* **4:** 368 – 376.

Addicott, K.W. (2014) Cloning, expression and partial characterization of a region of the *Plasmodium falciparum* PFC0760c protein. MSc Biochemistry dissertation, University of KwaZulu-Natal, South Africa.

Ahmad, I., Nawaz, N., Darwesh, N.M., ur Rahman, S., Mustafa, M.Z., Khan, S.B., and Patching, S.G. (2018) Overcoming challenges for amplified expression of recombinant proteins using *Escherichia coli. Protein Expression and Purification.* **144:** 12 – 18.

Ahn, T., Yang, S., and Yun, C.H. (2004) Enhanced expression of human cytochrome P450 1A2 by co-expression with human molecular chaperone Hsp70. *Toxicology Letters*. **153:** 267 – 272.

Altschul, S.F., Gish, W., Miller, W., Myers, E.W., and Lipman, D.J. (1990) Basic local alignment search tool. *Journal of Molecular Biology.* **215:** 403 – 410.

Aly, A.S.I., Mikolajczak, S.A., Rivera, H.S., Camargo, N., Jacobs-Lorena, V., Labaied, M., Coppens, I., and Kappe, S.H.I. (2008) Targeted deletion of SAP1 abolishes the expression of infectivity factors necessary for successful malaria parasite liver infection. *Molecular Microbiology.* **69:** 152 – 163.

Antinori, S., Galimberti, L., Milazzo, L., and Corbellino, M. (2012) Biology of human malaria Plasmodia including *Plasmodium knowlesi. Mediterraanean Journal of Hematology and Infectious Diseases.* **4:** doi: 10.4084/MJHID.2012.013.

Apostólico, J.D.S., Lunardelli, V.A.S., Coirada, F.C., Boscardin, S.B., and Rosa, D.S. (2016) Adjuvants: classification, *modus operandi*, and licensing. *Journal of Immunology Research.* doi: 10.1155/2016/1459394.

Ardito, F., Giuliani, M., Perrone, D., Troiano, G., and Muzio, L.L. (2017) The crucial role of protein phosphorylation in cell signaling and its use as targeted therapy. *International Journal of Molecular Medicine.* **40:** 271 – 280.

Baneyx, F. (1999) Recombinant expression in *Escherichia coli*. *Current Opinion in Biotechnology.* **10:** 411 – 421.

Bannister, L.H., Hopkins, J.M., Fowler, R.E., Krishna, S., and Mitchell, G.H. (2000) A brief illustrated guide to the ultrastructure of *Plasmodium falciparum* asexual blood stages. *Parasitology Today.* **16:** 427 – 433.

Barber, B.E., William, T., Grigg, M.J., Menon, J., Auburn, S., Marfurt, J., Anstey, N.M., and Yeo, T.W. (2013) A prospective comparative study of *knowlesi*, *falciparum* and *vivax* malaria in Sabah, Malaysia: high proportion with severe disease from *Plasmodium knowlesi* and *Plasmodium vivax*, but no mortality with early referral and artesunate therapy. *Clinical Infectious Diseases.* **56:** 383 – 397.

Barr, P.J., Green, K.M., Gibson, H.L., Bathurst, I.C., Quakyi, I.A., and Kaslow, D.C. (1991) Recombinant *Pfs*25 protein of *Plasmodium falciparum* elicits malaria transmission-blocking immunity in experimental animals. *Journal of Experimental Medicine.* **174:** 1203 – 1208.

Bartoloni, A., and Zammarchi, L. (2012) Clinical aspects of uncomplicated and severe malaria. *Mediterranean Journal of Hematology and Infectious Diseases.* **4:** doi: 10.4084/MJHID.2012.026

Bartual, S.G., Garcia-Doval, C., Alonso, J., Schoen, G., and van Raaij, M.J. (2010) Two-chaperone assisted soluble expression and purification of the bacteriophage T4 long fibre protein gp37. *Protein Expression and Purification.* **70:** 116 – 121.

Baum, J., Chen, L., Healer, J., Lopaticki, S., Boyle, M., Triglia, T., Ehlgen, F., Ralph, S.A., Beeson, J.G., and Cowman, A.F. (2009) Reticulocyte-binding protein homologue 5 – an essential adhesin involved in invasion of human erythrocytes by *Plasmodium falciparum. International Journal for Parasitology.* **39:** 371 – 380.

Beeson, J.G., Drew, D.R., Boyle, M.J., Feng, G., Fowkes, F.J.I., and Richards, J.S. (2016) Merozoite surface proteins in red blood cell invasion, immunity and vaccines against malaria. *Federation of European Microbiological Societies: Microbiology Reviews.* doi: 10.1093/femsre/fuw001.

Belen Cassera, M., Zhang, Y., Hazleton, K.Z., and Schramm, V.L. (2011) Purine and pyrimidine pathways as targets in *Plasmodium falciparum. Current Topics in Medicinal Chemistry.* **11:** 2103 – 2115.

Bell, S.L., Chiang, A.N., and Brodsky, J.L. (2011) Expression of a malarial Hsp70 improves defects in chaperone-dependent activities in *ssa1* mutant yeast. *Public Library of Science: ONE.* **6:** doi: 10.1371/journal.pone.0020047.

Bennet, B., Check, I.J., Olsen, M.R., and Hunter, R.L. (1992) A comparison of commercially available adjuvants for use in research. *Journal of Immunological Methods.* **153:** 31 – 40.

Berzins, K., Perlmann, H., Wåhlin, B., Carlsson, J., Wahlgren, M., Udomsangpetch, R., Björkman, A., Patarroyo, M.E., and Perlmann, P. (1986) Rabbit and human antibodies to a repeated amino acid sequence of a *Plasmodium falciparum* antigen, *Pf*155, react with the native protein and inhibit merozoite invasion. *Proceedings of the National Academy of Sciences.* **83:** 1065 – 1069.

Bijker, E.M., Borrmann, S., Kappe, S.H., Mordmüller, B., Sack, B.K., and Khan, S.M. (2015) Novel approaches to whole sporozoite vaccination against malaria. *Vaccine*. **33:** 7462 – 7468.

Birkett, A.J. (2016) Status of vaccine research and development of vaccines for malaria. *Vaccine.* **34:** 2915 – 2920.

Birkholtz, L.M., Blatch, G., Coetzer, T.L., Hoppe, H.C., Human, E., Morris, E.J., Ngcete, Z., Oldfield, L., Roth, R., Shonhai, A., Stephens, L., and Louw, A.I. (2008) Heterologous expression of plasmodial proteins for structural studies and functional annotation. *Malaria Journal.* **7:** doi: 10.1186/1475-2875-7-197.

Bliss, C.M., Drammeh, A., Bowyer, G., Sanou, G.S., Jagne, Y.J., Ouedraogo, O., Edwards, N.J., Tarama, C., Ouedraogo, N., Ouedraogo, M., Njie-Jobe, J., Diarra, A., Afolabi, M.O., Tiono, A.B., Yaro, J.B., Adetifa, U.J., Hodgson, S.H., Anagnostou, N.A., Roberts, R., Duncan, C.J.A., Cortese, R., Viebig, N.K., Leroy, O., Lawrie, A.M., Flanagan, K.L., Kampmann, B., Imoukhuede, E.B., Sirima, S.B., Bojang, K., Hill, A.V.S., Nébié, I., and Ewer, K.J. (2017) Viral vector malaria vaccines induce high-level T cell and antibody responses in West African children and infants. *Molecular Therapy.* **25:** 547 – 559.

Blum, T., Briesemeister, S., and Kohlbacher, O. (2009) MultiLoc2: integrating phylogeny and gene ontology terms improves subcellular protein localization prediction. *BioMed Central Bioinformatics*. **10:** doi: 10.1186/1471-2105-10-274.

Bodel, P.T., Nichols, B.A., and Bainton, D.F. (1977) Appearance of peroxidase reactivity within the rough endoplasmic reticulum of blood monocytes after surface adherence. *Journal of Experimental Medicine.* **145:** 264 – 274.

Boratyn, G.M., Camacho, C., Cooper, P.S., Coulouris, G., Fong, A., Ma, N., Madden, T.L., Matten, W.T., McGinnis, S.D., Merezhuk, Y., Raytselis, Y., Sayers, E.W., Tao, T., Ye, J., and Zaretskaya I. (2013) BLAST: a more efficient report with usability improvements. *Nucleic Acids Research.* **41:** W29 – W33.

Bornberg-Bauer, E., Rivals, E., and Vingron, M. (1998) Computational approaches to identify leucine zippers. *Nucleic Acids Research.* **26:** 2740 – 2746.

Bornhorst, J.A., and Falke, J.J. (2000) [16] Purification of proteins using polyhistidine affinity tags. In *Methods in Enzymology.* Academic Press. **326:** 245 – 254.

Borre, M.B., Dziegiel, M., Høgh, B., Petersen, E., Rieneck, K., Riley, E., Meis, J.F., Aikawa, M., Nakamura, K., Harada, M., Wind, A., Jakobsen, P.H., Cowland, J., Jepsen, S., Axelsen, N.H., and Vuust, J. (1991) Primary structure and localization of a conserved immunogenic *Plasmodium falciparum* glutamate rich protein (GLURP) expressed in both the preerythrocytic and erythrocytic stages of the vertebrate life cycle. *Molecular and Biochemical Parasitology.* **49:** 119 – 132.

Botha, M., Pesce, E.R., and Blatch, G.L. (2007) The pso40 genes of *Plasmodium falciparum* and other apicomplexa: regulating chaperone power in the parasite and the host. *International Journal of Biochemistry and Cell Biology.* **39:** 1781 – 1803.

Bousema, J.T., Schneider, P., Gouagna, L.C., Drakeley, C.J., Tostmann, A., Houben, R., Githure, J.I., Ord, R., Sutherland, C.J., Omar, S.A., and Sauerwein, R.W. (2006) Moderate effect of artemisinin-based combination therapy on transmission of *Plasmodium falciparum*. *The Journal of Infectious Diseases.* **193:** 1151 – 1159.

Bousema, T., Okell, L., Felger, I., and Drakeley, C. (2014) Asymptomatic malaria infections: detectability, transmissibility and public health relevance. *Nature Reviews Microbiology.* doi: 10.1038/nrmicro3364.

Boyle, M.J., Wilson, D.W., and Beeson, J.G. (2013) New approaches to studying *Plasmodium falciparum* merozoite invasion and insights into invasion biology. *International Journal for Parasitology.* **43:** 1 – 10.

Bozdech, Z., Zhu, J., Joachimiak, M.P., Cohen, F.E., Pulliam, B., and DeRisi, J.L. (2003a) Expression profiling of the schizont and trophozoite stages of *Plasmodium falciparum* with a long-nucleotide microarray. *Genome Biology.* **4:** doi: 10.1186/gb-2003-4-2-r9.

Bozdech, Z., Llinás, M., Pulliam, B.L., Wong, E.D., Zhu, J., and DeRisi, J.L. (2003b) The transcriptome of the intraerythrocytic developmental cycle of *Plasmodium falciparum. Public Library of Sciences Biology.* **1:** 85 – 100.

Bradford, M.M. (1976) A rapid and sensitive method for the quantitation of microgram quantities of protein utilizing the principle of protein-dye binding. *Analytical Biochemistry.* **72:** 248 – 254.

Brameier, M., Krings, A., and MacCallum, R.M. (2007) NucPred – Predicting nuclear localization of proteins. *Bioinformatics.* **23:** 1159 – 1160.

Brando, C., Ware, L.A., Freyberger, H., Kathcart, A., Barbosa, A., Cayphas, S., Demoitie, M.A., Mettens, P., Heppner, D.G., and Lanar, D.E. (2007) Murine immune responses to liver-stage antigen 1 protein FMP011, a malaria vaccine candidate, delivered with adjuvant AS01B or AS02A. *Infection and Immunity.* **75:** 838 – 845.

Brinke, A.T., Marek-Trzonkowska, N., Mansilla, M.J., Turksma, A.W., Piekarska, K., Iwaszkiewicz-Grześ, D., Passerini, L., Locafaro, G., Puñet-Ortiz, J., van Ham, M., Hernandez-Fuentes, M.P., Martínez-Cáceres, E.M., and Gregori, S. (2017) Monitoring T-cell responses in translational studies: optimization of dye-based proliferation assay for evaluation of antigen-specific responses. *Frontiers in Immunology.* **8:** doi: 10.3389/fimmu.2017.01870.

Brooker, A.S., and Berkowitz, K.M. (2014). The roles of cohesins in mitosis, meiosis, and human health and disease. In: Noguchi E., and Gadaleta M. (eds) *Cell Cycle Control. Methods in Molecular Biology.* Humana Press, New York, NY. **1170:** 229 – 266.

Brown, G.V., Culvernor, J.G., Crewther, P.E., Bianco, A.E., Coppel, R.L., Saint, R.B., Stahl, H.D., Kemp, D.J., and Anders, R.F. (1985) Localization of the ring-infected erythrocyte surface antigen (RESA) of *Plasmodium falciparum* in merozoites and ring-infected erythrocytes. *Journal of Experimental Medicine.* **162:** 774 – 779.

Burda, P. and Aebi, M. (1999) The dolichol pathway of *N*-linked glycosylation. *Biochimica et Biophysica Acta (BBA) – General Subjects.* **1426:** 239 – 257.

Burgess, R.R. (1996) [12] Purification of overproduced *Escherichia coli* RNA polymerase σ factors by solubilizing inclusion bodies and refolding from sarkosyl. In *Methods in Enzymology.* Academic Press. **273:** 145 – 149.

Burkhard, P., Stetefeld, J., and Strelkov, S.V. (2001) Coiled coils: a highly versatile protein folding motif. *Trends in Cell Biology.* **11:** 82 – 88.

Bustamante, L.Y., Bartholdson, S.J., Crosnier, C., Campos, M.G., Wanaguru, M., Nguon, C., Kwiatkowski, D.P., Wright, G.J., and Rayner, J.C. (2013) A full-length recombinant *Plasmodium falciparum Pf*RH5 protein induces inhibitory antibodies that are effective across common *Pf*RH5 genetic variants. *Vaccine.* **31:** 373 – 379.

Bygbjerg, I.C., Simonsen, L., and Schiøler, K.L. (2018) Elimination of falciparum malaria and emergence of severe dengue: an independent or interdependent phenomenon? *Frontiers in Microbiology.* **9:** doi: 10.3389/fmicb.2018.01120.

Camus, D., and Hadley, T.J. (1985) A *Plasmodium falciparum* antigen that binds to host erythrocytes and merozoites. *Science.* **230:** 553 – 556.

Cármenes, R.S., Freije, J.P., Molina, M.M., and Martin, J.M. (1989) Predict7, a program for protein structure prediction. *Biochemical and Biophysical Research Communications.* **159:** 687 – 693.

Carrió, M.M., Cubarsi, R., and Villaverde, A. (2000) Fine architecture of bacterial inclusion bodies. *Federation of European Biochemical Societies: Letters.* **471:** 7 – 11.

Ceroni, A., Passerini, A., Vullo, A., and Frasconi, P. (2006) DISULFIND: a disulfide bonding state and cysteine connectivity prediction server. *Nucleic Acids Research.* **34:** W177 – W181.

Chew, C.H., Lim, Y.A.L., Lee, P.C., Mahmud, R., and Chua, K.H. (2012) Hexaplex PCR detection system for identification of five human *Plasmodium* species with an internal control. *Journal of Clinical Microbiology.* **50:** 4012 – 4019.

Chhetri, G., Kalita, P., and Tripathi, T. (2015) An efficient protocol to enhance recombinant protein expression using ethanol in *Escherichia coli. MethodsX.* **2:** 385 – 391.

Choudhary, C., Weinert, B.T., Nishida, Y., Verdin, E., and Mann, M. (2014) The growing landscape of lysine acetylation links metabolism and cell signalling. *Nature Reviews Molecular Cell Biology.* **15:** 536 – 550.

Chowdhury, D.R., Angov, E., Kariuki, T., and Kumar, N. (2009) A potent malaria transmission blocking vaccine based on codon harmonized full length *Pfs*48/45 expressed in *Escherichia coli. Public Library of Science: ONE.* **4:** doi:10.1371/journal.pone.0006352.

Chua, C.L.L., Brown, G., Hamilton, J.A., Rogerson, S., and Boeuf, P. (2013) Monocytes and macrophages in malaria: protection or pathology? *Trends in Parasitology.* **29:** 26 – 34.

Clyde, D.F., McCarthy, V.C., Miller, R.M., and Woodward, W.E. (1975) Immunization of man against *falciparum* and vivax malaria by use of attenuated sporozoites. *American Journal of Tropical Medicine and Hygiene.* **24:** 397 – 401.

Collins, W.E., Anders, R.F., Pappaioanou, M., Campbell, G.H., Brown, G.V., Kemp, D.J., Coppel, R.L., Skinner, J.C., Andrysiak, P.M., Favaloro, J.M., Corcoran, L.M., Broderson, J.R., Mitchell, G.F., and Campbell, C.C. (1986) Immunization of *Aotus* monkeys with recombinant proteins of an erythrocyte surface antigen of *Plasmodium falciparum. Nature*. **323:** 259 – 262.

Collins, W.E., and Jeffery, G.M. (2007) *Plasmodium malariae*: parasite and disease. *Clinical Microbiology Reviews.* **20:** 579 – 592.

Cong, L., Liang, W., Wu, Y., Li, C., Chang, Y., Dong, L., Song, W., and Ma, J. (2014) High-level soluble expression of the functional peptide derived from the C-terminal domain of the sea cucumber lysozyme and analysis of its antimicrobial activity. *Electronic Journal of Biotechnology.* **17:** 280 – 286.

Cook, J., Aydin-Schmidt, B., González, I.J., Bell, D., Edlund, E., Nassor, M.H., Msellem, M., Ali, A., Abass, A.K., Mårtensson, A., and Björkman, A. (2015) Loop-mediate isothermal amplification (LAMP) for point-of-care detection of asymptomatic low-density malaria parasite carriers in Zanzibar. *Malaria Journal.* **14:** doi:10.1186/s12936-015-0573.

Coppel, R.L., Cowman, A.F., Anders, R.F., Bianco, A.E., Saint, R.B., Lingelbach, K.R., Kemp, D.J., and Brown, K.V. (1984) Immune sera recognize on erythrocytes a *Plasmodium falciparum* antigen composed of repeated amino acid sequences. *Nature.* **310:** 789 – 792.

Coppi, A., Pinzon-Ortiz, C., Hutter, C., and Sinnis, P. (2005) The *Plasmodium* circumsporozoite protein is proteolytically processed during cell invasion. *Journal of Experimental Medicine.* **201:** 27 – 33.

Craig, A.G., Khairul, M.F.M., and Patil, P.R. (2012) Cytoadherence and severe malaria. *Malaysian Journal of Medical Sciences.* **19:** 5 – 18.

Crewther, P.E., Matthew, M.L.S.M., Flegg, R.H., and Anders, R.F. (1996) Protective immune responses to apical membrane antigen 1 of *Plasmodium chabaudi* involve recognition of strain-specific epitopes. *Infection and Immunity.* **64:** 3310 – 3317.

Crompton, P.D., Pierce, S.K., and Miller, L.H. (2010) Advances and challenges in malaria vaccine development. *The Journal of Clinical Investigation.* **120:** 4168 – 4178.

Cummings, J.F., Spring, M.D., Schwenk, R.J., Ockenhouse, C.F., Kester, K.E., Polhemus, M.E., Walsh, D.S., Yoon, I.K., Prosperi, C., Juompan, L.Y., Lanar, D.E., Krzych, U., Hall, B.T., Ware, L.A., Stewart, V.A., Williams, J., Dowler, M., Nielsen, R.K., Hillier, C.J., Giersing, B.K., Dubovsky, F., Malkin, E., Tucker, K., Dubois, M.C., Cohen, J.D., Ballou, W.R., and Heppner Jr, D.G. (2010) Recombinant liver stage antigen-1 (LSA-1) formulated with AS01 or AS02 is safe, elicits high titer antibody and induces IFNɣ/IL-2 CD4+ T cells but does not protect against experimental *Plasmodium falciparum* infection. *Vaccine.* **28:** 5135 – 5144.

Daneshvar, C., Davis, T.M.E., Cox-Singh, J., Rafa'ee, M.Z., Zakaria, S.K., Divis, P.C.S., and Singh, B. (2009) Clinical and laboratory features of human *Plasmodium knowlesi* infection. *Clinical Infectious Diseases.* **49:** 852 – 860.

Davis, K.M., Gibson, L.E., Haselton, F.R., and Wright, D.W. (2014) Simple sample processing enhances malaria rapid diagnostic test performance. *Analyst.* **139:** 3026 – 3031.

Dekel, E., Rivkin, A., Heidenreich, M., Nadav, Y., Ofir-Birin, Y., Porat, Z., and Regev-Rudzki, N. (2017) Identification and classification of the malaria parasite blood developmental stages, using imaging flow cytometry. *Methods.* **112:** 157 – 166.

de Castro, E., Sigrist, C.J.A., Gattiker, A., Bulliard, V., Langendijk-Genevaux, P.S., Gasteiger, E., Bairoch, A., and Hulo, N. (2006) ScanProsite: detection of PROSITE signature matches and ProRule-associated functional and structural residues in proteins. *Nucleic Acids Research.* **34:** 362 – 365.

de Groot, N.S., and Ventura, S. (2006) Effect of temperature on protein quality in bacterial inclusion bodies. *Federation of European Biochemical Societies: Letters.* **580:** 6471 – 6476.

De Las Rivas, J., and Fontanillo, C. (2010) Protein-protein interactions essentials: key concepts to building and analyzing interactome networks. *Public Library of Sciences: Computational Biology.* **6:** doi: 10.1371/journal.pcbi.1000807.

de Marco, A. (2007) Protocol for preparing proteins with improved solubility by co-expressing with molecular chaperones in *Escherichia coli. Nature Protocols.* **2:** 2632 – 2639.

de Marco, A., Deuerling, E., Mogk, A., Tomoyasu, T., and Bukau, B. (2007) Chaperone-based procedure to increase yields of soluble recombinant proteins produced in *E. coli. BioMed Central: Biotechnology.* **7:** doi:10.1186/1472-6750-7-32.

Dhangadamajhi, G., Kar, S.K., and Ranjit, M. (2010) The survival strategies of malaria parasite in the red blood cell and host cell polymorphisms. *Malaria Research and Treatment.* doi: 10.4061/2010/973094.

Dodoo, D., Theisen, M., Kurtzhals, J.A.L., Akanmori, B.D., Koram, K.A., Jepsen, S., Nkrumah, F.K., Theander, T.G., and Hviid, L. (2000) Naturally acquired antibodies to the glutamate-rich protein are associated with protection against *Plasmodium falciparum* malaria. *The Journal of Infectious Diseases.* **181:** 1202 – 1205.

Douglas, A.D., Baldeviano, G.C., Lucas, C.M., Lugo-Roman, L.A., Crosnier, C., Bartholdson, S.J., Diouf, A., Miura, K., Lambert, L.E., Ventocilla, J.A., Leiva, K.P., Milne, K.H., Illingworth, J.J., Spencer, A.J., Hjerrild, K.A., Alanine, D.G.W., Turner, A.V., Moorhead, J.T., Edgel, K.A., Wu, Y., Long, C.A., Wright, G.J., Lescano, A.G., and Draper, S.J. (2015) A *Pf*RH5-based vaccine is efficacious against heterologous strain blood-stage *Plasmodium falciparum* infection in *Aotus* monkeys. *Cell Host and Microbe.* **17:** 130 – 139.

Dundas, K., Shears, M.J., Sun, Y., Hopp, C.S., Crosnier, C., Metcalf, T., Girling, G., Sinnis, P., Billker, O., and Wright, G.J. (2018) Alpha-v–containing integrins are host receptors for the *Plasmodium falciparum* sporozoite surface protein, TRAP. *Proceedings of the National Academy of Sciences.* **115:** 4477 – 4482.

D'Alessandro, U., Leach, A., Olaleye, B.O., Fegan, G.W., Jawara, M., Langerock, P., Greenwood, B.M., Drakeley, C.J., Targett, G.A.T., George, M.O., and Bennett, S. (1995) Efficacy trial of malaria vaccine S*Pf*66 in Gambian infants. *The Lancet.* **346:** 462 – 467.

Egan, J.E., Weber, J.L., Ballou, W.R., Hollingdale, M.R., Majarian, W.R., Gordon, D.M., Maloy, W.L., Hoffman, S.L., Wirtz, R.A., Schneider, I., Woollett, G.R., Young, J.F., and Hockmeyer, W.T. (1987) Efficacy of murine malaria sporozoite vaccines: implications for human vaccine development. *Science.* **236:** 453 – 456.

Ellis, R.D., Martin, L.B., Shaffer, D., Long, C.A., Miura, K., Fay, M.P., Narum, D.L., Zhu, D., Mullen, G.E.D., Mahanty, S., Miller, L.H., and Durbin, A.P. (2010) Phase 1 trial of the *Plasmodium falciparum*

blood stage vaccine MSP-1_{42}-C1/Alhydrogel with and without CPG 7909 in malaria naïve adults. *Public Library of Science: ONE.* **5:** doi: 10.1371/journal.pone.0008787.

El Sahly, H.M., Patel, S.M., Atmar, R.L., Lanford, T.A., Dube, T., Thompson, D., Sim, B.K.L., Long, C., and Keitel, W.A. (2010) Safety and immunogenicity of a recombinant nonglycosylated erythrocyte binding antigen 175 region II malaria vaccine in healthy adults living in an area where malaria is not endemic. *Clinical and Vaccine Immunology.* **17:** 1552 – 1559.

Emini, E.A., Hughes, J.V., Perlow, D.S., and Boger, J. (1985) Induction of hepatitis A virus-neutralizing antibody by a virus-specific synthetic peptide. *Journal of Virology.* **55:** 836 – 839.

Espinosa, D.A., Christensen, D., Muñoz, C., Singh, S., Locke, E., Anderson, P., and Zavala, F. (2017) Robust antibody and CD8+ T-cell responses induced by *P. falciparum* CSP adsorbed to cationic liposomal adjuvant CAF09 confer sterilizing immunity against experimental rodent malaria infection. *Nature Partner Journals: Vaccines.* **2:** doi: 10.1038/s41541-017-0011-y.

Ewer, K.J., O'Hara, G.A., Duncan, C.J.A., Collins, K.A., Sheehy, S.H., Reyes-Sandoval, A., Goodman, A.L., Edwards, N.J., Elias, S.C., Halstead, F.D., Longley, R.J., Rowland, R., Poulton, I.D., Draper, S.J., Blagborough, A.M., Berrie, E., Moyle, S., Williams, N., Siani, L., Folgori, A., Colloca, S., Sinden, R.E., Lawrie, A.M., Cortese, R., Gilbert, S.C., Nicosia, A., and Hill, A.V.S. (2013) Protective CD8+ T-cell immunity to human malaria induced by chimpanzee adenovirus-MVA immunisation. *Nature Communications.* **4:** doi: 10.1038/ncomms3836.

Fagerlund, R.D., Ooi P.L., and Wilbanks, S.M. (2012) Soluble expression and purification of tumor suppressor WT1 and its zinc finger domain. *Protein Expression and Purification.* **85:** 165 – 172.

Fairhurst, R.M., and Dondorp, A.M. (2016) Artemisinin-resistant *Plasmodium falciparum* malaria. *Microbiology Spectrum.* **4:** doi: 10.1128/microbiolspec.EI10-0013-2016.

Farazi, T.A., Waksman, G., and Gordon, J.I. (2001) The biology and enzymology of protein N-myristoylation. *Journal of Biological Chemistry.* **276:** 39501 – 39504.

Farrance, C.E., Chichester, J.A., Musiychuk, K., Shamloul, M., Rhee, A., Manceva, S.D., Jones, R.M., Mamedov, T., Sharma, S., Mett, V., Streatfield, S.J., Roeffen, W., van de Vegte-Bolmer, M., Sauerwein, R.W., Wu, Y., Muratova, O., Miller, L., Duffy, P., Sinden, R., and Yusibov, V. (2011a) Antibodies to plant-produced *Plasmodium falciparum* sexual stage protein *Pf*s25 exhibit transmission blocking activity. *Human Vaccines.* **7:** 191 – 198.

Farrance, C.E., Rhee, A., Jones, R.M., Musiychuk, K., Shamloul, M., Sharma, S., Mett, V., Chichester, J.A., Streatfield, S.J., Roeffen, W., van de Vegte-Bolmer, M., Sauerwein, R.W., Tsuboi, T., Muratova, O.V., Wu, Y., and Yusibov, V. (2011b) A plant-produced *Pf*s230 vaccine candidate blocks transmission of *Plasmodium falciparum. Clinical and Vaccine Immunology.* **18:** 1351 – 1357.

Fatih, F.A., Siner, A., Ahmed, A., Woon, L.C., Craig, A.G., Singh, B., Krishna, S., and Cox-Singh, J. (2012) Cytoadherence and virulence – the case of *Plasmodium knowlesi* malaria. *Malaria Journal.* **11:** doi: 10.1186/1475-2875-11-33.

Fecková, B., Kimáková, P., Ilkovičová, L., Szentpéteriová, E., Debeljak, N., Solárová, Z., Sačková, V., Šemeláková, M., Bhide, M., and Solár, P. (2016) Far-western blotting as a solution to the non-specificity of the anti-erythropoietin receptor antibody. *Oncology Letters.* **12:** 1575 – 1580.

Fidock, D.A., Gras-Masse, H., Lepers, J.P., Brahimi, K., Benmohamed, L., Mellouk, S., Guerin-Marchand, C., Londono, A., Raharimalala, L., and Meis, J.F. (1994) *Plasmodium falciparum* liver stage antigen-1 is well conserved and contains potent B and T cell determinants. *Journal of Immunology.* **153:** 190 – 204.

Fischer, B., Sumner, I., and Goodenough, P. (1993) Isolation, renaturation, and formation of disulfide bonds of eukaryotic proteins expressed in *Escherichia coli* as inclusion bodies. *Biotechnology and Bioengineering.* **41:** 3 – 13.

Flick, K., Ahuja, A., Chene, A., Bejarano, M.T., and Chen, Q. (2004) Optimized expression of *Plasmodium falciparum* erythrocyte membrane protein 1 domains in *Escherichia coli. Malaria Journal.* **3:** doi: 10.1186/1475-2875-3-50.

Florens, L., Washburn, M.P., Raine, J.D., Anthony, R.M., Grainger, M., Haynes, J.D., Moch, J.K., Muster, N., Sacci, J.B., Tabb, D.L., Witney, A.A., Wolters, D., Wu, Y., Gardner, M.J., Holder, A.A., Sinden, R.E., Yates, J.R., and Carucci, D.J. (2002) A proteomic view of the *Plasmodium falciparum* life cycle. *Nature.* **419:** 520 – 526.

Francis, S.E., Sullivan Jr, D.J., and Goldberg, D.E. (1997) Hemoglobin metabolism in the malaria parasite *Plasmodium falciparum. Annual Reviews in Microbiology.* **51:** 97 – 123.

Gamer, J., Multhaup, G., Tomoyasu, T., McCarty, J.S., Rüdiger, S., Schönfeld, H.J., Schirra, C., Bujard, H., and Bukau, B. (1996) A cycle of binding and release of the DnaK, DnaJ and GrpE chaperones regulates activity of the *Escherichia coli* heat shock transcription factor σ^{32}. *European Molecular Biology Organization Journal*. **15:** 607 – 617.

Garcia, C.R.S., Markus, R.P., and Madeira, L. (2001) Tertian and quartan fevers: temporal regulation in malarial infection. *Journal of Biological Rhythms.* **16:** 436 – 443.

García-Fruitós, E., González-Montalbán, N., Morell, M., Vera, A., Ferraz, M.R., Arís, A., Ventura, S., and Villaverde, A. (2005) Aggregation as bacterial inclusion bodies does not imply inactivation of enzymes and fluorescent proteins. *BioMed Central Microbial Cell Factories.* **4:** doi: 10.1186/1475-2859-4-27.

Gardner, M.J., Hall, N., Fung, E., White, O., Berriman, M., Hyman, R.W., Carlton, J.M., Pain, A., Nelson, K.E., Bowman, S., Paulson, I.T., James, K., Eisen, J.A., Rutherford, K., Salzberg, S.L., Craig, A., Kyes, S., Chan, M.S., Nene, V., Shallom, S.J., Suh, B., Peterson, J., Angiuoli, S., Pertea, M., Allen, J., Selengut, J., Haft, D., Mather, M.W., Vaidya, A.B. Martin, D.M.A., Fairlamb, A.H., Fraunholz, M.J., Roos, D.S., Ralph, S.A., McFadden, G.I., Cummings, L.M., Subramanian, G.M., Mungall, C., Venter, J.C., Carucci, D.J., Hoffman, S.L., Newbold, C., Davis, R.W., Fraser, C.M., and Barrell, B. (2002) Genome sequence of the human malaria parasite *Plasmodium falciparum. Nature.* **419:** 498 – 511.

Gaspar, M.P., Landes, G., Safavi, F., and Osterman, A.L. (2018) Accidental injection of Freund Complete Adjuvant with *Mycobacterium tuberculosis. The Journal of Hand Surgery.* **43:** doi: 10.1016/j.jhsa.2018.02.008.

Gasteiger, E., Hoogland, C., Gattiker, A., Duvaud, S., Wilkins, M.R., Appel, R.D., and Bairoch, A. (2005). Protein identification and analysis tools on the ExPASy server. In: Walker, J.M. (eds) *The Proteomics Protocols Handbook*. Humana Press, Totowa. 571 - 607.

Gatton, M.L., Martin, L.B., and Chen, Q. (2004) Evolution of resistance to sulfadoxine-pyrimethamine in *Plasmodium falciparum. Antimicrobial Agents and Chemotherapy.* **48:** 2116 – 2123.

Geissmann, F., Jung, S., and Littman, D.R. (2003) Blood monocytes consist of two principal subsets with distinct migratory properties. *Immunity.* **19:** 71 – 82.

Gibson, L.E., Markwalter, C.F., Kimmel, D.W., Mudenda, L., Mbambara, S., Thuma, P.E., and Wright, D.W. (2017) *Plasmodium falciparum* HRP2 ELISA for analysis of dried blood spot samples in rural Zambia. *Malaria Journal.* **16:** doi.org/10.1186/s12936-017-1996-4.

Giddam, A.K., Reiman, J.M., Zaman, M., Skwarczynski, M., Toth, I., and Good, M.F. (2016) A semi-synthetic whole parasite vaccine designed to protect against blood stage malaria. *Acta Biomaterialia.* **44:** 295 – 303.

Glover, J.R., and Lindquist, S. (1998) Hsp104, Hsp70, and Hsp40: a novel chaperone system that rescues previously aggregated proteins. *Cell.* **94:** 73 – 82.

Goh, L.L., Loke, P., Singh, M., and Sim, T.S. (2003) Soluble expression of a functionally active *Plasmodium falciparum* falcipain-2 fused to maltose-binding protein in *Escherichia coli. Protein Expression and Purification.* **32:** 194 – 201.

Good, M.F., and Doolan, D.L. (2010) Malaria vaccine design: immunological considerations. *Immunity.* **33:** 555 – 566.

Goodman, A.L., and Draper, S.J. (2010) Blood-stage malaria vaccines – recent progress and future challenges. *Annals of Tropical Medicine and Parasitology.* **104:** 189 – 211.

Goodman, A.L., Blagborough, A.M., Biswas, S., Wu, Y., Hill, A.V., Sinden, R.E., and Draper, S.J. (2011) A viral vectored prime-boost immunization regime targeting the malaria *Pfs*25 antigen induces transmission-blocking activity. *Public Library of Science: ONE.* **6:** doi:10.1371/journal.pone.0029428.

Gosling, R., and von Seidlein, L. (2016) The future of the RTS,S/AS01 malaria vaccine: an alternative development plan. *Public Library of Science: Medicine.* **13:** doi: 10.1371/journal.pmed.1001994.

Gragerov, A., Nudler, E., Komissarova, N., Gaitanaris, G.A., Gottesman, M.E., and Nikiforov, V. (1992) Cooperation of GroEL/GroES and DnaK/DnaJ heat shock proteins in preventing protein misfolding in *Escherichia coli. Proceedings of the National Academy of Sciences.* **89:** 10341 – 10344.

Greenfield, E.A. (2019) Preparing and using adjuvants. *Cold Spring Harbor Protocols.* **2019:** doi:10.1101/pdb.prot100214.

Guerra, Á.P., Calvo, E.P., Wasserman, M., and Chapparo-Olaya, J. (2016) Production of recombinant proteins from *Plasmodium falciparum* in *E. coli*. *Biomédica*. **36:** 97 – 108.

Hakimi, H., Goto, Y., Suganuma, K., Angeles, J.M.M., Kawai, S., Inoue, N., and Kawazu, S.I. (2015) Development of monoclonal antibodies against *Plasmodium falciparum* thioredoxin peroxidase 1 and its possible application for malaria diagnosis. *Experimental Parasitology.***154:** 62 – 66.

Hall, R.A. (2004) Studying Protein–Protein Interactions via Blot Overlay or Far Western Blot. In: Fu, H. (eds) *Protein-Protein Interactions: Methods in Molecular Biology.* Humana Press Inc. **261:** 167 – 174.

Hartl, F.U., and Hayer-Hartl, M. (2002) Molecular chaperones in the cytosol: from nascent chain to folded protein. *Science.* **295:** 1852 – 1858.

Harvey, S.H., Krien, M.J.E., and O'Connell, M.J. (2002) Structural maintenance of chromosomes (SMC) proteins, a family of conserved ATPases. *Genome Biology.* **3:** doi: 10.1186/gb-2002-3-2-reviews3003.

Hattori, A., Unno, H., Goda, S., Motoyama, K., Yoshimura, T., and Hemmi, H. (2015) *In vivo* formation of the protein disulfide bond that enhances the thermostability of diphosphomevalonate decarboxylase, an intracellular enzyme from the hyperthermophilic archaeon *Sulfolobus solfataricus. Journal of Bacteriology.* **197:** 3463 – 3471.

Hawthorne, P.L., Trenholme, K.R., Skinner-Adams, T.S., Spielmann, T., Fischer, K., Dixon, M.W.A., Ortega, M.R., Anderson, K.L., Kemp, D.J., and Gardiner, D.L. (2004) A novel *Plasmodium falciparum* ring stage protein, REX, is located in the Maurer's clefts. *Molecular and Biochemical Parasitology.* **136:** 181 – 189.

Hermsen, C.C., Verhage, D.F., Telgt, D.S.C., Teelen, K., Bousema, J.T., Roestenberg, M., Bolad, A., Berzins, K., Corradin, G., Leroy, O., Theisen, M., and Sauerwein, R.W. (2007) Glutamate-rich protein (GLURP) induces antibodies that inhibit *in vitro* growth of *Plasmodium falciparum* in a phase 1 malaria vaccine trial. *Vaccine.* **25:** 2930 – 2940.

Hill, A.V.S. (2011) Vaccines against malaria. *Philosophical Transactions of the Royal Society B: Biological Sciences.* **366:** 2806 - 2814.

Hillier, C.J., Ware, L.A., Barbosa, A., Angov, E., Lyon, J.A., Heppner, D.G., and Lanar, D.E. (2005) Process development and analysis of liver-stage antigen 1, a preerythrocyte-stage protein-based vaccine for *Plasmodium falciparum. Infection and Immunity.* **73:** 2109 – 2115.

Hlongwana, K.W., Mabaso, M.L.H., Kunene, S., Govender, D., and Maharaj, R. (2009) Community knowledge, attitudes and practices (KAP) on malaria in Swaziland: a country earmarked for malaria elimination. *Malaria Journal.* **8:** doi: 10.1186/1475-2875-8-29.

Hoffman, S.L., Goh, L.M.L., Luke, T.C.,Schneider, I., Le, T.P., Doolan, D.L., Sacci, J., de la Vega, P., Dowler, M., Paul, C., Gordon, D.M., Stoute, J.A., Church, L.W.P., Sedegah, M., Heppner, D.G., Ballou, W.R., and Richie, T.L. (2002) Protection of humans against malaria by immunization with radiation-attenuated *Plasmodium falciparum* sporozoites. *The Journal of Infectious Diseases.* **185:** 1155 – 1164.

Holder, A.A., Blackman, M.J., Burghaus, P.A., Chappel, J.A., Ling, I.T., McCallum-Deighton, N., and Shai, S. (1992) A malaria merozoite surface protein (MSP-1) – structure, processing and function. *Memórias do Instituto Oswaldo Cruz.* **87:** 37 – 42.

Hollingdale, M.R., and Sedegah, M. (2016) Development of whole sporozoite malaria vaccines. *Expert Review of Vaccines.* **16:** 45 – 54.

Hopp, T.P., and Woods, K.R. (1981) Prediction of protein antigenic determinants from amino acid sequences. *Proceedings of the National Academy of Sciences.* **78:** 3824 – 3828.

Hu, J.G., Ide, A., Yokoyama, T., and Kitagawa, T. (1989) Studies on the optimal immunization schedule of the mouse as an experimental animal. The effect of antigen dose and adjuvant type. *Chemical and Pharmaceutical Bulletin.* **37:** 3042 – 3046.

Huang, B.W., Pearman, E., and Kim, P.C. (2015) Mouse models of uncomplicated and fatal malaria. *Bio-Protocol.* **5:** e1514.

Ishizuka, A.S., Lyke, K.E., DeZure, A., Berry, A.A., Richie, T.L., Mendoza, F.H., Enama, M.E., Gordon, I.J., Chang, L.J., Sarwar U.N., Zephir, K.L., Holman, L.A., James, E.R., Billingsley, P.F., Gunasekera, A., Chakravarty, S., Manoj. A., Li, M., Ruben, A.J., Li, T., Eappen, A.G., Stafford, R.E., Natasha, K.C., Murshedkar, T., DeCederfelt, H., Plummer, S.H., Hendel, C.S., Novik, L., Costner, P.J.M., Saunders, J.G., Laurens, M.B., Plowe. C.V., Flynn, B., Whalen, W.R., Todd, J.P., Noor, J., Rao, S., Sierra-Davidson, K., Lynn, G.M., Epstein, J.E., Kemp, M.A., Fahle, G.A., Mikolajczak, S.A., Fishbaugher, M., Sack, B.K., Kappe, S.H.I., Davidson, S.A., Garver, L.S., Björkström, N.K., Nason, M.C., Graham, B.S., Roederer, M., Sim, B.K.L., Hoffman, S.L., Ledgerwood, J.E., and Seder, R.A. (2016) Protection against malaria at 1 year and immune correlates following *Pf*SPZ vaccination. *Nature Medicine*. **22:** doi: 10.1038/nm.4110.

Janin, J., Wodak, S., Levitt, M., and Maigret, B. (1978) Conformation of amino acid side-chains in proteins. *Journal of Molecular Biology.* **125:** 357 – 386.

Jans, D.A. (1995) The regulation of protein transport to the nucleus by phosphorylation. *Biochemistry Journal.* **311:** 705 – 716.

Johnston, S.P., Pieniazek, N.J., Xayavong, M.V., Slemenda, S.B., Wilkins, P.P., and da Silva, A.J. (2006) PCR as a confirmatory technique for laboratory diagnosis of malaria. *Journal of Clinical Microbiology.* **44:** 1087 – 1089.

Joice, R., Nilsson, S.K, Montgomery, J., Dankwa, S., Egan, E., Morahan, B., Seydel, K.B., Bertuccini, L., Alano, P., Williamson, K.C., Duraisingh, M.T., Taylor, T.E., Milner, D.A., and Marti, M. (2014) *Plasmodium falciparum* transmission stages accumulate in the human bone marrow. *Science Translational Medicine.* **6:** doi: 10.1126/scitransnlmed.3008882.

Jones, T.R., Narum, D.L., Gozalo, A.S., Aguiar, J., Fuhrmann, S.R., Liang, H., Haynes, J.D., Moch, J.K., Lucas, C., Luu, T., Magill, A.J., Hoffman, S.L., and Sim, B.K.L. (2001) Protection of *Aotus* monkeys by *Plasmodium falciparum* EBA-175 region II DNA prime–protein boost immunization regimen. *The Journal of Infectious Diseases.* **183:** 303 – 312.

Joseph, R.E., and Andreotti, A.H. (2008) Bacterial expression and purification of interleukin-2 tyrosine kinase: single step separation of the chaperonin impurity. *Protein Expression and Purification.* **60:** 194 – 197.

Kantari, C., Pederzoli-Ribeil, M., and Witko-Sarsat, V. (2008) The roles of neutrophils and monocytes in innate immunity. In: Egesten, A. Schmidt, A. Herwald, H. In *Trends in Innate Immunity*. Karger Publishers. **15:** 118 – 146.

Kapulu, M.C., Da, D.F., Miura, K., Li, Y., Blagborough, A.M., Churcher, T.S., Nikolaeva, D., Williams, A.R., Goodman, A.L., Sangare, I., Turner, A.V., Cottingham, M.G., Nicosia, A., Straschil, U., Tsuboi, T., Gilbert, S.C., Long, C.A., Sinden, R.E., Draper, S.J., Hill, A.V.S., Cohuet, A., and Biswas, S. (2015) Comparative assessment of transmission-blocking vaccine candidates against *Plasmodium falciparum*. *Scientific Reports.* **5:** doi: 10.1038/srep11193.

Karch, C.P., Doll, T.A.P.F., Paulillo, S.M., Nebie, I., Lanar, D.E., Corradin, G., and Burkhard, P. (2017) The use of a *P. falciparum* specific coiled-coil domain to construct a self-assembling protein nanoparticle vaccine to prevent malaria. *Journal of Nanobiotechnology.* **15:** doi: 10.1186/s12951-017-0295-0.

Karplus, P.A., and Schulz, G.E. (1985) Prediction of chain flexibility in proteins. *Naturwissenschaften.* **72:** 212 – 213.

Kaslow, D.C., Quakyi, I.A., Syin, C., Raum, M.G., Keister, D.B., Coligan, J.E., McCutchan, T.F., and Miller, L.H. (1988) A vaccine candidate from the sexual stage of human malaria that contains EGF-like domains. *Nature.* **333:** 74 – 76.

Kawai, T., and Akira, S. (2009) The role of TLRs, RLRs and NLRs in pathogen recognition. *International Immunology.* **21:** 317 – 337.

Kearse, M., Moir, R., Wilson, A., Stones-Havas, S., Cheung, M., Sturrock, S., Buxton, S., Cooper, A., Markowitz, S., Duran, C., Thierer, T., Ashton, B., Meintjes, P., and Drummond, A. (2012) Geneious Basic: an integrated and extendable desktop software platform for the organization and analysis of sequence data. *Bioinformatics.* **28:** 1647 – 1649.

Keitany, G.J., Kim, K.S., Krishnamurty, A.T., Hondowicz, B.D., Hahn, W.O., Dambrauskas, N., Sather, D.N., Vaughan, A.M., Kappe, S.H.I., and Pepper, M. (2016) Blood stage malaria disrupts humoral immunity to the pre-erythrocytic stage circumsporozoite protein. *Cell Reports.* **17:** 3193 – 3205.

Kester, K.E., Heppner Jr, D.G., Moris, P., Ofori-Anyinam, O., Krzych, U., Tornieporth, N., McKinney, D., Delchambre, M., Ockenhouse, C.F., Voss, G., Holland, C., Beckey, J.P., Ballou, W.R., Cohen, J., and the RTS,S/TRAP Group. (2014) Sequential phase 1 and phase 2 randomized, controlled trials of the safety, immunogenicity and efficacy of combined pre-erythrocytic vaccine antigens RTS,S and TRAP formulated with AS02 adjuvant system in healthy, malaria naïve adults. *Vaccine.* **32:** 6683 – 6691.

Khan, S., Parillo, M., Gutierrez, A.H., Terry, F.E., Moise, L., Martin, W.D., and De Groot, A.S. (2019) Immune escape and immune camouflage may reduce the efficacy of RTS,S vaccine in Malawi. *Human Vaccines and Immunotherapeutics.* doi: 10.1080/21645515.2018.1560772.

Kho, S., Marfurt, J., Handayuni, I., Pava, Z., Noviyanti, R., Kusuma, A., Piera, K.A., Burdam F.H., Kenangalem, E., Lampa, D.A., Engwerda, C.R., Poespoprodjo, J.R., Price, R.N., Anstey, N.M., Minigo, G., and Woodberry, T. (2016) Characterisation of blood dendritic and regulatory T cells in asymptomatic adults with sub-microscopic *Plasmodium falciparum* or *Plasmodium vivax* infection. *Malaria Journal.* **15:** doi: 10.1186/s12936-016-1382-7.

Khusmith, S., Sedegah, M., and Hoffman, S.L. (1994) Complete protection against *Plasmodium yoelii* by adoptive transfer of a CD8+ cytotoxic T-cell clone recognizing sporozoite surface protein 2. *Infection and Immunity.* **62:** 2979 – 2983.

Kilikian, B.V., Suárez, I.D., Liria, C.W., and Gombert, A.K. (2000) Process strategies to improve heterologous protein production in *Escherichia coli* under lactose or IPTG induction. *Process Biochemistry.* **35:** 1019 – 1025.

Kimura, E.A., Couto, A.S., Peres, V.J., Casal, O.L., and Katzin, A.M. (1996) N-linked glycoproteins are related to schizogony of the intraerythrocytic stage in *Plasmodium falciparum*. *Journal of Biological Chemistry*. **271:** 14452 – 14461.

Knapp, B., Hundt, E., and Küpper, H.A. (1990) *Plasmodium falciparum* aldolase: gene structure and localization. *Molecular and Biochemical Parasitology.* **40:** 1 – 12.

Koram, A.K., Adu, B., Ocran, J., Karikari, Y.S., Adu-Amankwah, S., Ntiri, M., Abuaku, B., Dodoo, D., Gyan, B., Kronmann, K.C., and Nkrumah, F. (2016) Safety and immunogenicity of EBA-175 RII-NG malaria vaccine administered intramuscularly in semi-immune adults: a phase 1, double-blinded placebo controlled dosage escalation study. *Public Library of Science: ONE.* **11:** doi: 10.1371/journal.pone.0163066.

Kosinski, M.J., Rinas, U., and Bailey, J.E. (1992) Isopropyl-*β*-D-thiogalactopyranoside influences the metabolism of *Escherichia coli. Applied and Microbial Biotechnology.* **36:** 782 – 784.

Kozicki, M., Czepiel, J., Biesiada, G., Nowak, P., Garlicki, A., and Wesełucha-Birczyńska, A. (2015) The ring-stage of *Plasmodium falciparum* observed in RBCs of hospitalized malaria patients. *Analyst.* **140:** 8007 – 8016.

Kram, K.E., and Finkel, S.E. (2015) Rich medium composition affects *Escherichia coli* survival, glycation, and mutation frequency during long-term batch culture. *Applied and Environmental Microbiology.* **81:** 4442 – 4450.

Krettli, A.U., and Miller, L.H. (2001) Malaria: a sporozoite runs through it. *Current Biology.* **11:** R409 – R412.

Krogh, A., Larsson, B., Von Heijne, G., and Sonnhammer, E.L.L. (2001) Predicting transmembrane protein topology with a hidden Markov model: application to complete genomes. *Journal of Molecular Biology.* **305:** 567 – 580.

Krzywinska, E., Dennison, N.J., Lycett, G.J., and Krzywinski, J. (2016) A maleness gene in the malaria mosquito *Anopheles gambiae. Science.* **353:** 67 – 69.

Kuehn, A., and Pradel, G. (2010) The coming-out of malaria gametocytes. *Journal of Biomedicine and Biotechnology*. **2010:** doi: 10.1155/2010/976827.

Kulangara, C., Luedin, S., Dietz, O., Rusch, S., Frank, G., Mueller, D., Moser, M., Kajava, A.V., Corradin, G., Beck, H.P., and Felger, I. (2012) Cell biological characterization of the malaria vaccine

candidate trophozoite exported protein 1. *Public Library of Science: ONE.* **7:** doi: 10.1371/journal.pone.0046112.

Kurtis, J.D., Hollingdale, M.R., Luty, A.J.F., Lanar, D.E., Krzych, U., and Duffy, P.E. (2001) Pre-erythrocytic immunity to *Plasmodium falciparum*: the case for an LSA-1 vaccine. *Trends in Parasitology.* **17:** 219 – 223.

Kyes, S., Horrocks, P., and Newbold, C. (2001) Antigenic variation at the infected red cell surface in malaria. *Annual Reviews in Microbiology.* **55:** 673 – 707.

Labaied, M., Camargo, N., and Kappe, S.H.I. (2007) Depletion of the *Plasmodium berghei* thrombospondin-related sporozoite protein reveals a role in host cell entry by sporozoites. *Molecular and Biochemical Parasitology.* **153:** 158 – 166.

LaCount, D.J., Vignali, M., Chettier, R., Phansalkar, A., Bell, R., Hesselberth, J.R., Schoenfeld, L.W., Ota, I., Sahasrabudhe, S., Kurschner, C., Fields, S., and Hughes, R.E. (2005) A protein interaction network of the malaria parasite *Plasmodium falciparum. Nature.* **438:** 103 – 107.

Laemmli, U.K. (1970) Cleavage of structural proteins during the assembly of the head of bacteriophage T4. *Nature.* **227:** 680 – 685.

Landschulz, W.H., Johnson, P.F., and McKnight, S.L. (1988) The leucine zipper: a hypothetical structure common to a new class of DNA binding proteins. *Science*. **240:** 1759 – 1764.

Larentis, A.L., Nicolau, J.F.M.Q., dos Santos Estevez, G., Vareschini, D.T., de Almeida, F.V.R., dos Reis, M.T., Galler, R., and Medeiros, M.A. (2014) Evaluation of pre-induction temperature, cell growth at induction and IPTG concentration on the expression of a leptospiral protein in *E. coli* using shaking flasks and a microbioreactor. *BioMed Central Research Notes.* **7:** doi: 10.1186/1756-0500-7-671.

LaVallie, E.R., DiBlasio, E.A., Kovacic, S., Grant, K.L., Schendel, P.F., and McCoy, J.F. (1993) A thioredoxin gene fusion expression system that circumvents inclusion body formation in the *E. coli* cytoplasm. *Nature Biotechnology.* **11:** 187 – 193.

Leehan K.M., and Koelsch K.A. (2015) T Cell ELISPOT: For the Identification of Specific Cytokine-Secreting T Cells. In: Kurien B., and Scofield R. (eds) *Western Blotting. Methods in Molecular Biology*. Humana Press, New York, NY. **1312:** 427 – 434.

Leenaars, P.P.A.M., Koedam, M.A., Wester, P.W., Baumans, V., Claassen, E., and Hendriksen, C.F.M. (1998) Assessment of side effects induced by injection of different adjuvant/antigen combinations in rabbits and mice. *Laboratory Animals.* **32:** 387 – 406.

Lessard, C.L. (2013) Growth media for *E. coli*. In *Methods in Enzymology.* Academic Press. **533:** 181 – 189.

Li, Q., Liu, H., Du, D., Yu, Y., Ma, C., Jiao, F., Yao, H., Lu, C., and Zhang, W. (2015) Identification of novel laminin- and fibronectin-binding proteins by far western blot: capturing the adhesins of *Streptococcus suis* type 2. *Frontiers in Cellular and Infection Microbiology.* **5:** doi:10.3389/fcimb.2015.00082.

Lindquist, S., and Craig, E.A. (1988) The heat shock proteins. *Annual Review of Genetics*. **22:** 631 - 677.

Ling, I.T., Ogun, S.A., and Holder, A.A. (1994) Immunization against malaria with a recombinant protein. *Parasite Immunology.* **16:** 63 – 67.

Lodish, H., Berk, A., Zipursky, S.L., Matsudaira, P., Baltimore, D., and Darnell, J. (2000) Section 7.1, DNA Cloning with Plasmid Vectors. In *Molecular Cell Biology.* 4th edition. New York: W. H. Freeman. Available from: https://www.ncbi.nlm.nih.gov/books/NBK21498/.

López, M.C., Silva, Y., Thomas, M.C., Garcia, A., Faus, M.J., Alonso, P., Martinez, F., Del Real, G., and Alonso, C. (1994) Characterization of S*Pf*(66)n: a chimeric molecule used as a malaria vaccine. *Vaccine.* **12:** 585 – 591.

Lu, X., Liu, T., Zhu, F., Chen, L., and Xu, W. (2017) A whole-killed, blood stage lysate vaccine protects against the malaria liver stage. *Parasite Immunology.* **39:** doi: 10.1111/pim.12386.

Luscombe, N.M., Greenbaum, D., and Gerstain, M. (2001) What is bioinformatics? A proposed definition and overview of the field. *Methods of Information in Medicine.* **40:** 346 – 358.

Lyke, K.E., Ishizuka, A.S., Berry, A.A., Chakravarty, S., DeZure, A., Enama, M.E., James, E.R., Billingsley, P.F., Gunasekera, A., Manoj, A., Li, M., Ruben, A.J., Li, T., Eappen, A.G., Stafford, R.E., Natasha, K.C., Murshedkar, T., Mendoza, F.H., Gordon, I.J., Zephir, K.L., Holman, L.A., Plummer, S.H., Hendel, C.S., Novik, L., Costner, P.J.M., Saunders, J.G., Berkowitz, N.M., Flynn, B.J., Nason, M.C., Garver, L.S., Laurens, M.B., Plowe, C.V., Richie, T.L., Graham, B.S., Roederer, M., Sim, B.K.L., Ledgerwood, J.E., Hoffman, S.L., and Seder, R.A. (2017) Attenuated *Pf*SPZ Vaccine induces strain-transcending T cells and durable protection against heterologous controlled human malaria infection. *Proceedings of the National Academy of Sciences.* **114:** 2711 – 2716.

MacDonald, N.J., Nguyen, V., Shimp, R., Reiter, K., Herrera, R., Burkhardt, M., Muratova, O., Kumar, K., Aebig, J., Rausch, K., Lambert, L., Dawson, N., Sattabongkot, J., Ambroggio, X., Duffy, P.E., Wu, Y., and Narum, D.L. (2016) Structural and immunological characterization of recombinant 6-cysteine domains of the *Plasmodium falciparum* sexual stage protein *Pf*s230. *Journal of Biological Chemistry.* **291:** 19913 – 19922.

Madar, D., Dekel, E., Bren, A., Zimmer, A., Porat, Z., and Alon, U. (2013) Promoter activity dynamics in the lag phase of *Escherichia coli*. *BioMed Central Systems Biology.* **7:** doi: 10.1186/1752-0509-7-136.

Mahajan, B., Berzofsky, J.A., Boykins, R.A., Majam, V., Zheng, H., Chattopadhyay, R., de la Vega, P., Moch, J.K., Haynes, J.D., Belyakov, I.M., Nakhasi, H.L., and Kumar, S. (2010) Multiple antigen peptide vaccines against *Plasmodium falciparum* malaria. *Infection and Immunity.* **78:** 4613 – 4624.

Mahanty, S., Miller, L.H., Saul, A., and Martin, L.B. (2007) Phase 1 study of two merozoite surface protein 1 ($MSP1_{42}$) vaccines for *Plasmodium falciparum* malaria. *Public Library of Science: Clinical Trials.* **2:** doi: 10.1371/journal.pctr.0020012.

Maharaj, R., Raman, J., Morris, N., Moonasar, D., Durrheim, D.N., Seocharan, I., Kruger, P., Shandukani, B., and Kleinschmidt, I. (2013) Epidemiology of malaria in South Africa: from control to elimination. *The South African Medical Journal.* **103:** 779 – 783.

Mahende, C., Ngasala, B., Lisungu, J., Yong, T.S., Lushino, P., Lemnge, M., Mmbando, B., and Premji, Z. (2016) Performance of rapid diagnostic test, blood-film microscopy and PCR for the diagnosis of malaria infection among febrile children from the Korogwe District, Tanzania. *Malaria Journal.* **15:** doi: 10.1186/s12936-016-1450-z.

Maier, R.M. (2000) Bacterial growth. In Maier, R.M., Pepper, I.L., and Gerba, C.P. (eds) *Environmental Microbiology*. 2nd edition. Oxford: Academic Press. 38 - 56.

Makhoba, X.H., Burger, A., Coertzen, D., Zininga, T., Birkholtz, L.M., and Shonhai, A. (2016) Use of a chimeric Hsp70 to enhance the quality of recombinant *Plasmodium falciparum* S-adenosylmethionine decarboxylase protein produced in *Escherichia coli*. *Public Library of Science: ONE.* **11:** doi: 10.1371/journal.pone.0152626.

Makobongo, M.O., Riding, G., Xu, H., Hirunpetcharat, C., Keough, D., De Jersey, J., Willadsen, P., and Good, M.F. (2003) The purine salvage enzyme hypoxanthine guanine xanthine phosphoribosyl transferase is a major target antigen for cell-mediated immunity to malaria. *Proceedings of the National Library of Sciences.* **100:** 2628 – 2633.

Malkin, E.M., Diemert, D.J., McArthur, J.H., Perreault, J.R., Miles, A.P., Giersing, B.K., Mullen, G.E., Orcutt, A., Muratova, O., Awkal, M., Zhou, H., Wang, J., Stowers, A., Long, C.A., Mahanty, S., Miller, L.H., Saul, Al., and Durbin, A.P. (2005) Phase 1 clinical trial of apical membrane antigen 1: an asexual blood-stage vaccine for *Plasmodium falciparum* malaria. *Infection and Immunity.* **73:** 3677 – 3685.

Malkin, E., Long, C.A., Stowers, A.W., Zou, L., Singh, S., MacDonald, M.J., Narum, D.L., Miles, A.P., Orcutt, A.C., Muratova, O., Moretz, S.E., Zhou, H., Diouf, A., Fay, M., Tierney, E., Leese, P.,

Maltha, J., Gillet, P., and Jacobs, J. (2013) Malaria rapid diagnostic tests in travel medicine. *Clinical Microbiology and Infection.* **19:** 408 – 415.

Marchler-Bauer, A., Bo, Y., Han, L., He, J., Lanczycki, C.J., Lu, S., Chitsaz, F., Derbyshire, M.K., Geer, R.C., Gonzales, N.R., Gwadz, M., Hurwitz, D.I., Lu, F., Marchler, G.H., Song, J.S., Thanki, N., Wang, Z., Yamashita, R.A., Zhang, D., Zheng, C., Geer, L.Y., and Bryant, S.H. (2017) CDD/SPARCLE: functional classification of proteins via subfamily domain architectures. *Nucleic Acids Research.* **45:** D200 – D203.

Markwalter, C.F., Davis, K.M., and Wright, D. (2016) Immunomagnetic capture and colorimetric detection of malarial biomarker *Plasmodium falciparum* lactate dehydrogenase. *Analytical Biochemistry.* **493:** 30 – 34.

Marsh, K., Forster, D., Waruiru, C., Mwangi, I., Winstanley, M., Marsh, V., Newton, C., Winstanley, P., Warn, P., Peshu, N., Pasvol, G., and Snow, R. (1995) Indicators of life-threatening malaria in African children. *The New England Journal of Medicine.* **332:** 1399 – 1404.

Marti, M., Baum, J., Rug, M., Tilley, L., and Cowman, A.F. (2005) Signal-mediated export of proteins from the malaria parasite to the host erythrocyte. *Journal of Cell Biology.* **171:** 587 – 592.

Martin, J. (1998) Protein folding assisted by the GroEL/GroES chaperonin system. *Biochemistry (Moscow)*. **63:** 374 – 381.

Matambo, T.S., Odunuga, O.O., Boshoff, A., and Blatch, G.L. (2004) Overproduction, purification, and characterization of the *Plasmodium falciparum* heat shock protein 70. *Protein Expression and Purification.* **33:** 214 – 222.

Mayhew, M., da Silva, A.C.R., Martin, J., Erdjument-Bromage, H., Tempst, P., and Hartl, F.U. (1996) Protein folding in the central cavity of the GroEL-GroES chaperonin complex. *Nature.* **379:** 420 – 426.

Mbewe, B., Chibale, K., and McIntosh, D.B. (2007) Purification of human malaria parasite hypoxanthine guanine xanthine phosphoribosyltransferase (HGXPRT) using immobilized Reactive Red 120. *Protein Expression and Purification.* **52:** 153 – 158.

McColm, A.A., and Dalton, L. (1983) Heterologous immunity in rodent malaria: comparison of the degree of cross-immunity generated by vaccination with that produced by exposure to live infection. *Annals of Tropical Medicine and Parasitology.* **77:** 355 – 377.

McFall, E., and Newman, E.B. (1996) 1996. Amino acids as carbon sources, p. 358-379. In F. C. Neidhardt, R. Curtiss III, J. L. Ingraham, E. C. C. Lin, K. B. Low, B. Magasanik, W. S. Reznikoff, M. Riley, M. Schaechter, and H. E. Umbarger (ed.), *Escherichia coli* and *Salmonella*: cellular and molecular biology, 2nd ed. ASM Press, Washington, D.C.

McPherson, A., and Gavira, J.A. (2014) Introduction to protein crystallization. *Acta Crystallographica Section F: Structural Biology Communications.* **70:** 2 – 20.

Mehlin, C., Boni, E., Buckner, F.S., Engel, L., Feist, T., Gelb, M.H., Haji, L., Kim, D., Liu, C., Mueller, N., Myler, P.J., Reddy, J.T., Sampson, J.N., Subramanian, E., Van Voorhis, W.C., Worthey, E., Zucker, F., and Hol, W.G.J. (2006) Heterologous expression of proteins from *Plasmodium falciparum:* results from 1000 genes. *Molecular and Biochemical Parasitology.* **148:** 144 – 160.

Melby, T.E., Ciampaglio, C.N., Briscoe, G., and Erickson, H.P. (1998) The symmetrical structure of structural maintenance of chromosomes (SMC) and MukB proteins: long, antiparallel coiled coils, folded at a flexible hinge. *Journal of Cell Biology.* **142:** 1595 – 1604.

Meraldi, V., Nebié, I., Tiono, A.B., Diallo, D., Sanogo, E., Theisen, M., Druilhe, P., Corradin, G., Moret, R., and Sirima, B.S. (2004) Natural antibody response to *Plasmodium falciparum* Exp-1, MSP-3 and GLURP long synthetic peptides and association with protection. *Parasite Immunology.* **26:** 265 – 272.

Miao, J., Lawrence, M., Jeffers, V., Zhao, F., Parker, D., Ge, Y., Sullivan Jr, W.J., and Cui, L. (2013) Extensive lysine acetylation occurs in evolutionarily conserved metabolic pathways and parasite-specific functions during *Plasmodium falciparum* intraerythrocytic development. *Molecular Microbiology.* **89:** 660 – 675.

Mikolajczak, S.A., Lakshmanan, V., Fishbaugher, M., Camargo, N., Harupa, A., Kaushansky, A., Douglass, A.N., Baldwin, M., Healer, J., O'Neill, M., Phuong, T., Cowman, A., and Kappe, S.H.I. (2014) A next-generation genetically attenuated *Plasmodium falciparum* parasite created by triple gene deletion. *Molecular Therapy.* **22:** 1707 – 1715.

Milek, R.L.B., Roeffen, W.F.G., Kocken, C.H.M., Jansen, J., Kaan, A.M., Eling, W.M.C., Sauerwein, R.W., and Konings, R.N.H. (1998) Immunological properties of recombinant proteins of the transmission blocking vaccine candidate, *Pfs*48/45, of the human malaria parasite *Plasmodium falciparum* produced in *Escherichia coli.* **20:** 377 – 385.

Miller, L.H., Ackerman, H.C., Su, X.Z., and Wellems, T.E. (2013) Malaria biology and disease pathogenesis: insights for new treatments. *Nature Medicine.* 156 – 167.

Minkah, N.K., Schafer, C., and Kappe, S.H.I. (2018) Humanized mouse models for the study of human malaria parasite biology, pathogenesis, and immunity. *Frontiers in Immunology.* **9:** doi: 10.3389/fimmu.2018.00807.

Moody, A. (2002) Rapid diagnostic tests for malaria parasites. *Clinical Microbiology Reviews.* **15:** 66 – 78.

Moorthy, V.S., Good, M.F., and Hill, A.V.S. (2004) Malaria vaccine developments. *The Lancet.* **363:** 150 – 156.

Muerhoff, A.S., Birkenmeyer, L.G., Coffey, R., Dille, B.J., Barnwell, J.W., Collins, W.E., Sullivan, J.S., Dawson, G.J., and Desai, S.M. (2010) Detection of *Plasmodium falciparum, vivax, ovale* and *malariae* MSP1-p19 antibodies in human malaria patients and experimentally infected non-human primates. *Clinical and Vaccine Immunology.* **17:** 1631 – 1638.

Muralidharan, V., Oksman, A., Pal, P., Lindquist, S., and Goldberg, D.E. (2012) *Plasmodium falciparum* heat shock protein 110 stabilizes the asparagine repeat-rich parasite proteome during malarial fevers. *Nature Communications.* **3:** doi:10.1038/ncomms2306.

Muralidharan, V., and Goldberg, D.E. (2013) Asparagine repeats in *Plasmodium falciparum* proteins: good for nothing? *Public Library of Science: Pathogens.* **9:** doi: 10.1371/journal.ppat.1003488.

Nahálka, J. (2008) Physiological aggregation of maltodextrin phosphorylase from *Pyrococcus furiosus* and its application in a process of batch starch degradation to α-D-glucose-1-phosphate. *Journal of Industrial Microbiology and Biotechnology.***35:** 219 – 223.

Nahálka, J., Gemeiner, P., and Bučko, M. (2006) Bioenergy beads: a tool for regeneration of ATP/NTP in biocatalytic synthesis. *Artificial Cells, Blood Substitutes, and Biotechnology.***34:** 515 – 521.

Nalivaeva, N.N., and Turner, A.J. (2001) Post-translational modifications of proteins: acetylcholinesterase as a model system. *Proteomics: International Edition.* **1:** 735 – 747.

Nambati, E.A., Kiarie, W.C., Kimani, F., Kimotho, J.H., Otinga, M.S., Too, E., Kaniaru, S., Limson, J., and Bulimo, W. (2018) Unclear association between levels of *Plasmodium falciparum* lactate dehydrogenase (*Pf*LDH) in saliva of malaria patients and blood parasitaemia: diagnostic implications? *Malaria Journal.* **17:** doi.org/10.1186/s12936-017-2151-y.

Nandakumar, D.N., Nagaraj, V.A., Vathsala, P.G., Rangarajan, P., and Padmanaban, G. (2006) Curcumin-artemisinin combination therapy for malaria. *Antimicrobial Agents and Chemotherapy.* **50:** 1859 – 1860.

Newton, P.N., Chotivanich, K., Chierakul, W., Ruangveerayuth, R., Teerapong, P., Silamut, K., Looareesuwan, S., and White, N.J. (2001) A comparison of the *in vivo* kinetics of *Plasmodium falciparum* ring-infected erythrocyte surface antigen-positive and -negative erythrocytes. *Blood.* **98:** 450 – 457.

Nijhawan, A., Jain, M., Tyagi, A.K. and Khurana, J.P. (2008) Genomic survey and gene expression analysis of the basic leucine zipper transcription factor family in rice. *Plant Physiology.* **146:** 333 – 350.

Nishihara, K., Kanemori, M., Kitagawa, M., Yanagi, H., and Yura, T. (1998) Chaperone co-expression plasmids: differential and synergistic roles of DnaK-DnaJ-GrpE and GroEL-GroES in assisting folding of an allergen of Japanese cedar pollen, Cryj2, in *Escherichia coli. Applied and Environmental Microbiology.* **64:** 1694 – 1699.

Noedl, H., Yingyuen, K., Laoboonchai, A., Fukuda, M., Sirichaisinthop, J., and Miller, R.S. (2006) Sensitivity and specificity of an antigen detection ELISA for malaria diagnosis. *American Journal of Tropical Medicine and Hygiene.* **75:** 1205 – 1208.

Nosten, F., Luxemburger, C., Kyle, D.E., Ballou, W.R., Wittes, J., Wah, E., Chongsuphajaisiddhi, T., Gordon, D.M., White, N.J., Sadoff, J.C., Heppner, D.G., and the Shoklo S*Pf*66 Malaria Vaccine Trial Group. (1996) Randomised double-blind placebo-controlled trial of S*Pf*66 malaria vaccine in children in northwestern Thailand. *The Lancet.* **348:** 701 – 707.

Notomi, T., Okayama, H., Masubuchi, H., Yonekawa, T., Watanabe, K., Amino, N., and Hase, T. (2000) Loop-mediated isothermal amplification of DNA. *Nucleic Acids Research.* **28:** e63.

Noya, O.G., Berti, Y.G., de Noya, B.A., Borges, R., Zerpa, N., Urbáez, J.D., Madonna, A., Garrido, E., Jimenéz, M.A., Borges, R.E., Garcia, P., Reyes, I., Prieto, W., Colmenares, C., Pabón, R., Barraez, T., de Caceres, L.G., Godoy, N., and Sifontes, R. (1994) A population-based clinical trial with the S*Pf*66 synthetic *Plasmodium falciparum* malaria vaccine in Venezuela. *The Journal of Infectious Diseases.* **170:** 396 – 402.

Nussenzweig, R.S., Vanderberg, J., Most, H., and Orton, C. (1967) Protective immunity produced by the injection of X-radiated sporozoites of *Plasmodium berghei. Nature.* **216:** 160 – 162.

Obaldia, N., Stockelman, M.G., Otero, W., Cockrill, J.A., Ganeshan, H., Abot, E.N., Zhang, J., Limbach, K., Charoenvit, Y., Doolan, D.L., Tang, D.C.C., and Richie, T.L. (2017) A *Plasmodium vivax* plasmid DNA- and adenovirus-vectored malaria vaccine encoding blood-stage antigens AMA1 and $MSP1_{42}$ in a prime/boost heterologous immunization regimen partially protects *Aotus* monkeys against blood stage challenge. *Clinical and Vaccine Immunology.* **24:** doi: 10.1128/CVI.00539-16.

Ockenhouse, C.F., Sun, P.F., Lanar, D.E., Wellde, B.T., Hall, B.T., Kester, K., Stoute, J.A., Magill, A., Krzych, U., Farley, L., Wirtz, R.A., Sadoff, J.C., Kaslow, D.C., Kumar, S., Church, L.W.P., Crutcher, J.M., Wizel, B., Hoffman, S., Lalvani, A., Hill, A.V.S., Tine, J.A., Guito, K.P., de Taisne, C., Anders, R., Horii, T., Paoletti, E., and Ballou, W.R. (1998) Phase I/IIa safety, immunogenicity, and efficacy trial of NYVAC-*Pf*7, a pox-vectored, multiantigen, multistage vaccine candidate for *Plasmodium falciparum* malaria. *The Journal of Infectious Diseases.* **177:** 1664 – 1673.

Ocker, R., Prompunjai, Y., Chutipongvivate, S., and Karanis, P. (2016) Malaria diagnosis by loop-mediated isothermal amplification (LAMP) in Thailand. *Journal of the Institute of Tropical Medicine of São Paulo.* **58:** doi.org/10.1590/S1678-9946201658027.

Oehring, S.C., Woodcroft, B.J., Moes, S., Wetzel, J., Dietz, O., Pulfer, A., Dekiwadia, C., Maeser, P., Flueck, C., Witmer, K., Brancucci, N.M.B., Niederwieser, I., Jenoe, P., Ralph, S.A., and Voss, T.S. (2012) Organellar proteomics reveals hundreds of novel nuclear proteins in the malaria parasite *Plasmodium falciparum. BioMed Central Genome Biology.* **13:** doi:10.1186/gb-2012-13-11-r108.

Oguonu, T., Shu, E., Ezeonwu, B.U., Lige, B., Derrick, A., Umeh, R.E., and Agbo, E. (2014) The performance evaluation of a urine malaria test (UMT) kit for the diagnosis of malaria in individuals with fever in south-east Nigeria: cross-sectional analytical study. *Malaria Journal.* **13:** doi: 10.1186/1475-2875-13-403.

Ogutu, B.R., Apollo, O.J., McKinney, D., Okoth, W., Siangla, J., Dubovsky, F., Tucker, K., Waitumbi, J.N., Diggs, C., Wittes, J., Malkin, E., Leach, A., Soisson, L.A., Milman, J.P., Otieno, L., Holland, C.A., Polhemus, M., Remich, S.A., Ockenhouse, C.F., Cohen, J., Ballou, W.R., Martin, S.K., Angov, E., Stewart, V.A., Lyon, J.A., Heppner Jr, D.G., and Withers, M.R. (2009) Blood stage malaria vaccine eliciting high antigen-specific antibody concentrations confers no protection to young children in Western Kenya. *Public Library of Sciences: ONE*. **4:** doi: 0.1371/journal.pone.0004708.

Ogwang, C., Kimani, D., Edwards, N.J., Roberts, R., Mwacharo, J., Bowyer, G., Bliss, C., Hodgson, S.H., Njuguna, P., Viebig, N.K., Nicosia, A., Gitau, E., Douglas, S., Illingworth, J., Marsh, K., Lawrie, A., Imoukhuede, E.B., Ewer, K., Urban, B.C., Hill, A.V.S., Bejon, P., and the MVVC group. (2015) Prime-boost vaccination with chimpanzee adenovirus and modified vaccinia Ankara encoding TRAP provides partial protection against *Plasmodium falciparum* infection in Kenyan adults. *Science Translational Medicine.* **7:** doi: 10.1126/scitranslmed.aaa2373.

Olins, P.O., Devine, C.S., Rangwala, S.H., and Kavka, K.S. (1988) The T7 phage gene 10 leader RNA, a ribosome-binding site that dramatically enhances the expression of foreign proteins in *Escherichia coli. Gene.* **73:** 227 – 235.

Opie, E.L., and Freund, J. (1937) An experimental study of protective inoculation with heat killed tubercle bacilli. *Journal of Experimental Medicine.* **66:** 761 – 788.

Ord, R.L., Caldeira, J.C., Rodriguez, M., Noe, A., Chackerian, B., Peabody, D.S., Gutierez, G., and Lobo, C.A. (2014) A malaria vaccine candidate based on an epitope of the *Plasmodium falciparum* RH5 protein. *Malaria Journal.* **13:** doi:10.1186/1475-2875-13-326.

Outchkorov, N.S., Roeffen, W., Kaan, A., Jansen, J., Luty, A., Schuiffel, D., van Gemert, G.J., van de Vegte-Bolmer, M., Sauerwein, R.W., and Stunnenberg, H.G. (2008) Correctly folded *Pfs*48/45 protein of *Plasmodium falciparum* elicits malaria transmission-blocking immunity in mice. *Proceedings of the National Academy of Sciences.* **105:** 4301 – 4305.

Oyibo, W.A., Ezeigwe, N., Ntadom, G., Oladosu, O.O., Rainwater-Loveth, K., O'Meara, W., Okpokoro, E., and Brieger, W. (2017) Multicenter pivotal clinical trial of urine malaria test for rapid diagnosis of *Plasmodium falciparum* malaria. *Journal of Clinical Microbiology.* **55:** 253 – 263.

O'Donnell, R.A., de Koning-Ward, T.F., Burt, R.A., Bockarie, M., Reeder, J.C., Cowman, A.F., and Crabb, B.S. (2001) Antibodies against merozoite surface protein (MSP)-1_{19} are a major component of the invasion-inhibitory response in individuals immune to malaria. *Journal of Experimental Medicine.* **193:** 1403 – 1412.

Pandey, R.K., Ali, M., Ojha, R., Bhatt, T.K., and Prajapati, V.K. (2018) Development of multi-epitope driven subunit vaccine in secretory and membrane protein of *Plasmodium falciparum* to convey protection against malaria infection. *Vaccine.* **36:**.4555 - 4565.

Patarroyo, M.E., Amador, R., Clavijo, P., Moreno, A., Guzman, F., Romero, P., Tascon, R., Franco, A., Murillo, L.A., Ponton, G., and Trujillo, G. (1988) A synthetic vaccine protects humans against challenge with asexual blood stages of *Plasmodium falciparum* malaria. *Nature.* **332:** 158 – 161.

Patel, S.N., Serghides, L., Smith, T.G., Febbraio, M., Silverstein, R.L., Kurtz, T.W., Pravenec, M., and Kain, K.C. (2004) CD36 mediates the phagocytosis of *Plasmodium falciparum*-infected erythrocytes by rodent macrophages. *The Journal of Infectious Diseases.* **189:** 204 – 213.

Pattnaik, P., Shakri, A.R., Singh, S., Goel, S., Mukherjee, P., and Chitnis, C.E. (2007) Immunogenicity of a recombinant malaria vaccine based on receptor binding domain of *Plasmodium falciparum* EBA-175. *Vaccine.* **25:** 806 – 813.

Pavadai, E., El Mazouni, F., Wittlin, S., de Kock, C., Phillips, M.A., and Chibale, K. (2016) Identification of new human malaria parasite *Plasmodium falciparum* dihydroorotate dehydrogenase inhibitors by pharmacore and structure-based viral screening. *Journal of Chemical Information and Modelling.* **56:** 548 – 562.

Payne, R.O., Silk, S.E., Elias, S.C., Miura, K., Diouf, A., Galaway, F., de Graaf, H., Brendish, N.J., Poulton, I.D., Griffiths, O.J., Edwards, N.J., Jin, J., Labbé, G.M., Alanine, D.G.W., Siani, L., Di Marco, S., Roberts, R., Green, N., Berrie, E., Ishizuka, A.S., Nielson, C.M., Bardelli, M., Partey, F.D., Ofori, M.F., Barford, L., Wambua, J., Murungi, L.M., Osier, F.H., Biswas, S., McCarthy, J.S., Minassian, A.M., Ashfield, R., Viebig, N.K., Nugent, F.L., Douglas, A.D., Vekemans, J., Wright, G.J., Faust, S.N., Hill, A.V.S., Long, C.A., Lawrie, A.M., and Draper, S.J. (2017) Human vaccination against RH5 induces neutralizing antimalarial antibodies that inhibit RH5 invasion complex interactions. *Journal of Clinical Investigation: Insight.* **2:** doi.org/10.1172/jci.insight.96381.

Pehrson, C., Mathiesen, L., Heno, K.K., Salanti, A., Resende, M., Dzikowski, R., Damm, P., Hansson, S.R., King, C.L., Schneider, H., Wang, C.W., Lavstsen, T., Theander, T.G., Knudsen, L.E., and Nielsen, M.A. (2016). Adhesion of *Plasmodium falciparum* infected erythrocytes in *ex vivo* perfused placental tissue: a novel model of placental malaria. *Malaria Journal*, **15:** doi: 10.1186/s12936-016-1342-2.

Perlman, R.L. (2016) Mouse models of human disease. *Evolution, Medicine and Public Health.* **2016:** 170 – 176.

Pichyangkul, S., Kum-Arb, U., Yongvanitchit, K., Limsalakpetch, A., Gettayacamin, M., Lanar, D.E., Ware, L.A., Stewart, V.A., Heppner, D.G., Mettens, P., Cohen, J.D., Ballou, W.R., and Fukuda, M.M. (2007) Preclinical evaluation of the safety and immunogenicity of a vaccine consisting of *Plasmodium falciparum* liver-stage antigen 1 with adjuvant AS01B administered alone or concurrently with the RTS,S/AS01B vaccine in rhesus primates. *Infection and Immunity.* **76:** 229 – 238.

Pinzon-Charry, A., McPhun, V., Kienzle, V., Hirunpetcharat, C., Engwerda, C., McCarthy, J., and Good, M.F. (2010) Low doses of killed parasite in CpG elicit vigorous CD4+ T-cell responses against blood stage malaria in mice. *Journal of Clinical Investigation.* **120:** 2967 – 2978.

Plassmeyer, M.L., Reiter, K., Shimp Jr, R.L., Kotova, S., Smith, P.D., Hurt, D.E., House, B., Zou, X., Zhang, Y., Hickman, M., Uchime, O., Herrera, R., Nguyen, V., Glen, J., Lebowitz, J., Jin, A.J., Miller, L.H., MacDonald, N.J., Wu, Y., and Narum, D.L. (2009) Structure of the *Plasmodium falciparum* circumsporozoite protein, a leading malaria vaccine candidate. *The Journal of Biological Chemistry.* **284:** 26951 – 26963.

Playfair, J.H.L., and de Souza, J.B. (1986) Vaccination of mice against malaria with soluble antigens. I. The effect of detergent, route of injection, and adjuvant. *Parasite Immunology.* **8:** 409 – 414.

Pombo, D.J., Lawrence, G., Hirunpetcharat, C., Rzepczyk, C., Bryden, M., Cloonan, N., Anderson, K., Mahukunkijchareon, Y., Martin, L.B., Wilson, D., Elliott. S., Elliott, S., Eisen, D.P., Weinberg, J.B., Saul, A., and Good, M.F. (2002) Immunity to malaria after administration of ultra-low doses of red cells infected with *Plasmodium falciparum. The Lancet.* **360:** 610 – 617.

Poon, L.L.M., Wong, B.W.Y., Ma, E.H.T., Chan, K.H., Chow, L.M.C., Abeyewickreme, W., Tangpukdee, N., Yuen, K.Y., Guan, Y., Looareesuwan, S., and Peiris, J.S.M. (2006) Sensitive and inexpensive molecular test for *falciparum* malaria: detecting *Plasmodium falciparum* DNA directly from heat-treated blood by loop-mediated isothermal amplification. *Clinical Chemistry.* **52:** 303 – 306.

Prasad, S., Khadatare, P.B., and Roy, I. (2011) Effect of chemical chaperones in improving the solubility of recombinant proteins in *Escherichia coli*. *Applied and Environmental Microbiology.* **77:** 4603 – 4609.

Prinz, W.A., Åslund, F., Holmgren, A., and Beckwith, J. (1997) The role of the thioredoxin and glutaredoxin pathways in reducing protein disulfide bonds in the *Escherichia coli* cytoplasm. *Journal of Biological Chemistry.* **272:** 15661 - 15667.

Przyborski, J.M., Diehl, M., and Blatch, G.L. (2015) *Plasmodial* HSP70s are functionally adapted to the malaria parasite life cycle. *Frontiers in Molecular Biosciences.* **2:** doi: 10.3389/fmolb.2015.00034.

Pusic, K.M., Hashimoto, C.N., Lehrer, A., Aniya, C., Clements, D.E., and Hui, G.S. (2011) T cell epitope regions of the *P. falciparum* $MSP1_{33}$ critically influence immune responses and *in vitro* efficacy of $MSP1_{42}$ vaccines. *Public Library of Sciences: ONE.* **6:** doi: 10.1371/journal.pone.0024782.

Radtke, A.J., Anderson, C.F., Riteau, N., Rausch, K., Scaria, P., Kelnhofer, E.R., Howard, R.F., Sher, A., Germain, R.N., and Duffy, P. (2017) Adjuvant and carrier protein-dependent T-cell priming promotes a robust antibody response against the *Plasmodium falciparum Pf*s25 vaccine candidate. *Scientific Reports.* **7:** doi: 10.1038/srep40312.

Raines, R.T., McCormick, M., Van Osbree, T.R., and Mierendorf, R.C. (2000) The S·tag fusion system for protein purification. In *Methods in Enzymology.* Academic Press. **326:** 362 – 376.

Ralph, P., and Nakoinz, I. (1975) Phagocytosis and cytolysis by a macrophage tumour and its cloned cell line. *Nature.* **257:** 393 – 394.

Rammensee, H.G., Bachmann, J., Emmerich, N.P.N., Bachor, O.A., and Stevanovi, S. (1999) SYFPEITHI: database for MHC ligands and peptide motifs. *Immunogenetics.* **50:** 213 – 219.

Rao, V.S., Srinivas, K., Sujini, G.N., and Kumar, G.N.S. (2014) Protein-protein interaction detection: methods and analysis. *International Journal of Proteomics.* **2014.** Available: http://dx.doi.org/10.1155/2014/147648.

Rehbein, H., and Karl, H. (1985) Solubilization of fish muscle proteins with buffers containing sodium dodecyl sulfate. *Zeitschrift für Lebensmittel-Untersuchung und Forschung.* **180:** 373 – 378.

Riley, E.M., Allen, S.J., Troye-Blomberg, M., Bennett, S., Perlmann, H., Andersson, G., Smedman, L., Perlmann, P., and Greenwood, B.M. (1991) Association between immune recognition of the malaria vaccine candidate antigen *Pf*155/RESA and resistance to clinical disease: a prospective study in a malaria-endemic region of West Africa. *Transactions of the Royal Society of Tropical Medicine and Hygiene.* **85:** 436 – 443.

Rodriguez, M., Lustigman, S., Montero, E., Oksov, Y., and Lobo, C.A. (2008) *Pf*RH5: a novel reticulocyte-binding family homolog of *Plasmodium falciparum* that binds to the erythrocyte, and an investigation of its receptor. *Public Library of Science: ONE.* **3:** doi:10.1371/journal.pone.0003300.

Rogl, H., Kosemund, K., Kühlbrandt, W., and Collinson, I. (1998) Refolding of *Escherichia coli* produced membrane protein inclusion bodies immobilised by nickel chelating chromatography. *Federation of European Biochemical Societies: Letters.* **432:** 21 – 26.

Rosano, G.L., and Ceccarelli, E.A. (2014) Recombinant protein expression in *Escherichia coli*: advances and challenges. *Frontiers in Microbiology.* **5:** doi: 10.3389/fmicb.2014.00172.

Rosas, J.E., Pedraz, J.L., Hernández, R.M., Gascón, A.R., Igartua, M., Guzmán, F., Rodríguez, R., Cortés, J., and Patarroyo, M.E. (2002) Remarkably high antibody levels and protection against *P. falciparum* malaria in *Aotus* monkeys after a single immunisation of S*Pf*66 encapsulated in PLGA microspheres. *Vaccine.* **20:** 1707 – 1710.

Rosenberg, A.H., Lade, B.N., Chui, D., Lin, S.W., Dunn, J.J., and Studier, F.W. (1987) Vectors for selective expression of cloned DNAs by T7 RNA polymerase. *Gene.* **56:** 125 – 135.

Rowe, J.A., Claessens, A., Corrigan, R.A., and Arman, M. (2009) Adhesion of *Plasmodium falciparum*-infected erythrocytes to human cells: molecular mechanisms and therapeutic implications. *Expert Reviews in Molecular Medicine.* **11:** doi: 10.1017/S1462399409001082.

RTS,S Clinical Trials Partnership (2015) Efficacy and safety of RTS,S/AS01 malaria vaccine with or without a booster dose in infants and children in Africa: final results of a phase 3, individually randomised, controlled trial. *The Lancet.* **386:** 31 – 45.

Ryabova, N.A., Marchenkov, V.V., Marchenokova, S.Y., Kotova, N.V., and Semisotnov, G.V. (2013) Molecular chaperone GroEL/ES: unfolding and refolding processes. *Biochemistry (Moscow).* **78:** 1405 – 1414.

Sambrook, J., Fritsch, E.F., and Maniatis, T. (1989) *Molecular cloning: a laboratory manual.* 2nd edition. New York: Cold Spring Harbor Laboratory Press.

Sampaio, N.G., Eriksson, E.M., and Schofield, L. (2018) *Plasmodium falciparum Pf*EMP1 modulates monocyte/macrophage transcription factor activation and cytokine and chemokine responses. *Infection and Immunity*. **86:** doi.org/10.1128/IAI.00447-17.

Scheele, G., and Jacoby, R. (1982) Conformational changes associated with proteolytic processing of presecretory proteins allow glutathione-catalyzed formation of native disulfide bonds. *The Journal of Biological Chemistry.* **257:** 12277 – 12282.

Schein, C.H. (1989) Production of soluble recombinant proteins in bacteria. *Nature Biotechnology.* **7:** 1141 – 1149.

Scherf, A., Lopez-Rubio, J.J., and Riviere, L. (2008) Antigenic variation in *Plasmodium falciparum. Annual Reviews of Microbiology.* **62:** 445 – 470.

Schlager, B., Straessle, A. and Hafen, E. (2012) Use of anionic denaturing detergents to purify insoluble proteins after overexpression. *BioMed Central Biotechnology.* **12:** doi: 10.1186/1472-6750-12-95.

Schönfeld, H.J., Schmidt, D., Schröder, H., and Bukau, B. (1995) The DnaK chaperone system of *Escherichia coli*: quaternary structures and interactions of the DnaK and GrpE components. *Journal of Biological Chemistry.* **270:** 2183 – 2189.

Schröder, H., Langer, T., Hartl, F.U., and Bukau, B. (1993) DnaK, DnaJ and GrpE form a cellular chaperone machinery capable of repairing heat-induced protein damage. *European Molecular Biology Organization Journal*. **12:** 4137 – 4144.

Schussek, S., Trieu, A., Apte, S.H., Sidney, J., Sette, A., and Doolan, D.L. (2013) Immunization with apical membrane antigen 1 confers sterile infection-blocking immunity against *Plasmodium* sporozoite challenge in a rodent model. *Infection and Immunity.* **81:** 3586 – 3599.

Sedegah, M., Charoenvit, Y., Minh, L., Belmonte, M., Majam, V.F., Abot, S., Ganeshan, H., Kumar, S., Bacon, D.J., Stowers, A., Narum, D.L., Carucci, D.J., and Rogers, W.O. (2004) Reduced immunogenicity of DNA vaccine plasmids in mixtures. *Gene Therapy.* **11:** 448 – 456.

Serbina, N.V., Jia, T., Hohl, T.M., and Pamer, E.G. (2008) Monocyte-mediated defense against microbial pathogens. *Annual Review of Immunology.* **26:** 421 – 452.

Sevier, C.S., and Kaiser, C.A. (2002) Formation and transfer of disulphide bonds in living cells. *Nature Reviews Molecular Cell Biology.* **3:** 836 – 847.

Shah, Z.H., Jones, D.R., Sommer, L., Foulger, R., Bultsma, Y., D'Santos, C., and Divecha, N. (2013) Nuclear phosphoinositides and their impact on nuclear functions. *Federation for European Biochemical Societies Journal*. **280:** 6295 – 6310.

Shahabuddin, M., Günther, Lingelbach, K., Aikawa, M., Schreiber, M., Ridley, R.G., and Scaife, J.G. (1992) Localisation of hypoxanthine phosphoribosyl transferase in the malaria parasite *Plasmodium falciparum*. *Experimental Parasitology.* **74:** 11 – 19.

Sharp, B.L., Ridl, F.C., Govender, D., Kuklinski, J., and Kleinschmidt, I. (2007) Malaria vector control by indoor residual insecticide spraying on the tropical island of Bioko, Equatorial Guinea. *Malaria Journal.* **6:** doi: 10.1186/1475-2875-6-52.

Shen, Y., Tolić, N., Purvine, S.O., and Smith, R.D. (2010) Identification of disulfide bonds in protein proteolytic degradation products using the *de novo*-protein unique sequence tags approach. *Journal of Proteome Research.* **9:** 4053 – 4060.

Shonhai, A., Boshoff, A., and Blatch, G.L. (2005) *Plasmodium falciparum* heat shock protein 70 is able to suppress the thermosensitivity of an *Escherichia coli* DnaK mutant strain. *Molecular Genetics and Genomics.* **274:** 70 – 78.

Siddiqui, W.A. (1977) An effective immunization of experimental monkeys against a human malaria parasite, *Plasmodium falciparum. Science.* **197:** 388 – 389.

Sievers, F., Wilm, A., Dineen, D., Gibson, T.J., Karplus, K., Li, W., Lopez, R., McWilliam, H., Remmert, M., Söding, J., Thompson, J.D., and Higgins, D.G. (2011) Fast, scalable generation of high-quality protein multiple sequence alignments using Clustal Omega. *Molecular Systems Biology.* **7:** doi:10.1038/msb.2011.75.

Silvie, O., Franetich, J.F., Charrin, S., Mueller, M.S., Siau, A., Bodescot, M., Rubinstein, E., Hannoun, L., Charoenvit, Y., Kocken, C.H., Thomas, A.W., van Gemert, G.J., Sauerwein, R.W., Blackman, M.J., Anders, R.F., Pluschke, G., and Mazier, D. (2004) A role for apical membrane antigen 1 during invasion of hepatocytes by *Plasmodium falciparum* sporozoites. *Journal of Biological Chemistry.* **279:** 9490 – 9496.

Singh, B., Sung, K.L., Matusop, A., Radhakrishnan, A., Shamsul, S.S., Cox-Singh, J., Thomas, A., and Conway, D.J. (2004) A large focus of naturally acquired *Plasmodium knowlesi* infections in human beings. *The Lancet.* **363:** 1017 – 1024.

Singh, S.M., and Panda, A.K. (2005) Solubilization and refolding of bacterial inclusion body proteins. *Journal of Bioscience and Bioengineering.* **99:** 303 – 310.

Sinigaglia, F., Guttinger, M., Kilgus, J., Doran, D.M., Matile, H., Etlinger, H., Trzeciak, A., Gillessen D., and Pink, J.L.R. (1988) A malaria T-cell epitope recognized in association with most mouse and human MHC class II molecules. *Nature.* **336:** 778 – 780.

Snel, B., Lehmann, G., Bork, P., and Huynen, M.A. (2000) STRING: a web-server to retrieve and display the repeatedly occurring neighbourhood of a gene. *Nucleic Acids Research.* **28:** 3442 – 3444.

Snounou, G., Viriyakosol, S., Zhu, X.P., Jarra, W., Pinheiro, L., do Rosario, V.E., Thaithong, S., and Brown, K.N. (1993) High sensitivity detection of human malaria parasites by the use of nested polymerase chain reaction. *Molecular and Biochemical Parasitology.* **61:** 315 – 320.

Soe, S., Theisen, M., Roussilhon, C., Aye, K.S., and Druilhe, P. (2004) Association between protection against clinical malaria and antibodies to merozoite surface antigens in an area of hyperendemicity in Myanmar: complementarity between responses to merozoite surface protein 3 and the 220-kilodalton glutamate-rich protein. *Infection and Immunity.* **72:** 247 – 252.

Soulard, V., Bosson-Vanga, H., Lorthiois, A., Roucher, C., Franetich, J.F., Zanghi, G., Bordessoulles, M., Tefit, M., Thellier, M., Morosan, S., Le Naour, G., Capron, F., Suemizu, H., Snounou, G., Moreno-Sabater, A., and Mazier, D. (2015) *Plasmodium falciparum* full life cycle and *Plasmodium ovale* liver stages in humanized mice. *Nature Communications.* **6:** doi: 10.1038/ncomms8690.

Sørensen, H.P., and Mortensen, K.K. (2005) Soluble expression of recombinant proteins in the cytoplasm of *Escherichia coli*. *Microbial Cell Factories.* **4:** doi:10.1186/1475-2859-4-1.**Spiegel, H., Boes, A., Fendel, R., Reimann, A., Schillberg, S., and Fischer, R.** (2017) Immunization with the malaria diversity-covering blood-stage vaccine candidate *Plasmodium falciparum* apical membrane antigen 1 DiCo in complex with its natural ligand *Pf*Ron2 does not improve the *in vitro* efficacy. *Frontiers in Immunology.* **8:** doi: 10.3389/fimmu.2017.00743.

Spring, M.D., Cummings, J.F., Ockenhouse, C.F., Dutta, S., Reidler, R., Angov, E., Bergmann-Leitner, E., Stewart, V.A., Bittner, S., Juompan, L., Kortepeter, M.G., Nielson, R., Krzych, U., Tierney, E., Ware, L.A., Dowler, M., Hermsen, C.C., Sauerwein, R.W., de Vlas, S.J., Ofori-Anyinam, O., Lanar, D.E., Williams, J.L., Kester, K.E., Tucker, K., Shi, M., Makin, E., Long, C., Diggs, C.L., Soisson, L., Dubois, M.C., Ballou, W.R., Cohen, J., and Heppner Jr, D.G. (2009) Phase 1/2a study of the malaria vaccine candidate apical membrane antigen-1 (AMA-1) administered in adjuvant system AS01B or AS02a. *Public Library of Science: ONE.* **4:** doi: 10.1371/journal.pone.0005254.

Spring, M., Murphy, J., Nielson, R., Dowler, M., Bennett, J.W., Zarling, S., Williams, J., de la Vega, P., Ware, L., Komisar, J., Polhemus, M., Richie, T.L., Epstein, J., Tamminga, C., Chuang, I., Richie, N., O'Neil, M., Heppner, G., Healer, J., O'Neill, M., Smithers, H., Finney, O.C., Mikolajczak, S.A., Wang, R., Cowman, A., Ockenhouse, C., Krzych, U., and Kappe, S.H.I. (2013) First-in-human evaluation of genetically attenuated *Plasmodium falciparum* sporozoites administered by bite of *Anopheles* mosquitoes to adult volunteers. *Vaccine*. **31:** 4975 – 4983.

Srinivasan, P., Ekanem, E., Diouf, A., Tonkin, M.L., Miura, K., Boulanger, M.J., Long, C.A., Narum, D.L., and Miller, L.H. (2014) Immunization with a functional protein complex required for erythrocyte invasion protects against lethal malaria. *Proceedings of the National Academy of Sciences.* **111:** 10311 – 10316.

Srinivasan, P., Baldeviano, G.C., Miura, K., Diouf, A., Ventocilla, J.A., Leiva, K.P., Lugo-Roman, L., Lucas, C., Orr-Gonzalez, S., Zhu, D., Villasante, E., Soisson, L., Narum, D.L., Pierce, S.K., Long, C.A., Diggs, C., Duffy, P.E., Lescano, A.G., and Miller, L.H. (2017) A malaria vaccine protects *Aotus* monkeys against virulent *Plasmodium falciparum* infection. *Nature Partner Journals: Vaccine.* **2:** doi: 10.1038/s41541-017-0015-7.

Stanisic, D.I., and Good, M.F. (2015) Whole organism blood stage vaccines against malaria. *Vaccine.* **33:** 7469 – 7475.

Steczko, J., Donoho, G.A., Dixon, J.E., Sugimoto, T., and Axelrod, B. (1991) Effect of ethanol and low-temperature culture on expression of soybean lipoxygenase L-1 in *Escherichia coli. Protein Expression and Purification.* **2:** 221 – 227.

Steffen, R., Fuchs, E., Schildknecht, J., Funk, M., Schlagenhauf, P., Phillips-Howard, P., Nevill, C., Naef, U., and Stürchler, D. (1993) Mefloquine compared with other malaria chemoprophylactic regimens in tourists visiting East Africa. *The Lancet.* **341:** 1299 – 1303.

Steiner-Monard, V., Kamaka, K., Karoui, O., Roethlisberger, S., Audran, R., Daubenberger, C., Fayet-Mello, A. Erdmann-Voisin, A., Felger, I., Geiger, K., Govender, L., Houard, S., Huber, E., Moyer, C., Mkindi, C., Portevin, D., Rusch, S., Schmidlin, S., Tiendrebeogo, R.W., Theisen, M., Thierry, A.C., Vallotton, L., Corradin, G., Leroy, O., Abdulla, S., Shekalaghe, S., Genton, B., Spertini, F., and Jongo, S.A. (2018) The candidate blood stage malaria vaccine P27A induces a robust humoral response in a fast track to the field phase I trial in exposed and nonexposed volunteers. *Clinical Infectious Diseases.* **68:** doi: 10.1093/cid/ciy514.

Stephens, L.L., Shonhai, A., and Blatch, G.L. (2011) Co-expression of the *Plasmodium falciparum* molecular chaperone, *Pf*Hsp70, improves the heterologous production of the antimalarial drug target GTP cyclohydrolase I, *Pf*GCHI. *Protein Expression and Purification.* **77:** 159 – 165.

Storm, J., and Craig, A.G. (2014) Pathogenesis of cerebral malaria – inflammation and cytoadherence. *Frontiers in Cellular and Infection Microbiology.* **4:** doi.org/10.3389/fcimb.2014.00100.

Stoute, J.A., Slaoui, M., Heppner, D.G., Momin, P., Kester, K.E., Desmons, P., Wellde, B.T., Garçon, N., Krzych, U., Marchand, M., Ballou, W.R., and Cohen, J. (1997) A preliminary evaluation of a recombinant circumsporozoite protein vaccine against *Plasmodium falciparum* malaria. *The New England Journal of Medicine.* **336:** 86 – 91.

Stowers, A.W., Kennedy, M.C., Keegan, B.P., Saul, A., Long, C.A., and Miller, L.H. (2002) Vaccination of monkeys with recombinant *Plasmodium falciparum* apical membrane antigen 1 confers protection against blood-stage malaria. *Infection and Immunity.* **70:** 6961 – 6967.

Strober, W. (2001) Trypan blue exclusion test of cell viability. *Current Protocols in Immunology*. **21:** Appendix 3B.

Studier, F.W. (2005) Protein production by auto-induction in high-density shaking cultures. *Protein Expression and Purification.* **41:** 207 – 234.

Sun, S., Mo, W., Ji, Y., and Liu, S. (2001) Preparation and mass spectrometric study of egg yolk antibody (IgY) against rabies virus. *Rapid Communications in Mass Spectrometry.* **15:** 708 – 712.

Sundström, C., and Nilsson, K. (1976) Establishment and characterization of a human histiocytic lymphoma cell line (U-937). *International Journal of Cancer.* **17:** 565 – 577.

Szabo, A., Langer, T., Schröder, H., Flanagan, J., Bukau, B., and Hartl, F.U. (1994) The ATP hydrolysis-dependent reaction cycle of the *Escherichia coli* Hsp7O system-DnaK, DnaJ, and GrpE. *Proceedings of the National Academy of Sciences.* **91:** 10345 – 10349.

Szklarczyk, D., Franceschini, A., Wyder, S., Forslund, K., Heller, D., Huerta-Cepas, J., Simonovic, M., Roth, A., Santos, A., Tsafou, K.P., Kuhn, M., Bork, P., Jensen, L.J., and von Mering, C. (2015) STRING v10: protein-protein interaction networks, integrated over the tree of life. *Nucleic Acids Research.* **43:** 447 – 452.

Tajuddin, S.M., Schick, U., Eicher, J.D., Chamie, N., Giri, A., Brody, J.A., Hill, W.D., Kacprowski, T., Li, J., Lyytikäinen, L.P., Manichaikul, A., Mihailov, E., O'Donoghue, M.L., Pankratz, N., Pazoki, R., Polfus, L.M., Smith, A.V., Schurmann, C., Vacchi-Suzzi, C., Waterworth, D.M., Evangelou, E., Yanek, L.R., Burt, A., Chen, M.H., van Rooij, F.J.A., Floyd, J.S., Greinacher, A., Harris, T.B., Highland, H.M., Lange, L.A., Liu, Y., Mägi, R., Nalls, M.A., Mathias, R.A., Nickerson, D.A., Nikus, K., Starr, J.M., Tardif, J.C., Tzoulaki, I., Velez Edwards, D.R., Wallentin, L., Bartz, T.M., Becker, L.C., Denny, J.C., Rattfield, L.M., Rioux, J.D., Friedrich, N., Fornage, M., Gao, H., Hirschhorn, J.N., Liewald, D.C.M., Rich, S.S., Uitterlinden, A., Bastarache, L., Becker, D.M., Boerwinkle, E., de Denus, S., Bottinger, E.P., Hayward, C., Hofman, A., Homuth, G., Lange, E., Launer, L.J.,

Lehtimäki, T., Lu, Y., Metspalu, A., O'Donnell, C.J., Quarells, P.C., Richard, M., Torstenson, E.S., Taylor, K.D., Vergnaud, A.C., Zonderman, A.B., Crosslin, D.R., Deary, I.J., Dörr, M., Elliott, P., Evans, M.K., Gudnason, V., Kähönen, M., Psaty, B.M. Rotter, J.I., Slater, A.J., Dehghan, A., White, H.D., Ganesh, S.K., Loos, R.J.F., Esko, T., Faraday, N., Wilson, J.G., Cushman, M., Johnson, A.D., Edwards, T.L., Zakai, N.A., Lettre, G., Reiner, A.P., and Auer, P.L. (2016) Large-scale exome-wide association analysis identifies loci for white blood cell traits and pleiotropy with immune-mediated diseases. *American Journal of Human Genetics.* **99:** 22 – 39.

Talaat, K.R., Ellis, R.D., Hurd, J., Hentrich, A., Gabriel, E., Hynes, N.A., Rausch, K.M., Zhu, D., Muratova, O., Herrera, R., Anderson, C., Jones, D., Aebig, J., Brockley, S., MacDonald, N.J., Wang, X., Fay, M.P., Healy, S.A., Durbin, A.P., Narum, D.L., Wu, Y., and Duffy, P.E. (2016) Safety and immunogenicity of *Pfs*25-EPA/Alhydrogel®, a transmission blocking vaccine against *Plasmodium falciparum*: an open label study in malaria naïve adults. *Public Library of Science: ONE.* **11:** doi.org/10.1371/journal.pone.0163144.

Tang, H.Y., and Speicher, D.W. (2004) Determination of disulfide-bond linkages in proteins. *Current Protocols in Protein Science.* **37:** doi: 10.1002/0471140864.ps1111s37.

Tangpukdee, N., Yew, H.S., Krudsood, S., Punyapradit, N., Somwong, W., Looareesuwan, S., Kano, S., and Wilairatana, P. (2008) Dynamic changes in white blood cell counts in uncomplicated *Plasmodium falciparum* and *P. vivax* malaria. *Parasitology International.* **57:** 490 – 494.

Targett, G.A., and Greenwood, B.M. (2008) Malaria vaccines and their potential role in the elimination of malaria. *Malaria Journal.* **7:** doi: 10.1186/1475-2875-7-S1-S10.

Teixeira, C., and Gomes, R. (2013) Experimental models in vaccine research: malaria and leishmaniasis. *Brazilian Journal of Medical and Biological Research.* **46:** 109 – 116.

Theisen, M., Vuust, J., Guttschau, A., Jepsen, S., and Høgh, B. (1995) Antigenicity and immunogenicity of recombinant glutamate-rich protein of *Plasmodium falciparum* expressed in *Escherichia coli. Clinical and Diagnostic Laboratory Immunology.* **2:** 30 – 34.

Theisen, M., Jore, M.M., and Sauerwein, R. (2017) Towards clinical development of a *Pfs*48/45-based transmission blocking malaria vaccine. *Expert Review of Vaccines.* **16:** 329 – 336..

Thera, M.T., Duombo, O.K., Coulibally, D., Laurens, M.B., Ouattara, A., Kone, A.K., Guindo, A.B., Traore, K., Traore, I., Kouriba, B., Diallo, D.A., Diarra, I., Daou, M., Dolo, A., Tolo, Y., Sissoko, M.S., Niangaly, A., Sissoko, M., Takala-Harrison, S., Lyke, K.E., Wu, Y., Blackwelder, W.C., Godeaux, O., Vekemans, J., Dubois, M.C., Ballou, W.R., Cohen, J., Thompson, D., Dube, T., Soisson, L., Diggs, C.L., House, B., Lanar, D.E., Dutta, S., Heppner, D.G. and Plowe, C.V. (2011) A field trial to assess a blood-stage malaria vaccine. *The New England Journal of Medicine.* **365:** 1004 – 1013.

Thinon, E., Serwa, R.A., Broncel, M., Brannigan, J.A., Brassat, U., Wright, M.H., Heal, W.P., Wilkinson, A.J., Mann, D.J., and Tate, E.W. (2014) Global profiling of co- and post-translationally *N*-myristoylated proteomes in human cells. *Nature Communications.* **5:** doi: 10.1038/ncomms5919.

Tiendrebeogo, R.W., Spallek, R., Oehlmann, W., Singh, M., Theisen, M., Nebie, I., Moret, R., Roussilhon, C., and Corradin, G. (2019) Immunogenicity of a recombinant fusion construct composed of intrinsically unstructured, low polymorphic segments derived from merozoite surface protein 2 and trophozoite exported protein 1. *Vaccine.* **37:** 5332 – 5340.

Tine, J.A., Lanar, D.E., Smith, D.M., Wellde, B.T., Schultheiss, P., Ware, L.A., Kauffman, E.B., Wirtz, R.A., de Taisne, C., Hui, G.S.N., Chang, S.P., Church, P., Hollingdale, M.R., Kaslow, D.C., Hoffman, S.L., Guito, K.P., Ballou, W.R., Sadoff, J.C., and Paoletti, E. (1996) NYVAC-*Pf*7: a poxvirus-vectored, multiantigen, multistage vaccine candidate for *Plasmodium falciparum* malaria. *Infection and Immunity.* **64:** 3833 – 3844.

Todryk, S.M., and Walther, M. (2005) Building better T-cell-inducing malaria vaccines. *Immunology.* **115:** 163 – 169.

Towbin, H., Staehelin, T., and Gordon, J. (1979) Electrophoretic transfer of proteins from polyacrylamide gels to nitrocellulose sheets: Procedure and some applications. *Proceedings of the National Academy of Sciences.* **76:** 4350 – 4354.

Trampuz, A., Jereb, M., Muzlovic, I., and Prabhu, R.M. (2003) Clinical review: severe malaria. *Critical Care. **7:** 315 – 323.*

Trieu, A., Kayala, M.A., Burk, C., Molina, D.M., Freilich, D.A., Richie, T.L., Baldi, P., Felgner, P.L., and Doolan, D.L. (2011) Sterile protective immunity to malaria is associated with a panel of novel *P. falciparum* antigens. *Molecular and Cellular Proteomics.* **10:** doi: 10.1074/mcp.M111.007948–1.

Triglia, T., Healer, J., Caruana, S.R., Hodder, A.N., Anders, R.F., Crabb, B.S., and Cowman, A.F. (2000) Apical membrane antigen 1 plays a central role in erythrocyte invasion by *Plasmodium* species. *Molecular Microbiology*.**38:** 706 – 718.

Trott, D.L., Hellestad, E.M., Yang, M., and Cook, M.E. (2008) Additions of killed whole cell bacteria preparations to Freund Complete adjuvant alter laying hen antibody response to soluble protein antigen. *Poultry Science.* **87:** 912 – 917.

Tsumoto, K., Ejima, D., Kumagai, I., and Arakawa, T. (2003) Practical considerations in refolding proteins from inclusion bodies. *Protein Expression and Purification.* **28:** doi: 10.1016/S1046-5928(02)00641-1.

Turner, L., Lavstsen, T., Berger, S.S., Wang, C.W., Peterson, J.E.V., Avril, M., Brazier, A.J., Freeth, J., Jespersen, J.S., Nielson, M.A., Magistrado, P., Lusingu, J., Smith, J.D., Higgins, M.K., and Theander, T.G. (2013) Severe malaria is associated with parasite binding to endothelial protein C receptor. *Nature.* **498:** 502 – 505.

Turrini, F., Ginsburg, H., Bussolino, F., Pescarmona, G.P., Serra, M.V., and Arese, P. (1992) Phagocytosis of *Plasmodium falciparum*-infected human red blood cells by human monocytes: involvement of immune and nonimmune determinants and dependence on parasite developmental stage. *Blood.* **80:** 801 – 808.

Tuteja, R. (2007) Malaria – an overview. *Federation of the European Biochemical Society Journal.* **274:** 4670 – 4679.

Ubillos, I., Ayestaran, A., Nhabomba, A.J., Dosoo, D., Vidal, M., Jiménez, A., Jairoce, C., Sanz, H., Aguilar, R., Williams, N.A., Díez-Padrisa, N., Mpina, M., Sorgho, H., Agnandji, S.T., Kariuki, S., Modrmüller, B., Daubenberger, C., Asante, K.P., Owusu-Agyei, S., Sacarlal, J., Aide, P., Aponte, J.J., Dutta, S., Gyan, B., Campo, J.J., Valim, C., Moncunill, G., and Dobaño, C. (2018) Baseline exposure, antibody subclass, and hepatitis B response differentially affect malaria protective immunity following RTS,S/AS01E vaccination in African children**.** *BioMed Central: Medicine.* **16:** doi.org/10.1186/s12916-018-1186-4.

Valero, M.V., Amador, R., Aponte, J.J., Narvaez, A., Galindo, C., Silva, Y., Rosas, J., Guzman, F., and Patarroyo, M.E. (1996) Evaluation of S*Pf*66 malaria vaccine during a 22-month follow-up field trial in the Pacific coast of Colombia. *Vaccine.* **14:** 1466 – 1470.

van Dooren, G.G., Marti, M., Tonkin, C.J., Stimmler, L.M., Cowman, A.F., and McFadden, G.I. (2005) Development of the endoplasmic reticulum, mitrochondrion and apicoplast during the asexual life cycle of *Plasmodium falciparum*. *Molecular Microbiology.* **57:** 405 – 419.

van Schaijk, B.C.L., Ploemen, I.H.J., Annoura, T., Vos, M.W., Foquet, L., van Gemert, G.J., Chevalley-Maurel, S., van de Vegte-Blomer, M., Sajid, M., Franetich, J.F., Lorthiois, A., Leroux-Roels, G., Meuleman, P., Hermsen, C.C., Mazier, D., Hoffman, S.L., Janse, C.J., Khan, S.M., and

Sauerwein, R.W. (2014) A genetically attenuated malaria vaccine candidate based on *P. falciparum b9/slarp* gene-deficient sporozoites. *eLife.* **3:** doi: 10.7554/eLife.03582.

Vaughan, A.M., Wang, R., and Kappe, S.H.I. (2010) Genetically engineered, attenuated whole cell vaccine approaches for malaria. *Human Vaccines.* **6:** 107 – 113.

Vedadi, M., Lew, J., Artz, J., Amani, M., Zhao, Y., Dong, A., Wasney, G.A., Gao, M., Hills, T., Brokx, S., Qiu, W., Sharma, S., Diassiti, A., Alam, Z., Melone, M., Mulichak, A., Wernimont, A., Bray, J., Loppnau, P., Plotnikova, O., Newberry, K., Sundararajan, E., Houston, S., Walker, J., Tempel, W., Bochkarev, A., Kozieradzki, I., Edwards, A., Arrowsmith, C., Roos, D., Kain, K., and Hui, R. (2007) Genome-scale protein expression and structural biology of *Plasmodium falciparum* and related Apicomplexan organisms. *Molecular and Biochemical Parasitology.* **151:** 100 – 110.

Veisi, K., Farajnia, S., Zarghami, N., Khorshid, H.R.K., Samadi, N., Khosroshahi, S.A., and Jaliani, H.Z. (2015) Chaperone-assisted soluble expression of a humanized anti-EGFR ScFv antibody in *E. coli. Advanced Pharmaceutical Bulletin.* **5:** 621 – 627.

Villard, V., Agak, G.W., Frank, G., Jafarshad, A., Servis, C., Nébié, I., Sirima, S.B., Felger, I., Arevalo-Herrera, M., Herrera, S., Heitz, F., Bäcker, Druihle, P., Kajava, A.V., and Corradin, G. (2007) Rapid identification of malaria vaccine candidates based on α-helical coiled coil protein motif. *Public Library of Science ONE.* **2:** e645.

Villaverde, A., and Carrió, M.M. (2003) Protein aggregation in recombinant bacteria: biological role of inclusion bodies. *Biotechnology Letters.* **25:** 1385 – 1395.

Verma, R., Tiwari, A., Kaur, S., Varshney, G.C., and Raghava, G.P.S. (2008) Identification of proteins secreted by malaria parasite into erythrocyte using SVM and PSSM profiles. *BioMed Central Bioinformatics.***9: doi:**10.1186/1471-2105-9-201.

Walsh, B.W., Lenhart, J.S., Schroeder, J.W., and Simmons, L.A. (2012) Far western blotting as a rapid and efficient method for detecting interactions between DNA replication and DNA repair proteins. In: Keck, J. (eds) *Single-Stranded DNA Binding Proteins. Methods in Molecular Biology (Methods and Protocols).* Totowa: Humana Press. **922:** 161 – 168.

Walsh, D.S., Pichyangkul, S., Gettayacamin, M., Tongtawe, P., Siegrist, C.A., Hansukjariya, P., Kester, K.E., Holland, C.A., Voss, G., Cohen, J., Stewart, A.V., Miller, R.S., Ballou, W.R., and Heppner Jr, D.G. (2004) Safety and immunogenicity of RTS,S+TRAP malaria vaccine, formulated in the AS02A adjuvant system, in infant rhesus monkeys. *American Journal of Tropical Medicine and Hygiene*. **70:** 499 – 509.

Weber, J.L. (1987) Analysis of sequences from the extremely A + T -rich genome of *Plasmodium falciparum. Gene.* **52:** 103 – 109.

Wedemeyer, W.J., Welker, E., Narayan, M., and Scheraga, H.A. (2000) Disulfide bonds and protein folding. *Biochemistry.* **39:** 4207 – 4216.

Weiss, W.R., Sedegah, M., Beaudoin, R.L., Miller, L.H., and Good, M.F. (1988) CD8+ T-cells (cytotoxic/suppressors) are required for protection in mice immunized with malaria sporozoites. *Proceedings of the National Academy of Sciences.* **85:** 573 – 576.

Wellems, T.E., and Plowe, C.V. (2001) Chloroquine-resistant malaria. *The Journal of Infectious Diseases.* **184:** 770 – 776.

Welling, G.W., Weijer, W.J., van der Zee, R., and Welling-Wester, S. (1985) Prediction of sequential antigenic regions in proteins. *Federation of European Biochemical Societies: Letters.* **188:** 215 – 218.

WHO (2018) World Health Organization. *World Malaria Report.*

William, T., Menon, J., Rajahram, G., Chan, L., Ma, G., Donaldson, S., Khoo, S., Fredrick, C., Jelip, J., Anstey, N.M., and Yeo, T.W. (2011) Severe *Plasmodium knowlesi* malaria in a tertiary care hospital, Sabah, Malaysia. *Emerging Infectious Diseases.* **17:** 1248 – 1255.

Wingfield, P.T. (2001) Use of protein folding reagents. *Current Protocols in Protein Science.* Appendix 3A. doi: 10.1002/0471140864.psa03as00.

Wipasa, J., Elliott, S., Xu, H., and Good, M.F. (2002) Immunity to asexual blood stage malaria and vaccine approaches. *Immunology and Cell Biology.* **80:** 401 – 414.

Wongsrichanalai, C., Barcus, M.J., Muth, S., Sutamihardja, A., and Wernsdorfer, W.H. (2007) A review of malaria diagnostic tools: microscopy and rapid diagnostic test (RDT). *American Journal of Tropical Medicine and Hygiene.* **77:** 119 – 217.

Woodberry, T., Pinzon-Charry, A., Piera, K.A., Panpisutchai, Y., Engwerda, C.R., Doolan, D.L., Salwati, E., Kenangalem, E., Tjitra, E., Price, R.N., Good, M.F., and Anstey, N.M. (2009) Human T cell recognition of the blood stage antigen *Plasmodium* hypoxanthine guanine xanthine phosphoribosyl transferase (HGXPRT) in acute malaria. *Malaria Journal.* **8:** doi:10.1186/1475-2875-8-12.

Wright, M.H., Clough, B., Rackham, M.D., Rangachari, K., Brannigan, K.A., Grainger, M., Moss, D.K., Bottrill, A.R., Heal, W.P., Broncel, M., Serwa, R.A., Brady, D., Mann, D.J., Leatherbarrow, R.J., Tewari, R., Wilkinson, A.J., Holder, A.A., and Tate, E.W. (2014) Validation of N-myristoyltransferase as an antimalarial drug target using an integrated chemical biology approach. *Nature Chemistry.* **6:** 112 – 121.

Wu, N., and Yu, H. (2012) The Smc complexes in DNA damage response. *Cell and Bioscience.* **2:** doi:10.1186/2045-3701-2-5.

Wu, Y., Li, Q., and Chen, X.Z. (2007) Detecting protein-protein interactions by far western blotting. *Nature Protocols.* **2:** 3278 – 3284.

Wu, Y., Ellis, R.D., Shaffer, D., Fontes, E., Malkin, E.M., Mahanty, S., Fay, M.P., Narum, D., Rausch, K., Miles, A.P., Aebig, J., Orcutt, A., Muratova, O., Song, G., Lambert, L., Zhu, D., Miura, K., Long, C.A., Saul, A., Miller, L.H., and Durbin, A.P. (2008) Phase 1 trial of malaria transmission blocking vaccine candidates *Pf*s25 and Pvs25 formulated with Montanide ISA 51. *Public Library of Science: ONE.* **3:** doi: 10.1371/journal.pone.0002636.

Wu, Y., Nelson, M.M., Quaile, A., Xia, D., Wastling, J.M., and Craig, A. (2009) Identification of phosphorylated proteins in erythrocytes infected by the human malaria parasite *Plasmodium falciparum. Malaria Journal.* **8:** doi:10.1186/1475-2875-8-105.

Wykes, M.N. (2013) Why haven't we made an efficacious vaccine for malaria? *European Molecular Biology Organization Reports*. **14:** 661.

Wykes, M.N., and Good, M.F. (2009) What have we learnt from mouse models for the study of malaria? *European Journal of Immunology.* **39:** doi: 10.1002/eji.200939552.

Xie, S.C., Dogovski, C., Hanssen, E., Chiu, F., Yang, T., Crespo, M.P., Stafford, C., Batinovic, S., Teguh, S., Charman, S., Klonis, N., and Tilley, L. (2016) Haemoglobin degradation underpins the sensitivity of early ring stage *Plasmodium falciparum* to artemisinins. *Journal of Cell Science.* **129:** 406 – 416.

Yang, F., Pan, Y., Chen, Y., Tan, S., Jin, M., Wu, Z., and Huang, J. (2015) Expression and purification of *Canis* interferon α in *Escherichia coli* using different tags. *Protein Expression and Purification.* **115:** 76 – 82.

Zhang, Y. (2008) I-TASSER server for protein 3D structure prediction. *BioMed Central Bioinformatics.* **9:** doi:10.1186/1471-2105-9-40.

Zhang, Z.H., Jiang, P.H., Li, N.J., Shi, M., and Huang, W. (2005) Oral vaccination of mice against rodent malaria with recombinant *Lactococcus lactis* expressing MSP-1_{19}. *World Journal of Gastroentrology.* **11:** 6975 – 6980.

Zhao, Y.O., Kurscheid, S., Zhang, Y., Liu, L., Zhang, L., Loeliger, K., and Fikrig, E. (2012) Enhanced survival of *Plasmodium*-infected mosquitoes during starvation. *Public Library of Science: ONE.* **7:** doi: 10.1371/journal.pone.0040556.

Zhou, J., Feng, G., Beeson, J., Hogarth, P.M., Rogerson, S.J., Yan, Y., and Jaworowski, A. (2015) $CD14^{hi}$CD16+ monocytes phagocytose antibody-opsonised *Plasmodium falciparum* infected erythrocytes more efficiently than other monocyte subsets, and require CD16 and complement to do so. *BioMed Central Medicine.* **13:** doi: 10.1186/s12916-015-0391-7.

Zhu, F., Liu, T., Zhao, C., Lu, X., Zhang, J., and Xu, W. (2017) Whole-killed blood-stage vaccine-induced immunity suppresses the development of malaria parasites in mosquitoes. *Journal of Immunology*. **198:** doi: 10.4049/jimmunol.1600979.

Zhu, J., and Hollingdale, M.R. (1991) Structure of *Plasmodium falciparum* liver stage antigen-1. *Molecular and Biochemical Parasitology.* **48:** 223 – 226.

Ziegler-Heitbrock, L. (2007) The CD14+ CD16+ blood monocytes: their role in infection and inflammation. *Journal of Leukocyte Biology.* **81:** 584 – 592.

Ziemienowicz, A., Skowyra, D., Zielstra-Ryalls, J., Fayet, O., Georgopoulos. C., and Zylicz, M. (1993) Both the *Escherichia coli* chaperone systems, GroEL/GroES and DnaK/DnaJ/GrpE, can reactivate heat-treated RNA polymerase. Different mechanisms for the same activity. *Journal of Biological Chemistry.* **268:** 25425 – 25431.

Appendix A: Annotated full-length amino acid sequence of *Pf*C0760c

An annotated full-length amino acid sequence for the *Pf*C0760c is shown. The sequence was obtained from the NCBI database, and subject to various online bioinformatics tools. Selected properties of the protein are indicated.

>gi|74764611|sp|O77384.1|LRR4_PLAF7 RecName: Full=Protein PFC0760c

MNNDFMKNEKDDYDKVNEEEYSLENFRGIDMNNNVDISNMNNNLNDVGELINIDNNDKYDEDQLSLIKESLEYGE
LLLSNVKEEDENNRREHFKKNDYMKDTEDVHYKESKIGQDKRFMHSL**C**VKELKSTEEGELFDDEKYKDKDTLINM
LRKKLEIKIKDYNLIMDTLILTKEE**C**SKKEEQLKDYKMKYNKMEKECYSLKNEIERKNNEKHLNIGSFSFYKNEY
DDMKYKLLKCEEKNKILLNKNQELHQTIIQMKNDSYNQNIKFKKDIDVLTEDKKNILIQNKNFTKQNKILIDKYL
RQEKIIYKLKKHNEEQEIIIKECHKKIEFVNKNSVNHLNKVRDVLNKSLIKSEEHVKLYTNLKKENDSLKIEYNK
SKTNIQQLNEQLVNYKNFIKEMEKKYKQLVVKNNSLFSITHDFINLKNSNIIIIRRTSDMKQIFKMYNLDIEHFN
EQDHLSVIYIYEILYNTNDNNNNDNDNNNDNNNNNNNNNDNNNNNNNDNNNNNNNYNNIMMMIENMNSGNHPNSN
NLHNYRHNTNDENNLSSLKTSFRYKINNKSGKSRSIKSRSHFSGDNEYIQDQLSNREMKDHYNYIERYNHSSNRN
DIHNLYYMEENVSHNNNKSDYDEDGDAENNNYYIKIKKNKYKKLNDLLNKAQMKIITLTRANEMFEKYCSNIKNT
LIRDDMKKFRKPDISDVHILHNEKIYLEKLLNEKLNYIKDIEKKLDELHGVINKNKEDIYILQVEKQTLIKVISS
VYDYTKMESENHIFKMNTTWNKMLNNVHMSSNKDYNNQNNQNIENNQNIENNQNNQNIENNQNIENNQNNQNNQN
NQNNQNNQNNQNNQNNAGIHISPDDFLKYRMSLEKFIQFTIKEHIVYIMKDEKKKTSNIIKESISLKKKHTKKSI
INNNNDNNNEDDDDNDMLSVMYSNDDVIKNKRKENNKEILEEHVSFSSFSNNEYIAHSFNSILLQLSNYIFNIEC
KQMEYFKNSNLLSYVDDYTITIELFYRLKKYNNIFSIEQILGTQYPSILQKLHDGIYCLKDNNKKKNNDGDNKSQ
EDDDGNKKKNNDGDNKSQEDDDGNKKKNNDGDNKSQEDDYGNKKNNDDDDDDSYKIELIVDELNKCKKNYTDEE
LYELMKGSDFDIFKKYKNFYLNHFININNIFSTIISFHIHNIEDKYKKVYERYFNLFNFNFSNVELSFDILIRRF
DKILRLTKKYEQLLEENYEKIKNKNEKEEYLHACIKELEMNLERYNNEKIILDEQINEKEKKINIINEKYLILEK
EYEEYQNKNIFINAQIENLEKEKKQLQEEIIQKDMINVKLNEKNCDIIKIYEKEKQYLHTLLQENKDSHNYLKDK
FENLLNLNEKLKYDHDISLNKINTLWLEEKENNKKNTFHMNNLRVENNNLLLKMKELQNKYNIIKKELNERIKQI
NVFRNNVSTLSLRDNRSTRGSIHQINNMYMNNTHLGFMGASKINNNISNLYYSNMIHMSHRGSIIKNKEDAEGNS
TQARMNNKDSTDNIINNIHNTDNINNMNNINNNTLNSINSNHLYYPFPFHNNVNSPKMVGMCDVTLASGVNKKDD
FLLNLEENEENSFLEYEIRIKSLQEELCDKESEILKIKGEKNILITCIETWKCFCKNSKEEISRLKEICKEQLEK
HKEFLLINKSNEDKLKYINSLLCDEKDKYDIVVKDIKNNMRNEIDKLNNDINEKSYEIKLLKHENNNLINEMNIL
KNKETENMNIKQKEEDYIKLIKKDKTNIQNEYNDLLEKYNEVVVKNNMLYNDMNVLLKEHKEEIFLLKENIKILQ
KDNTYLNDMFKNQINYVDNNLLKNRLDQLFNINQDLQKHLDTNQKHLEQLKYDYIEIKERLKIEKTKINKQEKYI
IQLQKDNNLILNDFNSTTTTTNNNNNNDNNNDNNNDNNNDNNNDTYQQFIHSLKANLENSRLELKELSNLNEKIQL
SDEKNRMKITILEDKLFKNEKDKMKLQQIIDDNNKNYMIQYNKLKTNLDMLSEENRMLLLNKEEYEKQIEQLNHD
HKLFISTKNNDIQIIENEKLQEQVDQYITTINEKDKIIVHLNLQIKKLANQNEHMRSRCDIFNVAHSQDNIKNDH
MVVGEDIMGDTNHDVNKNIDQGTNQHINQGTNQHINQGTNQHDTCDGPNYNYVKVQNATNREDNKNKERNLSQEI
YKYINENIDLTSELEKKNDMLENYKNELKEKNEEIYKLNNDIDMLSNNCKKLKESIMMMEKYKIIMNNNIQEKDE
IIENLKNKYNNKLDDLINNYSVVDKSIVSCFEDSNIMSPSCNDILNVFNNLSKSNKKVCTNMDICNENMDSISSI
NNVNNINNVNNINNVNNINNVNNINNVKNIVDINNYLVNNLQLNKDNDNIIIIKFNILKLFKLGS**C**YLYIINRNI
KEIQMLKNQILSLEESIKSLNEFINNLKNENEKNELIKINNFEEILKLKNNLQDNESCIQNLNNYLKKNEELNKI
NVKNIFKYKGYIIHLIQQSNVFCKIFKHFNENKIIDQSIINKLLYLKKSFDFYMYDSVIQEIRENKNIIINQDFL
TDEYFKHIQTFTKTCNVLIQRGYLSILKDTNNDFFIQNKQSNQQGNQNGNHINMCNIYPDDEINVTADQQIFDGT
ENVQQSLQNEEDYVNNEEMYTDKMDLDNNMNGDDDDDDDDDDDDDNNNNNNNNNNNNNNNMGDEDNHLVNAFNNH
NLLTNGNVKSDQINNETLERYEENIIQNIYTNDNVDNNQVIENINKILIKDKQDIINNDELKNEHNNLIRLINES
IENAHNLENVYVQNDANNLINDNIKKEETLTYVDEKDNVSNESNSKCDDDKKENEDIIQAKNENYPVSTHYDNND
DINKDNINNDNNNDNINDDNNNDNINNDNNNDNINNDNINNDNINNDNNNDNNNDNSNNGFVCELSSNINDFNNI
LNVNKDNFQGINKSNNFSTNLSEYNYDAYVKIVEAGSALENKKQQDKKRKYFSDSEITKENGYLGESNSIKIRKV
SVGGDNDNNDDDNNDDNDDDDNDDDNNDDDNNNDDDNDDSYDDEEKEQENYSNDVNTELNNHVTFEDISVHNNIQ
ENKKNYFSNVHENTFNLHVDENVHEDLQNYEDYVNNNNNNNDDDNEEESNNS**C**YIISSDDEGDKKNVSKQNDDDE
DDDDNGDDDDNEDDDDNEDDDNGDDDDNEDDDNGDDDDNEDDNYDDEDNDNYENEDDDNYANEDDDNYENDDDDN
YENDDDDNYENDDDNYENDDDDNYENGDDDNDNDHNDDNNDEEKYSCHDDKNEHTNNDLLNIDHDNNKNNITDEL
YSTYNVSVSHNKDPSNKENEIQNLISIDSSNENDENDENDENDENDENDENDENDENDENDENDEKDENDENDEN
DENFDNNNEGTLNEMNSEE

Figure A.1: Full-length amino acid sequence of PfC0760c with key sequences indicated. Red boxes: conserved peptides. Blue boxes: B-cell epitopes. Yellow highlight: acetylated lysine. Green: recombinant sequence. C in bold: conserved cysteine

Appendix B: BLAST output from PlasmoDB and ExPASy

The *Pf*C0760c protein sequence was subject to PlasmoDB BLAST. The accession numbers, species name and protein characteristics are illustrated in Table 1. The protein sequences were aligned with Clustal Omega and compared to the Clustal Omega output using protein sequences from NCBI BLASTp.

Table B.1: PlasmoDB BLAST analysis of PfC0760c protein sequence.

Accession number	*Plasmodium* species	Protein characteristics
PFIT_0317300	*P. falciparum* IT	conserved, unknown
PVP01_0822800	*P. vivax* P01	conserved, unknown
PVX_095365	*P. vivax* Sal-1	conserved hypothetical protein
PmUG01_08038800	*P. malariae* UG01	conserved, unknown
PKNH_0824500	*P. knowlesi* strain H	conserved, unknown
PKNOH_S100053000	*P. knowlesi* strain Malayan Strain Pk1 A	uncharacterised protein
PRG01_0320800	*P. reichenowi* G01	conserved, unknown
C922_02043	*P. inui* San Antonio 1	hypothetical protein
PBLACG01_0317800	*P. blacklocki* G01	conserved, unknown
PCOAH_00021130	*P. coatneyi* Hackeri	uncharacterised protein
PCYB_083240	*P. cynomolgi* strain B	hypothetical protein
PcyM_0824600	*P. cynomolgi* strain M	conserved, unknown
PGABG01_0316700	*P. gaboni* strain G01	conserved, unknown
PGSY75_0317300	*P. gaboni* strain SY75	hypothetical protein
PRCDC_0316600	*P. reichenowi* CDC	conserved, unknown
AK88_00579	*P. fragile* strain nilgiri	hypothetical protein
PADL01_0316200	*P. adleri* G01	conserved, unknown
PBILCG01_0316800	*P. billcollinsi* G01	conserved, unknown
PPRFG01_0318800	*P. praefalciparum* strain G01	conserved, unknown
PBANKA_0807900	*P. berghei* ANKA	conserved, unknown
PCHAS_0808200	*P. chabaudi chabaudi*	conserved, unknown
PY05757	*P. yoelii yoelii* 17XNL	hypothetical protein
PY07424	*P. yoelii yoelii* 17XNL	hypothetical protein
PY17X_0811100	*P. yoelii yoelii* 17X	conserved, unknown
PYYM_0810900	*P. yoelii yoelii* YM	conserved, unknown
YYE_01881	*P. vinckei vinckei* strain *vinckei*	hypothetical protein
YYG_01058	*P. vinckei petteri* strain CR	hypothetical protein
PGAL8A_00399000	*P. gallinaceum* 8A	conserved, unknown
PRELSG_0820800	*P. relictum* SGS1-like	conserved, unknown

The *Pf*C0760c protein sequence was subject to BLAST analysis using ExPASy. The accession numbers, species name and protein characteristics are illustrated in Table 2. The protein sequences were aligned with Clustal Omega and compared to the Clustal Omega output using protein sequences from NCBI BLASTp.

Table B.2: Protein sequences from ExPASy were aligned with PfC0760c using Clustal Omega.

Accession number	*Plasmodium species*	Protein function
A0A0J9VIP9 (PLAVI)	*P. vivax*	uncharacterised
A0A1D3PAQ5 (PLAMA)	*P. malariae*	uncharacterised
A0A060RNN0 (PLARE)	*P. reichenowi*	uncharacterised
A0A2P9BQW6 (9APIC)	*P. gaboni*	uncharacterised
A0A0D9QU16 (PLAFR)	*P. fragile*	uncharacterised
W7A291 (9APIC)	*P. inui*	uncharacterised
A0A1Y1JEH3 (PLAGO)	*P. gonderi*	uncharacterised
K6UJR3 (9APIC)	*P. cynomolgi*	uncharacterised
A0A1B1DYG9 (9APIC)	*P. coatneyi*	uncharacterised
A0A1D3RT35 (PLACH)	*P. chabaudi chabaudi*	uncharacterised
A0A1C6Y9T1 (PLACH)	*P. chabaudi adami*	uncharacterised
A0A077XDQ7 (PLABA)	*P. berghei* ANKA	uncharacterised
A0A0Y9VZ01 (PLABE)	*P. berghei*	uncharacterised
W7ARB4 (PLAVN)	*P. vinckei petteri*	uncharacterised
V7PPZ5 (9APIC)	*P. yoelii* 17X	uncharacterised
A0A078K6G8 (9APIC)	*P. yoelii*	uncharacterised
A0A1J1H4E4 (PLARL)	*P. relictum*	uncharacterised
A0A1J1GPR7 (PLAGA)	*P. gallinaceum*	uncharacterised